BioMed Research International

Current Biotechnological Advancements on Sustainable Metal and Nutrient Removal

Guest Editors: Li-Yuan Chai, Chong-Jian Tang, Qaisar Mahmood, and Xian-Wei Liu

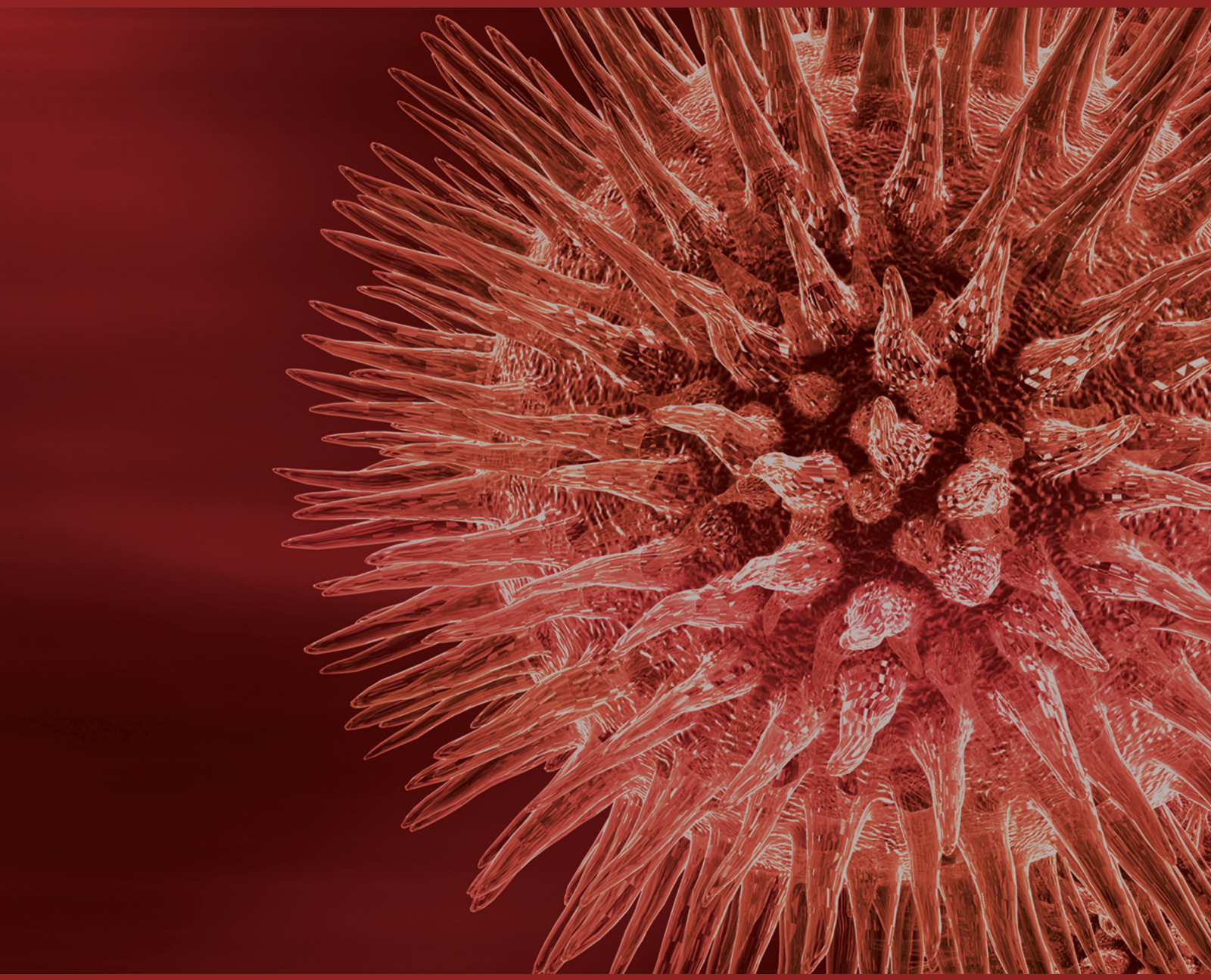

Current Biotechnological Advancements on Sustainable Metal and Nutrient Removal

BioMed Research International

Current Biotechnological Advancements on Sustainable Metal and Nutrient Removal

Guest Editors: Li-Yuan Chai, Chong-Jian Tang, Qaisar Mahmood, and Xian-Wei Liu

Contents

Hindawi Publishing Corporation
BioMed Research International
Volume 2014, Article ID 146796, 3 pages
http://dx.doi.org/10.1155/2014/146796

Editorial

Current Biotechnological Advancements on Sustainable Metal and Nutrient Removal

Li-Yuan Chai,[1] Chong-Jian Tang,[1] Qaisar Mahmood,[2] and Xian-Wei Liu[3]

[1] *Department of Environmental Engineering, School of Metallurgy and Environment, Central South University, Changsha, Hunan 410083, China*
[2] *Department of Environmental Sciences, COMSATS Institute of Information Technology, Abbottabad 22060, Pakistan*
[3] *The Biodesign Institute, Arizona State University, Tempe, AZ 85287, USA*

Correspondence should be addressed to Qaisar Mahmood; mahmoodzju@gmail.com

Received 9 January 2014; Accepted 9 January 2014; Published 27 February 2014

The prevalence of various pollutants like nitrogenous, sulphurous, phosphorous compounds, heavy metals, and organic compounds has seriously threatened the sustainability of natural ecosystems and is thus interfering with the natural biogeochemical cycling. Chemical pollution of water bodies can cause serious damage to environmental quality because many of these pollutants are extremely toxic and can in the worst case scenario wipe out entire ecosystems. The world still has not come up with the adequate monitoring system despite the fact that the global chemical pollution continues to grow because of the many "new" pollutants which have entered in use recently. Many thousands of new chemicals are introduced annually in USA alone. The long lasting effects of these pollutants are too varied and diverse and are no more a mystery now. Although nature often has great ability to recover from environmental stresses, the growing demands on water resources and land necessitate the professional application of fundamental knowledge of environmental remediation to ensure the maintenance of environmental quality.

Heavy metal pollution is one of the most important environmental problems today [1]. Various industries produce and discharge wastes containing different heavy metals into the environment, such as mining and smelting of metalliferous, surface finishing industry, energy and fuel production, fertilizer and pesticide industry and application, metallurgy, iron and steel, electroplating, electrolysis, electroosmosis, leatherworking, photography, electric appliance manufacturing, metal surface treating, and aerospace and atomic energy installation. They are widely used in all fields of life, that is, batteries, dyes, alloys, chemical compounds, and pharmaceutical and cosmetic products thus suggesting that the risk of pollution is very high. Thus, metals as resource are becoming a short in supply and also cause serious environmental pollution, threatening human health and ecosystem and also brings about serious environmental pollution, threatening human health and ecosystem. Three kinds of heavy metals are of concern, including toxic metals (such as Hg, Cr, Pb, Cd, and As), precious metals (such as Pd, Pt, Ag, Au, and Ru), and radionuclides (such as U, Th, Ra, and Am). The presence of heavy metal in atmosphere, soil, and water, even in traces, represents a severe risk to all organisms for their long-term toxicological effects. Heavy metal bioaccumulation and biomagnifications in the food chain can be extremely dangerous to human health [1].

Wastewater irrigation is not only used due to scarcity of fresh water but it is also used for protection of environment and for its high nutritive values [2]. Water pollution is a great problem throughout the world and ground water pollution occurs due to disposal of industrial effluents and domestic sewage into watercourses [3]. Wastewater not only provides the supplemental irrigation but also provides the useful nutrients, especially organic matter phosphorous and nitrogen to improve physical properties and fertility of soil [4]. The continuous utilization of raw water for irrigation of leafy and nonleafy vegetables results in metal deposition in soil as well as in undercultivated crops well over the maximum permissible level [5]. Heavy metals enter

the human body mainly through two routes, namely, inhalation and ingestion, ingestion being the main route of exposure to these elements in human population. Heavy metals intake by human populations through food chain has been reported in many countries [6]. The health risks of various heavy metals accumulated in these vegetables and crop plants need to be carefully assessed.

PAHs mainly generate from incomplete combustion of fossil fuels [7], oil refinery, and steelmaking [8]. PAHs are widely present in environment and organisms owing to high chemical stability, low water solubility, and high lipid solubility [9]. Food ingestion intake of PAHs increases with the higher trophic level of organisms in food chain through accumulating and transmitting [10]. Research has showed that PAHs have seriously damaged the health of marine mammals on the coast of California [11]. PAHs accumulated effectively in goats, intensifying the biotoxicity [12] and threatening human health, especially for those mainly depending on goat meat. The understanding of the distributions and mother-child transmission of PAHs in various food organisms is desirable and provides useful data to decrease human exposure risk.

The anaerobic bioreactor applies the principles of biotechnology and microbiology, and currently, it has been widely used in the wastewater treatment plants due to high efficiency, low energy use, and green energy generation. Anaerobic digestion is an attractive option for waste treatment practice in which both energy recovery and pollution control can be achieved. The anaerobic processes have become increasingly demanding in the treatment of complex industrial wastewaters, which have the ability to treat high concentrations of organics, and may contain toxic materials or complex substances and even low concentrations of domestic wastewater [13, 14]. Regarding the ability to attain environmental protection and resource preservation, anaerobic treatment process and anaerobic bioreactors have received great attention [13, 15, 16].

Nitrogen pollution has caused severe environmental problems. Since the first discovery of ANAMMOX in the early 1990s, this related technology is developing rapidly. A series of new and outstanding outcomes were achieved in the discovery of new ANAMMOX bacterial species including Brocadia sinica and sulfate-dependent ANAMMOX bacteria (Anammoxoglobus sulfate and *Bacillus benzoevorans*). Since the discovery of the ANAMMOX process [17], it has been regarded as a cost-effective and environment-friendly way to treat wastewater containing high ammonium concentrations [18]. By smart application of ANAMMOX in municipal treatment, wastewater treatment plants could be converted from energy-consuming into energy-producing systems [19]. It is a hot topic in the fields of microbiology and environmental science and engineering due to its merits of effective removal of both ammonium and nitrite under anaerobic conditions with high removal rate, little sludge production, and low operational cost [20–22].

In the recent years, the wastewater treatment strategies have been shifted to one of the most promising methods, that is, biological anaerobic treatment with the adoption of high rate anaerobic systems like up-flow anaerobic sludge blanket (UASB) and other related treatment systems. The outstanding characteristics of high rate anaerobic bioreactor (ABR) include the anaerobic microorganisms capable of aggregation, low operational and maintenance costs, energy recovery in the form of biogas, low energy consumption, and low production of digested sludge [23]. The ABR treated effluents can be employed for irrigation of various crops. However, such type of effluent may be high in chemical oxygen demand (COD), biochemical oxygen demand (BOD), and coliform [24]. As ABR effluents are anticipated to be rich in various nutrients, they can be treated in Constructed Wetlands (CW). CW is a low cost or economical on-site wastewater treatment technology which is not only effective but also aesthetically pleasing. Since 1980, the utilization of the CW for the treatment of a variety of wastewaters has quickly become widespread. The amount of nutrients removed by plants and stored in their tissues is highly relative which depends on the plant type, biomass, and nutrient concentration in tissues [25]. A variety of macrophytes are used in CW and most common are floating macrophytes (i.e., *Lemna* spp. or *Eichhornia crassipes*), submerged macrophytes (i.e., *Elodea canadiensis*), and rooted emergent macrophytes (i.e., *Phragmites australis* and *Typha angustifolia*). The plants roots create conducive environment for the microbial growth and in winter the plant litter acts as insulator. CW are attached growth biological reactors, which tender higher pollutant removal efficiency through physical, chemical, and biological mechanisms. The common removal mechanisms associated with wetlands include sedimentation, coagulation, adsorption, filtration, biological uptake, and microbial transformation [26, 27].

The role of bacteria in remediation of toxic compounds has been documented over the years and would continue to be a dominant technology for the remediation of organic and inorganic compounds [28]. Bacteria with the ability to tolerate, remove, or/and degrade several xenobiotics simultaneously are urgently needed for remediation of sites contaminated with more than one pollutant. Enzymatic reduction of metals to less toxic, nonsoluble lower oxidation states is employed by many bacteria for survival and can be used as a tool for bioremediation of heavy metals.

We hope that readers of CBA will find in this special issue accurate data and updated reviews on the various aspects of the subject. Some useful information has been presented on risk assessment of various pollutants, technological aspects of metal treatments, and strategies of metal recovery.

Li-Yuan Chai
Chong-Jian Tang
Qaisar Mahmood
Xian-Wei Liu

References

[1] Q. Mahmood, A. Rashid, S. S. Ahmad, M. R. Azim, and M. Bilal, "Current status of toxic metals addition to environment and its consequences," in *The Plant Family Brassicaceae: Contribution Towards Phytoremediation, Environmental Pollution*, N. A. Anjum et al., Ed., Springer, 2012.

[2] M. N. Jagtap, M. V. Kulkarni, and P. R. Puranik, "Flux of heavy metals in soils irrigated with urban wastewaters," *American-Eurasian Journal of Agricultural and Environmental Sciences*, vol. 8, no. 5, pp. 487–493, 2010.

[3] A. Mashiatullah, A. Riffat, M. Qureshi, A. Niaz, T. Javed, and A. Nisar, "Biological quality of ground water in Rawalpindi/Islamabad," *The Environmental Monitoring*, vol. 5, pp. 13–18, 2005.

[4] P. A. Gibbs, B. J. Chambers, A. M. Chaudri, S. P. McGrath, and C. H. Carlton-Smith, "Initial results from long-term field studies at three sites on the effects of heavy metal-amended liquid sludges on soil microbial activity," *Soil Use and Management*, vol. 22, no. 2, pp. 180–187, 2006.

[5] B. Nrgholi, "Investigation of the Firozabad 28. Hawley, J.K., 1985. Assessment of health risk wastewater quality-quantity variation for agricultural use," Final Report, Iranian Agricultural Engineering Research Institute, 2007.

[6] E. U. Islam, X.-E. Yang, Z.-L. He, and Q. Mahmood, "Assessing potential dietary toxicity of heavy metals in selected vegetables and food crops," *Journal of Zhejiang University B*, vol. 8, no. 1, pp. 1–13, 2007.

[7] B. J. Finlayson-Pitts and J. N. Pitts Jr., *Chemistry of the Upper and Lower Atmosphere: Theory, Experiments and Applications*, Academic Press, New York, NY, USA, 2000.

[8] N. Yassaa and A. Cecinato, "Composition of torched crude oil organic particulate emitted by refinery and its similarity to atmospheric aerosol in the surrounding area," *Chemosphere*, vol. 60, no. 11, pp. 1660–1666, 2005.

[9] J. Paasivirta, S. Sinkkonen, P. Mikkelson, T. Rantio, and F. Wania, "Estimation of vapor pressures, solubilities and Henry's law constants of selected persistent organic pollutants as functions of temperature," *Chemosphere*, vol. 39, no. 5, pp. 811–832, 1999.

[10] B. C. Kelly and F. A. P. C. Gobas, "Bioaccumulation of persistent organic pollutants in lichen-caribou-wolf food chains of Canada's Central and Western Arctic," *Environmental Science and Technology*, vol. 35, no. 2, pp. 325–334, 2001.

[11] J. S. Brown and S. A. Steinert, "DNA damage and biliary PAH metabolites in flatfish from Southern California bays and harbors, and the Channel Islands," *Ecological Indicators*, vol. 3, no. 4, pp. 263–274, 2004.

[12] K. Y. Kong, K. C. Cheung, C. K. C. Wong, and M. H. Wong, "The residual dynamic of polycyclic aromatic hydrocarbons and organochlorine pesticides in fishponds of the Pearl River delta, South China," *Water Research*, vol. 39, no. 9, pp. 1831–1843, 2005.

[13] L. Seghezzo, G. Zeeman, J. B. Van Lier, H. V. M. Hamelers, and G. Lettinga, "A review: the anaerobic treatment of sewage in UASB and EGSB reactors," *Bioresource Technology*, vol. 65, no. 3, pp. 175–190, 1998.

[14] S. Aiyuk, I. Forrez, D. K. Lieven, A. van Haandel, and W. Verstraete, "Anaerobic and complementary treatment of domestic sewage in regions with hot climates-A review," *Bioresource Technology*, vol. 97, no. 17, pp. 2225–2241, 2006.

[15] P. L. McCarty, "Anaerobic waste treatment fundamentals," *Public Works*, vol. 95, no. 9, pp. 107–112, 1964.

[16] S. Chong, T. K. Sen, A. Kayaalp, and H. M. Ang, "The performance enhancements of upflow anaerobic sludge blanket (UASB) reactors for domestic sludge treatment—a state-of-the-art review," *Water Research*, vol. 46, no. 11, pp. 3434–3470, 2012.

[17] A. Mulder, A. A. Van De Graaf, L. A. Robertson, and J. G. Kuenen, "Anaerobic ammonium oxidation discovered in a denitrifying fluidized bed reactor," *FEMS Microbiology Ecology*, vol. 16, no. 3, pp. 177–184, 1995.

[18] M. S. M. Jetten, S. Logemann, G. Muyzer et al., "Novel principles in the microbial conversion of nitrogen compounds," *Antonie van Leeuwenhoek, International Journal of General and Molecular Microbiology*, vol. 71, no. 1-2, pp. 75–93, 1997.

[19] B. Kartal, J. G. Kuenen, and M. C. M. Van Loosdrecht, "Sewage treatment with anammox," *Science*, vol. 328, no. 5979, pp. 702–703, 2010.

[20] M. Strous, J. A. Fuerst, E. H. M. Kramer et al., "Missing lithotroph identified as new planctomycete," *Nature*, vol. 400, no. 6743, pp. 446–449, 1999.

[21] Y. Tao, D.-W. Gao, Y. Fu, W.-M. Wu, and N.-Q. Ren, "Impact of reactor configuration on anammox process start-up: MBR versus SBR," *Bioresource Technology*, vol. 104, pp. 73–80, 2012.

[22] I. Tsushima, Y. Ogasawara, T. Kindaichi, H. Satoh, and S. Okabe, "Development of high-rate anaerobic ammonium-oxidizing (anammox) biofilm reactors," *Water Research*, vol. 41, no. 8, pp. 1623–1634, 2007.

[23] A. A. Khan, R. Z. Gaur, V. K. Tyagi et al., "Sustainable options of post treatment of UASB effluent treating sewage: a review," *Resources, Conservation and Recycling*, vol. 55, no. 12, pp. 1232–1251, 2011.

[24] M. A. El-Khateeb and A. Z. El-Bahrawy, "Extensive post treatment using constructed wetland," *Life Science Journal*, vol. 10, pp. 560–568, 2013.

[25] N. Korboulewsky, R. Wang, and V. Baldy, "Purification processes involved in sludge treatment by a vertical flow wetland system: focus on the role of the substrate and plants on N and P removal," *Bioresource Technology*, vol. 105, pp. 9–14, 2012.

[26] A. K. Mungray, Z. V. P. Murthy, and A. J. Tirpude, "Post treatment of up-flow anaerobic sludge blanket based sewage treatment plant effluents: a review," *Desalination and Water Treatment*, vol. 22, no. 1–3, pp. 220–237, 2010.

[27] C. Wendland, J. Behrendt, T. A. Elmitwalli et al., "ABR reactor followed by constructed wetland and UV radiation as an appropriate technology for municipal wastewater treatment in Mediterranean countries," in *Proceedings of the 7th specialized conference on small water and wastewater systems in Mexico*, 2006.

[28] A. B. Moldes, R. Paradelo, X. Vecino et al., "Partial characterization of biosurfactant from lactobacillus pentosus and comparison with sodium dodecyl sulphate for the bioremediation of hydrocarbon contaminated soil," *BioMed Research International*, vol. 2013, Article ID 961842, 6 pages, 2013.

Hindawi Publishing Corporation
BioMed Research International
Volume 2014, Article ID 839538, 8 pages
http://dx.doi.org/10.1155/2014/839538

Research Article

Impact Assessment of Cadmium Toxicity and Its Bioavailability in Human Cell Lines (Caco-2 and HL-7702)

Rukhsanda Aziz,[1] M. T. Rafiq,[1,2] Jie Yang,[3] Di Liu,[1] Lingli Lu,[1] Zhenli He,[4] M. K. Daud,[5] Tingqiang Li,[1] and Xiaoe Yang[1]

[1] *Ministry of Education Key, Laboratory of Environmental Remediation and Ecological Health, College of Environmental and Resource Sciences, Zhejiang University, Hangzhou 310058, China*
[2] *Department of Environmental Sciences, International Islamic University, Islamabad 44000, Pakistan*
[3] *College of Architecture and Environment, Sichuan University, Chengdu 610065, China*
[4] *Indian River Research and Education Center, Institute of Food and Agricultural Sciences, University of Florida, Fort Pierce, FL 34945, USA*
[5] *Department of Biotechnology & Genetic Engineering, Kohat University of Science and Technology, Kohat 26000, Pakistan*

Correspondence should be addressed to Tingqiang Li; litq@zju.edu.cn and Xiaoe Yang; xyang571@yahoo.com

Received 21 August 2013; Revised 23 October 2013; Accepted 9 November 2013; Published 16 February 2014

Academic Editor: Qaisar Mahmood

Cadmium (Cd) is a widespread environmental toxic contaminant, which causes serious health-related problems. In this study, human intestinal cell line (Caco-2 cells) and normal human liver cell line (HL-7702 cells) were used to investigate the toxicity and bioavailability of Cd to both cell lines and to validate these cell lines as *in vitro* models for studying Cd accumulation and toxicity in human intestine and liver. Results showed that Cd uptake by both cell lines increased in a dose-dependent manner and its uptake by Caco-2 cells (720.15 μg mg^{-1} cell protein) was significantly higher than HL-7702 cells (229.01 μg mg^{-1} cell protein) at 10 mg L^{-1}. A time- and dose-dependent effect of Cd on cytotoxicity assays (LDH release, MTT assay) was observed in both Cd-treated cell lines. The activities of antioxidant enzymes and differentiation markers (SOD, GPX, and AKP) of the HL-7702 cells were higher than those of Caco-2 cells, although both of them decreased significantly with raising Cd levels. The results from the present study indicate that Cd above a certain level inhibits cellular antioxidant activities and HL-7702 cells are more sensitive to Cd exposure than Caco-2 cells. However, Cd concentrations <0.5 mg L^{-1} pose no toxic effects on both cell lines.

1. Introduction

Cadmium (Cd) is one of the most concerned pollutants possessing high toxicity for both animals and plants [1]. The direct exposure of living beings, particularly human populations, to it may cause various health related problems such as Itai-Itai disease [2]. Cadmium is considered as a "guest" metal in Pb:Zn mining process and is widely dumped into the environment through various anthropogenic activities such as mining, smelting, and use of fertilizers [3]. It has been classified as a group I carcinogen by International Agency for Research in Cancer (IARC) and as a probable human carcinogen (group B1) by Environmental Protection Agency (EPA) [4]. Due to its toxic nature, it is now recognized that human exposure to Cd must either be stopped or minimized.

Cadmium salts, having greater solubility in water, can easily enter into our food chain through edible parts of the plant [5]. When grown in polluted soil, plants take up water, nutrients, and heavy metals that may then enter the food chain [6]. Khan et al. [7] found that Cd concentration in soils and food crops was above permissible limits in selected vegetables. They concluded that consuming such vegetables and food crops may result in Cd toxicity to both humans and grazing animals. Human beings are mostly exposed to Cd either by inhalation or ingestion, with oral intake being the major route. Understanding of the mechanisms of Cd absorption and circumventing the intestinal barrier is of prime interest. Available literature reports that, following oral exposure, Cd is absorbed in mammals preferentially in the duodenum and proximal jejunum [8]. After absorption Cd first reaches the

liver. In liver Cd induces the production of metallothionein. After continuous hepatocyte necrosis and apoptosis, Cd-metallothionein complexes are washed into sinusoidal blood. From here, some of the absorbed Cd enters into the enterohepatic cycle via secretion into the biliary tract in the form of Cd-glutathione conjugates. Enzymatically degraded to Cd-cysteine complexes in the biliary tract, Cd again enters the small intestine [9]. It is generally assumed that, after inhalation or ingestion of typical inorganic Cd compounds and after transferring across the alveolar membranes or intestinal wall, the major fraction of Cd initially accumulates in the liver [10]. *In vitro* and *in vivo* studies have depicted that low Cd concentrations (<5.0 μM) might enhance cell proliferation in a dose-dependent manner [11, 12], while its higher concentrations (>5.0 μM) could induce apoptosis in many tissues and organs [13].

Apoptosis is enhanced in cells in most cases upon Cd exposure [14]. Various assays such as LDH leakage, total protein contents, and the MTT are commonly employed for the detection of cytotoxicity or cell viability upon exposure to toxic substances. The LDH leakage assay measures the lactate dehydrogenase activity in the extracellular culture medium upon the loss of intracellular LDH and is an indicator of cell membrane damage [15]. 3-[4,5-Dimethylthiazol-2-yl]-2,5-diphenyltetrazolium bromide (MTT) is a water soluble tetrazolium salt, which is converted to an insoluble purple formazan within the mitochondria. Formazan accumulates only in healthy cells and its reduction in stressed cells has been reported [16].

Like any other environmental stress, Cd stress also causes oxidative stress in cultured cells due to the production of various reactive oxygen species (ROS) such as hydrogen peroxide, superoxide radical, and hydroxyl radical. Reactive oxygen species (ROS), normally produced during the aerobic metabolism, function as second messengers involved in many cellular functions. On the other hand, when ROS level increases because of oxidant treatments and defective antioxidant systems, these highly reactive compounds and radicals become dangerous toxic agents [17]. These ROS cause imbalance between oxidants and antioxidants of the cell tissues, which leads to the numerous degenerative diseases in humans. Either to avoid or to scavenge oxidative damage, mammalian cells possess inherent antioxidant machinery, which is comprised of superoxide dismutase (SOD), catalase, and glutathione peroxidase (GPx) [18]. However, there is scarce information regarding metabolic differences in oxidatively stressed intestinal cells compared to nonstressed cells. Due to its soluble nature, Cd can readily penetrate tissues after exposure and inhibit antioxidant enzymatic system [19] by affecting the cellular thiol redox balance [20], in particular with cellular glutathione. Several studies have shown that Cd indirectly generates ROS and consequently DNA, lipid, and protein oxidation in various cell lines [21].

The Caco-2 cell line is a human intestinal cellline and HL-7702 is normal human liver cell line that have been widely used as representative models of mammalian intestinal [22] and liver cells [23]. These cells have become useful tools for the study of uptake, toxicity, and transport of nutrients [22] and heavy metals [24]. The aims of this study were to (1) determine the bioavailability of Cd in the Caco-2 cells and HL-7702 cells; (2) study the effect of Cd on the activities of antioxidant enzymes (SOD, GPx) and differentiation marker enzyme (AKP); and (3) assess the health risk of the Cd in human small intestine and liver.

2. Materials and Methods

2.1. Chemicals and Reagents. $Cd(NO_3)_2$ was purchased from Sinopharm Chemical Reagent Co., Ltd. (Shanghai, China). Dulbecco's modified Eagle medium (DMEM with glucose 4.5 g L^{-1}), trypsin-EDTA, phosphate-buffered saline (PBS), fetal bovine serum (FBS), glutamine, nonessential amino acids, penicillin, and streptomycin were purchased from Gibco Life Technologies (Grand Island, NY). 3-[4,5-Dimethylthiazol-2-yl]-2,5-diphenyltetrazolium bromide (MTT) was purchased from Sigma-Aldrich (St. Louis, MO, USA). SOD, LDH, AKP, and GSH-Px testing kits were obtained from Nanjing KeyGen Biotech. Co., Ltd. (Nanjing, China). All of the other chemicals used in this study were of analytical grade purchased from local chemical suppliers. All reagents were prepared with deionized water (≤0.1 μS/cm) using a Milli-Q system (Millipore, Billerica, MA). All laboratory glassware used in the experiments were soaked in 10% HNO_3 for 24 h and subsequently rinsed with deionized water and air-dried.

2.2. Preparation of the Cadmium Solutions. The stock solution of cadmium nitrate was made in UHQ water and sterilized using a 0.22 mm filter. A working solution in the corresponding media (1 : 10 v/v) was prepared to give the concentrations of 0.25, 0.5, 2, 4, 8, and 10 mg L^{-1} in the culture medium.

2.3. Cell Culture. Caco-2 cells and HL-7702 cells were obtained from the Institute of Biochemistry and Cell Biology (SIBS, CAS, Shanghai, China) and used in assays at passage 20–33. The Caco-2 and HL-7702 cells were normally cultured in 25 cm^2 flasks (Corning Inc., NY, USA) and maintained in high glucose (4.5 g L^{-1}) DMEM, supplemented with 10% (v/v) fetal bovine serum, 1% (v/v) nonessential amino acids, 4 mM L-glutamine, and 1% (v/v) antibiotic solution (penicillin-streptomycin). The cells were maintained at 37°C in an incubator (Heraeus, BB15, Germany) with 5% CO_2 and 95% relative humidity. After being 80% confluent, the cells were washed with phosphate-buffered saline (PBS) to remove any unattached cells. The attached cells were then harvested using a trypsin-ethylenediaminetetraacetic acid (EDTA) solution. The cells were seeded in 6-well plates at a density of approximately 10×10^4 cells/mL. The medium was changed every 2 days, and the cultures were maintained for 13 days to reach the stationary growth phase and to allow for maximal functional differentiation. Confluent cultures of differentiated cells were used for further studies and were exposed to known concentrations of Cd in the culture medium and incubated for 2 and 12 h at 13 days after seeding. Cytological and biochemical assays were carried out on the cell lysate and culture medium for determination of markers of cell damage.

2.4. Cd Uptake. To assess the uptake of $Cd(NO_3)_2$, Caco-2 cells and HL-7702 cells, cultured in 6-well plates, were exposed to different concentrations of $Cd(NO_3)_2$ solution (0.25, 0.5, 2, 4, 8, and 10 mg L^{-1}), for 2 h at 37°C. Then the cells were washed twice with ice cold PBS to remove extracellular bound Cd. The cell monolayer was lysed by the addition of 2 mL of deionized water in the well and then harvested. The lysate was put into the digestion tubes and digested with HNO_3 (5 mL) and H_2O_2 (1 mL). After cooling the resultant solutions were diluted to 10 mL using deionized water. The concentrations of Cd in the final solution were determined by ICP-MS (Agilent 7500a, Agilent Technologies, CA, USA) following a standard procedure.

2.5. Cytotoxicity Assays

2.5.1. MTT Assay. Cytotoxicity induced by Cd was assessed by MTT assay. Caco-2 cells and HL-7702 cells were seeded at a density of 5×10^4 cells/well in a 96-well plate and incubated for 24 h. Cells were exposed to increasing concentrations of Cd (6 wells per concentration group plus 1 control group) for 2 h or 12 h at 37°C in an atmosphere of 5% CO_2 in air. Control groups consist of cells in media (minus chemical), which are processed identically and incubated simultaneously as treated groups. After various time intervals (2 and 12 h), medium was removed and replaced with 50 μL MTT solution (2 mg mL^{-1}) for another 4 h after which medium was removed. The medium is then replaced with 100 μL dimethyl lsulfoxide (DMSO), agitated for 5 min at room temperature. Finally, the absorbance was measured at 552 nm using a microplate reader (Bio-Rad-680, Bio-Rad, USA). Cell viability is expressed as a percentage of the control group. Cell MTT response (% control) was calculated from the equation:

$$\%\ \text{control} = \frac{\text{Absorbance}_{\text{treatment}}}{\text{Absorbance}_{\text{control}}} \times 100\%. \quad (1)$$

2.5.2. Lactate Dehydrogenase (LDH) Release. Cytotoxicity induced by Cd was assessed by lactate dehydrogenase (LDH) leakage into the culture medium. The activity of LDH in the medium was determined using a commercially available kit from Jiancheng Biochemical Co., Ltd. (Nanjing, China). The LDH assay is based on the conversion of lactate to pyruvate in the presence of LDH with parallel reduction of NAD to NADH. The change in the absorbance was recorded at 440 nm using a microplate spectrophotometer system (Bio-Rad-680, Bio-Rad, USA). Cell LDH release (% control) was calculated from the equation:

$$\%\ \text{control} = \frac{(\text{U LDH/mg cell protein})\ \text{treatment}}{(\text{U LDH/mg cell protein})\ \text{control}} \times 100\%. \quad (2)$$

2.6. Enzyme Assays

2.6.1. Glutathione Peroxidase (GPx). The cell glutathione peroxidase (GPx) activity was measured using the GPx cellular activity assay kit from Jiancheng Biochemical Co., Ltd. (Nanjing, China). This kit uses an indirect method, based on the oxidation of reduced glutathione (GSH) to oxidized glutathione (GSSG) catalyzed by GPx, which is then coupled with recycling GSSG back to GSH utilizing glutathione reductase and NADPH. The decrease in NADPH at 412 nm during oxidation of NADPH to NADP is indicative of GSH-Px activity. GSH-Px activity was expressed in terms of international units per mg of soluble cell proteins.

2.6.2. Superoxide Dismutase (SOD). The cell superoxide dismutase (SOD) activity was measured in Caco-2 cells and HL-7702 cells using the SOD cellular activity assay kit from Jiancheng Biochemical Co., Ltd. (Nanjing, China) based on the competition between pyrogallol oxidation by superoxide radicals and superoxide dismutation by SOD. The absorbance was measured at 550 nm using a microplate reader (Bio-Rad-680, Bio-Rad, USA). The SOD's one unit activity is defined as the amount of the enzyme required to prohibit the rate of pyrogallol autooxidation by 50%. SOD activity was expressed as international units per mg of soluble cell proteins.

2.6.3. Alkaline Phosphatase. The alkaline phosphatase activity was measured by the alkaline phosphatase testing kit. This assay is based on measuring the alkaline phosphatase activity by monitoring the color change as paranitrophenol phosphate which is colorless is converted to paranitrophenol + phosphate which is yellow. Activity was determined using a microplate reader (Bio-Rad-680, Bio-Rad, USA) at 520 nm.

2.7. Protein Assay. Bradford [25] assay was performed in order to measure cell protein in Caco-2 cells and HL-7702 cells. Its absorbance was measured at 595 nm with a spectrophotometer (VersaMax, Molecular Devices, Sunnyvale, CA, USA).

2.8. Statistical Analyses. Data were analyzed using the SPSS 18.0 (SPSS Inc., Chicago, USA). Results are presented as mean ± S.D. (standard deviation). Analysis of variance (ANOVA) was performed with the least significant difference (LSD) to compare means of different Cd concentrations with control. For comparison of the different cell lines, univariate ANOVA with LSD post hoc test was used [26]. Means were considered to be significantly different if P values were <0.05.

3. Results and Discussion

In recent years, heavy metal pollution, particularly cadmium, lead, arsenic, and chromium [1], has threatened living beings, causing adverse effects on human health such as renal and testicular dysfunction and pulmonary problems. In the present study, the cytotoxic effects of Cd on a normal human liver cell line (HL-7702 cells) and human intestinal cell line (Caco-2 cells) were evaluated by studying Cd uptake by both cell lines, cytotoxicity assays, ROS scavenger enzymes, and differentiation marker enzyme (AKP).

3.1. Cellular Cd Uptake. Cd accumulation in both cell lines was found significantly different due to difference in the

origin of cell lines. The Cd uptake by both cell lines is shown in Figure 1. Dose-dependent rise in Cd accumulation in Caco-2 cells and HL-7702 cells could be noticed ranging from 52.3 to 720.1 and from 11.3 to 229.0 $\mu g\,mg^{-1}$ of cellular protein, respectively. Increasing Cd levels in the incubation medium were significantly ($P < 0.05$) correlated with rising cellular Cd levels. It was also observed that the uptake of the Cd at 10 $mg\,L^{-1}$ by Caco-2 cells (720.15 $\mu g\,mg^{-1}$ cell protein) is higher as compared to HL-7702 cells (229.01 $\mu g\,mg^{-1}$ cell protein). Our results are in agreement with Templeton [27] who reported that Cd was absorbed from the gastrointestinal tract and was then taken up by the liver, the first organ after absorption which accumulates high Cd concentrations. Cd accumulation by the Caco-2 cells was augmented with the increasing Cd concentrations in the culture medium [28]. There can be various reasons regarding Cd uptake and its differential absorption in different organs of human body. Concentration-dependent Cd uptake in our present experiment might be due to its chemical and physical properties related to essential metals such as iron (Fe), zinc (Zn), or calcium (Ca). That is why Cd can be transported and taken up into the cells by a process referred to as "ionic and molecular mimicry" [29]. Intestinal absorption of Cd is characterized by a rapid rate of metal accumulation within the intestinal mucosa and a low rate of diffusive transfer into circulatory system [9]. In the present study we also found that the intestinal cells (Caco-2 cells) accumulated higher quantity of Cd as compared to the liver cells (HL-7702). There is a two-step process for the absorptive Cd movement from intestinal lumen into enterocytes: the first step consists of a nonspecific binding of Cd into the luminal plasma membrane and the second step consists of a transport across the luminal plasma membrane into enterocytes [30]. Much of the Cd absorbed in the intestines is delivered first to the liver through portal circulation, bound mainly to albumin, where it is taken up from the sinusoidal capillaries to the hepatocytes [31].

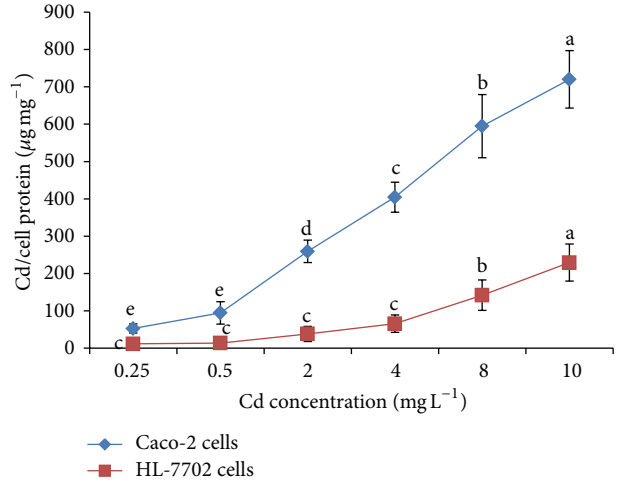

FIGURE 1: Bioavailability of cadmium (Cd) by HL-7702 and Caco-2 cells after 2 h. Values are presented as mean ± S.D.; $n = 3$. Different letters indicate significant differences at $P < 0.05$ by the least significant difference (LSD) test.

3.2. Effect of Cadmium on LDH Release and Mitochondrial Activity (MTT). The results obtained from the cytotoxicity assays indicate that there are differences between the two cell lines concerning their sensitivity to Cd exposure. HL-7702 cells appear to be more sensitive as indicated by the LDH and MTT assays (Figures 2 and 3). LDH release assay is an important method to assess cell membrane stability [13]. As shown in Figures 2(a) and 2(b), there was an increase in LDH release when Caco-2 cells and HL-7702 cells were exposed to different concentrations for 2 and 12 h. Increased concentrations and time of Cd exposure resulted in a significant increase of LDH release in culture media. At Cd concentrations greater than 0.5 $mg\,L^{-1}$, a significant ($P < 0.05$) increase in LDH release was observed for both cell lines, as compared with their respective controls. It was found that Cd dosage increased the LDH release from 99% to 178.5% in Caco-2 cells and from 100% to 198.4% in HL-7702 cells at the incubation time of 2 h. After 12 h, this increase was much larger at 10 $mg\,L^{-1}$ both in Caco-2 cells (264.6%) and HL-7702 cells (250.7%). In terms of LDH release, for both cell lines, Cd levels and exposure time significantly correlate ($P < 0.05$) with each other. The large increase in LDH release might also be due to cell rounding and loss of adherence found at the concentration of 10 $mg\,L^{-1}$ Cd. This noticeable increase of LDH release might be due to the increase of necrotic cell death as scavenging enzymes could be depleted by relatively high concentrations of Cd. Morphological changes (loss of adherence and cell rounding) based on 10 $mg\,L^{-1}$ Cd might be associated with loss of intercellular contacts and break down of desmosomes [26].

The MTT assay is mainly based on the enzymatic conversion of MTT in the mitochondria. It has been suggested that Cd disrupts mitochondrial function both *in vivo* [32] and *in vitro* [33]. Apoptosis mediated by mitochondria may be relevant in metal-induced cell death. Mitochondrial activity was significantly decreased by increasing concentrations and time of Cd exposure to both cells (Figures 3(a), and 3(b)). MTT assay was very low (<3%) in both cell lines treated with 0–0.5 $mg\,L^{-1}$ Cd. A significant decrease in MTT assay, compared to control cells, was noted in Caco-2 cells and HL-7702 cells subjected to Cd for 2 and 12 h. Initial cytotoxicity was observed for both cell lines at 2 $mg\,L^{-1}$ Cd. Cadmium dosage decreased cell viability by 84% and 44% in Caco-2 cells and by 75% and 38% in HL-7702 cells after 2 h while the percentage further decreased after 12 h in both Caco-2 cells (74% and 26%) and HL-7702 cells (60% and 24%) under different concentrations of Cd (2 $mg\,L^{-1}$ and 10 $mg\,L^{-1}$), as compared to their respective controls. These results indicated that Cd was able to induce cytotoxicity in a concentration- and time-dependent manner in the Caco-2 cells and HL-7702 cells. Similar findings were also reported by Nemmiche et al. [34] and Fotakis and Timbrell [15]. Cadmium toxicity primarily resulted from the binding of Cd to thiol groups in mitochondria, causing mitochondrial dysfunction and subsequent injury. Furthermore, Cd may enter mitochondria through Ca uniporter and interact with thiol groups

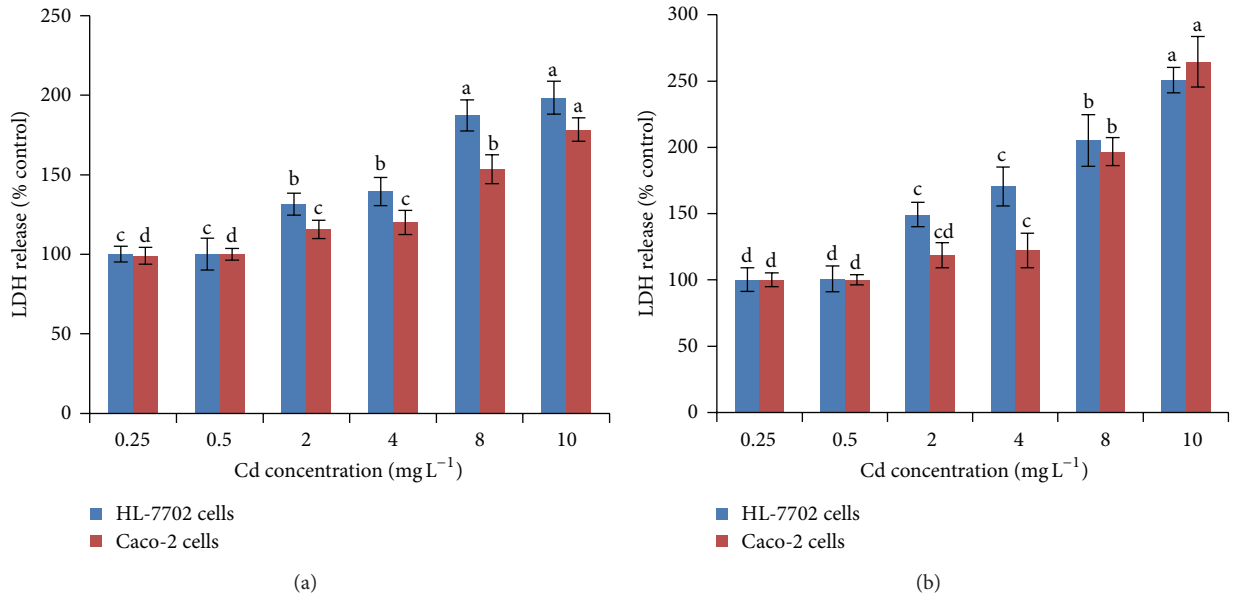

Figure 2: Effect of Cd on LDH release in Caco-2 and HL-7702 cells. Multiple range tests were conducted for Caco-2 and HL-7702 cells at different Cd levels after 2 h (a) and 12 h (b). Different letters indicate significant differences at $P < 0.05$ by the least significant difference (LSD) test. Values are presented as mean ± S.D.; $n = 3$.

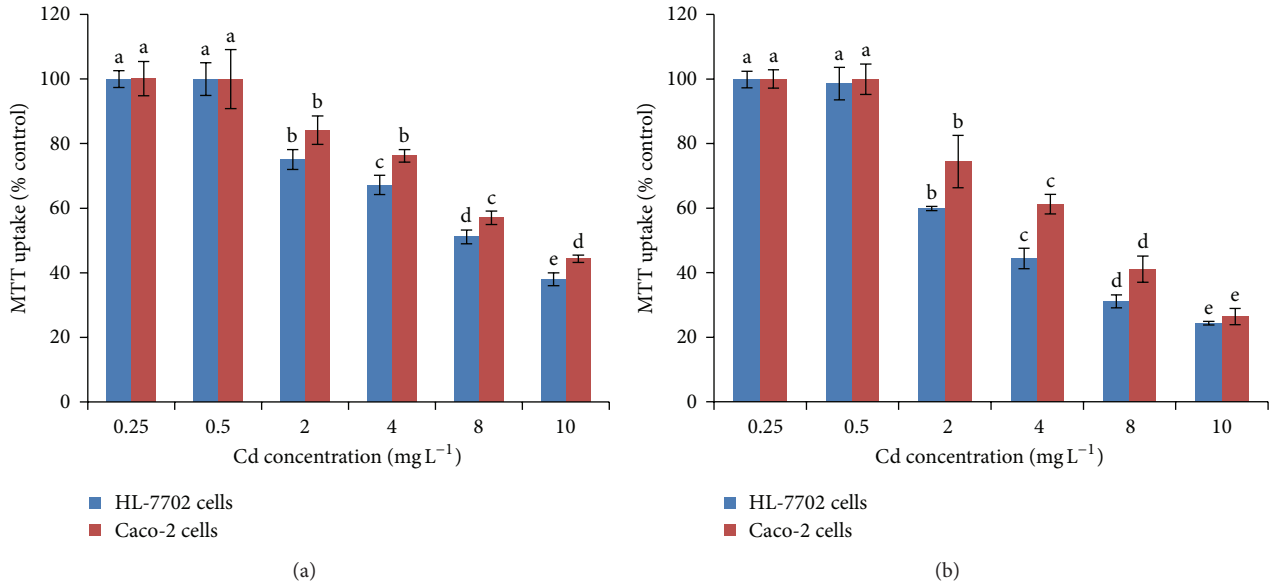

Figure 3: Effect of Cd on MTT assay in Caco-2 and HL-7702 cells. Multiple range tests were conducted for Caco-2 and HL-7702 cells at different Cd levels after 2 h (a) and 12 h (b). Different letters indicate significant differences at $P < 0.05$ by the least significant difference (LSD) test. Values are presented as mean ± S.D.; $n = 3$.

of adenine nucleotide translocator (ANT) to induce the Cytochrome c release and apoptosis. Xie et al. [23] also reported that Cd-induced apoptosis was dependent on Cd dose and exposure time in both normal (HL-7702) and tumor cells (Raji cells). Furthermore they [23] observed that Cd-induced Ca elevation was attenuated in HL-7702 cells coincubated with a Ca chelator. Therefore, Cd-induced apoptosis was mediated by the release of Ca from intracellular Ca storage but not an influx of extracellular Ca.

3.3. Effect of Cd on Antioxidant Enzymes Activity. Cadmium promotes an early oxidative stress and thus contributes to the development of serious pathological conditions because of its long retention in some tissues [35]. Physiologically, SOD is an important defense enzyme, which converts O_2 to H_2O_2 and thus protects against superoxide-induced damage [36]. GSH-Px, in particular, is highly dependent on glutathione concentration. The antioxidant enzymes (SOD, GPx) activities in Caco-2 cells and HL-7702 cells exposed to different

Table 1: Activities of antioxidants enzymes (SOD, GPX) and differentiation marker enzyme (AKP) in Caco-2 cells and HL-7702 cells at different Cd levels (after 2 hr exposure).

Parameters	Cell lines	Cd concentration (mg L^{-1})						
		0	0.25	0.5	2	4	8	10
GPx (U mg^{-1} cell protein)	Caco-2 cells	198.7 ± 0.7^{a}	190.9 ± 2.6^{b}	183.9 ± 3.2^{c}	133.7 ± 0.8^{d}	70.1 ± 1.1^{e}	48.09 ± 0.9^{f}	30.3 ± 0.7^{g}
	HL-7702 cells	306.9 ± 2.3^{a}	300.2 ± 8.7^{ab}	295.6 ± 5.3^{b}	207.2 ± 1.1^{c}	144.9 ± 0.8^{d}	100.3 ± 0.6^{e}	60.4 ± 0.6^{f}
SOD (U mg^{-1} cell protein)	Caco-2 cells	26.2 ± 1.8^{a}	25.1 ± 3^{a}	22.91 ± 2.4^{ab}	21.8 ± 0.5^{bc}	21.7 ± 0.9^{bc}	19.0 ± 2^{cd}	15.9 ± 0.3^{d}
	HL-7702 cells	26.0 ± 1.8^{a}	24.5 ± 0.6^{a}	24.0 ± 0.2^{a}	21.4 ± 1.0^{b}	20.03 ± 2.0^{b}	15.2 ± 0.5^{c}	11.1 ± 1.1^{d}
AKP (%Ck)	Caco-2 cells	100 ± 0.1^{a}	97.6 ± 3.3^{b}	95.3 ± 3.6^{b}	83.1 ± 0.7^{c}	79.41 ± 0.7^{d}	75.0 ± 1.0^{e}	66.1 ± 0.6^{f}
	HL-7702 cells	100 ± 0.4^{a}	95.5 ± 5.1^{b}	90.7 ± 3.7^{c}	65.32 ± 0.9^{d}	45.97 ± 1.0^{e}	28.31 ± 1.3^{f}	27.01 ± 1.0^{f}

Multiple comparison tests were for Caco-2 cells and HL-7702 cells at different Cd levels and different letters indicate significant differences at $P < 0.05$ as calculated by the least significant difference (LSD) test. Values are presented as mean ± S.D.; $n = 3$.

concentrations of Cd for 2 h are shown in Table 1. Significant changes in antioxidant enzymes activity were observed in both cell lines with the increase in Cd level, as compared with controls. Cd had no significant influence ($P > 0.05$) on SOD activity in both cell lines when the concentration was below 0.5 mg L^{-1}. However, the SOD activity was significantly decreased ($P < 0.05$) when the concentration of Cd was more than 0.5 mg L^{-1}. SOD activity of Caco-2 cells and the HL-7702 cells was decreased by 61.1% and 42.7%, respectively at 10 mg L^{-1} Cd level, as compared to their respective controls. The results of GPx activity showed a similar trend to SOD activity. The results showed that GPx activity in Cd-treated Caco-2 cells and HL-7702 cells ranged from 96% to 15.3% and 97.8% to 19.7%, respectively at 0.25 mg L^{-1} and 10 mg L^{-1} from control. Our results showed that antioxidant enzyme activities influenced by Cd in both cell lines differed significantly from their controls. In response to Cd stress, the activities of SOD and GPx in HL-7702 cells were considerably higher than those of Caco-2 cells.

According to our findings, the major toxic effects of increasing doses of Cd concentration involve decreased antioxidant enzyme levels. We presume that Cd also enters the mitochondria and inhibits the activities of many enzymes by binding to their −SH groups or by inhibiting the protein synthesis [37]. Cadmium binding to cysteine in reduced glutathione (GSH) results in the inactivation of GSH-Px, which, therefore, fails to convert H_2O_2 to water [38, 39]. Moreover, there is an increasing evidence that Cd interacts with Se and disrupts GSH-Px activity. This probably is the consequence of the intracellular accumulation of ROS with subsequent development of tissue injury.

3.4. Effect of Cd on Differentiation Marker Enzyme (AKP). Cadmium exposure had a significant ($P < 0.05$) effect on AKP activity in Caco-2 cells and HL-7702 cells (Table 1). AKP activity was highest in Caco-2 cells (97.6%) and HL-7702 cells (95.5%) when treated with 0.25 mg L^{-1} Cd, while at 10 mg L^{-1} its activity was decreased by 66.1% and 27.01%, respectively.

Our results showed that differentiation marker enzyme (AKP) was significantly decreased in both cell lines after 2 h Cd exposure. The inhibition of alkaline phosphatase activity has been already reported by others [40–42]. Also, El-Demerdash et al. [43] revealed that Cd *in vitro* caused significant inhibition of AKP activity in human plasma. The decrease in AKP activity may be due to changes in the permeability of plasma membrane in addition to changes in the balance between synthesis and degradation of enzyme [40]. Also, Lakshmi et al. [44] reported that the inhibition of AKP may be due to the breakdown of the membrane transport system and an inhibitory effect on cell growth and proliferation.

4. Conclusions

This study concludes that Caco-2 and HL-7702 cell models are in good agreement with the *in vivo* experiment after oral ingestion of Cd: low rate being transferred from the lumen into the body, higher accumulation in the intestinal cells than the liver cells. These results demonstrated that Cd is able to induce oxidative damage and apoptosis in both cell lines when its concentration exceeds 0.5 mg L^{-1}. Finally, our findings suggest that HL-7702 cells are more sensitive to Cd exposure than Caco-2 cells at the same concentration and exposure duration.

Conflict of Interests

Authors declare that they have no conflict of interests.

Acknowledgments

This study was supported by the Ministry of Science and Technology of China (Grant no. 2012AA101405), Ministry of Environmental Protection of China (Grant no. 2011467057) and the Fundamental Research Funds for the Central Universities of China.

References

[1] M. K. Daud, S. Ali, M. T. Variath et al., "Differential physiological, ultra-morphological and metabolic responses of cotton cultivars under cadmium stress," *Chemosphere*, vol. 93, no. 10, pp. 2593–2602, 2013.

[2] G. C. Lalor, "Review of cadmium transfers from soil to humans and its health effects and Jamaican environment," *Science of the Total Environment*, vol. 400, no. 1–3, pp. 162–172, 2008.

[3] M. K. Daud, Y. Sun, M. Dawood et al., "Cadmium-induced functional and ultrastructural alterations in roots of two transgenic cotton cultivars," *Journal of Hazardous Materials*, vol. 161, no. 1, pp. 463–473, 2009.

[4] J. C. Merrill, J. J. P. Morton, and S. D. Soileau, "Metals: cadmium," in *Principles and Methods of Toxicology*, A. W. Hayes, Ed., pp. 665–667, Taylor and Francis, London, UK, 2001.

[5] M. K. Daud, M. T. Variath, S. Ali et al., "Cadmium-induced ultramorphological and physiological changes in leaves of two transgenic cotton cultivars and their wild relative," *Journal of Hazardous Materials*, vol. 168, no. 2-3, pp. 614–625, 2009.

[6] P. N. Williams, M. Lei, G. Sun et al., "Occurrence and partitioning of cadmium, arsenic and lead in mine impacted paddy rice: Hunan, China," *Environmental Science and Technology*, vol. 43, no. 3, pp. 637–642, 2009.

[7] M. U. Khan, R. N. Malik, and S. Muhammad, "Human health risk from heavy metal via food crops consumption with wastewater irrigation practices in Pakistan," *Chemosphere*, vol. 93, no. 10, pp. 2230–2238, 2013.

[8] O. Andersen, J. B. Nielsen, J. A. Sorensen, and L. Scherrebeck, "Experimental localization of intestinal uptake sites for metals (Cd, Hg, Zn, Se) *in vivo* in mice," *Environmental Health Perspectives*, vol. 102, no. 3, pp. 199–206, 1994.

[9] R. K. Zalups and S. Ahmad, "Molecular handling of cadmium in transporting epithelia," *Toxicology and Applied Pharmacology*, vol. 186, no. 3, pp. 163–188, 2003.

[10] B. Elsenhans, G. J. Strugala, and S. G. Schäfer, "Small-intestinal absorption of cadmium and the significance of mucosal metallothionein," *Human and Experimental Toxicology*, vol. 16, no. 8, pp. 429–434, 1997.

[11] R. Arriazu, J. M. Pozuelo, N. Henriques-Gil et al., "Immunohistochemical study of cell proliferation, Bcl-2, p53, and caspase-3 expression on preneoplastic changes induced by cadmium and zinc chloride in the ventral rat prostate," *Journal of Histochemistry and Cytochemistry*, vol. 54, no. 9, pp. 981–990, 2006.

[12] D. Huang, Y. Zhang, Y. Qi, C. Chen, and W. Ji, "Global DNA hypomethylation, rather than reactive oxygen species (ROS), a potential facilitator of cadmium-stimulated K562 cell proliferation," *Toxicology Letters*, vol. 179, no. 1, pp. 43–47, 2008.

[13] P. Yang, H. Chen, J. Tsai, and L. Lin, "Cadmium induces Ca^{2+}-dependent necrotic cell death through calpain-triggered mitochondrial depolarization and reactive oxygen species-mediated inhibition of nuclear factor-κB activity," *Chemical Research in Toxicology*, vol. 20, no. 3, pp. 406–415, 2007.

[14] C. Shih, W. Ko, J. Wu et al., "Mediating of caspase-independent apoptosis by cadmium through the mitochondria-ROS pathway in MRC-5 fibroblasts," *Journal of Cellular Biochemistry*, vol. 91, no. 2, pp. 384–397, 2004.

[15] G. Fotakis and J. A. Timbrell, "Role of trace elements in cadmium chloride uptake in hepatoma cell lines," *Toxicology Letters*, vol. 164, no. 2, pp. 97–103, 2006.

[16] M. V. Berridge and A. S. Tan, "Characterization of the cellular reduction of 3-(4,5-dimethylthiazol-2- yl)-2,5-diphenyltetrazolium bromide (MTT): subcellular localization, substrate dependence, and involvement of mitochondrial electron transport in MTT reduction," *Archives of Biochemistry and Biophysics*, vol. 303, no. 2, pp. 474–482, 1993.

[17] M. R. Ruocco, F. Cecere, A. Iuliano et al., "Diclofenac-induced apoptosis in the neuroblastoma cell line SH-SY5Y: possible involvement of the mitochondrial superoxide dismutase," *Journal of Biomedicine and Biotechnology*, vol. 2010, Article ID 801726, 11 pages, 2010.

[18] S. S. Baker and R. D. Baker, "Antioxidant enzymes in the differentiated Caco-2 cell line," *In Vitro Cellular and Developmental Biology*, vol. 28, no. 9-10, pp. 643–647, 1992.

[19] S. Chater, T. Douki, A. Favier, M. Sakly, and H. Abdelmelek, "Changes in antioxidant status and biochemical parameters after orally cadmium administration in females rats," *Acta Biologica Hungarica*, vol. 60, no. 1, pp. 79–88, 2009.

[20] Y. Nzengue, R. Steiman, C. Garrel, E. Lefèbvre, and P. Guiraud, "Oxidative stress and DNA damage induced by cadmium in the human keratinocyte HaCaT cell line: role of glutathione in the resistance to cadmium," *Toxicology*, vol. 243, no. 1-2, pp. 193–206, 2008.

[21] Y. Wang, J. Fang, S. S. Leonard, and K. M. K. Rao, "Cadmium inhibits the electron transfer chain and induces reactive oxygen species," *Free Radical Biology and Medicine*, vol. 36, no. 11, pp. 1434–1443, 2004.

[22] V. Meunier, M. Bourrie, Y. Berger, and G. Fabre, "The human intestinal epithelial cell line Caco-2; pharmacological and pharmacokinetic applications," *Cell Biology and Toxicology*, vol. 11, no. 3-4, pp. 187–194, 1995.

[23] Z. Xie, Y. Zhang, A. Li, P. Li, W. Ji, and D. Huang, "Cd-induced apoptosis was mediated by the release of Ca^{2+} from intracellular Ca storage," *Toxicology Letters*, vol. 192, no. 2, pp. 115–118, 2010.

[24] C. Jumarie, P. G. C. Campbell, A. Berteloot, M. Houde, and F. Denizeau, "Caco-2 cell line used as an in vitro model to study cadmium accumulation in intestinal epithelial cells," *Journal of Membrane Biology*, vol. 158, no. 1, pp. 31–48, 1997.

[25] M. M. Bradford, "A rapid and sensitive method for the quantitation of microgram quantities of protein utilizing the principle of protein dye binding," *Analytical Biochemistry*, vol. 72, no. 1-2, pp. 248–254, 1976.

[26] B. Zödl, M. Zeiner, M. Sargazi et al., "Toxic and biochemical effects of zinc in Caco-2 cells," *Journal of Inorganic Biochemistry*, vol. 97, no. 4, pp. 324–330, 2003.

[27] D. M. Templeton, "Biomedical aspects of trace element speciation," *Fresenius' Journal of Analytical Chemistry*, vol. 363, no. 5-6, pp. 505–511, 1999.

[28] Y. Ui-Jeong, Y. So-Ra, C. Jae-Hwan et al., "Water spinach (Ipomoea aquatic Forsk.) reduced the absorption of heavy metals in an in vitro bio-mimicking model system," *Food and Chemical Toxicology*, vol. 50, pp. 3862–3866, 2012.

[29] D. A. Vesey, "Transport pathways for cadmium in the intestine and kidney proximal tubule: focus on the interaction with essential metals," *Toxicology Letters*, vol. 198, no. 1, pp. 13–19, 2010.

[30] E. C. Foulkes, "Transport of toxic heavy metals across cell membranes," *Proceedings of the Society for Experimental Biology and Medicine*, vol. 223, no. 3, pp. 234–240, 2000.

[31] N. J. DelRaso, B. D. Foy, J. M. Gearhart, and J. M. Frazier, "Cadmium uptake kinetics in rat hepatocytes: correction for albumin binding," *Toxicological Sciences*, vol. 72, no. 1, pp. 19–30, 2003.

[32] E. A. Belyaeva, V. V. Glazunov, and S. M. Korotkov, "Cyclosporin A-sensitive permeability transition pore is involved in Cd^{2+}-induced dysfunction of isolated rat liver mitochondria: doubts no more," *Archives of Biochemistry and Biophysics*, vol. 405, no. 2, pp. 252–264, 2002.

[33] J. Pourahmad and P. J. O'Brien, "A comparison of hepatocyte cytotoxic mechanisms for Cu^{2+} and Cd^{2+}," *Toxicology*, vol. 143, no. 3, pp. 263–273, 2000.

[34] S. Nemmiche, D. Chabane-Sari, M. Kadri, and P. Guiraud, "Cadmium chloride-induced oxidative stress and DNA damage in the human Jurkat T cell line is not linked to intracellular trace elements depletion," *Toxicology in Vitro*, vol. 25, no. 1, pp. 191–198, 2011.

[35] D. Bagchi, M. Bagchi, S. J. Stohs et al., "Free radicals and grape seed proanthocyanidin extract: importance in human health and disease prevention," *Toxicology*, vol. 148, no. 2-3, pp. 187–197, 2000.

[36] J. M. Matés, "Effects of antioxidant enzymes in the molecular control of reactive oxygen species toxicology," *Toxicology*, vol. 153, no. 1–3, pp. 83–104, 2000.

[37] M. Waisberg, P. Joseph, B. Hale, and D. Beyersmann, "Molecular and cellular mechanisms of cadmium carcinogenesis," *Toxicology*, vol. 192, no. 2-3, pp. 95–117, 2003.

[38] U. R. Acharya, M. Mishra, J. Patro, and M. K. Pan, "Effect of vitamins C and E on spermatogenesis in mice exposed to cadmium," *Reproductive Toxicology*, vol. 25, no. 1, pp. 84–88, 2008.

[39] F. M. Maiorino, R. Brigelius-Flohé, K. D. Aumann, A. Roveri, D. Schomburg, and L. Flohé, "Diversity of glutathione peroxidases," *Methods in Enzymology*, vol. 252, pp. 38–53, 1995.

[40] S. V. Rana, S. Rekha, and V. Seema, "Protective effects of few antioxidants on liver function in rats treated with cadmium and mercury," *Indian Journal of Experimental Biology*, vol. 34, no. 2, pp. 177–179, 1996.

[41] F. M. El-Demerdash, M. I. Yousef, F. S. Kedwany, and H. H. Baghdadi, "Cadmium-induced changes in lipid peroxidation, blood hematology, biochemical parameters and semen quality of male rats: protective role of vitamin E and β-carotene," *Food and Chemical Toxicology*, vol. 42, no. 10, pp. 1563–1571, 2004.

[42] F. M. El-Demerdash and E. I. Elagamy, "Biological effects in Tilapia nilotica fish as indicators of pollution by cadmium and mercury," *International Journal of Environmental Health Research*, vol. 9, no. 3, pp. 143–156, 1999.

[43] F. M. El-Demerdash, M. I. Yousef, and E. I. Elagamy, "Influence of paraquat, glyphosate, and cadmium on the activity of some serum enzymes and protein electrophoretic behavior (in vitro)," *Journal of Environmental Science and Health B*, vol. 36, no. 1, pp. 29–42, 2001.

[44] R. Lakshmi, R. Kundu, E. Thomas, and A. P. Mansuri, "Mercuric chloride induced inhibition of acid and alkaline phosphatase activity in the kidney of Mudskipper, Boleophthalmus dentatus," *Acta Hydrochimica et Hydrobiologica*, vol. 3, pp. 341–344, 1991.

Hindawi Publishing Corporation
BioMed Research International
Volume 2014, Article ID 831989, 8 pages
http://dx.doi.org/10.1155/2014/831989

Research Article

Chemodynamics of Methyl Parathion and Ethyl Parathion: Adsorption Models for Sustainable Agriculture

Noshabah Tabassum,[1] Uzaira Rafique,[1] Khaled S. Balkhair,[2] and Muhammad Aqeel Ashraf[3]

[1] *Department of Environmental Sciences, Fatima Jinnah Women University, The Mall, Rawalpindi 46000, Pakistan*
[2] *Department of Hydrology and Water Resources Management, King Abdulaziz University, Jeddah 22254, Saudi Arabia*
[3] *Department of Geology, Centre for Research in Biotechnology for Agriculture, University of Malaya, 50603 Kuala Lumpur, Malaysia*

Correspondence should be addressed to Muhammad Aqeel Ashraf; aqeelashraf@um.edu.my

Received 21 July 2013; Revised 4 December 2013; Accepted 24 December 2013; Published 6 February 2014

Academic Editor: Chong-Jian Tang

The toxicity of organophosphate insecticides for nontarget organism has been the subject of extensive research for sustainable agriculture. Pakistan has banned the use of methyl/ethyl parathions, but they are still illegally used. The present study is an attempt to estimate the residual concentration and to suggest remedial solution of adsorption by different types of soils collected and characterized for physicochemical parameters. Sorption of pesticides in soil or other porous media is an important process regulating pesticide transport and degradation. The percentage removal of methyl parathion and ethyl parathion was determined through UV-Visible spectrophotometer at 276 nm and 277 nm, respectively. The results indicate that agricultural soil as compared to barren soil is more efficient adsorbent for both insecticides, at optimum batch condition of pH 7. The equilibrium between adsorbate and adsorbent was attained in 12 hours. Methyl parathion is removed more efficiently (by seven orders of magnitude) than ethyl parathion. It may be attributed to more available binding sites and less steric hindrance of methyl parathion. Adsorption kinetics indicates that a good correlation exists between distribution coefficient (Kd) and soil organic carbon. A general increase in Kd is noted with increase in induced concentration due to the formation of bound or aged residue.

1. Introduction

Sustainable agriculture demands high and good quality food production. Increase in agricultural base has become a challenge for the growers and farmers. This compels extensive use of insecticides that lead to growing accumulation of pollutants in environment over the last decade. The environment and human health are adversely affected by irrational and high pesticides use [1]. The toxicological and ecotoxicological effect is manifested as pesticides remain chemically active and rapidly broke down into other chemicals [2]. Pesticides when applied on crops get transported to various environmental compartments [3] like soil, plant, and water, while only a small part of the chemical stays in the area where it is applied.

Organophosphates have been detected in air, snow, fog, rainwater [4, 5], and in the pine needles in the mountains [6], miles away from the agricultural spraying area. Toxicity of organophosphates for nontarget organisms has also been the subject of extensive research [7]. Organophosphates are extensively used in China, Colombia, and Pakistan. Use of chemicals to control pests is increasing at the rate of 25% a year [8] in Pakistan.

Organophosphates are esters of phosphoric acid and exist in two forms, Thion and Oxon [9]. Parathions (methyl and ethyl) are a group of highly toxic compounds used extensively in agricultural crops especially cotton, soybean, corn, wheat, alfalfa, vegetables, fruit trees, and domestic activities [10] leading to different hazards.

Methyl parathion, $C_8H_{10}NO_5PS$ [11], also known as metaphos, is a broad-spectrum agricultural insecticide and acaricide that is released to the environment primarily through spraying using aircraft or ground spray equipment [12]. Methyl parathion is rapidly removed from the atmosphere [13] by wet and dry deposition and forms bound

residues restricting its movement in soils [14–16], where its adsorption is influenced by organic matter and CEC of the soil [17]. However, its mobility and leaching into the soil-water system is affected by pH. Methyl parathion when introduced into the environment is degraded by hydrolysis, photolysis, or microorganisms, whereas degradation appears to be significantly retarded [18, 19] when its concentration is high, as in bulk disposal and spills.

Ethyl parathion, $C_{10}H_{14}NO_5PS$, also known as thiophos, has little or no potential for groundwater contamination [11]. The major metabolites of ethyl parathion are amino parathion and 4-nitrophenol. However, in soils that have received multiple applications, 4-nitrophenol is the only metabolite and rate of degradation is faster. Soil act as a buffer and offer degradation potential for the stored pollutants with the help of soil organic carbon [20]. Pesticides also bind to soil particles thus reducing chemical availability and transportation to different environmental compartments. Chemodynamics of pesticides is generally considered to be effectively controlled through adsorption process by offering high adsorption capacity, extra ordinary surface area, and microporous structure of adsorbents.

To remediate the adverse effects and chemical accumulation of active metabolites of applied insecticides in soil fields, different control methods are in use. Solid-phase adsorption is one of the most efficient technologies for the treatment of pesticide [21].

The adsorption of organophosphorus pesticides onto activated carbon has attracted many researchers due to its high removal efficiency [22, 23], but high cost inhibits its application on a large scale [24].

To overcome these and other limitations associated with commercial adsorbent materials, the researchers continue their work to find out more economical and easily available materials [25] to be used as potential adsorbents.

Knowing the fact that sorption of organic chemicals to soil is a process that can affect mobility, degradation, and toxicity by reducing availability, the present investigation is designed with the following objectives:

(i) explore the use of most abundantly available soil as natural adsorbent for the removal of organophosphate pesticides;

(ii) quantify the fate and transport process of organophosphates for understanding their behavior in the environment;

(iii) determine the factors affecting binding of pesticide with soil through batch adsorption experiment.

Pakistan is a developing country with agro-based economy. Its life line and development rest on sustainable agricultural practices. Improving soil conditions of agricultural fields can ensure best growing conditions and can also offset the adverse effects of applied pesticides; for example, organic matter in soil has multiple functions. It revolves nutrient storage, improves soil structure, maintains tilt, minimizes erosion, and binds the unwanted chemical to be removed thereafter.

Table 1: Physiochemical analysis of soil fields.

Sample fields	Wheat field (WF I)	Wheat field (WF II)	Wheat field (WF III)	Barren field (BF I)	Barren field (BF II)
pH	7.42	7.61	7.57	8.75	8.78
Electrical conductivity μS at 25°C	73.2	54.4	54.8	37.4	36.1
Bulk density g/cm^3	1.33	1.36	1.37	1.5	1.6
Organic content (%)	4.2	4.4	4.5	3.1	3.2
Moisture content (%)	3.7	2.33	3.5	5.5	5.1

The present study will facilitate the prediction of the exposure level of humans and nontarget organisms to organophosphate pesticides and its active ingredients. The development of low cost soil adsorbent will suggest a pest control product for environmental remediation and sustainable agriculture.

2. Materials and Methods

Two different sampling areas of Jhelum, that is, agricultural (wheat) and barren (suburbs of wheat), were selected for sampling with the objective to represent varying organic matter. Topsoil (4-5 inches) 90 samples from agricultural and 60 of barren area were collected in X and zigzag pattern, respectively. Composite sieved (2 mm) soil sample of each type was prepared by mixing the subsoil samples in agate mortar and pestle. pH and temperature were noted on site.

Each soil sample was analyzed for physicochemical parameters of pH, bulk density, electrical conductivity, and organic matter content following standard methods. The pH and EC of all solutions were recorded by pH (inoLab pH 720) and conductivity meter (con-500, Cyberscan), respectively. Color of samples was observed using Munsell color chart. Results of physicochemical parameters are summarized in Table 1.

The physicochemical characteristics of oil samples reveal that agricultural fields have relatively lower pH than barren. It may be related to the higher organic content due to more fulvic and humic acid. The range is generally alkaline for both classes of soil. Pakistani soil is mostly alkaline in nature ranging from 7.5 to 8.5 [26].

The low value of bulk density is indicative of higher organic matter content and large pore size [27]. Soil with higher content of organic matter is more porous and has relatively low bulk density [28].

EC of the soil sample decreases with decrease in % age organic matter (see Table 1). It may be attributed to the fact that ionic concentration is greater in alkaline soils [29] and the higher the ionic species, the higher the conductivity [30].

2.1. Batch Adsorption. Nine series of batch experiments for each pesticide were conducted as a function of time to determine the percentage concentration of the pesticide

removed by adsorption on each soil. The following general procedure for a batch experiment was adopted.

Aqueous solution of known concentration of the pesticide was induced to fixed mass (5 g) of soil adsorbent, adjusted at known pH at room temperature. Solution pH was adjusted to the desired value (pH 4, 7 and 10) by adding sodium acetate and acetic acid (pH 4), 0.1 M NH_3, and NH_4OH for pH 7 to 10 solutions [31].

The mixture was allowed to shake on Isothermal shaker (Lab-Companion SK-300). After regular contact time interval (one hour), pesticide was extracted using equimolar solvent mixture of acetone and n-hexane. The extracted aliquot was run on UV-Visible spectrophotometer (UV1601, Shimadzu) to determine the absorbance of the solution against blank. The concentration was calculated from standard calibration curve. The process continued till equilibrium was attained between adsorbate and adsorbent.

The same procedure was repeated for varying adjusted pH (4, 7 and 10) and variable induced concentration in μg/L (10, 30 and 50) for each selected pesticide.

The percentage removal of methyl parathion and ethyl parathion by different soils at equilibrium is calculated using the following mass balance equation:

$$q_e = \frac{C_i - C_e}{S}, \tag{1}$$

where q_e is amount (in μg/kg) of the pesticide removed, C_i is initial concentration of pesticide in solution (μg/L), and C_e is equilibrium concentration of pesticide in solution (μg/L).

The dose concentration S is expressed as $S = m/v$, where v is initial volume of pesticide solution used and m is mass of soil used.

K_d and K_{oc} were also calculated using the following equations:

$$K_d = \frac{\text{amount of pesticide in adsorbent}}{\text{amount of pesticide in solution}}, \tag{2}$$

(see [32]),

$$K_{oc} = \frac{K_d}{OC}, \tag{3}$$

(see [33]).

K_d is the distribution coefficient so $K_d = X/S$, where X is the amount of adsorbent and S is the amount of pesticide in solution. K_{oc} is the distribution coefficient of organic carbon and OC is the organic carbon.

2.2. Kinetic Studies. The adsorption kinetics was computed to optimize the appropriate correlation for equilibrium adsorption behavior. Rate was determined through application of first order, pseudo-first-order [34], pseudo-second-order [35], and intraparticle diffusion [36].

2.3. Adsorption Models. Adsorption models of Freundlich and Langmuir [37] are commonly used to describe the adsorption process. Equations are tabulated in Table 2.

3. Results and Discussion

3.1. Effect of pH. The effect of different pH (4, 7 and 10) on the adsorption of methyl parathion and ethyl parathion by different soil samples is studied. The results are graphically presented in Figures 1 and 2.

It is observed that pH has a momentous effect in adsorption capacity. In moving from pH 4 to 7, an increase in methyl parathion adsorption followed by a decrease at pH 10 is observed for agricultural and barren soil. The presence of hydronium ions on the adsorbent surface at lower pH may enhance the interaction of pesticide molecules with the binding sites of adsorbent material. It is further suggested that carbonaceous functional groups are dissociated at different pH values and consequently take part in the sorption process.

Same trend is noted for adsorption of ethyl parathion on both soil types in terms of variable pH (see Figure 2).

The present study behavior of organophosphates (parathion) is in contrast to Lindane and Carbofuran [38] reporting that adsorption increases with increase in pH of neutral molecules.

Decrease in percent adsorption with time is accompanied by a reduction in the adsorption capacity while extending to basic pH in both soil types. The reduction in adsorption capacity at higher pH is also reported by other authors [39]. It may also be attributed to the lesser adhesive forces between adsorbate and adsorbent than the cohesive forces of the adsorbate (due to alkaline soil and adjusted alkaline media).

The study concludes that pH 7 is optimum evident to both pesticides, showing maximum removal efficiency for methyl and ethyl parathions as 83% and 80% for agricultural soil, whereas 82% and 79% for barren soil.

It reflects preference of organic matter content in agricultural soil for adsorption; the higher is the organic content, the more is the adsorption. Soil high in organic matter and clay are more adsorptive than coarse sandy soil because a clay or organic soil has more particle surface area or more sites into which pesticide can bind [40]. The closeness in percent adsorption on two types of soil at pH 7 (neutral) is highly encouraging as sustainable agricultural approach suggests that little or no modification is required in soil characteristics for optimum removal of parathion.

3.2. Effect of Concentration. In order to study the effect of concentration on adsorption, batch experiment was administered at induced pesticide concentration of 10, 30, and 50 μg/L for each soil type. The results are presented in Figures 3 and 4.

It is noted that adsorption potential of agricultural soil for removal of methyl and ethyl parathions is found to be 72%, 78%, and 83% and 75%, 79%, and 80%, respectively, on increasing the concentration from 10 through 30 to 50 μg/L (see Figure 3).

As reported in the literature the maximum loading capacity of the adsorbent and the rate of adsorption were found to increase with increase in the pesticide initial concentration [24].

A different behavior is depicted by barren soil field samples for the removal of methyl parathion with change

Table 2: Adsorption models along with their parameters.

Isotherms	Linear expression	Plot	Parameters
Langmuir (1918)	$\frac{C_e}{q_e} = \frac{1}{q_m K_L} + \frac{C_e}{q_m}$	$\frac{C_e}{q_e}$ v C_e	$q_m = \frac{1}{\text{slope}}$ $K_L = \frac{\text{slope}}{\text{intercept}}$
Freundlich (1906)	$\log q_e = \log K_F + \frac{1}{n} \log C_e$	$\log q_e$ v $\log Ce$	$n = \frac{1}{\text{slope}}$ K_F = Antilog (intercept)
Pseudo-first-order	$\log (q_e - q_t) = \log q_e - \left(\frac{k_1}{2.303}\right) t$	$\log (q_e - q_t)$ v t	k_1 = slope q_e = Antilog (intercept)
Pseudo-second-order	$\frac{t}{q_t} = \frac{1}{k_2 q_e^2} + \left(\frac{1}{q_e}\right) t$	$\frac{t}{q_t}$ v t	q_e = slope h = intercept $k_2 = \frac{\text{intercept}}{(\text{slope})^2}$
Intraparticle diffusion	$q_t = k_{\text{ip}} t^{0.5} + C$	q_t v t	k_{ip} = slope C = intercept

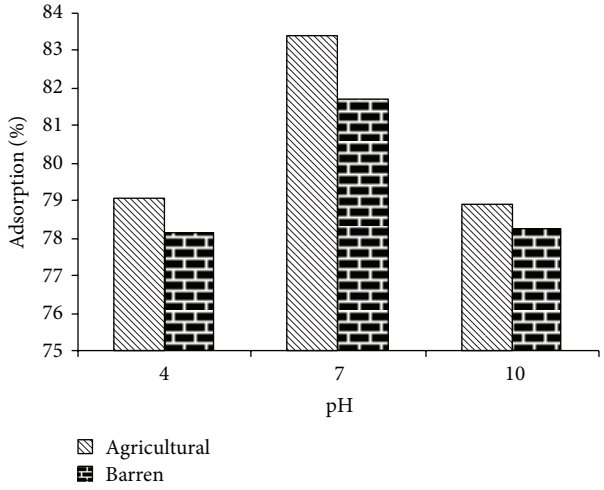

Figure 1: Effect of pH on %-adsorption of methyl parathion.

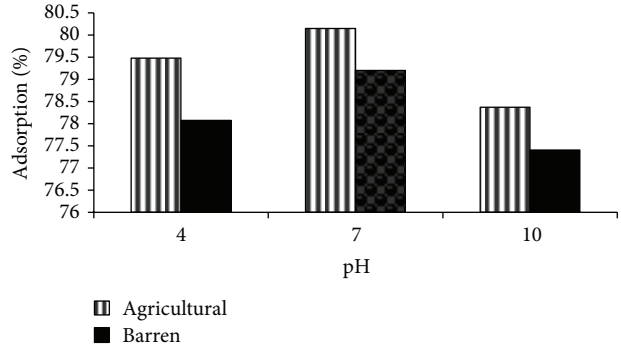

Figure 2: Effect of pH on %-adsorption of ethyl parathion.

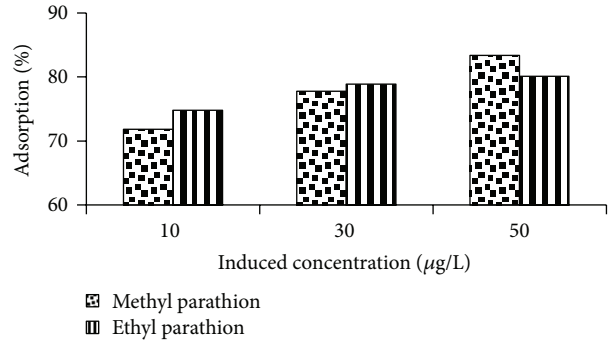

Figure 3: Effect of induced concentration on %-adsorption of methyl parathion.

in concentration. An initial decrease of 8 orders followed by 14 orders increase in adsorption is observed in moving from 10 μg/L to 50 μg/L (see Figure 4). This peculiar feature of methyl parathion adsorption is affected by the chemical properties of the pesticide [41].

The general lower adsorption behavior on barren soil is demonstrated by soil parameters like higher moisture content, significantly lower EC, and high density allowing less number of sites available.

On the other hand, barren soil behaves similarly to agricultural soil for the removal of ethyl parathion showing a gradual increase in adsorption with a regular increase in concentration. This is due to the fact that increased concentration provides necessary driving force to overcome the resistances to the mass transfer of pesticide between aqueous and solid phase. This behavior is comparable and supported by other studies [38].

The study concludes that optimum adsorption takes place at higher induced concentration (50 μg/L). However, the induced concentration on average impact slightly shows more

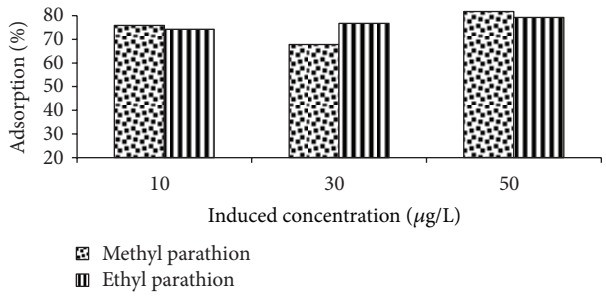

Figure 4: Effect of induced concentration on %-adsorption of ethyl parathion.

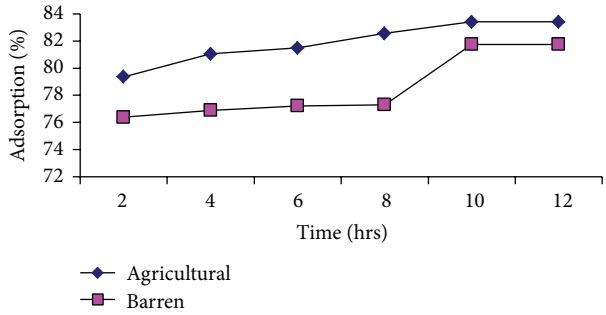

Figure 5: Effect of contact time on %-adsorption of methyl parathion.

adsorption for methyl parathion than ethyl parathion. It may be due to insignificant structural difference between two pesticides.

3.3. Effect of Contact Time. Batch experiment was conducted with regular intervals of time in order to determine the equilibrium between adsorbate and adsorbent.

It is generally observed that adsorption increases with increase in contact time for both pesticides. The removal was rapid in early stages and finally attained almost constant value for longer contact time (see Figures 5 and 6). Obviously, the initial high adsorption rate is due to the abundance of free binding sites [24].

It is interesting to note that the first adsorption equilibrium for both pesticides is attained in 10 hours time. This is also supported by other studies. However, the rate of adsorption follows a very slow increase for barren soil till equilibrium. Agricultural soil shows a rapid increase in adsorption for the first 6 hours followed by almost the same adsorption rate till equilibrium.

3.4. Adsorption Kinetics. The average values of the adsorption kinetic parameters for both pesticides on two soil types are tabulated in Table 3.

It can be seen that pseudo-second-order kinetic fits the adsorption data equally best for both soil types and both pesticides with correlation coefficient R^2 (0.999) at optimum operating conditions of pH and induced concentration.

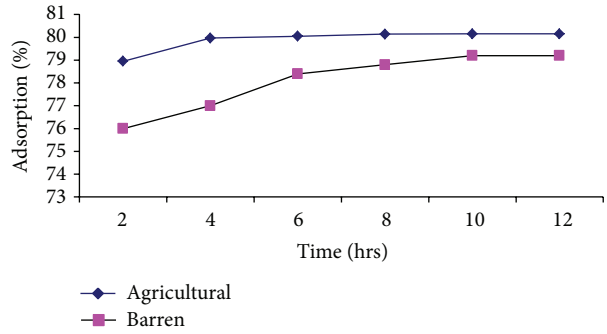

Figure 6: Effect of contact time on %-adsorption of ethyl parathion.

Intraparticle diffusion kinetics also provides a good description of sorption data. A set of correlation coefficients of 0.979, 0.918 and 0.976, 0.961 is comparable for methyl and ethyl parathions on agricultural and barren soils, respectively.

It can be seen from Table 3 that distribution of methyl parathion in agricultural soil samples is comparatively higher than ethyl parathion. This is also in conformity with higher adsorption of the former on agricultural soil.

The sequence of distribution constant as a function of pH follows pH 7 < pH 4 < pH 10 on agricultural and barren soil for both pesticides. On further investigation, a direct relation of K_d and K_{oc} is found verifying the trend that agricultural soils are relatively proven to be better adsorbent and work optimally at pH 7. Direct relation of K_d and K_{oc} depicting higher values for agricultural than barren soil is reported by other researchers [42] (see Table 4).

3.5. Adsorption Isotherms. Both Freundlich and Langmuir isotherms are best fit for experimental data. The magnitude of K_f (see Table 5) shows relatively good adsorption capacity. Dada et al. reported K_f value of 7.61 mg/g for adsorption of Zn onto modified rice husk [43]. Good fit of Freundlich isotherm describes that the adsorbent surface is heterogeneous in nature [44].

On the other hand, Langmuir also holds best sorption data with average R^2 (0.998). Langmuir model suggests formation of a monolayer adsorbate on the outer surface of the adsorbent and equilibrium distribution between the solid and liquid phases [45].

4. Conclusions

The present study concludes with the following:

(i) the batch adsorption experiment provides an efficient, convenient, and simple method for the removal of selected pesticides attaining equilibrium in 10 hours;

(ii) the parameters of paramount significance are found to be organic matter content, pH and induced concentration, optimum being higher organic matter, pH 7, and higher (50 μg/L) induced concentration for the removal of both pesticides;

Table 3: Kinetic models for methyl parathion and ethyl parathion.

Soil type	Kinetic models	Parameters	Methyl parathion	Ethyl parathion
Agricultural	Pseudo-first-order	K_1	−0.0011	−0.0011
		q_e	2.896	2.8903
		R^2	0.402	0.393
Barren	Pseudo-first-order	K_1	−0.0011	−0.0011
		q_e	2.8813	2.880
		R^2	0.3634	0.4023
Agricultural	Pseudo-second-order	K_2	0.1387	0.1295
		q_e	0.0014	0.0011
		R^2	0.999	0.999
Barren	Pseudo-second-order	K_2	0.0181	0.0255
		q_e	0.1059	0.0011
		R^2	0.5486	0.999
Agricultural	Intraparticle diffusion	A	0.0098	0.0105
		$\log K_{id}$	1.8802	1.8925
		R^2	0.979	0.918
Barren	Intraparticle diffusion	A	0.0064	0.0167
		$\log K_{id}$	1.8716	1.8763
		R^2	0.976	0.961

q_e is in μg/L.

Table 4: K_d and K_{oc} values of agricultural and barren soil samples.

	K_d			K_{oc}		
	pH 4	pH 7	pH 10	pH 4	pH 7	pH 10
Methyl parathion						
Agricultural	48.966	63.33	42.500	3726.71	3804.80	3079.71
Barren	44.516	51.429	42.500	3548.23	3632.48	3413.11
Ethyl parathion						
Agricultural	63.333	66.957	53.585	589.37	851.92	259.78
Barren	3.375	3.474	3.310	288.50	296.94	282.91

Table 5: Adsorption isotherm for methyl parathion and ethyl parathion.

Adsorption isotherm	Soil types	Parameters	Methyl parathion	Ethyl parathion
Freundlich	Agricultural	n	−1.606	−1.597
		K_f	3.25	3.257
		R^2	0.999	0.999
	Barren	n	−1.602	−1.65
		K_f	3.325	3.332
		R^2	0.999	0.999
Langmuir	Agricultural	b	−3.325	−3.271
		Q_o	0.335	0.322
		R^2	0.999	0.998
	Barren	b	−3.161	−3.512
		Q_o	0.282	0.332
		R^2	0.998	0.995

(iii) methyl parathion is found to be more effectively removed than ethyl parathion due to lower molecular weight and less steric hindrance;

(iv) pseudo-second-order, intraparticle diffusion, Langmuir and Freundlich models explain the experimental data to the best fit.

The authors propose that adsorption attains equilibrium between adsorbate and adsorbent upon contact of 10 hours. The goodness of Langmuir suggests monolayer adsorption and nature of adsorbent (soil) is determined to be heterogeneous. It also reveals that pores are not uniformly distributed. kinetics reveals that pseudo-second-order is in good agreement for agricultural soil samples suggesting its dependence on concentration of organic content. On the other hand, intraparticle diffusion is found to be equally appropriate for both soils suggesting that diffusion is not characteristics of physical characteristics of soil and pore size is the same in both soil samples.

Conflict of Interests

The authors certify that there is no conflict of interests with any financial organization regarding the material discussed in the paper.

Acknowledgments

The research was financially supported by the University of Malaya Grant nos. BKP (BK006-2013), UMRG (RG257-13AFR), and FRGS (FP038-2013B).

References

[1] C. Wilson and C. Tisdell, "Why farmers continue to use pesticides despite environmental, health and sustainability costs," *Ecological Economics*, vol. 39, no. 3, pp. 449–462, 2001.

[2] C. P. Cai, M. Liang, and R. R. Wen, "Rapid multiresidue screening method for organophosphate pesticides in vegetables," *Chromatographia*, vol. 40, no. 7-8, pp. 417–420, 1995.

[3] FAO/WHO, "Joint FAO/WHO meeting on pesticide residues," WHO/PCS/96.48, World Health Organization, Geneva, Switzerland, 1996.

[4] J. R. Plimmer, "Dissipation of pesticides in the environment," in *Fate of Pesticides and Chemicals in the Environment*, J. L. Schnoor, Ed., pp. 79–90, Wiley-Interscience, New York, NY, USA, 1992.

[5] J. M. Zabik and J. N. Seiber, "Atmospheric transport of organophosphate pesticides from California's Central Valley to the Sierra Nevada mountains," *Journal of Environmental Quality*, vol. 22, no. 1, pp. 80–90, 1993.

[6] L. S. Aston and J. N. Seiber, "Exchange of airborne organophosphorus pesticides with pine needles," *Journal of Environmental Science and Health B*, vol. 31, no. 4, pp. 671–698, 1996.

[7] C. Bauer and J. Römbke, "Factors influencing the toxicity of two pesticides on three Lumbricid species in laboratory tests," *Soil Biology and Biochemistry*, vol. 29, no. 3-4, pp. 705–708, 1997.

[8] M. I. Tariq, S. Afzal, and I. Hussain, "Pesticides in shallow groundwater of Bahawalnagar, Muzafargarh, D.G. Khan and Rajan Pur districts of Punjab, Pakistan," *Environment International*, vol. 30, no. 4, pp. 471–479, 2004.

[9] J. LaDou, "The asbestos cancer epidemic," *Environmental Health Perspectives*, vol. 112, no. 3, pp. 285–290, 2004.

[10] L. G. Costa, "Organophosphorus compounds," in *Recent Advances in Nervous System Toxicology*, C. L. Galli, L. Manzo, and P. S. Spencer, Eds., vol. 100 of *NATO ASI Series*, pp. 203–246, Plenum Press, New York, NY, USA, 1988.

[11] NPIRS, *National Pesticide Information Retrieval System (Database). Chemical Fact Sheet for: Methyl Parathion*, U.S. Environmental Protection Agency, Office of Pesticide Programs, Washington, DC, USA, 1986, IARC 1983; NPIRS 1986; Spencer 1982.

[12] T. A. Albanis, P. J. Pomonis, and A. T. Sdoukos, "Movement of methyl parathion, lindane and atrazine through lysimeters in field conditions," *Toxicological & Environmental Chemistry* , vol. 17, no. 1, pp. 35–45, 1988.

[13] M. D. Jackson and R. G. Lewis, "Volatilization of two methyl parathion formulations from treated fields," *Bulletin of Environmental Contamination and Toxicology* , vol. 20, no. 1, pp. 793–796, 1978.

[14] W. A. Jury, A. M. Winer, W. F. Spencer, and D. D. Focht, "Transport and transformation of organic chemicals in the soil-air-water ecosystems," *Reviews of Environmental Contamination and Toxicology*, vol. 99, pp. 119–164, 1987.

[15] J. E. McLean, R. C. Sims, and W. J. Doucette, "Evaluation of mobility of pesticides in soil using U.S. EPA Methodology," *Journal of Environmental Engineering* , vol. 114, no. 3, pp. 689–703, 1988.

[16] K. S. Reddy and R. P. Gambrell, "Factors affecting the adsorption of 2,4-D and methyl parathion in soils and sediments," *Agriculture, Ecosystems & Environment*, vol. 18, no. 3, pp. 231–241, 1987.

[17] L. C. Butler, D. C. Staiff, and J. E. Davis, "Methyl parathion persistence in soil following simulated spillage," *Archives of Environmental Contamination and Toxicology*, vol. 10, no. 4, pp. 451–458, 1981.

[18] EPA, "Health and environmental effects profile for methyl parathion," NTIS PB88-180534, U.S. Environmental Protection Agency, Environmental Criteria and Assessment Office, Cincinnati, Ohio, USA, 1984.

[19] M. Nousiainen, K. Peräkorpi, and M. Sillanpää, "Determination of gas-phase produced ethyl parathion and toluene 2,4-diisocyanate by ion mobility spectrometry, gas chromatography and liquid chromatography," *Talanta*, vol. 72, no. 3, pp. 984–990, 2007.

[20] P. Burauel and F. Baßmann, "Soils as filter and buffer for pesticides—experimental concepts to understand soil functions," *Environmental Pollution*, vol. 133, no. 1, pp. 11–16, 2005.

[21] I. Ali and V. K. Gupta, "Adsorbents for water treatment: development of low-cost alternatives to carbon," in *Encyclopedia of Surface and Colloid Science*, pp. 149–184, Taylor & Francis, New York, NY, USA, 2nd edition, 2006.

[22] H. Murayama, N. Moriyama, H. Mitobe et al., "Evaluation of activated carbon fiber filter for sampling of organochlorine pesticides in environmental water samples," *Chemosphere*, vol. 52, no. 5, pp. 825–833, 2003.

[23] S. J. T. Pollard, G. D. Fowler, C. J. Sollars, and R. Perry, "Low-cost adsorbents for waste and wastewater treatment: a review," *Science of the Total Environment*, vol. 116, no. 1-2, pp. 31–52, 1992.

[24] B. Hameed and A. Ahmad, "Batch adsorption of methylene blue from aqueous solution by garlic peel, an agricultural waste

biomass," *Journal of Hazardous Materials*, vol. 164, no. 2-3, pp. 870–875, 2009.

[25] R. T. Meister, *Farm Chemicals Handbook*, Meister, Willoughby, Ohio, USA, 1992.

[26] Soil Survey of Pakistan, "Soil conservation and agriculture development in the Barani areas of Punjab," Lahore, Pakistan, 1975.

[27] J. P. Harsh, F. E. Koehler, C. D. Moodie, and B. L. McNeal, *Laboratory Manual for Soil Analysis: Chemistry and Fertility*, Department of Agronomy and Soils, Washington State University, Pullman, Wash, USA, 1988.

[28] L. M. Thompson and F. R. Troen, *Soils and Soil Fertility*, McGraw-Hill, New York, NY, USA, 3rd edition, 1973.

[29] A. Rashid and K. S. Memon, *Soil Science*, National Book Foundation, Islamabad, Pakistan, 2001.

[30] J. D. Rhoades, N. A. Manteghi, P. J. Shouse, and W. J. Alves, "Soil electrical conductivity and soil salinity: new formulations and calibrations," *Soil Science Society of America Journal*, vol. 53, no. 2, pp. 433–439, 1989.

[31] D. D. Perrin and B. Dempsey, *Buffers for pH and Metal Ion Control*, Chapman & Hall, London, UK, 1974.

[32] C. E. Beste, *Herbicide Handbook of the Weed Science Society of America*, vol. 3, Weed Science Society of America, Champaign, Ill, USA, 5th edition, 1983.

[33] M. Özacar, "Equilibrium and kinetic modelling of adsorption of phosphorus on calcined alunite," *Adsorption*, vol. 9, no. 2, pp. 125–132, 2003.

[34] F. C. Wu, R. L. Tseng, and R. S. Juang, "Kinetic modeling of liquid-phase adsorption of reactive dyes and metal ions on chitosan," *Water Research*, vol. 35, no. 3, pp. 613–618, 2001.

[35] E. Demirbaş, M. Kobya, S. Öncel, and S. Sencan, "Removal of Ni(II) from aqueous solution by adsorption onto hazelnut shell activated carbon: equilibrium studies," *Bioresource Technology*, vol. 84, no. 3, pp. 291–293, 2002.

[36] W. T. Tsai, K. J. Hsien, and J. M. Yang, "Silica adsorbent prepared from spent diatomaceous earth and its application to removal of dye from aqueous solution," *Journal of Colloid and Interface Science*, vol. 275, no. 2, pp. 428–433, 2004.

[37] Y. Sudhakar and A. K. Dikshit, "Competitive sorption of pesticides onto treated wood charcoal and the effect of organic and inorganic parameters on adsorption capacity," *Journal of Environmental Engineering*, vol. 136, no. 10, pp. 1096–1104, 2010.

[38] Z. Al-Qodah, A. T. Shawaqfeh, and W. K. Lafi, "Adsorption of pesticides from aqueous solutions using oil shale ash," *Desalination*, vol. 208, no. 1–3, pp. 294–305, 2007.

[39] G. Z. Memon, M. I. Bhanger, J. R. Memon, and M. Akhtar, "Adsorption of methyl parathion from aqueous solutions using mango kernels: equilibrium, kinetic and thermodynamic studies," *Bioremediation Journal*, vol. 13, no. 2, pp. 102–106, 2009.

[40] K. V. Ragnarsdottir, "Environmental fate and toxicology of organophosphate pesticides," *Journal of the Geological Society*, vol. 157, no. 4, pp. 859–876, 2000.

[41] K. M. Spark and R. S. Swift, "Effect of soil composition and dissolved organic matter on pesticide sorption," *Science of the Total Environment*, vol. 298, no. 1–3, pp. 147–161, 2002.

[42] K. M. Scow, S. Fan, C. Johnson, and G. M. Ma, "Biodegradation of sorbed chemicals in soil," *Environmental Health Perspectives*, vol. 103, supplement 5, pp. 93–95, 1995.

[43] A. O. Dada, A. P. Olalekan, A. M. Olatunya, and O. Dada, "Langmuir, freundlich, temkin and Dubinin-Radushkevitch isotherms studies of equilibrium sorption of Zn^{2+} unto phosphoric acid modified rice husk," *IOSR Journal of Applied Chemistry*, vol. 3, no. 1, pp. 38–45, 2012.

[44] N. D. Hutson and R. T. Yang, "Theoretical basis for the Dubinin-Radushkevitch (D-R) adsorption isotherm equation," *Adsorption*, vol. 3, no. 3, pp. 189–195.

[45] K. R. Hall, L. C. Eagleton, A. Acrivos, and T. Vermeulen, "Pore- and solid-diffusion kinetics in fixed-bed adsorption under constant-pattern conditions," *Industrial & Engineering Chemistry Fundamentals*, vol. 5, no. 2, pp. 212–223, 1966.

Hindawi Publishing Corporation
BioMed Research International
Volume 2014, Article ID 841573, 10 pages
http://dx.doi.org/10.1155/2014/841573

Review Article

Characteristics, Process Parameters, and Inner Components of Anaerobic Bioreactors

Awad Abdelgadir,[1,2] Xiaoguang Chen,[1] Jianshe Liu,[1] Xuehui Xie,[1] Jian Zhang,[1] Kai Zhang,[1] Heng Wang,[1] and Na Liu[1]

[1] *State Environmental Protection Engineering Center for Pollution Control in Textile, College of Environmental Science and Engineering, Donghua University, Shanghai 201620, China*
[2] *Industrial Research and Consultancy Center (IRCC), Khartoum 13314, Sudan*

Correspondence should be addressed to Xiaoguang Chen; cxg@dhu.edu.cn

Received 20 September 2013; Revised 6 November 2013; Accepted 6 November 2013; Published 23 January 2014

Academic Editor: Chong-Jian Tang

The anaerobic bioreactor applies the principles of biotechnology and microbiology, and nowadays it has been used widely in the wastewater treatment plants due to their high efficiency, low energy use, and green energy generation. Advantages and disadvantages of anaerobic process were shown, and three main characteristics of anaerobic bioreactor (AB), namely, inhomogeneous system, time instability, and space instability were also discussed in this work. For high efficiency of wastewater treatment, the process parameters of anaerobic digestion, such as temperature, pH, Hydraulic retention time (HRT), Organic Loading Rate (OLR), and sludge retention time (SRT) were introduced to take into account the optimum conditions for living, growth, and multiplication of bacteria. The inner components, which can improve SRT, and even enhance mass transfer, were also explained and have been divided into transverse inner components, longitudinal inner components, and biofilm-packing material. At last, the newly developed special inner components were discussed and found more efficient and productive.

1. Introduction

Anaerobic digestion (AD) is an attractive option for waste treatment practice in which both energy recovery and pollution control can be achieved. Anaerobic degradation or digestion involves the breakdown of biomass by a concerted action of a wide range of microorganisms in the absence of oxygen. The biological processes are essentially used to remove contaminants, in wastewater treatment, and nowadays many biological treatment options are available and have shown encouraging results over the treatment of complex organic matter [1, 2]. Comparing between anaerobic and aerobic process, anaerobic process is especially considered as a suitable treatment option due to low-energy requirements and little quantities of sludge production. Therefore, anaerobic process has become increasingly demanding in the treatment of complex industrial wastewater, which may contain toxic materials, or even low concentrations of domestic wastewater [3, 4]. The ability to attain environmental protection and resource preservation, anaerobic treatment process, and anaerobic bioreactors has received great attention [3, 5, 6].

The anaerobic digestion process is a simple and applied energy source. A simple digester consists of a digestion chamber, a dome, an inlet, an outlet for biogas, and an outlet for slurry. The biogas trapped by the dome flows under pressure through the outlet, where it can be used as an energy source. The use of anaerobic reactor began in 1859 with the first anaerobic digester that was built by a leper colony in Bombay, India [7]. And then in 1895, the technology was developed in Exeter, England, where a septic tank was used to generate gas for the sewer gas destructor lamp, a type of gas lighting. Thereafter, in the 1930s, anaerobic digestion gained academic recognition through scientific research [8]. The septic tank represents the first generation of anaerobic bioreactor (AB). In the late 1970s, the upflow anaerobic sludge blanket (UASB) process was developed by Dr. Gatze Lettinga and colleagues to represent the second generation of AB [9, 10]. In the beginning, a

Table 1: Advantages and disadvantages of anaerobic process [3, 15].

Advantages	Disadvantages
(i) Reduction of greenhouse gas emissions through methane recovery.	(i) Long recovery time: it may take longer time for the system to return to normal operating conditions if shock loading happens.
(ii) High treatment efficiency for biodegradable sludge.	(ii) Low pathogen and nutrient removal.
(iii) Production of methane gas (potential source of fuel).	(iii) Long startup.
(iv) A high degree of waste stabilization is possible.	(iv) Possible bad odors.
(v) Simplicity.	(v) High sensitivity of methanogenic bacteria to a large number of chemical compounds.
(vi) Flexibility: anaerobic treatment can easily be applied on either a very large or a very small scale.	(vi) Small- and middle-scale anaerobic technology for the treatment of solid waste in middle- and low-income countries is still relatively new.
(vii) Space saving (higher loading rates require smaller reactor volumes thereby saving on disposal cost).	
(viii) Less requirement of energy and oxygen.	
(ix) Inoffensive residual sludge may be used as soil conditioner.	
(x) Low nutrients and chemicals requirement.	

UASB reactor was just like an empty tank (thus an extremely simple and inexpensive design), but an important inner component, the three-phase separator, is added to avoid washout of granular sludge occurred. The third generation of AB, such as expanded granular sludge bed (EGSB) and internal circulation (IC) reactor, was developed on the foundation of the second generation. For instance, the faster rate of upward-flow velocity is designed for the wastewater passing through the sludge bed. The increased flux permits partial expansion (fluidization) of the granular sludge bed, improving wastewater-sludge contact as well as enhancing segregation of small inactive suspended particle from the sludge bed. The increased flow velocity is either accomplished by utilizing tall reactors or by incorporating an effluent recycle (or both) [3, 11–13]. Some super-high-rate anaerobic bioreactors (SAB) were developed recently by Chen et al. [11–13]. The development of the third generation anaerobic bioreactors and SAB shows that the process parameters such as upflow velocity, Sludge Retention Time (SRT) and Hydraulic Retention Time (HRT); and bioreactor structure (inner components) are the two most important factors for microorganisms' cultivation for anaerobic bioreactors [3, 11–13]. Therefore, This work will present the advantages and disadvantages of anaerobic process and explain the representative characteristics of anaerobic bioreactor. It also introduces main process parameters, inner components, and their effects on the performance of wastewater treatment in anaerobic bioreactors.

2. Advantages and Disadvantages of Anaerobic Process

Anaerobic treatment (digestion) is a proven way and efficient method to produce biogas (methane) that can be used for the production of renewable heat and power and a compost like output. The principle of anaerobic treatment is the utilization of anaerobic bacteria (biomass) to convert organic matter (pollutants) or COD (chemical oxygen demand) into methane rich biogas in the absence of oxygen.

The early stages of the formation of anaerobic granules follow the same principles in the formation of biofilm of bacteria on solid surfaces. There is strong evidence that inert carriers play an important positive role in granulation. Many researchers conclude that *Methanosaeta concilii* is a key organism in granulation [14].

When the system is in balance, the methanogenic bacteria use the acid intermediates as rapidly as they appear. However, if the methane bacteria are not present in suitable numbers or are being slowed down by unfavorable environmental conditions, they will not use the acids as rapidly as they are produced by the acid formers, and the volatile acids will increase in concentration. Thus, an increase in acid concentration indicates that the methane formers are not in balance with the acid formers [5]. Classification of bacteria depends upon temperature classes, where mesophiles bacteria are like mesophilic temperature, while thermophiles bacteria are like thermophilic temperature. Advantages and disadvantages of anaerobic treatment processes are shown in Table 1.

3. Characteristics of Anaerobic Bioreactor

3.1. Inhomogeneous System. Anaerobic reactor operates under an inhomogeneous system that means that the anaerobic treatment is done through three phases, solid (sludge), liquid (wastewater), and gas (methane).

3.1.1. Solid Phase. Solid phase consists of sludge granules, which have a diameter around 0.5 to 2 mm [14], which exist in the lower part of the reactor. Sludge granules play an important role for successful operation of UASB and EGSB technology, a sludge granules are the sum of microorganisms (Bacteria) forming during the treatment of wastewater in an environment with a constant upflow hydraulic regime, without any support matrix, the surrounding and suitable environment for bacteria survive is occurring during flow conditions, and therefore bacteria able to contact together and start growth and proliferate.

3.1.2. Liquid Phase. Liquid (wastewater) flows upwards through a sludge bed located in the lower part of the reactor, while the upper part contains a three phases (solid, liquid, and gas) of separation system. Three-phase separation device is the most characteristic feature of UASB reactor. It facilitates the collection of biogas and also provides internal recycling of sludge by disengaging adherent biogas bubbles from rising sludge particles.

3.1.3. Gas Phase. Biogas typically refers to a gas produced by bacteria that breakdown organic matter in the absence of oxygen (organic waste such as dead plant and animal material, animal feces, and kitchen waste or industrial organic waste can be converted into a gaseous fuel called biogas). The

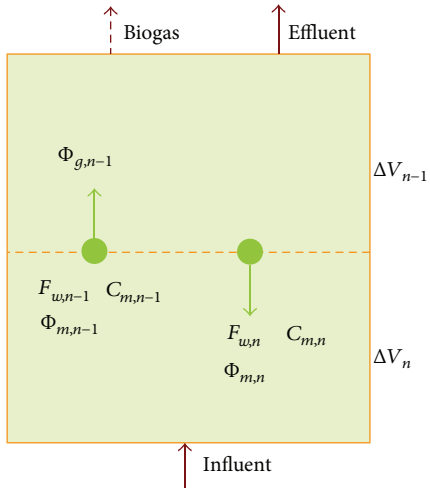

Figure 1: The granular sludge dynamic behavior.

most important thing is that biogas can result in the dynamic behavior of granular sludge [13].

In Figure 1, $\phi_{g,n-1}$ is gas production in ΔV_{n-1}, $m^3\,h^{-1}$, $\phi_{m,n}$ is downwards transport of sludge from ΔV_n to ΔV_{n-1}, $kg\,h^{-1}$, $\phi_{m,n-1}$ is sludge transport flux from ΔV_{n-1} to ΔV_n, $kg\,h^{-1}$, $C_{m,n}$ is sludge concentration (TSS) in ΔV_n, $kg\,m^{-3}$, $C_{m,n-1}$ is sludge concentration (TSS) in ΔV_{n-1}, $kg\,m^{-3}$, $F_{w,n-1}$ is up-moving wake stream in ΔV_{n-1}, $m^3\,h^{-1}$, and $F_{w,n}$ is backmix stream in ΔV_n, $m^3\,h^{-1}$.

Figure 1 explains the relationships that happen, while the movements of sludge up and down due to gas production, and therefore the transport power of sludge resulted from the upward fluid flow led by influence and the up-moving wake stream ($F_{w,n-1}$, $m^3\,h^{-1}$) led by gas production ($\phi_{g,n-1}$). Buijs et al. (1982) reported that the sludge transport efficiency of up-moving biogas can reach up to $20.2 \pm 2.1\,m^3/m^3$ (sludge/biogas) in a UASB reactor [16]. Figure 1 suggested that the downward transport of sludge ($\phi_{m,n}$, $Kg\,h^{-1}$) from ΔV_n to ΔV_{n-1} was caused due to the settling of sludge and by the back mix stream [13].

3.2. Time Instability. Anaerobic Bioreactor is used for treatment of wastewater, consisting of complex organic matters. It is become more complicated with the change in production cycles and quantities. Various industrial processes operating under different conditions (times, temperature, and pH) with a different range, throughout the four seasons of the year, have created a challenge on AB. Due to the inherent limitations of anaerobic treatment technologies, there is a need to focus on the improvement of these drawbacks, thus challenging the designers and engineers [6].

Many small sewage treatment plants are operated independently in local cities, due to encouraging processing by anaerobic digestion at a centralized sewage treatment plant (STP); high-solid sewage sludge is helpful because it reduces the energy and cost required for transporting the sludge from other STPs. Hidaka et al. [17] reported that under mesophilic

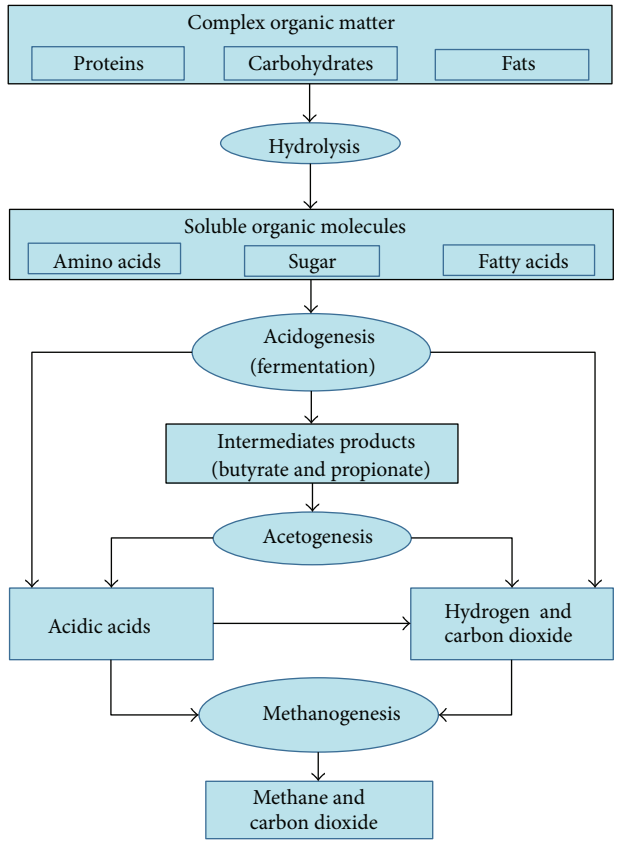

Figure 2: The key process stages of anaerobic digestion.

condition, anaerobic digestion of sewage sludge of total solids concentrations (TS) of 10% was successfully treated, while under the thermophilic condition, sewage sludge of 7.5% TS was not successfully treated when the total ammonia concentration was over 2000 mg N/L. But thermophilic anaerobic digestion successfully reduced *Salmonella* spp., and *Escherichia coli* is below detection limits but not *Clostridium perfringens* Spores. Thus, the final product met Class A biosolids' final disposal regulations, but further investigation is needed in order to satisfy the future European legislation [18].

3.3. Space Instability. The microbial consortia which achieve the conversion of complex organic matter into biogas are formed of several groups and each performs a specific function in the digestion process. Together they achieve the conversion of organic matter into biogas through a sequence of stages. The initial stages generate short chain or volatile fatty acids (VFA). The final stage is methanogenesis (methane formation) where methanogenic precursors, primarily acetic acid and hydrogen, are converted to methane and CO_2. Figure 2 explains the key process stages of anaerobic digestion [19].

The first stage of digestion process is hydrolysis. This step is very important for the anaerobic digestion process since polymers cannot be directly utilized by the fermentative microorganisms. Therefore, the insoluble complex organic

matter, such as cellulose, converts into soluble molecules such as sugars, amino acids, and fatty acids. The complex polymeric matter is hydrolyzed to monomer, for example, cellulose to sugars or alcohols and proteins to peptides or amino acids, by hydrolytic enzymes (lipases, proteases, cellulases, amylases, etc.), secreted by microbes, and make them available for other bacteria [20, 21]. Equation (1) shows an example of a hydrolysis reaction where a polysaccharide is broken down into glucose [20, 21].

Hydrolysis reactions is as follows:

$$\begin{gathered}\text{Lipids} \longrightarrow \text{Fatty Acids} \\ \text{Polysaccharides} \longrightarrow \text{Monosaccharides} \\ \text{Protein} \longrightarrow \text{Amino Acids} \\ \text{C}_{24}\text{H}_{40}\text{O}_{20} : \text{H}_2\text{O} + 3\text{H}_2\text{O} \longrightarrow 4\text{C}_6\text{H}_{12}\text{O}_6\end{gathered} \quad (1)$$

In the second stage acidogenesis (fermentation), acidogenic bacteria transform the products of the first reaction (such as sugars and amino acids) into carbon dioxide, hydrogen, ammonia, and organic acids. The principal acidogenesis stage products are acetic acid (CH_3COOH), propionic acid (CH_3CH_2COOH), butyric acid ($CH_3CH_2CH_2COOH$), and ethanol (C_2H_5OH). In an equilibrated system, most of the organic matter is converted into readily available substrates for methanogenic microbes (acetate, hydrogen, and carbon dioxide), but a significant part (approximately 30%) is transformed into short chain fatty acids or alcohols [15]. From these products, the hydrogen, carbon dioxide, and acetic acid will skip the third stage (acetogenesis) and be utilized directly by the methanogenic bacteria in the final stage (methanogenesis). Equations (2), (3) [22], and (4) [15] represent three typical acidogenesis reactions where glucose is converted to ethanol, propionate, and acetic acid, respectively,

$$\text{C}_6\text{H}_{12}\text{O}_6 \longrightarrow 2\text{CH}_3\text{CH}_2\text{OH} + 2\text{CO}_2 \quad (2)$$

$$\text{C}_6\text{H}_{12}\text{O}_6 + 2\text{H}_2 \longrightarrow 2\text{CH}_3\text{CH}_2\text{COOH} + 2\text{H}_2\text{O} \quad (3)$$

$$\text{C}_6\text{H}_{12}\text{O}_6 + 2\text{H}_2\text{O} \longrightarrow 2\text{CH}_3\text{COOH} + 2\text{CO}_2 + 4\text{H}_2 \quad (4)$$

In the third stage, acetogenic bacteria convert the organic acids that resulting from the second stage and the rest of the acidogenesis products into acetic acid, hydrogen, and carbon dioxide. Equation (5) represents the conversion of propionate to acetate, only achievable at low hydrogen pressure. Glucose (6) and ethanol (7) among others are also converted to acetate during the third stage of anaerobic digestion process [22]. The products formed during acetogenesis are due to a number of different microbes, for example, *syntrophobacter wolinii*, *a propionate decomposer* and *sytrophomonos wolfei, a butyrate decomposer*. Other acid formers are *Clostridium* spp., *Peptococcus anaerobius, Lactobacillus,* and *Actinomyces* [15],

$$\begin{gathered}\text{CH}_3\text{CH}_2\text{COO}^- + 3\text{H}_2\text{O} \\ \longrightarrow \text{CH}_3\text{COO}^- + \text{H}^+ + \text{HCO}_3{}^- + 3\text{H}_2\end{gathered} \quad (5)$$

$$\text{C}_6\text{H}_{12}\text{O}_6 + 2\text{H}_2\text{O} \longrightarrow 2\text{CH}_3\text{COOH} + 2\text{CO}_2 + 4\text{H}_2 \quad (6)$$

$$\text{CH}_3\text{CH}_2\text{OH} + 2\text{H}_2\text{O} \longrightarrow \text{CH}_3\text{COO}^- + 2\text{H}_2 + \text{H}^+ \quad (7)$$

The fourth and final stage is called methanogenesis. In this stage, methane is produced by bacteria called methanogens (also known as methane former) in two ways: either by means of cleavage of acetic acid molecules to generate carbon dioxide and methane (8) or by reduction of carbon dioxide with hydrogen (9). Methane production is higher from reduction of carbon dioxide, but limited hydrogen concentration in digesters results in that the acetate reaction is the primary producer of methane [21]. The methanogenic bacteria include *Methanobacterium, Methanobacillus, Methanococcus,* and *Methanosarcina.* Methanogens can also be divided into two groups: acetate and H_2/CO_2 consumers. Also, *Methanosaeta* is considered to be important in AD as both acetate and H_2/CO_2 consumers [21, 23]:

$$\text{CH}_3\text{COOH} \longrightarrow \text{CH}_4 + \text{CO}_2 \quad (8)$$

Carbon dioxide reduction is as follows:

$$\text{CO}_2 + 4\text{H}_2 \longrightarrow \text{CH}_4 + 2\text{H}_2\text{O} \quad (9)$$

The challenges facing anaerobic digestion such as low methane yield and process instability, preventing this technology from being widely applied. A wide variety of inhibitory substances are the primary cause of anaerobic digester upset or failure since they are present in substantial concentrations in wastes. Considerable research efforts have been made to identify the mechanism and the controlling factors of inhibition. The methane forming bacteria is strictly anaerobic and even small quantities of oxygen are harmful to them [5]. Nitrogen is an essential nutrient for anaerobic organisms [24]. The ammonia concentration must be maintained in excess of at least 40–70 mg N L^{-1} to prevent reduction of biomass activity [25]. And high ammonia concentrations may lead to inhibition of the anaerobic digestion process [26–28].

However, improved reactor configuration can reduce the space instability as soon as possible. For example, the compartmentalized anaerobic reactor (CAR) [29] was separated into a distribution zone, a reaction zone, and a separation zone by adding three inners, which seem to keep the space stability. As a result, the CAR displays a great potential for its application.

4. Process Parameters of Anaerobic Bioreactor

Degradation of unwanted components/contaminants in the anaerobic treatment depends on several parameters. The main parameters are related to reactor operating conditions (temperature, pH, organic loading rate (OLR), HRT, SRT, and upflow velocity) and influent characteristics such as particle size distribution. These parameters and their effects are discussed in the following paragraphs.

4.1. Temperature. Temperature an important physical characteristic that affects the acceptability of water as well as water chemistry and water treatment [30]. Anaerobic bacteria are classified into "temperature classes" on the basis of the optimum temperature; the mesophiles survive in mesophilic temperature around 30°C to 40°C, while thermophiles are

considered the first microorganism existing at thermophilic temperature around 50°C to 65°C [31]. Temperature even affects all wastewater treatment processes to some degree [30], for example,

(i) biological waste treatment: cold water reduces the efficiency of high-rate trickling filters by approximately 30%; low temperature inhibits nitrification (by 75% from 30°C to 10°C) more than BOD (biological oxygen demand) removal;

(ii) digestion: the minimum solid retention time varies from 2 days at 35°C to 10 days at 20°C; the heat requirement of the digester depends on outside temperature;

(iii) microbial growth: temperature affected the richness and diversity of microbial populations [32].

Temperature affects particle removal through influencing the wastewater viscosity and conversion of organic matter [33]. Because water viscosity is physically coupled to temperature, changes in temperature can influence the activity of microscopic organisms through both physiological and physical means [34]. Increasing the wastewater temperature leads to enhancing mixing by reducing viscosity, more hydraulic turbulence in a reactor, enhanceing the sedimentation, and better entrapment and adsorption due to contact between sludge and solids, and more biogas will be produced [33]. A sudden temperature changes can lead to a change in the physical and chemical properties of the wastewater, which can considerably affect the design and operation of the treatment system [35].

4.1.1. Low Temperatures. Generally temperature has a significant effect on the intracellular and extracellular environment of bacteria, and it also acts as an accelerator of the conversion processes. At low temperatures the startup period may take longer, but it can be successfully accomplished by inoculating the reactor with digested sludge. Anaerobic treatment of raw domestic sewage (COD = 500–700 g m^{-3}) on different UASB reactors can be accomplished at 12–18°C (HRTs of 7–12 h with total COD and BOD removal efficiencies of 40–60% and 50–70%, resp.) [3]. And also the possibility of applying anaerobic digestion of dilute dairy waste water at 10°C at OLRs up to 2 kg COD m^{-3} d^{-1} can gain over 84% of OD removal efficiency [36].

4.1.2. High Temperatures. The rates of reaction proceed much faster at higher temperatures, therefore producing more efficient operation and smaller tank sizes. And also treatment proceeds much more rapidly at thermophilic temperatures (around 50°C to 65°C), and the digestion under high temperature conditions offers many advantages such as higher metabolic rates, consequently higher specific growth rates, but frequently also higher death rates as compared to mesophilic bacteria, but also the additional heat required to maintain such temperatures may offset the advantage obtained. Then, most treatment systems are designed to operate in the mesophilic range or lower [5, 37, 38].

4.2. pH. pH is an expression of the intensity of the basic or acid condition of a liquid, a measure of the acidity of a solution. Commonly, methanogens in wastewater treatment systems are most active in the neutral pH range (7.0) [39]. The concentration range suitable for most organisms is 6.0–9.0 [30]; beyond this range, digestion can proceed, but with less efficiency. The biomass inhibited at pH 9 was able to regain activities after adjusting the pH to neutrality, but that inhibited at pH 5 was not [40]. At acidic conditions produced can become quite toxic to the methane bacteria. For this reason, it is important that the pH is not allowed to drop below 6.2 for a significant period of time. Because this parameter is very important, thus the system needs to control the pH. When the methane gas production stabilizes, the pH remains between 7.2 and 8.2 [19].

McCarty [5] reported that an optimum pH range of anaerobic treatment is about 7.0 to 7.2, but it can proceed quite well with a pH varying from about 6.6 to 7.6.

4.3. Hydraulic Retention Time (HRT). HRT also known as hydraulic residence time is a measure of the average length of time that a soluble compound remains in a constructed bioreactor. Hydraulic retention time is the volume of the aeration tank divided by the influent flow rate:

$$\text{HRT [d]} = \frac{\text{Volume of aeration tank } \left[\text{m}^3\right]}{\text{Influent flow rate } \left[\text{m}^3/\text{d}\right]} = \frac{V}{Q}, \quad (10)$$

where HRT is hydraulic retention time (d) and usually expressed in hours (or sometimes days), the V is the volume of aeration tank or reactor volume (m^3), and Q is the influent flow rate (m^3/d).

Generally HRT is a good operational parameter that is easy to control and also a macroconceptual time for the organic material to stay in the reactor. In bioreaction engineering studies, the reverse of HRT is defined as dilution rate, for which if it is bigger than the growth rate of microbial cells in the reactor, the microbe will be washed out, and otherwise the microbe will be accumulated in the reactor. Either of these situations may result in the breakdown of the biological process happening in the reactor.

4.4. Organic Loading Rate (OLR). At the industrial scale a range of high-rate anaerobic fluidized-bed (AFB) reactors such as upflow anaerobic sludge blanket (UASB), upflow-staged sludge bed (USSB), expanded granular sludge bed (EGSB), internal circulation (IC), and inverse anaerobic fluidized bed (IAFB) reactors can bear very high loading rates, up to 40 kg COD/(m^3·d) [41]. The organic loading rate (OLR) and volumetric biogas production (VBP) of the spiral automatic circulation (SPAC) reactor in our laboratory could reach up to 306 kg COD/(m^3·d) [41–43]. Several authors reported that up to a certain limit, the treatment efficiency of complex wastewaters, for example, potato maize, slaughterhouse, in high rate anaerobic reactors increases with increase in OLR. A further increase in OLR will lead to operational problems like sludge bed flotation and excessive foaming at the gas-liquid interface in the gas-liquid-solid (GLS)

separator, as well as accumulation of undigested ingredients. As a result, the treatment efficiency deteriorates [44, 45]. Also accumulation of biogas in the sludge bed was noticed, forming stable gas pockets that lead to incidental lifting of parts of the bed and a pulse-like eruption of the gas from this zone [45, 46]. The OLR can be varied by changing the influent concentration and by changing the flow rate. Thus, implies changing the HRT and by changing the flow rate, under these conditions OLR can be expressed in the following form:

$$\mathrm{OLR} = \frac{(Q \times \mathrm{COD})}{V}, \tag{11}$$

where OLR is organic loading rate (kg COD/m^3·d), Q is flow rate (m^3/d), COD is chemical oxygen demand (kg COD/m^3), and V is reactor volume (m^3). By using (10), the OLR can be simplified:

$$\mathrm{OLR} = \frac{\mathrm{COD}}{\mathrm{HRT}}. \tag{12}$$

When the solids removal efficiency in upflow reactors is related to the OLR, it becomes crucial to distinguish between these parameters. For this reason, OLR is an inadequate design parameter to assure good performance of anaerobic reactors.

4.5. Sludge Retention Time (SRT). SRT is known to be the key parameter affecting biochemical and physical properties of sludge [47]. The success of UASB reactors is mainly dependent on the sludge retention time (SRT) [48], which is the key factor determining the ultimate amount of hydrolysis and methanogenesis in a UASB system at certain temperature conditions [49]. The SRT should be long enough to provide sufficient methanogenic activity at the prevailing conditions. The SRT is determined by the loading rate, the fraction of suspended solid (SS) in the influent, the removal of SS in the sludge bed, and the characteristics of the SS (biodegradability, composition, etc.) [3].

Methanogenesis starts at SRT between 5 and 15 days at 25°C and between 30 and 50 days at 15°C, the maximum methanogenesis found at 25°C amounted to 51% and 25% at 15°C. Maximum hydrolysis occurs at 75 days SRT and amounted to 50% at 25°C and 24% at 15°C [47]. The SRT and temperature have a significant influence on the hydrolysis of proteins, carbohydrates, and lipids. The most substantial portion of the digestion of proteins, carbohydrates, and lipids occurs within the first 15 and 10 days at process temperatures of 25°C and 35°C, respectively [50].

4.6. Upflow Velocity. The upflow velocity is one of the main factors affecting the efficiency of upflow reactors. An increase in upflow velocity from 1.6 to 3.2 m/h resulted in a relatively small loss in SS removal efficiency, from 55% to nearly 50%, which indicates the role of adsorption and entrapment [51].

4.7. Particle Size Distribution. The particle-size distribution (PSD) of a powder, granular material, or particles dispersed in fluid is a list of values or a mathematical function that defines the relative amount, typically by mass, of particles present according to size. The effluent quality from classical filters is highly related to the specific size of the filtering media. Most studies indicate that smaller media size gives more efficient removal [52].

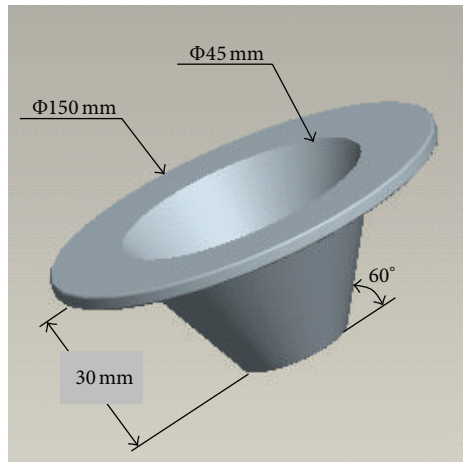

Figure 3: Structural sketch diagram of funnel-shape inner component.

5. Inner Components of Anaerobic Bioreactor

The inner components play an important role in enhancing OLR of the reactor, help in improving the quality of fluidization, separate the gas bubble from the sludge granules, and therefore enhance the treatment efficiency and so on. The inner components in a biological fluidized bed reactor can be divided into the transverse inner components, longitudinal inner components, and biofilm-packing material.

5.1. Transverse Inner Components. The most significant function of transverse inner components is (1) to keep the sludge in AB effectively and (2) to improve the quality of fluidization, break bubbles, and enhanced mass transfer significantly. To keep sludge effectively, following a three-phase separator developed in the early 1990s by Lettinga et al. [53], many investigators set inner components in the reactor by applying the three-phase separation principle. Chelliapan et al. [54] set a 45° angle of the three-phase separator baffle in the outlet of upflow anaerobic a multistage reactor (UASR) and held the granular sludge efficientively (5850 g VSS·m^{-3}). In order to reduce the short flow, improve the flow pattern, and enhance mass transfer, many researchers set different inner components in AB. Figure 3 shows that the funnel-shaped diversion components were located in the top of the reactor resulting in a 15% increase in the volumetric oxygen transfer coefficient, and liquid mixing time is reduced by 10% to 25% [55].

Karim et al. [56] studied the effect of bottom configuration and a hanging baffle on the mixing inside a gas-lift digester filled with non-Newtonian sludge (Figure 4 and Table 2). Their results showed that to change the configuration of the bottom of the reactor (Figures 4(a) and 4(c)),

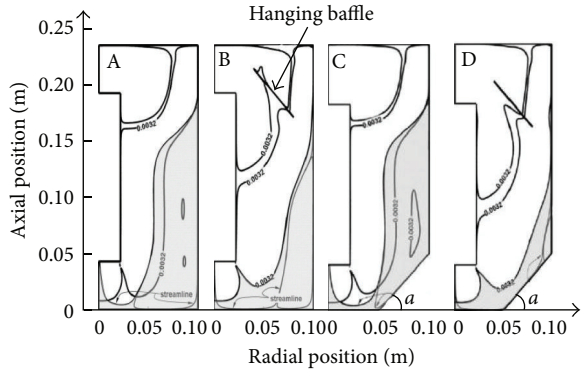

Figure 4: Comparison of fluidization quality for different conical bottom digesters with and without hanging inner component.

Table 2: Comparison of fluidization quality for different conical bottom digesters with and without hanging inner component.

Bottom configuration	The short flow area of the total volume (%)	
	No inner components	Inner components
Flat-bottomed head	33.6	21.4
Conical head ($\alpha = 25^{\circ}$)	31.9	15.8
Conical head ($\alpha = 45^{\circ}$)	29.6	11.7

the figures demonstrate that the conical bottoms resulted in only slight improvement, but Figures 4(b) and 4(d) show additional suspended inner component to permit fluid flow to the inner wall of the reactor. Under the action of an inverted conical head, the fluid flows within the draft tube, thereby constituting internal circulation, and reducing short-stream and the dead zone.

The data in Table 2 shows that the change in digester bottom configuration resulted in about 2–4% reduction in the poorly mixed zone. However, the introduction of a hanging baffle reduced the percentage of poorly mixed zones by 12%, 16%, and 18% in the case of flat, 25° and 45° bottom digesters, respectively. Therefore, it is clear that a combination of a hopper bottom and a hanging baffle would significantly improve the mixing efficacy inside gas-lift digesters.

5.2. Longitudinal Inner Components. Recent research at home and abroad shows that the future development trend of longitudinal inner components is organic integration of the components within the multigroup, in order to optimize the flow field and reduce the intermediate product inhibition. Van Lier et al. [57] set a number of three-phase separators baffle in the sludge bed of an upflow staged sludge bed (USSB) reactor (Figure 5). Its performance compared to that of an upflow anaerobic sludge bed (UASB) reactor operating at the same operational conditions, and the reaction zone in (USSB) is divided into several compartments, and each compartment can collect produced gas [58, 59].

Guyuan et al. and Ji et al. [60, 61] studied the performance of the inner components having a certain inclination multilayer baffle deflector driven in the spiral upflow reactor (SUFR) by software simulation (Figure 6). Hong-lin et al.

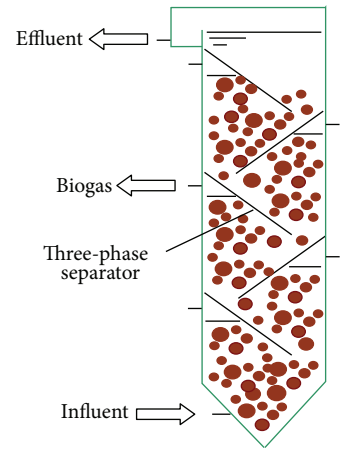

Figure 5: Structural and setup sketch of 3-phase separator baffle in USSB.

[62–64] reported that the plurality of sets of helical blades combined inner longitudinal component used in fluidized bed reactor to enhance the reactor coagulation, granulation, and biological degradation.

5.3. Biofilm-Packing Material. In 1978, Weber Jr. et al. [65] placed in a fluidized bed reactor dosing activated carbon particles and explored the inner structures of biofilm as the first of its kind. Granular activated carbon dosing has three functions to provide huge growth of microbial attachment specific surface area, enhanced biosorption, and biodegradation of synergies, greatly improve the matrix of the particle surface and oxygen concentration, effectively enhance the performance of microbial oxidation, effectively relieve hydraulic shearing action, and maintain a high concentration of microorganisms. In1980s, fixed filler was placed by McCarty and Smith [66] in the bioreactor as the inner component. High concentrations of anaerobic activated sludge was achieved, and thus anaerobic filter (AF) was developed [67]. Since then, many researchers added activated carbons [68], sand [69] calcium alginate [70], and porous polymer carrier [71] and so on as inner component in AF, and achieved some remarkable efficiency.

6. Super-High-Rate Anaerobic Bioreactor (SAB)

Under high load conditions, the biogas produced in the anaerobic reactor does not escape granular sludge in a timely manner, can reduce the particle density, and increase bed slugging. In laboratory-scale biological fluidized bed, slugging cause paralysis of the mechanical operation of the reactor. In response to this situation, Zheng's research group has developed a new spiral automatic circulation (SPAC) anaerobic reactor [42] (Figure 7), after more than two years, OLR of SPAC can reach up to 300 Kg COD·m^{-3}·$d^{-1,}$ much higher than the performance level of the existing high-rate anaerobic reactor [43]. Its main advantages are to effectively eliminate the slugging phenomenon and ensure the smooth operation

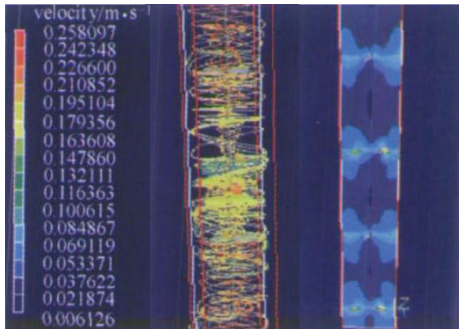

Figure 6: Simulation of flow field in SUFR.

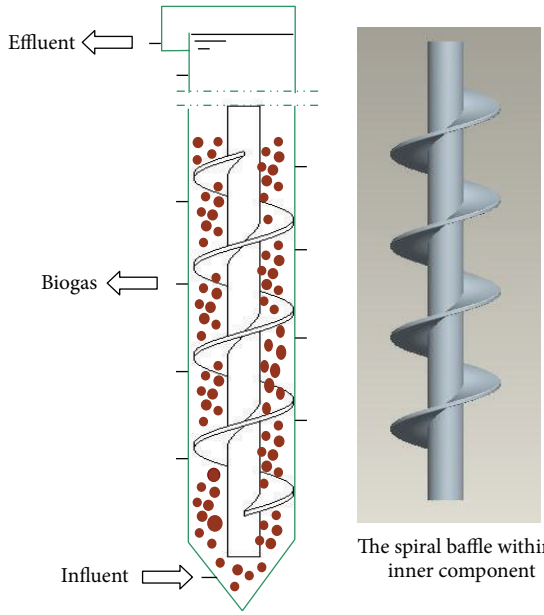

Figure 7: Structural and setup sketch of spiral baffle.

of the reactor by means of the reaction force of the spiral plate reactor.

7. Conclusion

(i) Anaerobic treatment is a proven way and efficient method to produce biogas (methane) that can be used for the production of renewable heat and power and a compost like output. Inhomogeneous system, time instability, and space instability are three main characteristics of anaerobic bioreactor (AB).

(ii) Anaerobic treatment efficiency has a deep effect by several parameters such as temperature, pH, OLR, SRT, HRT, upflow velocity, and size distribution, cause of anaerobic reactor operates under inhomogeneous system (Gas-liquid-solid). Therefore anaerobic treatment needs especial kind of setting because anaerobic processes successful depends on bacteria living and growth inside the reactor.

(iii) The reactor inner components play an important role in enhancing the treatment efficiency, and the most significant functions of inner components are (1) effective to improve the retention sludge reactor capacity and (2) significantly improve the quality of fluidization, broken bubbles, and enhanced mass transfer. And they can be divided into the transverse inner components, longitudinal inner components, and biofilm-packing material.

Conflict of Interests

The authors declare that there is no conflict of interests regarding the publication of this paper.

Acknowledgments

The authors would like to thank the National Natural Science Foundation of China (Grant no. 51208087), the Shanghai Natural Science Foundation of China (Grant no. 12ZR1400800), Doctoral Fund of Ministry of Education of China (New Teachers) (Project no. 20120075120001), and the central university special funds, free exploration program.

References

[1] G. S. Mittal, "Treatment of wastewater from abattoirs before land application—a review," *Bioresource Technology*, vol. 97, no. 9, pp. 1119–1135, 2006.

[2] S. Wijetunga, X.-F. Li, and C. Jian, "Effect of organic load on decolourization of textile wastewater containing acid dyes in upflow anaerobic sludge blanket reactor," *Journal of Hazardous Materials*, vol. 177, no. 1-3, pp. 792–798, 2010.

[3] L. Seghezzo, G. Zeeman, J. B. Van Lier, H. V. M. Hamelers, and G. Lettinga, "A review: the anaerobic treatment of sewage in UASB and EGSB reactors," *Bioresource Technology*, vol. 65, no. 3, pp. 175–190, 1998.

[4] S. Aiyuk, I. Forrez, D. K. Lieven, A. van Haandel, and W. Verstraete, "Anaerobic and complementary treatment of domestic sewage in regions with hot climates-A review," *Bioresource Technology*, vol. 97, no. 17, pp. 2225–2241, 2006.

[5] P. L. McCarty, "Anaerobic waste treatment fundamentals," *Public Works*, vol. 95, no. 9, pp. 107–112, 1964.

[6] S. Chong, T. K. Sen, A. Kayaalp, and H. M. Ang, "The performance enhancements of upflow anaerobic sludge blanket (UASB) reactors for domestic sludge treatment - A State-of-the-art review," *Water Research*, 2012.

[7] P.-J. Meynell, *Methane: Planning a Digester*, Schocken Books, New York, NY, USA, 1976.

[8] P. J. Reddy, *Municipal Solid Waste Management: Processing-Energy Recovery-Global Examples*, CRC Press, 2011.

[9] G. Lettinga et al., "Use of the upflow sludge blanket (USB) reactor concept for biological wastewater treatment, especially for anaerobic treatment," *Biotechnology and Bioengineering*, vol. 22, no. 4, pp. 699–734, 1980.

[10] M. T. Kato, J. A. Field, P. Versteeg, and G. Lettinga, "Feasibility of expanded granular sludge bed reactors for the anaerobic treatment of low-strength soluble wastewaters," *Biotechnology and Bioengineering*, vol. 44, no. 4, pp. 469–479, 1994.

[11] X.-G. Chen, P. Zheng, Y.-J. Guo, Q. Mahmood, C.-J. Tang, and S. Ding, "Flow patterns of super-high-rate anaerobic bioreactor," *Bioresource Technology*, vol. 101, no. 20, pp. 7731–7735, 2010.

[12] X. Chen, Z. Ping, S. Ding et al., "Specific energy dissipation rate for super-high-rate anaerobic bioreactor," *Journal of Chemical Technology and Biotechnology*, vol. 86, no. 5, pp. 749–756, 2011.

[13] X.-G. Chen, P. Zheng, M. Qaisar, and C.-J. Tang, "Dynamic behavior and concentration distribution of granular sludge in a super-high-rate spiral anaerobic bioreactor," *Bioresource Technology*, vol. 111, pp. 134–140, 2012.

[14] L. W. Hulshoff Pol, S. I. De Castro Lopes, G. Lettinga, and P. N. L. Lens, "Anaerobic sludge granulation," *Water Research*, vol. 38, no. 6, pp. 1376–1389, 2004.

[15] K. M. Kangle, V. S. Kore, and G. S. Kulkarni, "Recent trends in anaerobic codigestion: a review," *Universal Journal of Environmental Research and Technology*, vol. 2, no. 4, pp. 210–219, 2012.

[16] C. Buijs, P. M. Heertjes, and R. R. van der Meer, "Distribution and behavior of sludge in upflow reactors for anaerobic treatment of wastewater," *Biotechnology and Bioengineering*, vol. 24, no. 9, pp. 1975–1989, 1982.

[17] T. Hidaka, F. wang, T. Togari et al., "Comparative performance of mesophilic and thermophilic anaerobic digestion for high-solid sewage sludge," *Bioresource Technology*, vol. 149, pp. 177–183, 2013.

[18] E. Lloret, L. Pastor, P. Pradas, and J. Pascual, "Semi full-scale thermophilic anaerobic digestion (TAnD) for advanced treatment of sewage sludge: stabilization process and pathogen reduction," *Chemical Engineering Journal*, vol. 232, pp. 42–50, 2013.

[19] T. Abbasi, S. M. Tauseef, and S. A. Abbasi, "Anaerobic digestion for global warming control and energy generation - An overview," *Renewable and Sustainable Energy Reviews*, vol. 16, no. 5, pp. 3228–3242, 2012.

[20] M. T. Madigan, J. M. Martinko, D. Stahl, and D. P. Clark, *Brock Biology of Microorganisms*, Benjamin-Cummings, Reading, Mass, USA, 2008.

[21] M. Kayhanian, "Biodegradability of the organic fraction of municipal solid waste in a high-solids anaerobic digester," *Waste Management and Research*, vol. 13, no. 2, pp. 123–136, 1995.

[22] K. Ostrem, *Greening Waste: Anaerobic Digestion for Treating the Organic Fraction of Municipal Solid Wastes*, Earth Engineering Center Columbia University, 2004.

[23] S. Berger, C. Welte, and U. Deppenmeier, "Acetate activation in methanosaeta thermophila: characterization of the key enzymes pyrophosphatase and acetyl-CoA synthetase," *Archaea*, 2012.

[24] R. A. Mah, M. R. Smith, and L. Baresi, "Studies on an acetate-fermenting strain of Methanosarcina," *Applied and Environmental Microbiology*, vol. 35, no. 6, pp. 1174–1184, 1978.

[25] M. Takashima and R. E. Speece, "Mineral nutrient requirements for high-rate methane fermentation of acetate at low SRT," *Research Journal of the Water Pollution Control Federation*, vol. 61, no. 11-12, pp. 1645–1650, 1989.

[26] K. H. Hansen, I. Angelidaki, and B. K. Ahring, "Anaerobic digestion of swine manure: inhibition by ammonia," *Water Research*, vol. 32, no. 1, pp. 5–12, 1998.

[27] M. Kayhanian, "Ammonia inhibition in high-solids biogasification: an overview and practical solutions," *Environmental Technology*, vol. 20, no. 4, pp. 355–365, 1999.

[28] S. Sung and T. Liu, "Ammonia inhibition on thermophilic anaerobic digestion," *Chemosphere*, vol. 53, no. 1, pp. 43–52, 2003.

[29] J. Y. Ji, K. Zheng, Y. J. Xing, and P. Zheng, "Hydraulic characteristics and their effects on working performance of compartmentalized anaerobic reactor," *Bioresource Technology*, vol. 116, pp. 47–52, 2012.

[30] N. G. Adrien, "Processing water, wastewater, residuals, and excreta for health and environmental protection," in *An Encyclopedic Dictionary*, 2008.

[31] M. T. Agler, Z. Aydinkaya, T. A. Cummings, A. R. Beers, and L. T. Angenent, "Anaerobic digestion of brewery primary sludge to enhance bioenergy generation: a comparison between low- and high-rate solids treatment and different temperatures," *Bioresource Technology*, vol. 101, no. 15, pp. 5842–5851, 2010.

[32] W. J. Gao, K. T. Leung, W. S. Qin, and B. Q. Liao, "Effects of temperature and temperature shock on the performance and microbial community structure of a submerged anaerobic membrane bioreactor," *Bioresource Technology*, vol. 102, no. 19, pp. 8733–8740, 2011.

[33] N. Mahmoud, G. Zeeman, H. Gijzen, and G. Lettinga, "Solids removal in upflow anaerobic reactors, a review," *Bioresource Technology*, vol. 90, no. 1, pp. 1–9, 2003.

[34] M. K. Winkler, J. P. Bassin, R. Kleerebezem, R. G. van der Lans, and M. C. van Loosdrecht, "Temperature and salt effects on settling velocity in granular sludge technology," *Water Research*, vol. 46, no. 12, pp. 3897–3902, 2012.

[35] G. Lettinga, S. Rebac, and G. Zeeman, "Challenge of psychrophilic anaerobic wastewater treatment," *Trends in Biotechnology*, vol. 19, no. 9, pp. 363–370, 2001.

[36] D. C. Katarzyna Bialek and V. O'Flaherty, "Low-Temperature (10°C) anaerobic digestion of dilute dairy wastewater in an EGSB bioreactor: microbial community structure, population dynamics, and kinetics of methanogenic populations," *Archaea*, 2013.

[37] H. M. El-Mashad, G. Zeeman, W. K. P. Van Loon, G. P. A. Bot, and G. Lettinga, "Effect of temperature and temperature fluctuation on thermophilic anaerobic digestion of cattle manure," *Bioresource Technology*, vol. 95, no. 2, pp. 191–201, 2004.

[38] H. Ge, P. D. Jensen, and D. J. Batstone, "Increased temperature in the thermophilic stage in temperature phased anaerobic digestion (TPAD) improves degradability of waste activated sludge," *Journal of Hazardous Materials*, vol. 187, no. 1-3, pp. 355–361, 2011.

[39] L. Florencio, A. Nozhevnikova, A. Van Langerak, A. J. M. Stams, J. A. Field, and G. Lettinga, "Acidophilic degradation of methanol by a methanogenic enrichment culture," *FEMS Microbiology Letters*, vol. 109, no. 1, pp. 1–6, 1993.

[40] H. H. P. Fang and X.-S. Jia, "Soluble microbial products (SMP) of acetotrophic methanogenesis," *Bioresource Technology*, vol. 66, no. 3, pp. 235–239, 1998.

[41] X.-G. Chen, P. Zheng, J. Cai, and M. Qaisar, "Bed expansion behavior and sensitivity analysis for super-high-rate anaerobic bioreactor," *Journal of Zhejiang University*, vol. 11, no. 2, pp. 79–86, 2010.

[42] P. Zheng, J. W. Chen, and C. J. Tang, "A new type of spiral automatic circulation anaerobic reactor," ZL200720106182.6, 2008. (Chinese).

[43] J. Chen, C. Tang, P. Zheng, and L. Zhang, "Performance of lab-scale SPAC anaerobic bioreactor with high loading rate," *Chinese Journal of Biotechnology*, vol. 24, no. 8, pp. 1413–1419, 2008.

[44] I. Ruiz, M. C. Veiga, P. De Santiago, and R. Blázquez, "Treatment of slaughterhouse wastewater in a UASB reactor and an anaerobic filter," *Bioresource Technology*, vol. 60, no. 3, pp. 251–258, 1997.

[45] S. Kalyuzhnyi, L. Estrada De Los Santos, and J. R. Martinez, "Anaerobic treatment of raw and preclarified potato-maize wastewaters in a UASB reactor," *Bioresource Technology*, vol. 66, no. 3, pp. 195–199, 1998.

[46] T. A. Elmitwalli, M. H. Zandvoort, G. Zeeman, H. Burning, and G. Lettinga, "Low temperature treatment of domestic sewage in

upflow anaerobic sludge blanket and anaerobic hybrid reactors," *Water Science and Technology*, vol. 39, no. 5, pp. 177–185, 1999.

[47] M. Halalsheh, J. Koppes, J. Den Elzen, G. Zeeman, M. Fayyad, and G. Lettinga, "Effect of SRT and temperature on biological conversions and the related scum-forming potential," *Water Research*, vol. 39, no. 12, pp. 2475–2482, 2005.

[48] V. H. Varel, A. G. Hashimoto, and Y. R. Chen, "Effect of temperature and retention time on methane production from beef cattle waste," *Applied and Environmental Microbiology*, vol. 40, no. 2, pp. 217–222, 1980.

[49] W. J. Jewell, "Anaerobic sewage treatment," *Environmental Science and Technology*, vol. 21, no. 1, pp. 14–21, 1987.

[50] N. Mahmoud, G. Zeeman, H. Gijzen, and G. Lettinga, "Anaerobic stabilisation and conversion of biopolymers in primary sludge - Effect of temperature and sludge retention time," *Water Research*, vol. 38, no. 4, pp. 983–991, 2004.

[51] G. Zeeman, W. T. M. Sanders, K. Y. Wang, and G. Lettinga, "Anaerobic treatment of complex wastewater and waste activated sludge—application of an upflow anaerobic solid removal (UASR) reactor for the removal and pre-hydrolysis of suspended COD," *Water Science and Technology*, vol. 35, no. 10, pp. 121–128, 1997.

[52] H. Landa, A. Capella, and B. Jiménez, "Particle size distribution in an efluent from an advanced primary treatment and its removal during filtration," *Water Science and Technology*, vol. 36, no. 4, pp. 159–165, 1997.

[53] G. Lettinga, J. A. Field, R. Sierra-Alvarez, J. B. Van Lier, and J. Rintala, "Future perspectives for the anaerobic treatment of forest industry wastewaters," *Water Science and Technology*, vol. 24, no. 3-4, pp. 91–102, 1991.

[54] S. Chelliapan, T. Wilby, and P. J. Sallis, "Performance of an up-flow anaerobic stage reactor (UASR) in the treatment of pharmaceutical wastewater containing macrolide antibiotics," *Water Research*, vol. 40, no. 3, pp. 507–516, 2006.

[55] C. Wei, L. Li, J. Wu, C. Wu, and J. Wu, "Influence of funnel-shape internals on hydrodynamics and mass transfer in internal loop three-phase fluidized bed," *Journal of Chemical Industry and Engineering*, vol. 58, no. 3, pp. 591–595, 2007.

[56] K. Karim, G. J. Thoma, and M. H. Al-Dahhan, "Gas-lift digester configuration effects on mixing effectiveness," *Water Research*, vol. 41, no. 14, pp. 3051–3060, 2007.

[57] J. B. Van Lier, J. L. Sanz Martin, and G. Lettinga, "Effect of temperature on the anaerobic thermophilic conversion of volatile fatty acids by dispersed and granular sludge," *Water Research*, vol. 30, no. 1, pp. 199–207, 1996.

[58] P. N. L. Lens, M. C. Van Den Bosch, L. W. Hulshoff Pol, and G. Lettinga, "Effect of staging on volatile fatty acid degradation in a sulfidogenic granular sludge reactor," *Water Research*, vol. 32, no. 4, pp. 1178–1192, 1998.

[59] H. Yanling, *Anaerobic Biological Treatment of Wastewater*, China Light Industry Press, Beijing, China, 1998, (Chinese).

[60] L. Guyuan, D. Junfeng, J. I. Fangying, and L. Ning, "Study on the characteristic of spiral Up-flow reactor system and its performance on biological nitrogen and phosphorus removal," *Acta Scientiae Circumstantiae*, vol. 24, no. 1, pp. 15–20, 2004 (Chinese).

[61] T. Ji, G. Luo, D. Wang, X. Xu, and L. Zhu, "Effect of prolonged sludge age on biological nutrient removal in spiral up-flow reactor system and flow pattern interpretation," *Journal of Chemical Industry and Engineering*, vol. 58, no. 10, pp. 2613–2618, 2007.

[62] Y. Hong-lin, L. Yong-jun, and W. Xiao-chang, "Microbial community structure and dynamic changes of fluidized-Pellet-Bee Bioreactor," *Journal of Microbiology*, vol. 27, no. 2, pp. 1–5, 2007 (Chinese).

[63] Y. Honglin, W. Xiaochang, and W. Li, "Comparison of microbial growth in a fluidized-pellet-bed bioreactor and an A~2/O process," *Acta Scientiae Circumstantiae*, vol. 27, no. 6, pp. 973–978, 2007.

[64] H. L. Yuan and Y. J. Liu, "Pilot study of a fluidized pellet—bed bioreactor for simultaneous biodegradation and solid/liquid separation in municipal wastewater treatment future of urban wastewater systems decentralization and reuse," in *Proceedings of IWA Conference*, pp. 253–260, Xian, China, 2005.

[65] W. J. Weber Jr., M. Pirbazari, and G. L. Melson, "Biological growth on activated carbon: an investigation by scanning electron microscopy," *Environmental Science and Technology*, vol. 12, no. 7, pp. 817–819, 1978.

[66] P. L. McCarty and D. P. Smith, "Anaerobic wastewater treatment," *Environmental Science and Technology*, vol. 20, no. 12, pp. 1200–1206, 1986.

[67] F. X. Zheng Ping, *Waste Biological Treatment*, Higher Education Press, Beijing, China, 2006.

[68] A. Tanyolaç and H. Beyenal, "Prediction of substrate consumption rate, average biofilm density and active thickness for a thin spherical biofilm at pseudo-steady state," *Biochemical Engineering Journal*, vol. 2, no. 3, pp. 207–216, 1998.

[69] F. K. J. Rabah and M. F. Dahab, "Biofilm and biomass characteristics in high-performance fluidized-bed biofilm reactors," *Water Research*, vol. 38, no. 19, pp. 4262–4270, 2004.

[70] N. F. Y. Tam and Y. S. Wong, "Effect of immobilized microalgal bead concentrations on wastewater nutrient removal," *Environmental Pollution*, vol. 107, no. 1, pp. 145–151, 2000.

[71] X. G. Chen, Y. Dayong, and H. Zhaoji, "Experimental study on a three-phase outer circulating fluidized bed by a sequencing batch reactor of biofilm process," in *Seminar on Engineering Education Cooperation & Academic Research for Chinese-French Universities*, p. 367370, 2005.

Hindawi Publishing Corporation
BioMed Research International
Volume 2013, Article ID 374063, 10 pages
http://dx.doi.org/10.1155/2013/374063

Research Article

Cadmium-Induced Upregulation of Lipid Peroxidation and Reactive Oxygen Species Caused Physiological, Biochemical, and Ultrastructural Changes in Upland Cotton Seedlings

Muhammad Daud Khan,[1,2] Lei Mei,[1] Basharat Ali,[1] Yue Chen,[1] Xin Cheng,[1] and S. J. Zhu[1]

[1] *Institute of Crop Science, College of Agriculture and Biotechnology, Zhejiang University, Zijingang Campus, Hangzhou, China*
[2] *Department of Biotechnology and Genetic Engineering, Kohat University of Science and Technology, Kohat 26000, Pakistan*

Correspondence should be addressed to S. J. Zhu; shjzhu@zju.edu.cn

Received 29 August 2013; Accepted 28 October 2013

Academic Editor: Qaisar Mahmood

Cadmium (Cd) toxicity was investigated in cotton cultivar (ZMS-49) using physiological, ultrastructural, and biochemical parameters. Biomass-based tolerance index decreased, and water contents increased at 500 μM Cd. Photosynthetic efficiency determined by chlorophyll fluorescence and photosynthetic pigments declined under Cd stress. Cd contents were more in roots than shoots. A significant decrease in nutrient levels was found in roots and stem. A significant decrease in nutrient levels was found in roots and stems. In response to Cd stress, more MDA and ROS contents were produced in leaves than in other parts of the seedlings. Total soluble proteins were reduced in all parts except in roots at 500 μM Cd. Oxidative metabolism was higher in leaves than aerial parts of the plant. There were insignificant alterations in roots and leaves ultrastructures such as a little increase in nucleoli, vacuoles, starch granules, and plastoglobuli in Cd-imposed stressful conditions. Scanning micrographs at 500 μM Cd showed a reduced number of stomata as well as near absence of closed stomata. Cd depositions were located in cell wall, vacuoles, and intracellular spaces using TEM-EDX technology. Upregulation of oxidative metabolism, less ultrastructural modification, and Cd deposition in dead parts of cells show that ZMS-49 has genetic potential to resist Cd stress, which need to be explored.

1. Introduction

Cadmium (Cd) like other heavy metals such as arsenic, lead, and chromium is a persistent inorganic toxic pollutant, which comes mainly through various anthropogenic activities such as industrialization and mining [1]. It can be readily taken up by plant roots because of its relatively high mobility in the soil-plant system [2] and can pose serious threats to human health by entering into the food chain. Its presence in the environment poses several problems for both plants and animals at various functional levels. Plants are more prone to Cd stress than animals and experience various physiological, ultrastructural, and biochemical disturbances upon exposure to Cd. Physiological retardations such as limited water and nutrients' transportation, reduced mitochondrial respiration, low production of photosynthates, stunted growth, and reproduction have been observed due to Cd stress in plants [3]. Ultrastructural anomalies in plants like increase in number of nucleoli and vacuoles [4], condensed cytoplasm, reduced mitochondrial cristae, severe plasmolysis, highly condensed chromatin materials, enlarged vacuoles, disorganized chloroplastic structure and disrupted nuclear envelope [5], disorganized granal and stromal thylakoids and appearance of enlarged plastoglobuli in chloroplasts, and dilated thylakoid membranes have also been reported [6].

In Cd stressed conditions, the ultrastructural studies reveal the appearance of electron dense precipitates, which need to be analyzed for their chemical composition. Their analyses as well as distribution in cellular compartments are important to better comprehend the tolerance mechanisms in plant species [7]. This can be performed with various analytical technologies, such as energy-dispersive

X-ray analyses (EDX) and electron energy loss spectroscopy (EELS), which are equipped with transmission and scanning electron microscopes. These are useful tools for studying subcellular distribution, compartmentalization, and speciation of heavy metals [8] and can precisely localize different heavy elements in the cellular compartments [7].

Cd stress can also inhibit various metabolic events in plants. Resultantly, cellular energy deficiency and oxidative stress are accelerated [9], which lead to the increased production of various free radicals and reactive oxygen species (ROS). They are such as the superoxide ($O_2^{\bullet-}$), hydrogen peroxide (H_2O_2), and hydroxyl ($OH^{\bullet}$) radicals. They can directly damage the cells through peroxidation of poly unsaturated fatty acid of lipid membranes [10], protein oxidation, and DNA damage [3] and cause oxidative stress in cells. To avoid or to minimize the stressful effects of these radicals, various mechanisms get activated. For example, they either lower down Cd absorption and uptake, bind and sequester biomolecules, or synthesize antioxidant molecules [10, 11].

Antioxidant molecules are composed of various ROS-scavenging enzymatic and nonenzymatic antioxidants [3]. They are, for example, superoxide dismutase (SOD), peroxidase (POD), catalase (CAT), ascorbate peroxidase (APX), glutathione reductase (GR), and so forth. SOD catalyzes the dismutation of $O_2^{\bullet-}$ to H_2O_2. CAT can dismutate H_2O_2 to oxygen and water, and APX reduces H_2O_2 to water by utilizing ascorbate as specific electron donor. Nonenzymatic antioxidant ROS detoxification mechanisms are mainly composed of ascorbate and glutathione (reduced and oxidized), as well as vitamins, flavonoids, alkaloids, and carotenoids [12].

Phytoremediation is a promising plant-based remediation of contaminated soils. Woody species such as willow and poplar have been widely exploited in recent years due to their resistance and accumulation potential of various metals [13]. Cotton is a woody perennial tree, which is widely grown as fiber and oil crop. It can tolerate various abiotic and biotic stress factors. The present study was designed to investigate responses of cotton seedlings to Cd short-term stress. They were subjected to various physiological, biochemical, and ultrastructural modifications and localization studies.

2. Materials and Methods

2.1. Plant Culture Conditions. An upland cotton cultivar (ZMS-49) was used in the present experiment. Uniform-sized seeds were surface sterilized using 70% ethanol for 3 min and then in 0.1% $HgCl_2$ for 8–10 min. After several times washing with ddH_2O, seeds were soaked overnight in dH_2O. Next day, they were sown in a mixture of peat and vermiculite (7 : 3, v : v) for ten days under controlled growth chamber conditions. Seeds were kept in complete dark conditions for the first three days and thereafter a 16 h photoperiod of 50 $\mu molm^{-2}s^{-1}$ under white fluorescent light was provided for for the next 7 days at a temperature of 28 ± 2°C culture temperature and 60% relative humidity. At the end of 10-day growth period, uniform seedlings were transferred to modified Hoagland solution for four hours acclimatization period. Hoagland media were composed of 500 μM $(NH_4)_2SO_4$, 500 μM $MgSO_4$, 200 μM K_2SO_4, 1000 μM KNO_3, 600 μM $Ca(NO_3)_2{\cdot}4\,H_2O$, 200 μM KH_2PO_4, 100 μM Na_2-EDTA, 10 μM $FeSO_4{\cdot}7H_2O$, 0.5 μM $MnSO_4{\cdot}H_2O$, 0.25 μM $ZnSO_4{\cdot}7H_2O$, 0.05 μM $CuSO_4{\cdot}5H_2O$, 100 μM H_3BO_3, and 0.02 μM $(NH_4)_6Mo_7O_{24}$. After that, seedlings were transferred to fresh Hoagland medium having two levels of Cd (applied as $CdCl_2{\cdot}2.5\,H_2O$), that is, 0 and 500 μM. Seedlings were grown in the Cd stressful media for 24 hours. Next day, seedlings' roots were thoroughly washed with 20 mM EDTA-Na_2 for 15 min to remove adhering metals. Then, seedlings were divided into roots, stems, and leaves for physiological, biochemical, and ultrastructural studies.

2.2. Measurements of Physiological Parameters. After 24-hour Cd stress, seedling roots, stems, and leaves were separated for the measurements of biomass-based tolerance indices and water contents. The fresh and dry biomass-based per plant tolerance indices and per plant water contents in roots, stems, and leaves were determined according to [4, 6], respectively. For each measurement, three replications were kept with different number of plants. Regarding fresh and dry biomasses, three plants per replication were taken.

2.3. Measurements of Photosynthesis and Light Harvesting Pigments. In order to evaluate leaf efficiency regarding its photosynthesis and chlorophyll fluorescence, method described by [14] was used. For the determination of chlorophyll pigments, 0.1 g FW per sample per replication was used. Leaves were first dark adapted for 15 min in order to measure all chlorophyll fluorescence parameters. Nonphotochemical quenching (NPQ) was measured using the protocol of [15]. And all measurements were taken from the same leaf. There were three replications and in each replication, three leaves were randomly selected from three different plants. And for every replication, the mean values were calculated for 15 different locations of the three different leaves.

2.4. Measurements of Cd Concentrations and Important Micro- and Macronutrients. For elemental analyses including Cd contents in roots, stem, and leaves, fifteen seedlings from each replicate were selected. At the end of the experiment, seedlings were washed three times first with tap and then with distilled water. To remove adhering metals from roots, they were immersed in 20 mM EDTA-Na_2 for 15 min and were washed with dH_2O for three-four times. Seedlings' roots, stems, and leaves were oven dried at 80°C for 48 hour. A 0.2 g of each sample was digested with a mixture of 5 mL HNO_3 + 1 mL of $HClO_4$, which was diluted to 25 mL using 2% HNO_3 and then filtered. The concentrations of Cd and various micro- and macroelements in the filtrate were determined using inductively coupled plasma atomic emission spectroscope (ICP-AES, IRIS/AP optical emission spectrometer, Thermo Jarrel Ash, San Jose, CA) following standard procedures.

2.5. Quantification of MDA Contents, ROS, Total Soluble Proteins, and Antioxidants. Quantifications of oxidative stress markers such as MDA contents, hydrogen peroxide,

Table 1: Tolerance indices/plant based on biomass (fresh and dry) and water content (%)/plant of different parts of cotton seedlings grown under Cd stress.

Parts	Tolerance index (FW)		Tolerance index (DW)		Water contents (%)	
	0 μM Cd	500 μM Cd	0 μM Cd	500 μM Cd	0 μM Cd	500 μM Cd
Roots	100.00 ± 0.00[a] (0.00)	62.86 ± 2.44[b] (−37.14)	100.00 ± 0.00[a] (0.00)	26.11 ± 3.89[b] (−73.89)	92.47 ± 0.29[b] (0.00)	96.78 ± 0.73[a] (4.67)
Stems	100.00 ± 0.00[a] (0.00)	74.58 ± 6.73[b] (−25.42)	100.00 ± 0.00[a] (0.00)	65.00 ± 5.00[b] (−35.00)	91.10 ± 0.22[b] (0.00)	92.22 ± 0.29[a] (1.23)
Leaves	100.00 ± 0.00[a] (0.00)	99.33 ± 9.66[a] (−0.97)	100.00 ± 0.00[a] (0.00)	85.39 ± 2.56[b] (−14.61)	90.22 ± 0.85[a] (0.00)	91.50 ± 0.64[a] (1.42)

Values are the means ± SE of three replications. Variants possessing the same letter are not statistically significant at $P < 0.05$. Values in parenthesis show percent relative increase (+) or decrease (−) over the related controls.

superoxide radical ($O_2^{\bullet -}$), extracellular hydroxyl radicals (OH^-), total soluble proteins, and ROS-scavenging antioxidant activities were performed using established protocols described by [16]. A 0.5 g fresh sample of leaves, stems, and roots was used for all assays.

2.6. Ultramorphological and Microlocalization Studies. Cd-induced ultrastructural modifications in root meristem and leaf mesophyll cells were observed under transmission electron microscopy. Root and leaf samples were prepared according to [4, 6]. For scanning electron microscopy, leaf samples were first fixed with 2.5% glutaraldehyde in phosphate buffer (pH 7.0) for more than 4 hours and were washed three times with phosphate buffer for 15 min at each step. Then samples were postfixed with 1% OsO_4 in phosphate buffer (pH 7.0) for 1 hour and washed three times with the same phosphate buffer for 15 min. The specimens were first dehydrated by a graded series of ethanol (50%, 70%, 80%, 90%, 95%, and 100%) for about 15 to 20 minutes at each step, transferred to the mixture of alcohol and iso-amyl acetate (v : v = 1 : 1) for about 30 minutes, and then transferred to pure iso-amyl acetate for about 1 hour. In the end, the specimens were dehydrated in Hitachi Model HCP-2 critical point dryer with liquid CO_2. The dehydrated specimen was coated with gold-palladium and observed in Hitachi Model TM-1000 SEM.

For the Cd localization experiment, thin sections of 120 nm of both roots and leaves were prepared according to [4, 6]. They were observed in EDAX GENESIS XM2 30TEM energy spectrometer at 80 KV.

2.7. Statistical Analyses. The data obtained were subjected to one-way analysis of variance (ANOVA) using STATIX9. All the results are the means ± SE of three replications. Means were separated by Least Significant Difference (LSD) test at 5% level of significance.

3. Results and Discussion

Heavy metals-based pollution is a serious environmental threat for all living organisms. Cd is a highly phytotoxic heavy metal. Because of its water soluble nature [4], it is readily taken up by roots and transported to the vegetative and reproductive organs of plants. Resultantly, the mineral nutrition and homeostasis in plant shoot and root growth and developments [17] are greatly disturbed. Also, Cd can affect biochemical and structural aspects of cell by inducing oxidative stress and disruption of membrane composition and function [4, 6, 18].

3.1. Effect of Cd Stress on Tolerance Indices and Water Contents of Upland Cotton Seedlings. Biomass-based tolerance index is the indirect measurement of plant growth efficiency under stressful conditions. Tolerance index per plant based on both fresh and dry biomasses and water content percentage of roots, stems, and leaves of cotton seedlings is shown in Table 1. Mean data regarding tolerance index of both fresh and dry biomass revealed downward trends in roots, stems, and shoots at 500 μM Cd as compared with the control. Greater and significant decline could be observed in tolerance index of dry biomass. As a whole, greater decline in tolerance index of roots followed by stem and leaves was noticed. Similar trend was observed by [19] in mustard cultivars under Cd stress. Cd-induced reduction in tolerance index directly reveals the growth inhibition of these parts. Inhibited growth may be due to Cd interference with the vital metabolic processes such as photosynthesis and translocation of photosynthetic products and essential nutrients [17]. That is why a general decline in the photosynthesis related parameters and essential nutrients was observed under Cd stress in the present experiments.

Measurement of water contents based on difference in fresh and dry biomass production is very helpful to investigate Cd-induced secondary stress, that is, water stress [6]. All parts of the seedlings absorbed more water at 500 μM Cd as compared with the control. The root water content was significantly ($P < 0.05$) higher (4.67%) in comparison with leaves (1.42%) and stem (1.23%). As a whole, roots absorbed more water than leaves and stems, which are contrary to our previous findings [6] as well as those of [20] in pea and of [21] in *Lactuca* sp. This difference could be due to several reasons such as (a). We could not observe any wilting situation in cotton seedlings, (b). Ultramicroscopic observations revealed that most of the cells were in turgid conditions, (c). Upregulation of methionine synthase protein (as revealed by our proteomic studies, data not given here) might have caused greater lignification of the cell wall and

Table 2: Chlorophyll pigments and fluorescence of leaves of cotton seedlings grown under Cd stress.

Cd levels	Chlorophyll pigments			Chlorophyll fluorescence			
	Chl a	Chl b	Chl a/b	F_m	F_m'	F_v/F_m	NPQ $(F_m/F_m' - 1)$
0 μM	0.044 ± 0.00^a (0.00)	2.72 ± 0.13^a (0.00)	0.016 ± 0.003^a (0.00)	0.49 ± 0.05^a (0.00)	0.49 ± 0.01^a (0.00)	0.81 ± 0.02^a (0.00)	0.03 ± 0.08^a (0.00)
500 μM	0.021 ± 0.01^b (−52.27)	2.22 ± 0.27^a (−19.12)	0.011 ± 0.005^a (−33.83)	0.33 ± 0.03^b (−32.65)	0.34 ± 0.01^b (−30.61)	0.65 ± 0.02^b (−19.75)	0.05 ± 0.03^a (55.17)

Values are the means ± SE of three replications. Variants possessing the same letter are not statistically significant at $P < 0.05$. Values in parenthesis show percent relative increase (+) or decrease (−) over the related controls.

more resistance to allow intracellular water out in Cd stressful conditions.

3.2. Effect of Cd on Photosynthetic Parameters of Cotton Seedlings. Photosynthesis is a major source of ROS production in plants, which performs active role in metabolism and formation of ROS [16]. Quantification of photosynthesis-related parameters gives a clear idea about the stressful effects of any external stimuli. Table 2 shows various parameters of chlorophyll pigments and fluorescence. The mean data of chlorophyll pigments such as chlorophyll a, b and chlorophyll a/b ratio showed variable responses to Cd stress. The highest and statistically significant decline (52%) was observed only in chlorophyll a. Chlorophyll a and chlorophyll a/b ratio showed a decrease of 19% and 34%, respectively; however, this decrease was statistically nonsignificant. A similar trend in chlorophyll pigments composition was observed in *Brassica* under Cd stress [22].

The results for fluorescence parameters such as F_m, F_m', and F_v/F_m and nonquenching parameter (NPQ) reveal that Cd stress significantly inhibited the photosynthetic parameters with the exception of NPQ, which upregulated. Percent inhibition in the chlorophyll fluorescence parameters was in the order of F_m (33%) > F_m' (31%) > F_v/F_m (20%). A decrease in the chlorophyll fluorescence was also observed in barley under Al stress [23] and in tomato under Cd stress [14]. Such reduction in chlorophyll pigments and fluorescence may lead to reduced photosynthesis and growth [24]. These inhibitory effects could be possibly due to indirect interaction of Cd with micronutrients (such Fe, Mn, Zn), which are made unavailable to act as cofactors of enzymes, pigments, and structural components of the photosynthetic apparatus [25]. Fe deficiency in leaves observed in the present experiments can be a responsible factor in Cd-induced inhibition of photosynthesis [26].

3.3. Analyses of Cd and Macro- and Micronutrients. There is a direct relationship of metal uptake in plants and its concentration in soil or medium [6]. Table 3 shows concentrations of Cd and various macro- and micronutrients in different parts of cotton seedlings grown for 24 hour in Cd stressed and nonstressed conditions. Under controlled conditions, Cd concentrations in roots, stems, and leaves of seedlings were almost negligible as compared to seedlings grown in 500 μM of Cd, where all parts of the seedlings absorbed significant amounts of Cd. The highest Cd concentration (2.29 mg/g DW) was found in roots followed by stem (2.27 mg/g DW) and leaves (0.55 mg/g DW). Root retained more Cd and only a small portion was transported to aerial parts. Similar findings have been reported by [27].

Cadmium can interact with the availability of nutrients [28] and may imbalance the uptake and distribution of certain essential nutrients in plants [29]. In the present experiment, Cd stress had adverse effects on most of the macronutrients levels in roots, stems, and leaves as compared to their relevant controls (Table 3). Levels of macronutrients such as N, P, K, and Mg decreased in both roots and stems, while their levels enhanced in leaves at 500 μM Cd as compared to their related controls. However, S level in all parts of cotton seedlings was upregulated. As a whole, maximum decrease was observed in K, which was in roots (75%), while significant enhancement was found in N in leaves (120%) as compared to their related controls. Furthermore, downregulation of macronutrients in roots was more than in stems. S contents levels showed a nonsignificant upward trend. Our present findings are contradictory to those of [20] in pea and [30] in birch.

Table 3 further depicts the micronutrients status in different parts of the cotton seedlings under Cd stress. The data reveal that Cd had a negative influence on the levels of various micronutrients except Fe and B. In roots of cotton seedlings, Fe contents nonsignificantly increased (21%) over the control, while the B contents levels in all parts of the cotton seedlings enhanced. Greater incline in B contents could be observed in roots, which was 235% as compared with the control, followed by stem (40%) and leaves (32%). As a whole the nutritional status of leaves and roots greatly altered. Almost similar trend was reported in pea [20]. Different factors like the involvement of different transporters in nutrients/elements translocation, variable affinity of phytochelatins for specific metals [20], and morphological changes of the conducting xylem tissues [31] could be the possible reasons for the differential uptake of these elements under Cd stress. Similar to our findings, Cd stress reduced the concentration of most of the nutrients in durum wheat [32] and barley [33].

3.4. Cd Stress Upregulated the MDA and ROS Contents and Downregulated the Total Soluble Protein Contents. MDA production is a cytotoxic product of lipid peroxidation [34], which is produced under stressful conditions. The production of superoxide radicals ($O_2^{\bullet -}$), hydrogen peroxide (H_2O_2), and hydroxyl radicals (OH^-) under Cd stress [16] has been

Table 3: Cd uptake by different parts of cotton seedlings and macro- and micronutrients concentration in different parts of the cotton seedlings under Cd stress.

Elements (mg/g DW)	Roots		Stems		Leaves	
	0 μM Cd	500 μM Cd	0 μM Cd	500 μM Cd	0 μM Cd	500 μM Cd
Cd	0.04 ± 0.004^{b} (0.00)	2.29 ± 0.07^{a} (6206.61)	0.004 ± 0.001^{b} (0.00)	2.27 ± 0.02^{a} (55561.05)	0.002 ± 0.003^{b} (0.00)	0.55 ± 0.04^{a} (30798.29)
Macronutrients						
N	19.51 ± 0.83^{a} (0.00)	9.78 ± 1.40^{b} (−49.84)	5.24 ± 0.58^{a} (0.00)	3.15 ± 0.97^{a} (−39.84)	1.11 ± 0.23^{b} (0.00)	2.45 ± 0.73^{a} (120.28)
P	5.51 ± 0.94^{a} (0.00)	2.80 ± 0.56^{a} (−49.12)	9.06 ± 1.52^{a} (0.00)	7.73 ± 0.41^{a} (−14.68)	10.68 ± 0.96^{a} (0.00)	12.95 ± 0.91^{a} (21.29)
K	33.29 ± 1.63^{a} (0.00)	8.30 ± 0.75^{b} (−75.06)	27.59 ± 1.32^{a} (0.00)	23.32 ± 1.41^{a} (−15.51)	18.70 ± 1.45^{a} (0.00)	21.65 ± 1.56^{a} (15.77)
Mg	8.48 ± 0.35^{b} (0.00)	4.67 ± 0.56^{a} (−44.88)	5.73 ± 0.39^{a} (0.00)	5.24 ± 0.47^{a} (−8.58)	5.19 ± 0.79^{a} (0.00)	6.24 ± 0.28^{a} (20.35)
S	15.68 ± 0.92^{a} (0.00)	19.59 ± 1.79^{a} (25.00)	7.66 ± 0.69^{a} (0.00)	12.32 ± 1.73^{a} (60.74)	9.76 ± 0.43^{a} (0.00)	11.62 ± 0.76^{a} (18.98)
Micronutrients						
Fe	0.94 ± 0.12^{a} (0.00)	1.14 ± 0.13^{a} (21.15)	0.06 ± 0.01^{a} (0.00)	0.05 ± 0.001^{a} (−21.67)	0.15 ± 0.005^{a} (0.00)	0.12 ± 0.003^{b} (−21.68)
Zn	0.29 ± 0.004^{a} (0.00)	0.13 ± 0.01^{b} (−54.91)	0.08 ± 0.006^{a} (0.00)	0.06 ± 0.004^{a} (−19.35)	0.10 ± 0.004^{a} (0.00)	0.080 ± 0.006^{a} (−16.61)
Cu	0.02 ± 0.001^{a} (0.00)	0.02 ± 0.001^{b} (−33.33)	0.01 ± 0.001^{a} (0.00)	0.01 ± 0.000^{b} (−23.17)	0.01 ± 0.000^{a} (0.00)	0.01 ± 0.001^{a} (−8.28)
Ca	7.65 ± 0.24^{a} (0.00)	4.20 ± 0.4^{b} (−45.09)	20.52 ± 0.81^{a} (0.00)	16.97 ± 0.35^{b} (−17.29)	21.04 ± 0.79^{a} (0.00)	19.90 ± 0.65^{a} (−5.51)
Mn	54.81 ± 0.004^{a} (0.00)	31.52 ± 0.003^{b} (−42.50)	19.07 ± 0.003^{a} (0.00)	17.26 ± 0.001^{a} (−9.50)	93.97 ± 0.003^{a} (0.00)	83.94 ± 0.002^{b} (−10.67)
Ni	0.01 ± 0.001^{a} (0.00)	0.01 ± 0.001^{a} (−36.05)	0.02 ± 0.000^{a} (0.00)	0.002 ± 0.000^{a} (−13.07)	0.002 ± 0.000^{a} (0.00)	0.001 ± 0.000^{a} (−16.25)
B	0.04 ± 0.000^{a} (0.00)	0.05 ± 0.000^{a} (234.54)	0.01 ± 0.004^{a} (0.00)	0.01 ± 0.002^{a} (40.04)	0.04 ± 0.002^{a} (0.00)	0.050 ± 0.004^{a} (32.40)

Values are the means ± SE of three replications. Variants possessing the same letter are not statistically significant at $P < 0.05$. Values in parenthesis show percent relative increase (+) or decrease (−) over the related controls.

reported. They can damage membrane and inactivate various enzymes due to reactions with proteins, lipids, and nucleic acids [35].

The main objective of the present study was to determine the effect of Cd stress on MDA contents and production of reactive oxygen species. Data in Table 4 reveal an increase in MDA and ROS in all parts of the cotton seedlings in response to Cd stress. Superoxide radical was produced in greater amount followed by H_2O_2, OH^-, and MDA. Moreover, greater production of $O_2^{\bullet -}$, H_2O_2, and MDA in leaves, while that OH^- in roots was found. Statistically significant variations were more in H_2O_2 and MDA at 5% probability level.

The total soluble proteins in all parts of the cotton seedlings were also determined in this study (Table 4). The tabulated data showed that in seedlings roots, protein contents were significantly higher (98%) in Cd treated seedlings, while in other parts it was lower (33% in stem and 37% in leaves), in comparison with the respective control. Similar upward trend in MDA and H_2O_2 was observed in *Brassica* under Cd stress [16, 22] and in wheat under heavy metal stress [36]. This increase in their production of these species indicates that Cd stress might have caused damage to membranes. This assumption is supported by the fractured plasma membrane, misshaped chloroplast, and enlarged vacuoles observed under Cd stress. Similar upregulation in MDA and ROS contents was observed in *Sedum alfredii* Hance [11] and *J. effuses* [18] under Cd stress. Such decline can be due to pigment loss, reduction in the photosynthetic efficiency, decreased RNA levels, and so forth. [37]. Increase in total soluble proteins in roots might be due to increase in number of nuclei, which might have synthesized greater amount of amino acids [4].

3.5. Effect of Cd Stress on Oxidative Metabolism Levels in Cotton Seedlings. Antioxidative enzymes play active roles in scavenging of ROS produced in plants under environmental stresses. Table 5 shows the status of oxidative metabolism in different parts of cotton seedlings grown for 24 hours in Cd stressed and nonstressed conditions. Data regarding SOD activity showed an enhancement in its activity in all parts of the seedlings, which was statistically significant in roots and leaves. Greater percent enhancement was found in

Table 4: Effect of Cd stress on MDA (ηM/mg protein) and ROS (H_2O_2, $O_2^{\bullet -}$, $OH^{\bullet}$) contents (μM/gFW) as well as total soluble proteins (mg/gFW) in different parts of cotton seedlings.

Traits	Parts					
	Roots		Stems		Leaves	
	0 μM Cd	500 μM Cd	0 μM Cd	500 μM Cd	0 μM Cd	500 μM Cd
MDA	9.18 ± 0.24^b (0.00)	11.25 ± 0.23^a (22.55)	10.83 ± 0.24^a (0.00)	11.73 ± 0.27^a (8.47)	13.14 ± 21.61^b (0.00)	21.61 ± 2.24^a (64.46)
H_2O_2	20.92 ± 6.21^a (0.00)	34.17 ± 12.34^a (63.30)	42.44 ± 9.91^b (0.00)	80.69 ± 8.37^a (90.13)	68.18 ± 10.09^b (0.00)	164.16 ± 26.16^a (140.77)
$O_2^{\bullet -}$	22.15 ± 9.00^a (0.00)	33.66 ± 22.85^a (51.95)	75.23 ± 36.76^a (0.00)	102.78 ± 42.28^a (36.62)	19.29 ± 1.09^b (0.00)	126.96 ± 6.18^a (558.16)
$OH^{\bullet}$	0.10 ± 0.01^b (0.00)	0.15 ± 1.53^a (103.36)	0.13 ± 0.03^a (0.00)	0.19 ± 0.03^a (52.72)	0.13 ± 0.08^a (0.00)	0.15 ± 0.08^a (13.83)
Proteins	8.89 ± 0.19^b (0.00)	17.63 ± 0.86^a (98.34)	13.06 ± 4.31^a (0.00)	8.74 ± 0.17^a (−33.08)	14.81 ± 1.71^a (0.00)	9.33 ± 0.65^b (−36.99)

Values are the means ± SE of three replications. Variants possessing the same letter are not statistically significant at $P < 0.05$. Values in parenthesis show percent relative increase (+) or decrease (−) over the related controls.

Table 5: Antioxidants status in different parts of cotton seedlings upon their exposure to Cd stress for 24-hour duration.

Antioxidants	Parts					
	Roots		Stems		Leaves	
	0 μM Cd	500 μM Cd	0 μM Cd	500 μM Cd	0 μM Cd	500 μM Cd
SOD (U/mg protein)	275.25 ± 1.69^b (0.00)	324.67 ± 6.13^a (17.95)	267.13 ± 8.21^a (0.00)	284.50 ± 1.94^a (6.50)	255.82 ± 21.26^b (0.00)	344.92 ± 5.09^a (34.83)
APX (μM/min/mg protein)	0.51 ± 0.17^a (0.00)	0.41 ± 0.24^a (−20.04)	1.43 ± 0.95^a (0.00)	0.37 ± 0.10^a (−74.50)	3.31 ± 0.16^a (0.00)	1.84 ± 0.35^a (−44.43)
CAT (μM/min/mg protein)	0.030 ± 0.02^a (0.00)	0.035 ± 0.01^a (12.37)	0.11 ± 0.02^a (0.00)	0.02 ± 0.010^b (−83.17)	0.21 ± 0.010^a (0.00)	0.57 ± 0.02^a (169.09)
POD (μM/min/mg protein)	7.48 ± 0.69^a (0.00)	4.93 ± 0.33^b (−34.09)	2.62 ± 0.13^b (0.00)	3.72 ± 0.15^a (41.85)	5.07 ± 0.14^b (0.00)	8.03 ± 0.39^a (58.26)
GR (μM/min/mg protein)	0.22 ± 0.03^a (0.00)	0.03 ± 0.08^a (−85.10)	0.05 ± 0.02^b (0.00)	0.18 ± 0.02^a (244.76)	0.17 ± 0.02^b (0.00)	0.27 ± 0.03^a (54.59)

Values are the means ± SE of three replications. Variants possessing the same letter are not statistically significant at $P < 0.05$. Values in parenthesis show percent relative increase (+) or decrease (−) over the related controls.

leaves (35%) followed by roots (18%) and stems (7%). Greater activity in leaves might be due the fact that Cd might have caused senescence-like situation in leaves. Such enhancement in SOD activity under Cd stress has also been previously reported in *Sedum alfredii* by [11]. Under Cd stress, the APX activity was reduced in different parts of the seedlings, but this effect was statistically not significant. Similar to our findings, a marked reduction in APX activity in roots of HE *Sedum alfredii* has been observed [11]. At higher Cd concentration (i.e., 500 μM), activities of POD and GR were reduced by 34 and 85%, respectively, in roots, and the activity of CAT was reduced in stems by 83%. However, their activities were enhanced in all other parts of cotton seedlings. Greater relative increase in the activities of CAT, POD, and GR was observed in leaves (169, 58%) and stems (245%), respectively. However, POD activity enhanced in leaves under Cd stress. Our present findings are not in line with those of [20]. Its activity was also increased in *B. juncea* under Cd stress [38]. As a whole, significant percent inhibition (85%) was in GR activity of roots, while significant percent enhancement (245%) was also found in the GR activity of stem. Such increase has also been found in mustard under cadmium stress [37].

3.6. Effect of Cd Stress on Ultrastructure of Roots and Leaves. Ultrastructural studies in plants are important tools to peep into the cellular mechanisms being involved in the detoxification of Cd. The ultrastructural changes, in combination with metabolic activities, help devise a strategy to reduce the effects of Cd stress in plants. Ultrastructural alterations in root meristem and leaf mesophyll cells of ZMS-49 were not so severe at 500 μM Cd as compared with the control (Figures 1(a)–1(d)). At 0 μM Cd, the cells of root meristems had typical structural features. They possessed granular cytoplasm with a number of vacuoles, mitochondria, and endoplasmic reticulum. Membranous structures such as plasma, nucleus and mitochondria were smooth. Cytoplasm was dense with centrally located nucleus (Figure 1(a)). At 500 μM Cd level, ultrastructural changes such as increase in number of vacuoles, nucleoli, mitochondria, misshaped nucleus, and fractured nuclear membrane were observed.

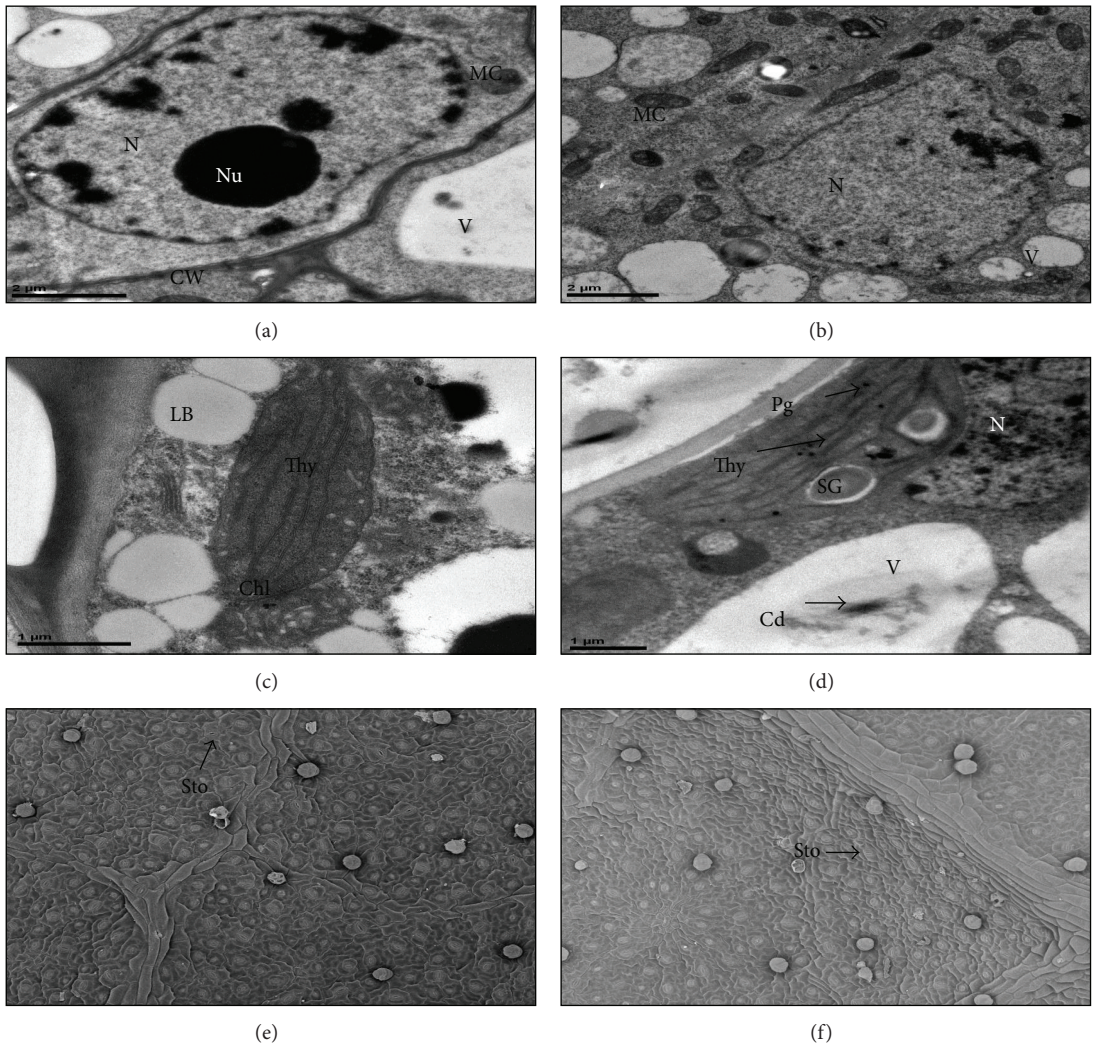

Figure 1: Transmission electron micrographs of roots meristem cells ((a), (b)), leaf mesophyll cells ((c), (d)), and scanning micrographs EM of leaves ((e), (f)) of cotton seedlings under normal ((a), (c), (e)) and Cd stress ((b), (d), (f)) conditions. MC: mitochondria, CW: cell wall, N: nucleus, Nu: nucleolus, V: vacuole, Chl: chloroplast, Thy: thylakoids, LB: lipid bodies, Pg: plastoglobuli, SG: starch granules, Sto: stomata.

However, plasmolysis was almost absent and electron dense precipitates, probably Cd, were observed in vacuoles and intracellular spaces as well as attached to the cell walls (Figure 1(b)).

The transmission electron microscopy images of leaf mesophyll cells are shown in Figures 1(c) and 1(d). Under normal conditions, thin and clean cell walls were seen, with well-shaped nucleus and few lipid bodies. The chloroplasts were of regular shape with well-arranged thylakoids (Figure 1(c)). However, some alterations were observed at whole leaf mesophyll as well as chloroplast levels. Greater modifications could be seen in vacuolar, nuclear, and chloroplastic regions. An increase in number of lipid bodies, starch granules, and plastoglobuli could be noticed (Figure 1(d)). Electron dense precipitates, probably Cd, were mostly seen in the vacuolar and cell walls regions. Such observations have also been made in previous studies [4, 6, 16, 18, 22]. Increase in number of starch granules is a general sign of stress in plants [18]. Increased nutrient deficiency or disturbed vein loading system [6] due to high Cd translocation into shoot may lead to starch accumulation in the chloroplast. Their deposition in these regions shows that ZMS-49 can play a significant role in Cd tolerance by preventing the circulation of free Cd ions in the cytosol [4]. Our findings are further supported by [39, 40].

Figures 1(e) and 1(f) also show the scanning micrographs of the abaxial side of cotton leaf. These micrographs show that almost outer surfaces were smooth in both Cd stressed and nonstressed leaves of cotton seedlings. Less number of stomata was found closed in the Cd treated leaf mesophyll cells. The number of stomata was almost the same in both types of cells. Trichome was less turgid in the Cd treated leaf mesophyll cells as compared with the nonstressed leaves. Such observations are against those of [20]. Taking together observations at transmission and scanning microscopic levels, it is argued that Cd stress caused very little alterations in both roots and leaves. There was observed

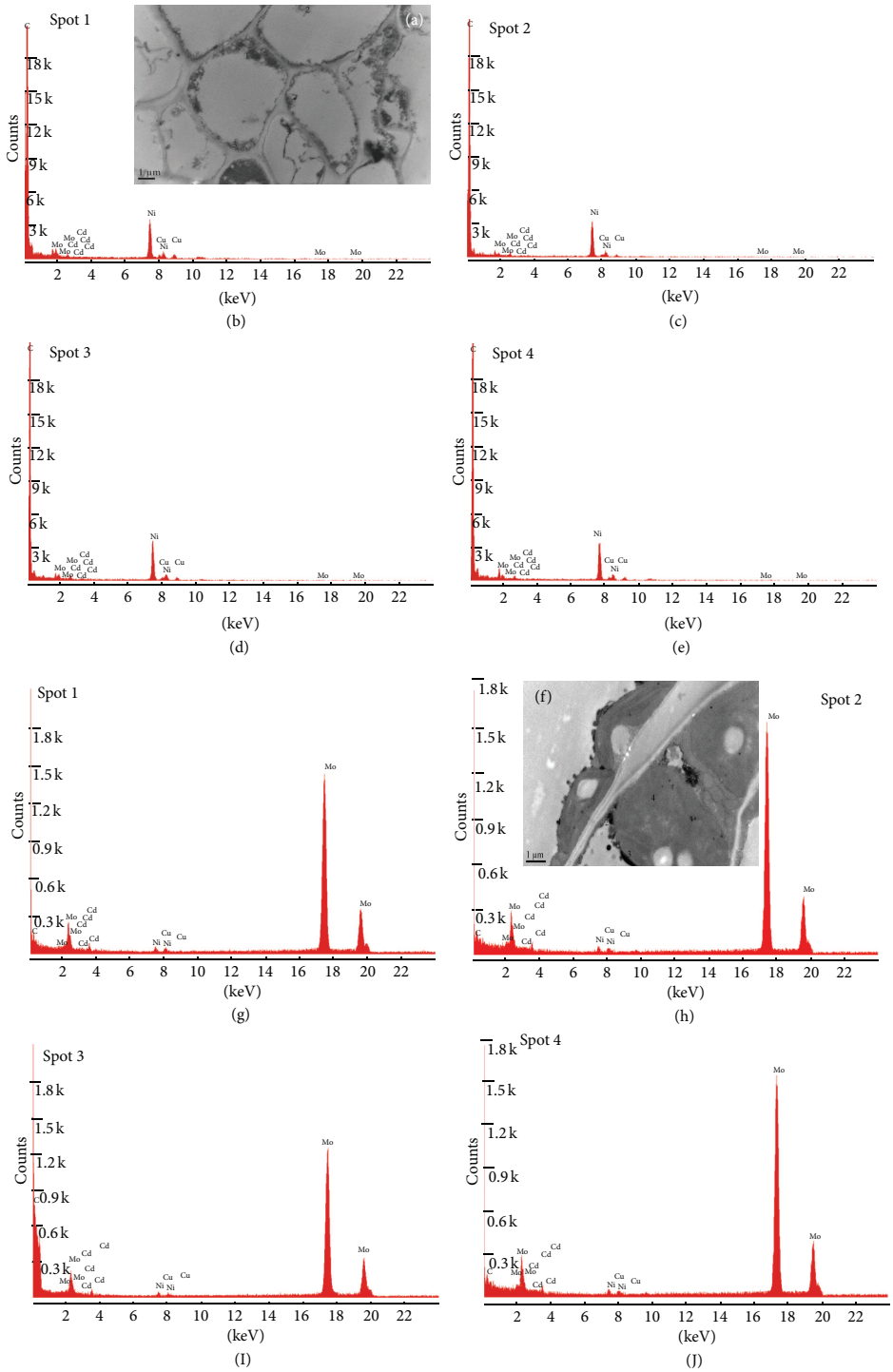

FIGURE 2: Energy dispersive X-ray analysis of both roots ((a)–(e)) and leaves ((f)–(j)) under Cd stress. Peaks show the presence of Cd in vacuoles and cell walls of these samples.

some senescent-like situation in cellular compartments of the cells of these parts, mostly in leaves, which might be due to increased production of MDA and various ROS.

3.7. Microlocalization of Cd. Compartmentalization and complexation of heavy metals at a subcellular level play an important role in detoxification of heavy metals in plant tissues [41]. In our present experiment, we found electron dense precipitates in the Cd treated root meristems and leaf mesophyll cells (Figures 2(a) and 2(f)). These were confirmed by EDX technology. For every root and leaf samples, we analyzed four different spots. The EDX spectra obtained

confirmed the presence of Cd mostly in the dead parts of the cell such as cell wall, vacuoles, and intracellular spaces (Figures 2(b)–2(e) and 2(g)–2(j)). We only observed the Cd treated samples of roots and leaves for the microlocalization of Cd because such precipitates were not clearly observed in the control samples. Such observations have also been previously made by [7].

4. Conclusions

From the present study, it can be concluded that

(i) Cd stress disturbed photosynthetic machinery and nutrient levels, which indirectly reduced biomass-based tolerance index;

(ii) there was an increase in the water contents in different parts of the cotton seedlings in order to combat such stressful situation;

(iii) there was a rise in MDA and ROS contents in all parts, which were scavenged by various ROS-scavenging antioxidants due to their upregulation;

(iv) the active involvement of ROS-scavenging antioxidant machinery caused less disruption of cellular organelles both in roots and leaves as well as Cd deposition in cell wall and vacuole.

Abbreviations

APX: Ascorbate peroxidase
CAT: Catalase
MDA: Malondialdehyde
POD: Peroxidase
ROS: Reactive oxygen species
SOD: Superoxide dismutase
H_2O_2: Hydrogen peroxide.

Conflict of Interests

All authors declare that they have no conflict of interests regarding the submitted paper to BioMed Research International.

Acknowledgments

The project was financially supported by 973 Project of National Natural Science Foundation of China and the National High Technology Research and Development Program of China. The authors greatly acknowledge Dr. Noor and Dr. Aziz, Kohat University of Science and Technology, Kohat, Pakistan, for their contribution regarding the final editing of their paper. The submitted paper is a part of the first author postdoctoral research project titled Metabolomic, Proteomic, and Transcriptomic Changes in Upland Cotton under Heavy Metal Stresses.

References

[1] M. K. Daud, S. Ali, M. T. Variath et al., "Differential physiological, ultramorphological and metabolic responses of cotton cultivars under cadmium stress," *Chemosphere*, vol. 93, no. 10, pp. 2593–2602, 2013.

[2] M. D. Groppa, M. P. Ianuzzo, E. P. Rosales, S. C. Vázquez, and M. P. Benavides, "Cadmium modulates NADPH oxidase activity and expression in sunflower leaves," *Biologia Plantarum*, vol. 56, no. 1, pp. 167–171, 2012.

[3] S. S. Gill and N. Tuteja, "Reactive oxygen species and antioxidant machinery in abiotic stress tolerance in crop plants," *Plant Physiology and Biochemistry*, vol. 48, no. 12, pp. 909–930, 2010.

[4] M. K. Daud, Y. Sun, M. Dawood et al., "Cadmium-induced functional and ultrastructural alterations in roots of two transgenic cotton cultivars," *Journal of Hazardous Materials*, vol. 161, no. 1, pp. 463–473, 2009.

[5] P. Aravind and M. N. V. Prasad, "Cadmium-Zinc interactions in a hydroponic system using *Ceratophyllum demersum* L.: adaptive ecophysiology, biochemistry and molecular toxicology," *Brazilian Journal of Plant Physiology*, vol. 17, no. 1, pp. 3–20, 2005.

[6] M. K. Daud, M. T. Variath, S. Ali et al., "Cadmium-induced ultramorphological and physiological changes in leaves of two transgenic cotton cultivars and their wild relative," *Journal of Hazardous Materials*, vol. 168, no. 2-3, pp. 614–625, 2009.

[7] M. Wójcik and A. Tukiendorf, "Cadmium uptake, localization and detoxification in *Zea mays*," *Biologia Plantarum*, vol. 49, no. 2, pp. 237–245, 2005.

[8] D. E. R. Meyers, P. M. Kopittke, G. J. Auchterlonie, and R. I. Webb, "Characterization of lead precipitate following uptake by roots of *Brassica juncea*," *Environmental Toxicology and Chemistry*, vol. 28, no. 11, pp. 2250–2254, 2009.

[9] G. Lannig, A. S. Cherkasov, and I. M. Sokolova, "Temperature-dependent effects of cadmium on mitochondrial and whole-organism bioenergetics of oysters (*Crassostrea virginica*)," *Marine Environmental Research*, vol. 62, no. 1, pp. S79–S82, 2006.

[10] A. Kumar, M. N. V. Prasad, M. M. V. V. Achary et al., "Elucidation of lead-induced oxidative stress in *Talinum triangulare* roots by analysis of antioxidant responses and DNA damage at cellular level," *Environmental Science and Pollution Research*, vol. 20, pp. 4551–4561, 2012.

[11] X. Jin, X. Yang, E. Islam, D. Liu, and Q. Mahmood, "Effects of cadmium on ultrastructure and antioxidative defense system in hyperaccumulator and non-hyperaccumulator ecotypes of *Sedum alfredii* Hance," *Journal of Hazardous Materials*, vol. 156, no. 1–3, pp. 387–397, 2008.

[12] C. H. Foyer and G. Noctor, "Managing the cellular redox hub in photosynthetic organisms," *Plant, Cell and Environment*, vol. 35, no. 2, pp. 199–201, 2012.

[13] M. N. Dos Santos Utmazian, G. Wieshammer, R. Vega, and W. W. Wenzel, "Hydroponic screening for metal resistance and accumulation of cadmium and zinc in twenty clones of willows and poplars," *Environmental Pollution*, vol. 148, no. 1, pp. 155–165, 2007.

[14] G. J. Ahammed, S. P. Choudhary, S. Chen et al., "Role of brassinosteroids in alleviation of phenanthrene-cadmium co-contamination-induced photosynthetic inhibition and oxidative stress in tomato," *Journal of Experimental Botany*, vol. 63, pp. 695–709, 2012.

[15] W. Bilger and O. Björkman, "Role of the xanthophyll cycle in photoprotection elucidated by measurements of light-induced absorbance changes, fluorescence and photosynthesis in leaves of *Hedera canariensis*," *Photosynthesis Research*, vol. 25, no. 3, pp. 173–185, 1990.

[16] B. Ali, Q. Tao, Y. Zhou et al., "5-Aminolevolinic acid mitigates the cadmium-induced changes in *Brassica napus* as revealed by the biochemical and ultra-structural evaluation of roots," *Ecotoxicology and Environmental Safety*, vol. 92, pp. 271–280, 2013.

[17] A. Metwally, V. I. Safronova, A. A. Belimov, and K.-J. Dietz, "Genotypic variation of the response to cadmium toxicity in *Pisum sativum* L.," *Journal of Experimental Botany*, vol. 56, no. 409, pp. 167–178, 2005.

[18] U. Najeeb, G. Jilani, S. Ali, M. Sarwar, L. Xu, and W. Zhou, "Insights into cadmium induced physiological and ultra-structural disorders in *Juncus effusus* L. and its remediation through exogenous citric acid," *Journal of Hazardous Materials*, vol. 186, no. 1, pp. 565–574, 2011.

[19] S. S. Gill, N. A. Khan, and N. Tuteja, "Differential cadmium stress tolerance in five indian mustard (*Brassica juncea* L) cultivars: an evaluation of the role of antioxidant machinery," *Plant Signaling and Behavior*, vol. 6, no. 2, pp. 293–300, 2011.

[20] L. M. Sandalio, H. C. Dalurzo, M. Gómez, M. C. Romero-Puertas, and L. A. Del Río, "Cadmium-induced changes in the growth and oxidative metabolism of pea plants," *Journal of Experimental Botany*, vol. 52, no. 364, pp. 2115–2126, 2001.

[21] I. Ramos, E. Esteban, J. J. Lucena, and A. Gárate, "Cadmium uptake and subcellular distribution in plants of *Lactuca* sp. Cd-Mn interaction," *Plant Science*, vol. 162, no. 5, pp. 761–767, 2002.

[22] B. Ali, C. R. Huang, Z. Y. Qi et al., "5-Aminolevulinic acid ameliorates cadmium-induced morphological, biochemical, and ultrastructural changes in seedlings of oilseed rape," *Environmental Science and Pollution Research*, vol. 20, no. 10, pp. 7256–7267, 2013.

[23] M. Dawood, F. Cao, M. M. Jahangir, G. Zhang, and F. Wu, "Alleviation of aluminum toxicity by hydrogen sulfide is related to elevated ATPase, and suppressed aluminum uptake and oxidative stress in barley," *Journal of Hazardous Materials*, vol. 209-210, pp. 121–128, 2012.

[24] F. A. Bazzaz, G. L. Rolfe, and R. W. Carlson, "Effect of Cd on photosynthesis and transpiration of excised leaves of corn and sunflower," *Physiologia Plantarum*, vol. 32, no. 4, pp. 373–377, 1974.

[25] M. K. Joshi and P. Mohanty, "Chlorophyll A fluorescence as a probe of heavy metal ion toxicity in plants," in *Chlorophyll A Fluorescence: Advances in Photosynthesis and Respiration*, vol. 19, pp. 637–661, Springer, Dordrecht, The Netherlands, 2004.

[26] Á. Solti, L. Gáspár, I. Mészáros, Z. Szigeti, L. Lévai, and É. Sárvári, "Impact of iron supply on the kinetics of recovery of photosynthesis in Cd-stressed poplar (*Populus glauca*)," *Annals of Botany*, vol. 102, no. 5, pp. 771–782, 2008.

[27] A. Vassilev, T. Tsonev, and I. Yordanov, "Physiological response of barley plants (*Hordeum vulgare*) to cadmium contamination in soil during ontogenesis," *Environmental Pollution*, vol. 103, no. 2-3, pp. 287–293, 1998.

[28] N. A. Khan, N. A. Anjum, R. Nazar et al., "Increased activity of ATP-sulfurylase and increased contents of cysteine and glutathione reduce high cadmium-induced oxidative stress in mustard cultivar with high photosynthetic potential," *Russian Journal of Plant Physiology*, vol. 5, pp. 670–677, 2009.

[29] G. Dražić, N. Mihailović, and Z. Stojanović, "Cadmium toxicity: the effect on macro- and micro-nutrient contents in soybean seedlings," *Biologia Plantarum*, vol. 48, no. 4, pp. 605–607, 2004.

[30] M. Gussarsson, H. Asp, S. Adalsteinsson, and P. Jensén, "Enhancement of cadmium effects on growth and nutrient composition of birch (*Betula pendula*) by buthionine sulphoximine (BSO)," *Journal of Experimental Botany*, vol. 47, no. 295, pp. 211–215, 1996.

[31] A. Ros Barceló, "Lignification in plant cell walls," *International Review of Cytology*, vol. 176, pp. 87–132, 1997.

[32] A. Jalil, F. Selles, and J. M. Clarke, "Effect of cadmium on growth and the uptake of cadmium and other elements by durum wheat," *Journal of Plant Nutrition*, vol. 17, no. 11, pp. 1839–1858, 1994.

[33] Y.-Z. Huang, K. Wei, J. Yang, F. Dai, and G.-P. Zhang, "Interaction of salinity and cadmium stresses on mineral nutrients, sodium, and cadmium accumulation in four barley genotypes," *Journal of Zhejiang University Science B*, vol. 8, no. 7, pp. 476–485, 2007.

[34] Y. Li, S. Zhang, W. Jiang et al., "Cadmium accumulation, activities of antioxidant enzymes, and malondialdehyde (MDA) content in *Pistia stratiotes* L.," *Environmental Science and Pollution Research*, vol. 20, pp. 1117–1123, 2013.

[35] X. Tian and Y. Lei, "Nitric oxide treatment alleviates drought stress in wheat seedlings," *Biologia Plantarum*, vol. 50, no. 4, pp. 775–778, 2006.

[36] S. K. Panda, I. Chaudhury, and M. H. Khan, "Heavy metals induce lipid peroxidation and affect antioxidants in wheat leaves," *Biologia Plantarum*, vol. 46, no. 2, pp. 289–294, 2003.

[37] A. Masood, N. Iqbal, and N. A. Khan, "Role of ethylene in alleviation of cadmium-induced photosynthetic capacity inhibition by sulphur in mustard," *Plant, Cell and Environment*, vol. 35, no. 3, pp. 524–533, 2012.

[38] M. Mobin and N. A. Khan, "Photosynthetic activity, pigment composition and antioxidative response of two mustard (*Brassica juncea*) cultivars differing in photosynthetic capacity subjected to cadmium stress," *Journal of Plant Physiology*, vol. 164, no. 5, pp. 601–610, 2007.

[39] H. Küpper, E. Lombi, F.-J. Zhao, and S. P. McGrath, "Cellular compartmentation of cadmium and zinc in relation to other elements in the hyperaccumulator *Arabidopsis halleri*," *Planta*, vol. 212, no. 1, pp. 75–84, 2000.

[40] D. Liu and I. Kottke, "Subcellular localization of cadmium in the root cells of *Allium cepa* by electron energy loss spectroscopy and cytochemistry," *Journal of Biosciences*, vol. 29, no. 3, pp. 329–335, 2004.

[41] L. Zheng, T. Peer, V. Seybold, and U. Lütz-Meindl, "Pb-induced ultrastructural alterations and subcellular localization of Pb in two species of *Lespedeza* by TEM-coupled electron energy loss spectroscopy," *Environmental and Experimental Botany*, vol. 77, pp. 196–206, 2012.

Hindawi Publishing Corporation
BioMed Research International
Volume 2013, Article ID 396487, 9 pages
http://dx.doi.org/10.1155/2013/396487

Research Article

Start-Up Characteristics of a Granule-Based Anammox UASB Reactor Seeded with Anaerobic Granular Sludge

Lei Xiong,[1,2] Yun-Yan Wang,[1,2] Chong-Jian Tang,[1,2] Li-Yuan Chai,[1,2] Kang-Que Xu,[1,2] Yu-Xia Song,[1,2] Mohammad Ali,[1,2] and Ping Zheng[3]

[1] *School of Metallurgy and Environment, Central South University, Changsha 410083, China*
[2] *National Engineering Research Center for Control and Treatment of Heavy Metal Pollution, Changsha 410083, China*
[3] *Department of Environmental Engineering, Zhejiang University, Zijingang Campus, Hangzhou 310058, China*

Correspondence should be addressed to Chong-Jian Tang; chjtang@csu.edu.cn

Received 20 September 2013; Accepted 22 November 2013

Academic Editor: Qaisar Mahmood

The granulation of anammox sludge plays an important role in the high nitrogen removal performance of the anammox reactor. In this study, anaerobic granular sludge was selected as the seeding sludge to start up anammox reactor in order to directly obtain anammox granules. Results showed that the anammox UASB reactor was successfully started up by inoculating anaerobic granular sludge, with substrate capacity of 4435.2 mg/(L·d) and average ammonium and nitrite removal efficiency of 90.36% and 93.29%, respectively. During the start-up course, the granular sludge initially disintegrated and then reaggregated and turned red, suggesting the high anammox performance. Zn-Fe precipitation was observed on the surface of granules during the operation by SEM-EDS, which would impose inhibition to the anammox activity of the granules. Accordingly, it is suggested to relatively reduce the trace metals concentrations, of Fe and Zn in the conventional medium. The findings of this study are expected to be used for a shorter start-up and more stable operation of anammox system.

1. Introduction

Anaerobic ammonia oxidation (anammox) is one of the latest additions to the biogeochemical nitrogen cycle initially discovered in the 1990s [1]. It involves the autotrophic oxidation of ammonium to dinitrogen gas using nitrite as electron acceptor under anaerobic conditions (1) [1, 2]. The process is performed by microorganisms belonging to the order Brocadiales and affiliated to the Planctomycetes:

$$\mathrm{NH_4^+} + 1.32\mathrm{NO_2^-} + 0.066\mathrm{HCO_3^-} + 0.13\mathrm{H^+} \rightarrow 1.0\mathrm{N_2} + 0.26\mathrm{NO_3^-} + 0.066\mathrm{CH_2O_{0.5}N_{0.15}} + 2.03\mathrm{H_2O} \quad (1)$$

In contrast to conventional biological nitrogen removal processes, anammox presents advantages in less operational costs and higher nitrogen removal efficiency due to its low dependency of oxygen, none organic carbon consumption, and less sludge production [2, 3]. Thus, anammox has attracted much attention in the fields of environmental science and engineering. Several full-scale anammox plants have been employed for nitrogen removal from ammonium-rich wastewaters with maximum nitrogen removal rate (NRR) up to 9500 mg/(L · d) [3, 4].

However, the anammox microbes are characterized by a very slow growth rate with their doubling time best estimated at 7–11 d [5]. The enrichment of anammox bacteria from a mixed inoculum requires the optimization of conditions favorable for the anammox bacteria and generally takes 200–300 days [3, 6, 7]. The long start-up has been becoming one choke point on the application of the anammox process.

Study of anammox start-up has been focused on factors that have been found to have an impact on cultivation of anammox bacteria including hydraulic retention time (HRT), dissolved oxygen (DO), inoculum, temperature, wastewater composition, nitrogen compound concentration, and reactor

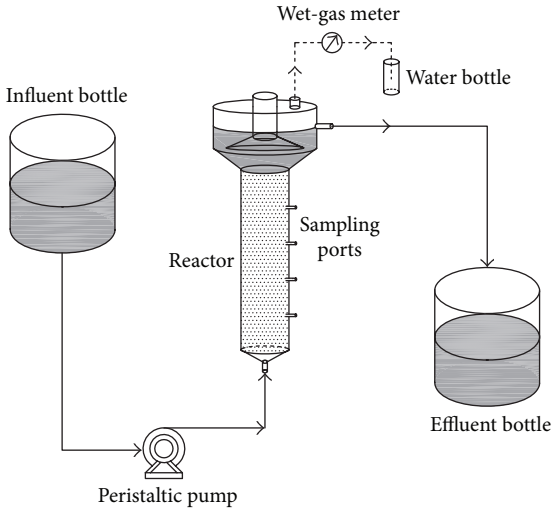

Figure 1: Schematic diagram of the anammox UASB system.

configuration [8–15]. Among researches on anammox start-up course seeded by various conventional sludges [11, 16–23], anaerobic granular sludge has been reported as a preferable inoculum based on compact structure with very good settling properties, high removal efficiency, and strong shock load capacity [24]. During the start-up course, the anaerobic granular sludge can be directly converted into red anammox granules, which plays a crucial role in stable and efficient operation of anammox reactor. However, researches on start-up characteristics of anammox seeded with anaerobic granular sludge are still inadequate, and anaerobic granular sludge's variable properties are currently unclear. In this study, a granule-based anammox UASB reactor seeded with anaerobic granular sludge was started up, and start-up properties were investigated.

2. Materials and Methods

2.1. Anammox Reactor. A plexiglass upflow anaerobic sludge blanket (UASB) reactor (Figure 1) was used in this study. The reactor had a functional working volume of 1.0 L with an internal diameter of 0.5 dm. It was covered with black cloth as conducted by van der Star et al. (2008) [5] to avoid light inhibition, growth of phototrophic organisms, and subsequent oxygen production. The reactor was operated at the temperature of 35 ± 1°C by using a thermostatic water bath.

2.2. Synthetic Wastewater. In this study, the anammox reactor was constantly fed with synthetic wastewater based on tap water, which contained NaH_2PO_4 0.01 g/L, $CaCl_2 \cdot 2H_20$ 0.0056 g/L, $MgS0_4 \cdot 7H_20$ 0.3 g/L, $KHCO_3$ 1.25 g/L and 1 ml/L trace element solution I and II. The concentration of nitrite ($NaNO_2$) and ammonium ($(NH_4)_2SO_4$) was supplied as needed. Trace element solution I consisted of $FeSO_4$ 5 g/L, EDTA 5 g/L. Trace element solution II consisted of EDTA 15 g/L $ZnSO_4 \cdot 7H_2O$ 0.430 g/L, $CuSO_4 \cdot 5H_2O$ 0.250 g/L, $NiCl_2 \cdot 6H_2O$ 0.190 g/L, $NaMoO_4 \cdot 2H_2O$ 0.22 g/L, and H_3BO_4 0.014 g/L [25]. The pH of the influent was set at 6.8.

Table 1: Physical and chemical characteristics of seeding sludge.

Seed sludge	SS/g·L^{-1}	VSS/g·L^{-1}	VSS/SS	Diameter/mm
Anaerobic granular sludge	50.6	42.5	0.84	1-2

2.3. Seed Sludge. The seeding anaerobic granular sludge was taken from an IC reactor in a paper mill wastewater treatment plant located in Hunan Province, China. The characteristics of the seeding sludge are illustrated in Table 1. Before the inoculation, seed granules were washed several times using phosphate buffer (0.14 g/L KH_2PO_4 and 0.75 g/L K_2HPO_4) until the supernatant COD concentration decreased to 10 mg/L.

2.4. Analytical Procedures. The influent and effluent samples were collected on daily basis and were analyzed immediately. Ammonium, nitrite, and nitrate concentrations were determined spectrophotometrically; biomass concentrations were determined as volatile suspended solids (VSS), according to standard methods (APHA, 1998 [26]). Cu and Fe concentrations in the wastewater samples were determined through ICP-AES (iCAP6300). The pH of the wastewater samples was determined by the HANNA pH 211 type acidometer with a selective electrode. Digital macrophotography was performed by the Canon EOS 600D Digital Single Lens Reflex. The energy dispersive spectrum (EDS) is acquired based on the SEM technique.

2.5. SEM. Morphological characteristics of the biomass specimens were observed using SEM model JEOL JSM-6360LV. The biomass specimens were fixed by glutaraldehyde in paraformaldehyde solution for 3 h, subsequently, dehydrated through a graded series of ethanol solution 25%, 50%, 75%, 90%, and 100% (thrice for each concentration), then gold-coated by a sputter, and finally observed under scanning electron microscopy.

3. Results and Discussion

3.1. Start-Up and Performance of the Anammox Reactor. The start-up of anammox reactor, essentially includes activation of bacteria in the system, biomass expansion, and the enhancement of reaction [12]. In this study, reducing hydraulic retention time (HRT) and increasing the inflow nitrogen concentration were alternatively adopted to increase volumetric nitrogen loading rate of the reactor.

According to Tang et al. (2009) [12], the overall start-up of the anammox reactors was divided into four phases, namely, cell lysis phase, lag phase, activity elevation phase, and stationary phase. During cell lysis phase (days 1–29), ammonium concentration of outflow exceeded that of inflow, and ammonium removal rate was below zero (Figure 2(a)). These phenomena could be attributed to the autolysis of

heterotrophic bacteria, which were the dominant microbe of seed sludge. Heterotrophic bacteria went through starving and then died when exposed in medium absence of organic, releasing ammonium to the water through mineralization and finally leading to higher outflow ammonium concentration over inflow [17]. Disintegration of granular sludge was observed by visual observation in the reactor at this time. The autolysis of heterotrophic bacteria released organic matter simultaneously, which was used by denitrifying bacteria as electron donor to denitrify NO_2^--N to nitrogen gas. The effluent nitrite concentration was detected to be zero; meanwhile, apparent gas production was observed in the reactor, suggesting that denitrification did occur in the reactor. In addition, the observed higher outflow pH (Figure 2(d)) further confirmed the hypothesis since denitrification is alkali-induced reaction. As shown in Figure 2(a), the effluent ammonium concentration at the beginning and the end of lag phase was 87.78 mg/L and 62.22 mg/L (when influent ammonium concentration was average 70 mg/L), with the corresponding ammonium removal rate of −42.67 mg/(L · d) and 31.11 mg/(L · d), respectively, (Figure 2(b)), indicating the attenuation of bacteria autolysis. Accordingly, the organic matter (electron donor) in the reactor decreased and denitrification reduced gradually, resulting in the increase of effluent nitrite concentration. The effluent nitrite concentration at the beginning and the end of lag phase was 0 and 7 mg/L (when influent nitrite concentration was average 70 mg/L), with nitrite removal rate slightly decreased from 165 mg/(L·d) to 145 mg/(L · d).

On day 30, the influent and effluent ammonium concentrations were nearly the same, indicating that the start-up turned into the lag phase [12]. This phase was characterized by sharp variations in effluent ammonium concentration (Figure 2(a)) and ammonium removal efficiency (Figure 2(c)). Yang et al. [14] seeded anaerobic granular sludge to start up anammox reactor, and the lag phase lasted for 27 days. Even under sulfate press and seed with nitrifying sludge, the time of the lag phase to start an anammox reactor was no more than 49 day. However, in the present study, no signal indicating the end of lag phase was observed after 73 days of lag phase.

As reported by van der Star et al. [3] and Tang et al. [10, 23, 27, 28], addition of a very small amount of red anammox sludge could significantly enhance the anammox performance in the reactor system, which was confirmed by the experience of start-up of the first full scale anammox reactor in Rotterdam, The Netherland [3]. Therefore, in order to shorten the lag phase and accelerate start-up of the anammox UASB reactor, 10 mL matured red anammox sludge cultivated in our lab-scale high-rate anammox reactors was added to the tested reactor. Soon after the addition, anammox reaction appeared and the nitrogen removal efficiency enhanced continuously, suggesting that the start-up course turned into activity elevation phase (104–148 d). During this phase, ammonium and nitrite concentrations of influent were progressively increased from both 70 mg/L to 229 mg/L and 252 mg/L, respectively. Meanwhile, HRT was reduced from 10 h to 2.5 h gradually. The nitrogen loading rate was continuously elevated from 336 mg/(L · d) to 4617.6 mg/(L · d), along with a progressive increase in the ammonium removal rate from 95.47 mg/(L · d) to 1722 mg/(L · d), and the total nitrogen removal rate was significantly increased to 3768 mg/(L · d). At the same time, effluent nitrite concentration was maintained below 50 mg/L during the whole operation. Based on the mass balance, the percentage of nitrite conversion via anammox rose from 25% to 96%, which indicated that anammox finally dominated the system. Effluent nitrate concentration increased with the average value of 68.73 mg/L. The stoichiometric ratio of the ammonium conversion, nitrite removal, and nitrate production was 1 : 1.26 : 0.44 (Figure 2(e)), which was close to the theoretical value (1 : 1.32 : 0.26) reported by Strous et al. [2]. Higher nitrate production in this research might be associated with trace oxide brought by tap water due to the predeoxidized treatment with influent. During this period, granules' color turned from black to brown and then red subsequently, implying the significant enhancement in the activity of anammox bacteria.

Based on the start-up standard proposed by Jin et al. (2008) [29] (the nitrogen removal rate was higher than 0.5 kg/(m^3 · d)), the anammox UASB reactor was successfully started up. However, the subsequent increase of nitrite concentration after reaching 252 mg/L no longer improved the volumetric substrate nitrogen removal rate (149–164 d), the function of anammox became close to saturation, and the start-up course came into the stationary phase [12]. In order to further increase ammonium removal efficiency and consequently lower effluent ammonium concentration, the ratio of ammonium and nitrite concentration in the influent was set at 1 : 1.2, on the basis of practical reacting ratio value. The reactor ran steadily, certified by ammonium and nitrite removal efficiency up to 95.35% and 100%. Under the total nitrogen loading rate of 4435.2 mg/(L · d), the ammonium and nitrite concentrations in effluent were below 50 mg/L and 25 mg/L, respectively, attaining average ammonium and nitrite removal rate of 1841.6 and 2209.9 mg/(L · d), respectively.

3.2. Characteristics of the Anammox Granules during the Start-up. The apparent characteristics of the seeding anaerobic granular sludge taken from an IC reactor treating paper mill wastewater are shown in Figure 3(a). As shown in Figure 3(a), the anaerobic granules possessed black color and close-to-sphere shape, with a diameter range of 1–3 mm. Scanning electron microscopy (SEM) was used to observe the surface of aggregates along the experiment. The surface of the anaerobic granules was smooth without any acute angle and mainly consisted of bacilli. Filamentous bacteria were also observed (Figures 4(a) and 4(b)).

On day 45, in the start-up course, distinct crack appeared along with the generation of sediment, which has not been mentioned in the anammox literature seen (Figure 4(c)). Moreover, the granular surface became rough. These may be associated with the autolysis of bacteria in the reactor, as illustrated above. Since there is no continuous supply of organic matter, the aboriginal heterotrophic bacteria in the anaerobic granular sludge were starved to death, which might be a leading reason for the granular disintegration.

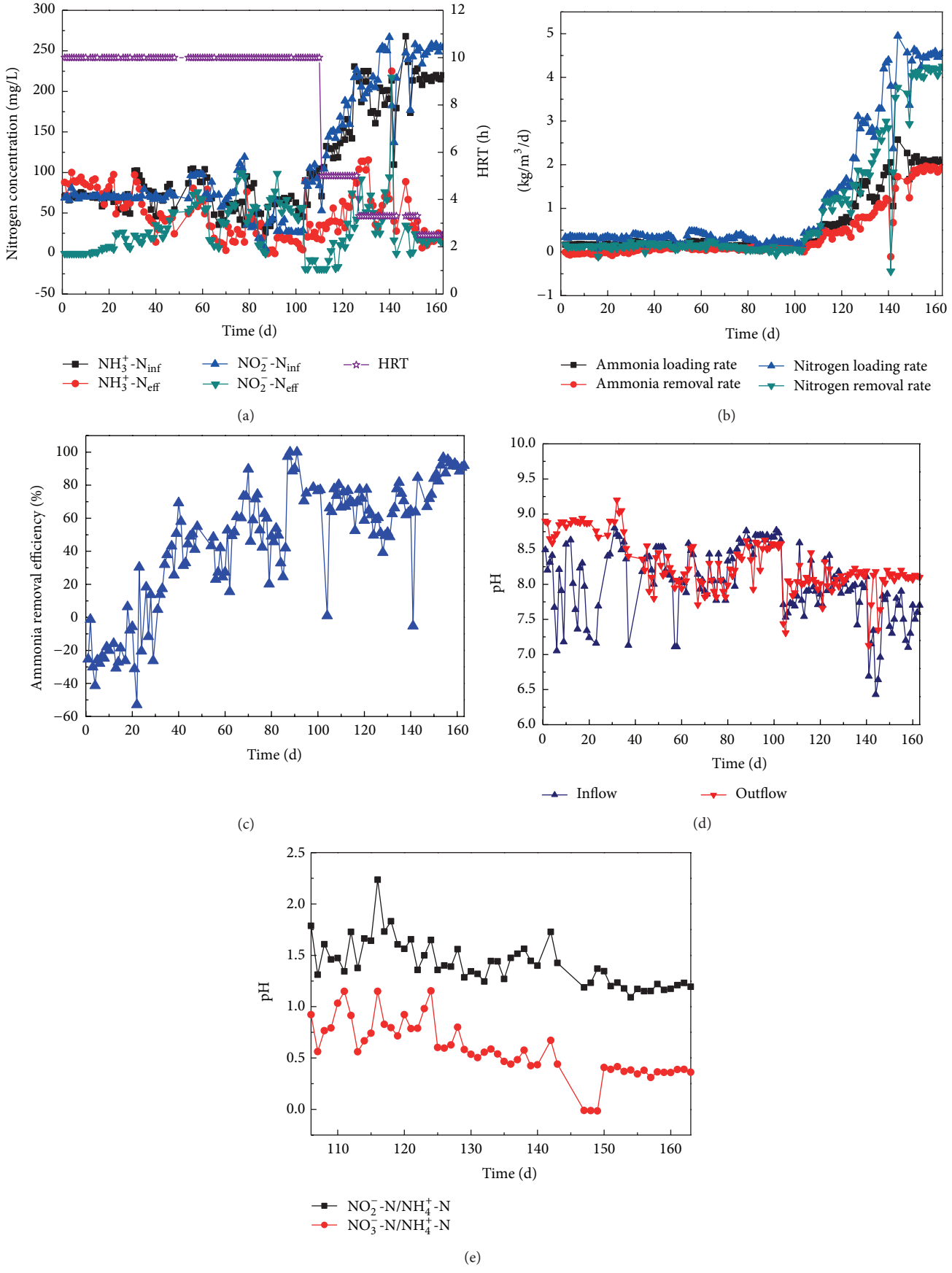

Figure 2: Performance of the anammox reactor.

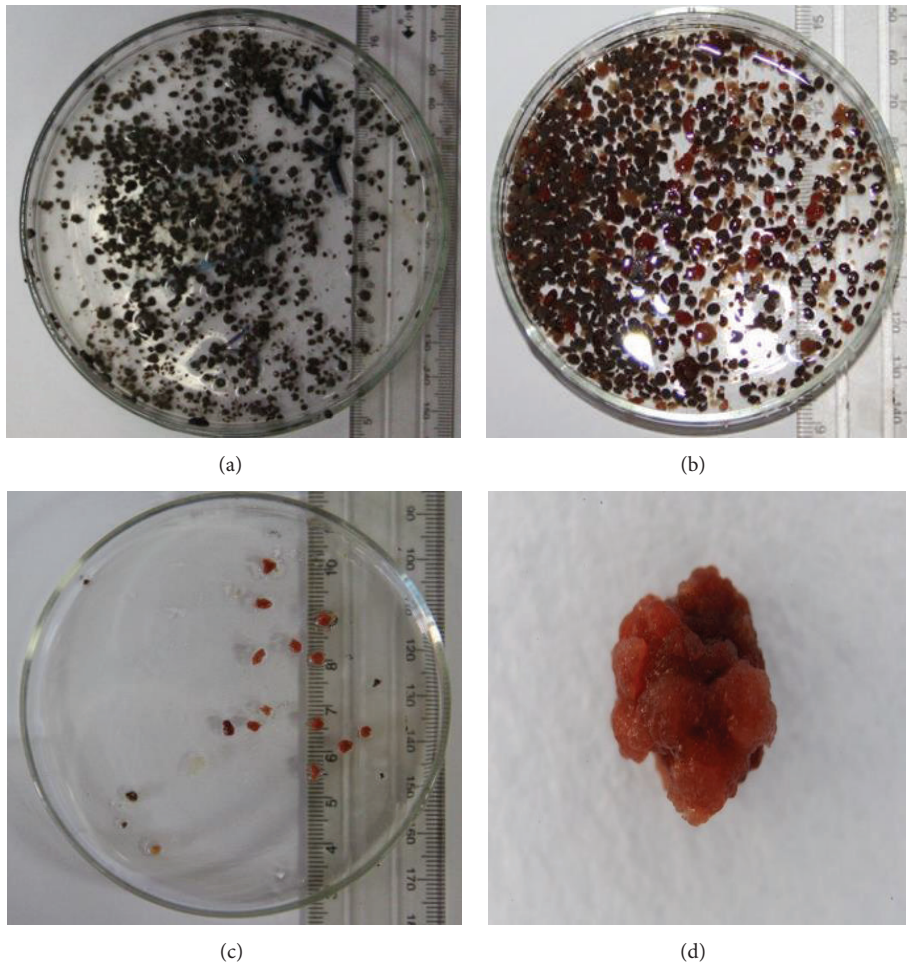

Figure 3: Photograph of granules of biomass (a, b, and c) and a granule (d) on day 0 (a) and day 150 (b, c, and d).

On day 140, the volumetric nitrogen removal rate was up to 3000 mg/(L · d) after the anammox reactor was started up. According to Tang et al. [10], Schmid et al. [30], and Klotz et al. [31], anammox bacteria contained two key enzymes rich in heme *c*, that is, hydroxylamine oxidoreductase and hydrazine oxidoreductase, both of which are important during the anammox metabolic pathway. Thus, anammox granule possessed uniquely carmine color. As shown in Figure 3(b), the proportion of carmine anammox granules was notably larger at this time. The new generated anammox granules were inordinately shaped in contrast with the anoxic seeding granules, with a diameter range of 2-3 mm (Figure 3(d)). Furthermore, SEM observations showed the granules with a high degree of compactness, compact areas on the surface of the granules, fissures with irregular depression surface, morphology, and the sludge hollow phenomenon (Figures 4(e) and 4(f)).

3.3. Precipitation on the Granular Surface. When granular sludge was observed by SEM with a broad view at low magnification, sediments adhering to the granular surface were discovered, as indicated in Figures 5(a) and 5(c). In order to exactly analyze the mineral contents of the precipitation, EDS analysis based on SEM was carried out in the present study. Results showed that the main elements in the sediment were O, S, Fe, and Zn, among which Zn and Fe took a more ascendant part with mass percent of 72% and 8.47% and atomic number ratio of 53% and 7.26%, respectively. It showed that a series of precipitation reactions may occur to generate insoluble Fe-Zn deposits in the reactor. This is a new discovery that was not available in references and would be a new field for the subsequent anammox research.

Based on ICP-AES analysis, the trace metals Fe, and Zn concentrations in the influent and effluent were 1.3, 0.8, and 1.0, 0.3 mg/L, respectively. Based on the mass balances, 0.3 and 0.5 mg/L decrements of Fe and Zn concentrations were observed. Fe and Zn were relatively excess in effluent, revealing that trace elements Fe and Zn were considerably surplus for anammox start-up. Since the number of anammox bacteria was very low in the initial start-up phases, the removal of Fe and Zn by anammox metabolism might be very little. The observed Fe and Zn precipitate on granular surface

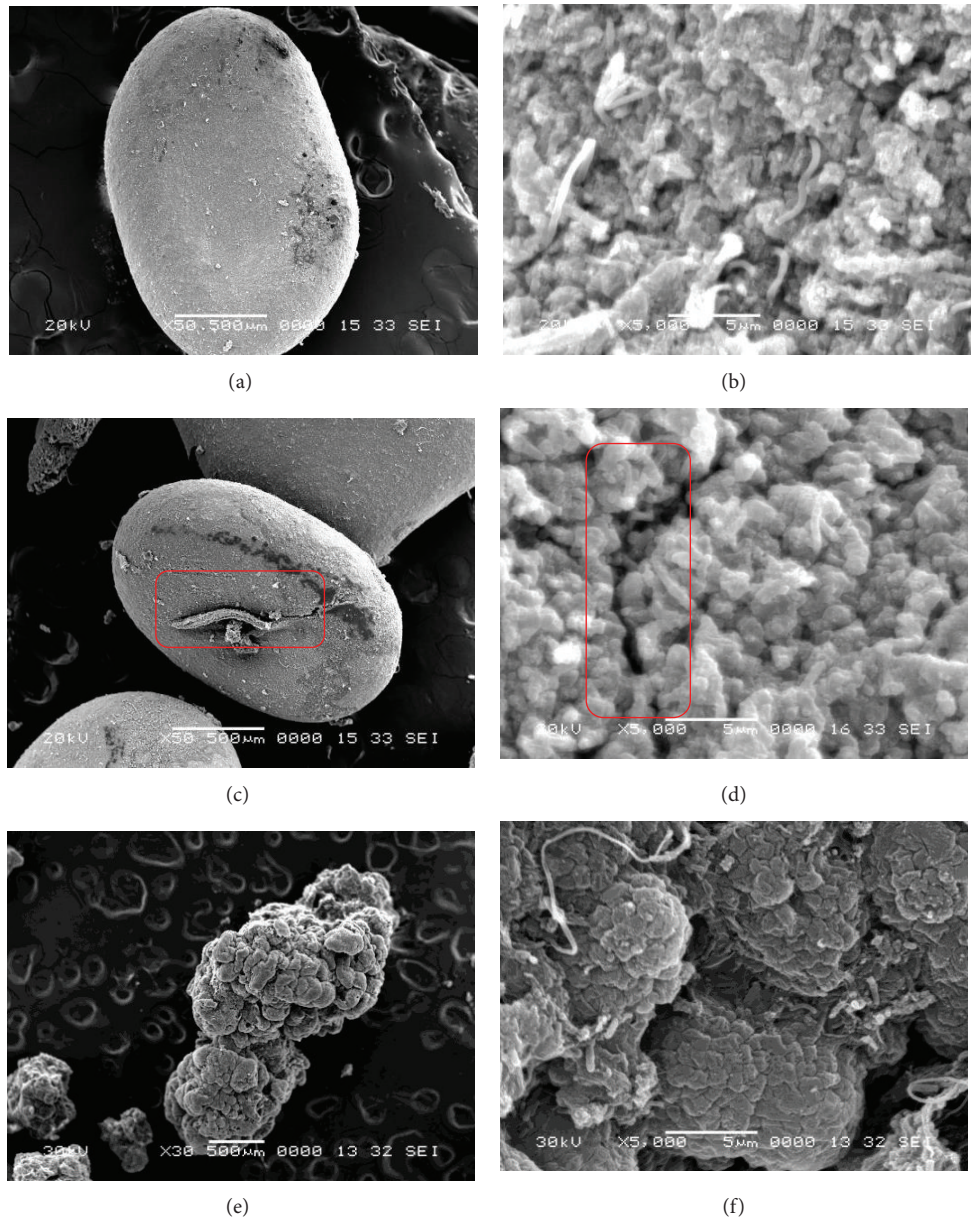

Figure 4: SEM observation of the sludge on day 0 (a, b), day 45 (c, d), and day 150 (e, f) of the start-up. The red square indicates the crack on the granular surface.

further reduced their bioavailability in wastewater, which was not helpful for the anammox process especially in the start-up.

As reported by Trigo et al. (2006) [15], after feeding with the mineral medium proposed by van de Graaf et al. (1995) [25] with 226 mg/L $CaCl_2 \cdot 2H_2O$ and 50 mg/L KH_2PO_4 for 10 days, the reactor performance underwent a sharp decrease from 100 mg/(L · d) to 10 mg/(L · d). The red granules' color gradually changed to light chestnut with time that occurred simultaneously with the observed NVSS accumulation. Salt precipitation was observed and considered as a feasible reason of these phenomena. Elemental analysis of the biomass surface showed that mass percentage of 17.3% calcium and 7.8% phosphorus was detected, and the molar relationship between Ca and P was 1.71, which is close to that of 1.5 of calcium phosphate, indicating that the precipitates were formed by calcium salts, especially by the calcium phosphate salt. After decreasing the calcium and phosphorus concentrations to 5.65 mg/L $CaCl_2 \cdot 2H_2O$ and 10 mg/L KH_2PO_4, both the activity and the nitrogen uptake of the system increased quickly. A maximum nitrogen removal rate of 710 mg/(L · d) was obtained after 185 days' operation. The concentration of NVSS was kept approximately constant around 0.2 g/L, indicating that no additional salt precipitation took place. Additionally, biomass color varied from light chestnut to red color. Therefore, it is concluded that salts precipitation on the

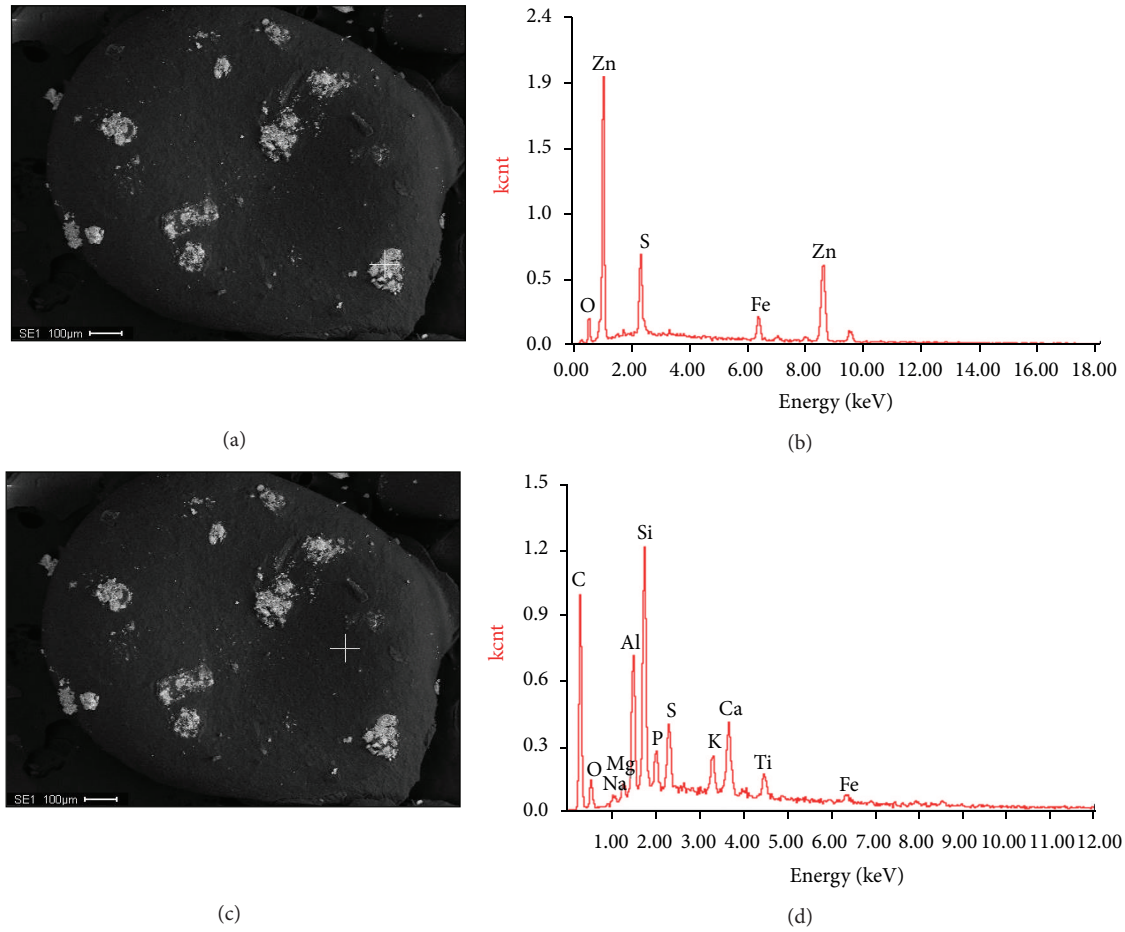

Figure 5: Elemental analysis based on SEM-EDS carried out on day 45 of the start-up, indicating the percentage composition by the mass of the most abundant elements of the precipitate (a, b) and other areas on biomass surface (c, d), respectively.

biomass surface interfered with microbial activity and caused a decrease of the nitrogen removal rate.

In this study, the optimized mineral medium of Trigo et al. (2006) [15] was used to cultivate anammox biomass. During the operation, no calcium phosphate precipitation was detected although the low distribution of calcium and phosphorus on the granular surface was observed (Figures 5(c) and 5(d)). However, Fe-Zn precipitation was surprisingly observed on the granular surface. The chemical precipitates might also interfere with microbial activity and, thus, delay the start-up of anammox reactor, as demonstrated above. Therefore, it is suggested by the present study to relatively reduce the Fe and Zn concentrations in the mineral medium to prevent Fe-Zn precipitation, under which microbial growth might be further ensured.

4. Conclusions

Anammox UASB reactor was successfully started up by inoculating anaerobic granular sludge in the present study. The nitrogen removal performance was enhanced to 4435.2 mg/(L · d) and HRT was minimized to 2.5 h, attaining average ammonium and nitrite removal efficiency of 90.36% and 93.29%, respectively. During the start-up course, the granular sludge experienced a process of initial disintegration and subsequent reaggregation. Disintegration of granules was probably caused by bacteria autolysis. In addition, Zn-Fe precipitation was firstly discovered on the surface of granules during the operation, which could impose inhibition to microbial activity and penalize the start-up of anammox reactor. Therefore, it is suggested to adequately decrease the concentrations of Fe and Zn in mineral medium to avoid Fe-Zn precipitation during the start-up of anammox reactors.

Conflict of Interests

The authors declare that there is no conflict of interests regarding the publication of this paper.

Acknowledgments

The authors acknowledge the financial support by National Funds for Distinguished Young Scientists of China (50925417), the National Natural Science Foundation of

China (51204213), the key project of the Science and Technology Program of Hunan Province (2013WK2007), the Special National Postdoctoral Science Foundation of China (2013T60782), the National Postdoctoral Science Foundation of China (2012M511769), and the Postdoctoral Foundation of Central South University, China.

References

[1] A. Mulder, A. A. Graaf, L. A. Robertson, and J. G. Kuenen, "Anaerobic ammonium oxidation discovered in a denitrifying fluidized bed reactor," *FEMS Microbiology Ecology*, vol. 16, no. 3, pp. 177–184, 1995.

[2] M. Strous, J. G. Kuenen, and M. S. M. Jetten, "Key physiology of anaerobic ammonium oxidation," *Applied and Environmental Microbiology*, vol. 65, no. 7, pp. 3248–3250, 1999.

[3] W. R. L. van der Star, W. R. Abma, D. Blommers et al., "Startup of reactors for anoxic ammonium oxidation: experiences from the first full-scale anammox reactor in Rotterdam," *Water Research*, vol. 41, no. 18, pp. 4149–4163, 2007.

[4] A. Joss, D. Salzgeber, J. Eugster et al., "Full-scale nitrogen removal from digester liquid with partial nitritation and anammox in one SBR," *Environmental Science and Technology*, vol. 43, no. 14, pp. 5301–5306, 2009.

[5] W. R. van der Star, A. I. Miclea, U. G. van Dongen, G. Muyzer, C. Picioreanu, and M. van Loosdrecht, "The membrane bioreactor: a novel tool to grow anammox bacteria as free cells," *Biotechnology and Bioengineering*, vol. 101, no. 2, pp. 286–294, 2008.

[6] A. Dapena-Mora, J. L. Campos, A. Mosquera-Corral, M. S. M. Jetten, and R. Méndez, "Stability of the ANAMMOX process in a gas-lift reactor and a SBR," *Journal of Biotechnology*, vol. 110, no. 2, pp. 159–170, 2004.

[7] M. Jetten, I. Cirpus, B. Kartal et al., "1994–2004: 10 Years of research on the anaerobic oxidation of ammonium," *Biochemical Society Transactions*, vol. 33, no. 1, pp. 119–123, 2005.

[8] S. Suneethi and K. Joseph, "ANAMMOX process start up and stabilization with an anaerobic seed in anaerobic membrane bioreactor (AnMBR)," *Bioresource Technology*, vol. 102, no. 19, pp. 8860–8867, 2011.

[9] Y. Tao, D. Gao, Y. Fu, W. Wu, and N. Ren, "Impact of reactor configuration on anammox process start-up: MBR versus SBR," *Bioresource Technology*, vol. 104, pp. 73–80, 2012.

[10] C.-J. Tang, P. Zheng, B.-L. Hu, J.-W. Chen, and C.-H. Wang, "Influence of substrates on nitrogen removal performance and microbiology of anaerobic ammonium oxidation by operating two UASB reactors fed with different substrate levels," *Journal of Hazardous Materials*, vol. 181, no. 1–3, pp. 19–26, 2010.

[11] I. Tsushima, T. Kindaichi, and S. Okabe, "Quantification of anaerobic ammonium-oxidizing bacteria in enrichment cultures by real-time PCR," *Water Research*, vol. 41, no. 4, pp. 785–794, 2007.

[12] C.-J. Tang, P. Zheng, Q. Mahmood, and J.-W. Chen, "Start-up and inhibition analysis of the Anammox process seeded with anaerobic granular sludge," *Journal of Industrial Microbiology and Biotechnology*, vol. 36, no. 8, pp. 1093–1100, 2009.

[13] S. Bagchi, R. Biswas, and T. Nandy, "Start-up and stabilization of an Anammox process from a non-acclimatized sludge in CSTR," *Journal of Industrial Microbiology and Biotechnology*, vol. 37, no. 9, pp. 943–952, 2010.

[14] Z. Yang, S. Zhou, and Y. Sun, "Start-up of simultaneous removal of ammonium and sulfate from an anaerobic ammonium oxidation (anammox) process in an anaerobic up-flow bioreactor," *Journal of Hazardous Materials*, vol. 169, no. 1–3, pp. 113–118, 2009.

[15] C. Trigo, J. L. Campos, J. M. Garrido, and R. Méndez, "Start-up of the Anammox process in a membrane bioreactor," *Journal of Biotechnology*, vol. 126, no. 4, pp. 475–487, 2006.

[16] K. Pynaert, B. F. Smets, D. Beheydt, and W. Verstraete, "Start-up of autotrophic nitrogen removal reactors via sequential biocatalyst addition," *Environmental Science and Technology*, vol. 38, no. 4, pp. 1228–1235, 2004.

[17] N. Chamchoi and S. Nitisoravut, "Anammox enrichment from different conventional sludges," *Chemosphere*, vol. 66, no. 11, pp. 2225–2232, 2007.

[18] J. Nakajima, M. Sakka, T. Kimura, K. Furukawa, and K. Sakka, "Enrichment of anammox bacteria from marine environment for the construction of a bioremediation reactor," *Applied Microbiology and Biotechnology*, vol. 77, no. 5, pp. 1159–1166, 2008.

[19] Z.-X. Quan, S.-K. Rhee, J.-E. Zuo et al., "Diversity of ammonium-oxidizing bacteria in a granular sludge anaerobic ammonium-oxidizing (anammox) reactor," *Environmental Microbiology*, vol. 10, no. 11, pp. 3130–3139, 2008.

[20] J. van de Vossenberg, J. E. Rattray, W. Geerts et al., "Enrichment and characterization of marine anammox bacteria associated with global nitrogen gas production," *Environmental Microbiology*, vol. 10, no. 11, pp. 3120–3129, 2008.

[21] B. Ni, Y. Chen, S. Liu, F. Fang, W. Xie, and H. Yu, "Modeling a granule-based anaerobic ammonium oxidizing (ANAMMOX) process," *Biotechnology and Bioengineering*, vol. 103, no. 3, pp. 490–499, 2009.

[22] K. W. Lawrence, H. L. Howard, and T. H. Yung, *Waste Treatment in the Process Industries*, CRC Press, New York, NY, USA, 2005.

[23] C.-J. Tang, P. Zheng, C.-H. Wang, and Q. Mahmood, "Suppression of anaerobic ammonium oxidizers under high organic content in high-rate Anammox UASB reactor," *Bioresource Technology*, vol. 101, no. 6, pp. 1762–1768, 2010.

[24] A. Franco, E. Roca, and J. M. Lema, "Granulation in high-load denitrifying upflow sludge bed (USB) pulsed reactors," *Water Research*, vol. 40, no. 5, pp. 871–880, 2006.

[25] A. A. van de Graaf, A. Mulder, P. De Bruijn, M. S. M. Jetten, L. A. Robertson, and J. G. Kuenen, "Anaerobic oxidation of ammonium is a biologically mediated process," *Applied and Environmental Microbiology*, vol. 61, no. 4, pp. 1246–1251, 1995.

[26] American Public Health Association (APHA), *Standard Methods for the Examination of Water and Waste Water*, American Public Health Association, Washington, DC, USA, 20th edition, 1998.

[27] C.-J. Tang, P. Zheng, C.-H. Wang et al., "Performance of high-loaded ANAMMOX UASB reactors containing granular sludge," *Water Research*, vol. 45, no. 1, pp. 135–144, 2011.

[28] C.-J. Tang, P. Zheng, L. Zhang et al., "Enrichment features of anammox consortia from methanogenic granules loaded with high organic and methanol contents," *Chemosphere*, vol. 79, no. 6, pp. 613–619, 2010.

[29] R.-C. Jin, P. Zheng, A.-H. Hu, Q. Mahmood, B.-L. Hu, and G. Jilani, "Performance comparison of two anammox reactors: SBR and UBF," *Chemical Engineering Journal*, vol. 138, no. 1–3, pp. 224–230, 2008.

[30] M. C. Schmid, A. B. Hooper, M. G. Klotz et al., "Environmental detection of octahaem cytochrome c hydroxylamine/hydrazine oxidoreductase genes of aerobic and anaerobic ammonium-oxidizing bacteria," *Environmental Microbiology*, vol. 10, no. 11, pp. 3140–3149, 2008.

[31] M. G. Klotz, M. C. Schmid, M. Strous, H. J. M. Op Den Camp, M. S. M. Jetten, and A. B. Hooper, "Evolution of an octahaem cytochrome c protein family that is key to aerobic and anaerobic ammonia oxidation by bacteria," *Environmental Microbiology*, vol. 10, no. 11, pp. 3150–3163, 2008.

Hindawi Publishing Corporation
BioMed Research International
Volume 2013, Article ID 957853, 8 pages
http://dx.doi.org/10.1155/2013/957853

Research Article

Combined Industrial Wastewater Treatment in Anaerobic Bioreactor Posttreated in Constructed Wetland

Bibi Saima Zeb,[1] Qaisar Mahmood,[1] Saima Jadoon,[2] Arshid Pervez,[1] Muhammad Irshad,[1] Muhammad Bilal,[1] and Zulfiqar Ahmad Bhatti[1]

[1] *Department of Environmental Sciences, COMSATS Institute of Information Technology, Abbottabad 22060, Pakistan*
[2] *Department of Natural Resources Engineering and Management, University of Kurdistan, Hewler, Iraq*

Correspondence should be addressed to Qaisar Mahmood; mahmoodzju@gmail.com

Received 17 October 2013; Accepted 13 November 2013

Academic Editor: Chong-Jian Tang

Constructed wetland (CW) with monoculture of *Arundo donax* L. was investigated for the posttreatment of anaerobic bioreactor (ABR) treating combined industrial wastewater. Different dilutions of combined industrial wastewater (20, 40, 60, and 80) and original wastewater were fed into the ABR and then posttreated by the laboratory scale CW. The respective removal efficiencies of COD, BOD, TSS, nitrates, and ammonia were 80%, 78–82%, 91.7%, 88–92%, and 100% for original industrial wastewater treated in ABR. ABR was efficient in the removal of Ni, Pb, and Cd with removal efficiencies in the order of Cd (2.7%) > Ni (79%) > Pb (85%). Posttreatment of the ABR treated effluent was carried out in lab scale CW containing *A. donax* L. CW was effective in the removal of COD and various heavy metals present in ABR effluents. The posttreatment in CW resulted in reducing the metal concentrations to 1.95 mg/L, 0 mg/L, and 0.004 mg/L for Ni, Pb, and Cd which were within the permissible water quality standards for industrial effluents. The treatment strategy was effective and sustainable for the treatment of combined industrial wastewater.

1. Introduction

Pakistan's current population of 180 million is expected to grow to about 221 million by the end of year 2025 [1]. In Pakistan and other developing countries, water pollution is a major threat to the livelihood of people [2]. The heavy metals contamination of aquatic and terrestrial ecosystems is a major environmental problem. Each pollution problem calls for specific optimal and cost-effective solution; if one technology proves less or ineffective, the other takes its place. It is indispensable to treat industrial wastewaters for their subsequent use for irrigation, drinking, and other purposes. In addition, due to an increased scarcity of clean water, there is a need for appropriate management of available water resources [3]. The factors like profound demographic, economic changes and global energy crisis are compelling the implementation of low-cost natural treatment systems for the domestic and industrial wastewaters [1].

In the recent years, the wastewater treatment strategies have been shifted to one of the most promising methods, that is, biological anaerobic treatment with the adoption of high rate anaerobic systems like upflow anaerobic sludge blanket (UASB) and other related treatment systems. The outstanding characteristics of high rate ABR include the anaerobic microorganisms capable of aggregation, low operational and maintenance costs, energy recovery in the form of biogas, low energy consumption, and low production of digested sludge [4–7]. In developing countries like India, Brazil, and Colombia, where financial resources are generally scarce due to high energy costs, the process is familiar as one of the most feasible methods for the wastewater treatment. Despite several modifications, the quality of ABR treated effluent hardly ever meets the discharge standards [6, 8]. Lettinga and coresearchers applied ABR process for municipal wastewater treatment since early 1980 [9–13] and reported that about 70% of chemical oxygen demand (COD) removal can be achieved under warm climates [6, 14, 15]. Since its inception, wider hype has been gained by this process [16, 17]. The ABR treated effluents can be employed for irrigation of various crops. However, such type of effluent may be high in chemical oxygen demand (COD), biochemical oxygen demand (BOD), and coliforms [18]. Thus, additional posttreatment strategy

is mandatory for the ABR treated effluents if further use is desired [19–21].

CW wastewater treatment systems are engineered structures specifically designed for treating wastewater by optimizing the physical, chemical, and biological processes that occur in natural wetland ecosystems [1, 18, 22–24]. CW is known as green technology which uses plants for the removal of contaminants from a specified area, and process is known as phytoremediation [25]. CW is a low-cost or economical on-site wastewater treatment technology which is not only effective but also aesthetically pleasing. Since 1980 the utilization of the CW for the treatment of variety of wastewater has quickly become widespread. The amount of nutrients removed by plants and stored in their tissues is highly relative which depends on the plant type, biomass, and nutrient concentration in tissues [26].

The plant species, media like sand and gravel of specific ratio and size, and containers are the foundation materials for CW. There are two major types of CW, subsurface flowing water (SSF) CW and free water surface (FWS) flowing CW. A variety of macrophytes are used in CW and most common are floating macrophytes (i.e., *Lemna* spp. or *Eichhornia crassipes*), submerged macrophytes (i.e., *Elodea canadensis*), and rooted emergent macrophytes (i.e., *Phragmites australis* and *Typha angustifolia*). The plants roots create conducive environment for the microbial growth and in winter the plant litter acts as insulator. CW is attached growth biological reactors, which tender higher pollutant removal efficiency through physical, chemical, and biological mechanisms. The common removal mechanisms associated with wetlands include sedimentation, coagulation, adsorption, filtration, biological uptake, and microbial transformation [3, 24, 27].

CW technology is well known at present, but it is not well documented for treating specific industrial effluents [28–30]. A variety of posttreatment configurations based on various combinations with ABR have been studied; ABR followed by final polishing units (FPU) or polishing pond (PP) is a common process used in India, Colombia, and Brazil due to its simplicity in operation [6, 31–33]. The implementation of low-cost, simple mitigation measures is required for the timely control and sustainable management of pollution problems in developing countries. The objective of this study was to evaluate the performance of ABR for the treatment of combined industrial wastewater followed by posttreatment in CW planted with *A. donax.*

2. Materials and Methods

2.1. Collection of Wastewater and Treatment. The industrial wastewater was collected from combined drain at Hattar Industrial Estate, Hattar, Pakistan, as grab samples. The physicochemical parameters like pH, turbidity, and EC were determined onsite while the rest were analyzed in the laboratory within 24 h. As a treatment strategy and to avoid toxic effects of the pollutants, various dilutions of wastewater included 20, 40, 60, and 80% to feed into ABR, after which original wastewater was also treated in ABR and then CW.

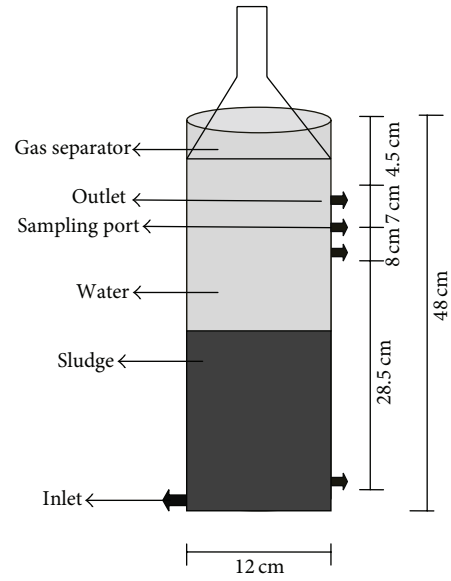

Figure 1: Schematic diagram of a lab scale anaerobic bioreactor with its dimensions.

2.2. ABR Experimental Setup. This research work was carried out in the bioremediation laboratory of COMSATS Institute of Information Technology, Abbottabad, Pakistan. In this study ABR was used as a primary treatment step. A lab scale ABR was operated in upflow mode with biomass retention as shown in Figure 1. The reactor is made of Perspex with a working volume of 5 liters. The influent was pumped into ABR using peristaltic pump from the influent vessel to the reactor (Figure 1). The flow rate was adjusted according to results of startup study. A recycling pump was used to mix the influent (substrate) and sludge (biocatalyst) and to decrease possible substrate inhibition. The ratio of recycle flow to the influent flow was set at about 2.5–3. Bioreactor startup was carried out by feeding synthetic wastewater and nutrient solution at various organic loading rate (OLR) and COD by using organic compounds, at a fixed Hydraulic retention time (HRT) but increasing OLR and at fixed OLR but decreasing HRT.

Industrial wastewater samples were collected from Hattar Industrial Estate (Haripur, Pakistan) after characterization and were fed into the ABR. Different dilutions of real industrial wastewater were made to avoid the reactor disturbances before feeding to ABR.

2.3. Experimental Setup. The lab scale experimental constructed wetland consists of two independent rectangular basins (length: 120 cm, width: 90 cm, and depth: 40 cm). The basins were filled with gravel, sand, and soil from bottom to top with one layer of each as shown in Figure 2. Each basin had a 10% slope and was equipped with a nozzle outlet for discharging the treated effluent. The CW was planted with *A. donax* (6 shoots/m^2) taken from the botanical garden of the institute.

An unplanted bed served as a control. Treated effluents were collected directly from the lab scale experimental plant

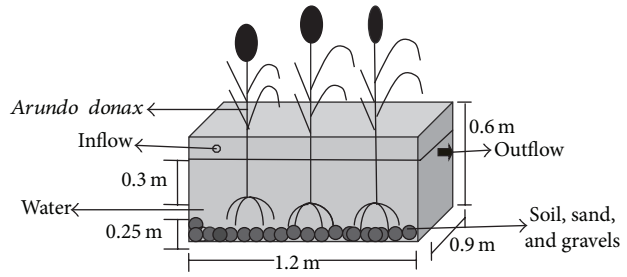

Figure 2: Schematic diagram of a laboratory scale CW for the treatment of combined industrial wastewater.

Table 1: Dimensions and operating conditions of experimental CW.

Dimensions of CW	
Length	1.2 m
Width	0.9 m
Total height	0.6 m
Total container volume	0.432 m^3
Water depth	0.3 m
Substrate depth	0.25 m
Plant name	*Arundo donax* L. (giant reed)
No. of rhizome/m^2	3
Operating conditions	
OLR	538 kg/ha/d
HRT	3 days
HLR	862 m^3/ha/d

of the wastewater treatment laboratory. The operational conditions of the experimental setup of CW are shown in Table 1. All plants, sand, and gravel were properly washed before planting to CW system.

Pollutant removal rates (%) were calculated according to the following equation:

$$R\ (\%) = \left[1 - \left(\frac{Cf}{Ci}\right)\right] \times 100, \quad (1)$$

where R is the removal rate, Ci is the concentration (mg/L) of the considered parameter in the untreated WW (influent), and Cf is the concentration (mg/L) of the considered parameter in the treatment bed effluent.

2.4. Analytical Procedures. Raw and treated samples were analyzed for their BOD, COD, EC, pH, turbidity, and so forth, according to the standard methods [34]. For COD determination closed reflux, calorimetric method included digestion at 150°C for 2 h in COD vials followed by spectrophotometer reading at 530 nm [34]. The pH was measured using a digital pH meter (HANNA, HI 991003 Sensor Check pH) and TDS and conductivity by HANNA, HI9835 Microprocessor for conductivity and TDS. Heavy metals were analyzed through atomic absorption spectrophotometer. At least three readings were taken for each parameter each time and then mean value was calculated.

2.5. Statistical Analysis. Collected data were analyzed by the descriptive statistics and arithmetic averages of percent removal were calculated using Microsoft Excel XP version 2010 and Origin Lab 8.

3. Results and Discussion

3.1. Characterization of Combined Industrial Wastewater. Physicochemical characteristics of industrial wastewater were depicted in Table 2. Four different dilutions (20%, 40%, 60%, and 80%) and original WW from HIE had the following characteristics.

3.2. Pretreatment of Combined Industrial Wastewater in ABR. The ABR was fed with combined industrial wastewater for treatment at retention time of 12 h. The treated effluent characteristics and percent removal efficiency was showed in Table 3.

The results described the performance of the ABR for the treatment of combined industrial wastewater, as the concentrations of COD before pretreatment were 70, 189, 284, 379, and 474 mg/L, respectively, for four different dilutions of 20, 40, 60, and 80 and original wastewater. After pretreatment with ABR the COD was reduced to 42, 54, 121, 159, and 297 mg/L with 40.0, 40.8, 57.3, 58.0, and 37.3% removal efficiency, respectively. The results in Figure 3 showed the maximum COD removal efficiency for the 80% dilution of the wastewater through ABR. The ABR also reduced the BOD concentrations of the dilutions from 78 to 82% as shown in Figure 3. The BOD concentration reduced from 23.3, 25.4, 50.9, 77.0 and 84.8 mg/L to 18.5, 4.16, 5.1, 10.2, and 18.5, respectively. It was observed from the results that ABR showed excellent removal efficiency for BOD removal.

Total solids were tremendously removed by 91.7% with the corresponding concentration of 1400 mg/L for original wastewater. The concentration of NO_3-N was reduced from 24, 59, 83, 98, and 145 to 1.8, 6.1, 9.23, 8.9, and 16 mg/L for 20, 40, 60, and 80 and original wastewater. ABR showed 88 to 92% removal efficiency for the NO_3-nitrogen as shown in Figure 4.

Similarly, the removal efficiency of NH_4-N was 87.6, 90.8, 90, 85.9, and 87.8% for the four different dilutions 20, 40, 60, and 80 and original wastewater, respectively, as shown in Figure 4. The concentrations of NH_4-N 17, 23, 45, 57, and 82 mg/L were reduced to 2.1, 2.1, 4.5, 8, and 10 mg/L. On the other hand, Pb, Ni, and Cd removal by reactor was 2.7%, 79%, and 85% for real industrial wastewater. The heavy metals removal were found in order Cd > Ni > Pb shown in Figure 5.

The previous workers observed that the treatment of complex industrial wastewater reduced the efficiency of the ABR as in the present study [35]. During anaerobic digestion processes of organic matter the biochemical reaction takes place which is affected by the heavy metals presence [35]. It is clear from the results that soluble heavy metals rapidly decreased at the initial concentrations. It depends on which chemical form the heavy metal is existed. The most common and important form of the heavy metals are precipitation (as sulfides, carbonates, and hydrocarbons) and sorption on to

Table 2: Characterization of four different dilutions and original WW of combined industrial wastewater.

Parameters	Influent/raw wastewater dilutions				
	20%	40%	60%	80%	Original WW
pH	8.1	8.48	8.6	8.76	10.2
Conductivity (μs)	627	646	645	676	702
TDS	378	330	344	394	411
TS	712	812	780	1333	1400
VS	600	520	1050	1160	1960
COD	70	189	284	379	474
BOD	23.3	25.4	50.9	77	84.8
Nitrates	24	59	83	98	145
Ammonia	17	23	45	57	82
Lead	0.131	0.653	1.335	1.851	2.337
Nickel	0.117	0.225	0.315	0.271	0.403
Cadmium	0.026	0.021	0.009	0.026	0.048

The values are given as mg/L except pH and conductivity.

Table 3: The performance of ABR in treating combined industrial effluents.

Parameters	Influent/raw wastewater					ABR effluent					% removal				
	20%	40%	60%	80%	Original WW	20%	40%	60%	80%	Original WW	20%	40%	60%	80%	Original WW
pH	8.1	8.48	8.6	8.76	10.2	7.89	8.31	8.52	8.66	8.41	—	—	—	—	—
Conductivity (μs)	627	646	645	676	702	654	616	645	687	702	—	—	—	—	—
TDS	378	330	344	394	411	339	324	334	357	365	10	2	3	9	11
TS	712	812	780	1333	1400	83	85	93	215	115	88	89.5	88	83.8	91.7
VS	600	520	1050	1160	1960	45	86.3	163.9	97.2	305	92	83.5	86	90	84
COD	70	189	284	379	474	42	54	121	159	297	40	47.8	57.3	58.04	37.34
BOD	23.3	25.4	50.9	77	84.8	18.5	4.16	5.1	10.2	18.5	82	80	80	81	78
Nitrates	24	59	83	98	145	1.8	6.1	9.23	8.9	16	92.5	89.6	88.8	90.9	88.9
Ammonia	17	23	45	57	82	2.1	2.1	4.5	8	10	87.6	90.8	90	85.9	87.8
Lead	0.131	0.653	1.335	1.851	2.337	0.558	0.653	1.222	2.109	2.703	64	27.8	8.46	7.4	2.7
Nickle	0.117	0.225	0.315	0.271	0.403	0.079	0.015	0.035	0.074	1.014	92.1	93.4	87	79	79
Cadmium	0.026	0.021	0.009	0.026	0.048	0.009	0.008	0.001	0.009	0.007	65.4	62	88.9	96.2	85.4

The values are given as mg/L except pH and conductivity.

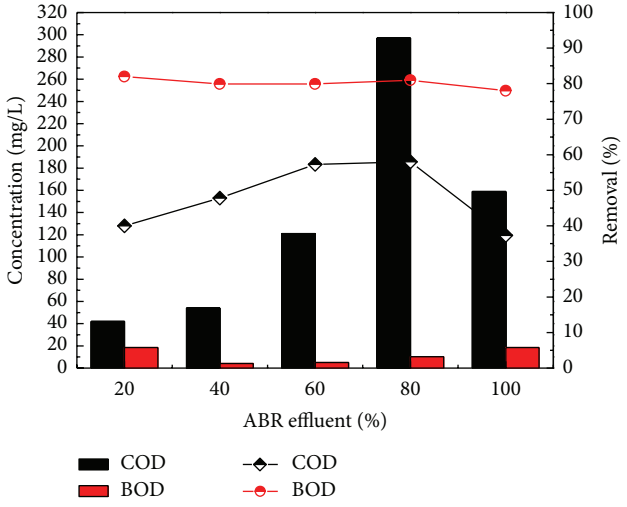

Figure 3: COD removal efficiency of a lab scale ABR reactor for combined industrial wastewater.

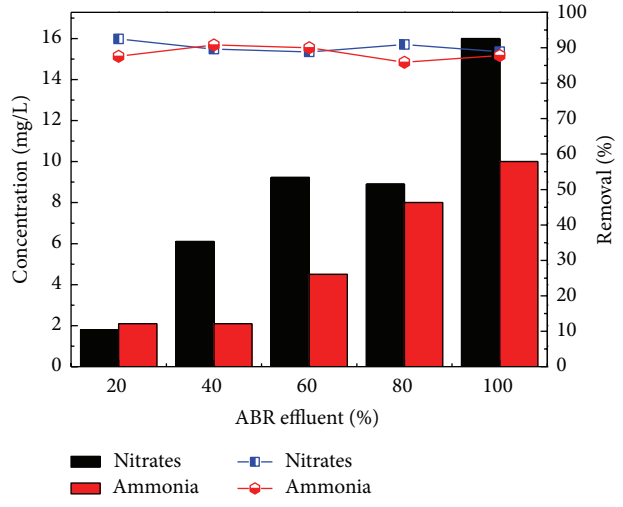

Figure 4: Nitrates Removal efficiency of pretreatment of combined industrial wastewater with ABR.

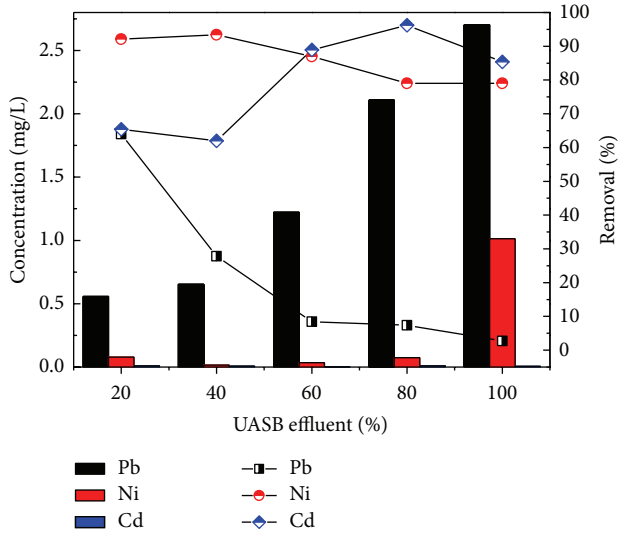

Figure 5: Removal efficiency of Pb, Ni, and Cd by ABR.

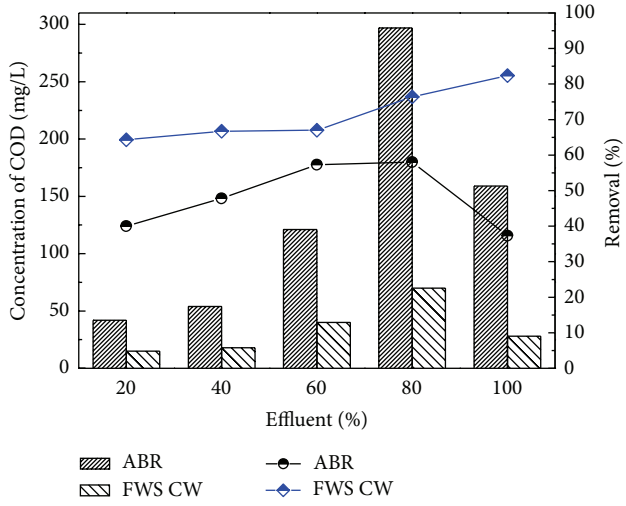

Figure 6: Comparison of ABR and CW for COD removal.

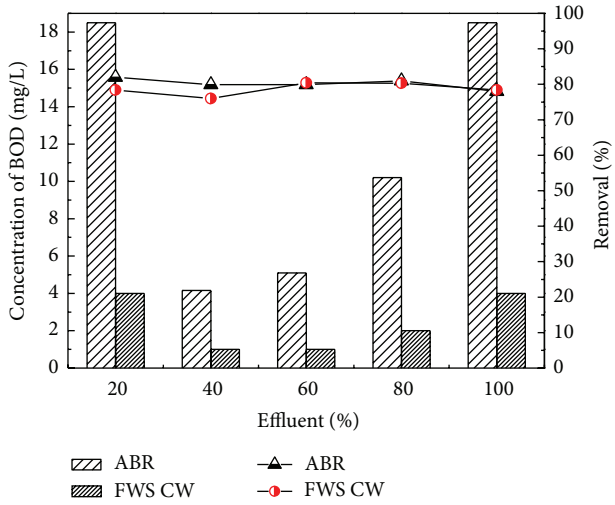

Figure 7: Comparison of ABR and CW for BOD removal.

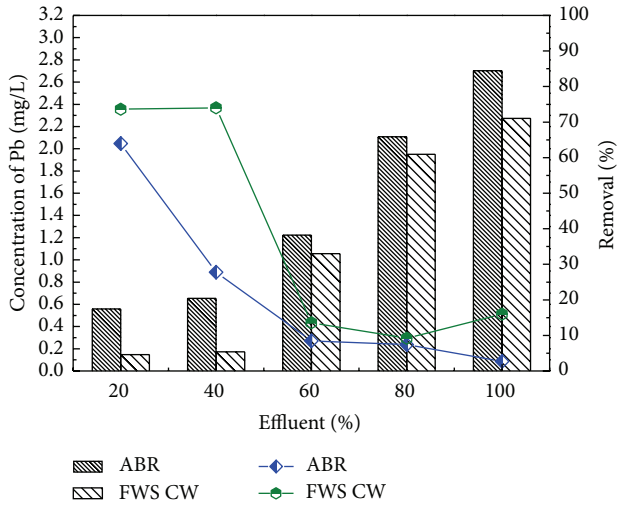

Figure 8: Comparison of % removal efficiency of Pb in ABR and FWS CW.

solid form (Inhibition effect of heavy metals on anaerobic sludge) [36]. Ni could be bound in all forms. So it was cleared that high initial concentrations were tolerated by the ABR sludge and thus showed the satisfactory removal of the heavy metals.

However, the residual concentration of organic (BOD and COD) and heavy metals in the anaerobic reactor effluent usually exceeds the maximum permissible level prescribed by the effluent discharge standards of most developing countries [20, 37, 38]. From this standpoint, posttreatment of anaerobic effluent is necessary to reduce these contaminants to the required level [39].

3.3. Posttreatment of ABR Effluent with Constructed Wetland. The pretreated effluent was then further treated by CW at HRT of 3 days for each dilution. The results for FWS CW effluent are shown in Figures 6, 7, 8, 9, and 10 with pollutant percent removal efficiency.

The results of treatment in CW showed efficient removal efficiency for COD, BOD, TS, nitrates, ammonia, and heavy metals like Pb, Ni, and Cd. The residual concentration of COD and BOD was 64.3, 66.7, 67, 76.4, and 82.4 and 78.4, 76, 80.3, 80.3, and 78.4 mg/L, respectively, for the corresponding dilutions of 20, 40, 60, and 80 and original WW as shown in Figures 6 and 7. The CW showed the highest COD removal efficiency of 82.4% for original WW, but at the same dilution the BOD was reduced to 78.4%. Nitrates and ammonia removal efficiency was found to be 95, 82, 86, 72, and 75% for the respective concentrations of 1.8, 6.1, 9.23, 8.9, and 16 mg/L of the corresponding four different dilutions and original pretreated effluent. Ammonia removal was not satisfactory as compared to other parameters and the highest removal efficiency was 70.1% by CW.

CW normally improves the DO in wetland. The introduction of excess organic matter may result in a depletion of oxygen from an aquatic system. Prolonged exposure to low

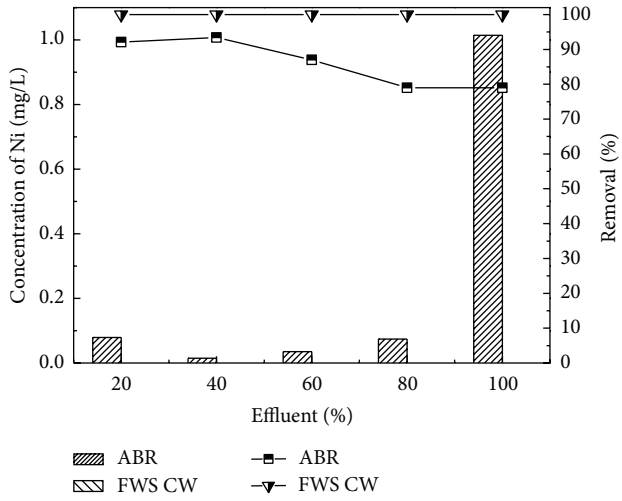

Figure 9: Comparison of percent removal efficiency of Ni in ABR and FWS SCW.

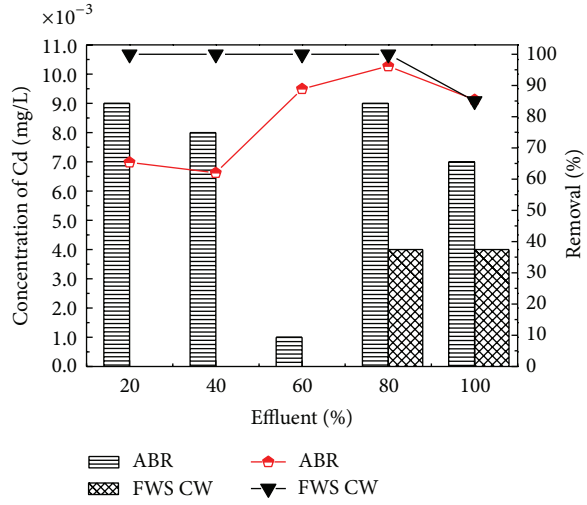

Figure 10: Comparison of % removal efficiency of Cd in ABR and FWS CW.

dissolved oxygen levels (<5.0-6.0 mg/L) may not directly kill an organism but will increase its susceptibility to other environmental stresses. Exposure to <30% saturation (<2.0 mg/L oxygen) for one to four days kills most of the biota in a system. If oxygen-requiring organisms perish, the remaining organisms will be air-breathing insects and anaerobic (not requiring oxygen) bacteria [40]. If all oxygen is depleted, aerobic (oxygen-consuming) decomposition ceases. So, treating pollutants in wetlands may help to increase DO which is consumed by the other aerobes. In this experiment during the posttreatment by CW the DO increased up to 8.8 mg/L.

Industrial wastewater was treated in two-stage constructed wetland [41] planted with *Typha latifolia* and *Phragmites australis*. For tannery wastewater, CW may be an interesting treatment option. Two-stage series of horizontal subsurface flow CW with *Phragmites australis* (UP series) and *Typha latifolia* (UT series) provided high removal of organics from tannery wastewater, up to 88% of biochemical oxygen demand ($BOD_{(5)}$) (from an inlet of 420 to 1000 mg/L) and 92% of chemical oxygen demand (COD) (from an inlet of 808 to 2449 mg/L) and of other contaminants, such as nitrogen, operating at hydraulic retention times of 2, 5, and 7 days. Overall mass removals of up to 1294 kg COD/ha/d and 529 kg $BOD_{(5)}$/ha/d were achieved for a loading ranging from 242 to 1925 kg COD ha/d and from 126 to 900 kg $BOD_{(5)}$/ha/d. Plants were resilient to the conditions imposed; however *P. australis* exceeded *T. latifolia* in terms of propagation. In the present study, *A. donax* was used in the CW for post treatment which showed the efficient performance for the further removal of pollutants from the ABR pretreated effluent. The results confirmed that effluent showed traces of heavy metals Ni and Cd with the corresponding ABR treated wastewater at almost all the levels of dilutions of 20, 40, 60, and 80 and original wastewater. CW showed the maximum removal efficiency for Ni and Cd as depicted in Figures 9 and 10, respectively. CW posttreatment of Pb was not satisfactory in the reduction of its concentration. Using the San Joaquin Marsh constructed wetlands, the removal efficiencies for four heavy metal elements Cd, Cu, Pb, and Zn were evaluated. It was found that the effluent metal concentrations were not substantially lower than the influent. The removal efficiencies of 23.9%, 10.6%, and 17.6% were found for Cd, Cu, and Zn, respectively. No significant reduction was observed for concentrations of Pb [42].

Metal and metalloid removal in constructed wetlands from industrial waste water have been investigated [43]. The removal of metals and metalloids from contaminated waters was investigated in constructed wetlands. Metal removal rates in wetlands depend on the type of element (Hg > Mn > Fe 1/4 Cd >Pb 1/4 Cr > Zn 1/4 Cu > Al > Ni > As), their ionic forms, substrate conditions, season, and plant species. Standardized procedures and data are lacking for efficiently comparing properties of plants and substrates. The study depicted the relative treatment efficiency index (RTEI) to quantify treatment impacts on metal removal in constructed wetlands.

Various mechanisms, including sedimentation, filtration, chemical precipitation, adsorption, microbial interactions, and uptake by vegetation, have been attributed with the removal of metal within CW. Specifically, the major processes that are responsible for metal removal in CW are binding to sediments and soils, precipitation as insoluble salts, and uptake by plants and bacteria [44]. In CW, substrate interactions remove most metals from contaminated water [45]. The anoxic condition of wetland soil helps create an environment for immobilization of heavy metals in the highly reduced sulfite or metallic form [46]. Wetland plants adsorb and accumulate metals in tissues, which can play an important role in CW pollutant treatment efficiency [47]. Phytoremediation, using vegetation to remove, detoxify, or stabilize heavy metal pollutants, is an accepted tool for cleaning polluted soils and waters [48]. Research has also shown that metal storage in the sediment is influenced by vegetation. Concentrations of metals were significantly higher in the vegetated sediments than in the nonvegetated sediments [49].

4. Conclusion

This paper presented the evaluation results on removal efficiencies for COD, BOD, nitrates, phosphates, TS, and heavy metals (Cd, Ni, and Pb) in ABR and posttreated by a lab scale *Arundo donax* based CW. It was clearly observed that posttreatment accomplished tremendous removal of the COD, BOD, TS Ni, and Cd. The efficiency of both the treatment systems was not too much satisfactory for Pb removal. Because of the positive effects of vegetation on metal removal efficiency, CWs containing *A. donax* is recommended for HIE combined wastewater treatment.

Conflict of Interests

The authors have neither any conflict of interests nor financial gain from the present paper.

References

[1] Q. Mahmood, A. Pervez, B. S. Zeb et al., "Natural treatment systems as sustainable ecotechnologies for the developing countries," *Biomed Research International*, vol. 2013, Article ID 796373, 19 pages, 2013.

[2] B. S. Zeb, Q. Mahmood, and A. Pervez, "Characteristics and performance of anaerobic wastewater treatment (a review)," *Journal of Chemical Society of Pakistan*, vol. 35, pp. 217–232, 2013.

[3] A. K. Mungray, Z. V. P. Murthy, and A. J. Tirpude, "Post treatment of up-flow anaerobic sludge blanket based sewage treatment plant effluents: a review," *Desalination and Water Treatment*, vol. 22, no. 1–3, pp. 220–237, 2010.

[4] A. C. van Haandel and G. Lettinga, *Anaerobic Sewage Treatment, a Practical Guide for Regions with a Hot Climate*, John Wiley & Sons, New York, NY, USA, 1994.

[5] C. Y. Gomec, "High-rate anaerobic treatment of domestic wastewater at ambient operating temperatures: a review on benefits and drawbacks," *Journal of Environmental Science and Health A*, vol. 45, no. 10, pp. 1169–1184, 2010.

[6] A. A. Khan, R. Z. Gaur, V. K. Tyagi et al., "Sustainable options of post treatment of UASB effluent treating sewage: a review," *Resources, Conservation and Recycling*, vol. 55, no. 12, pp. 1232–1251, 2011.

[7] J. Y. Ji, Y. J. Xing, Z. T. Ma, M. Zhang, and P. Zheng, "Acute toxicity of pharmaceutical wastewaters containing antibiotics to anaerobic digestion treatment," *Chemosphere*, vol. 91, pp. 1094–1098, 2013.

[8] B. Lew, M. Belavski, S. Admon, S. Tarre, and M. Green, "Temperature effect on UASB reactor operation for domestic wastewater treatment in temperate climate regions," *Water Science and Technology*, vol. 48, no. 3, pp. 25–30, 2003.

[9] G. Lettinga, A. F. M. van Velsen, S. W. Hobma, W. D. Zecuw, and A. Klapwijk, "Use of the upflow sludge blanket (USB) reactor concept for biological wastewater treatment, especially for anaerobic treatment," *Biotechnolgy and Bioengineering*, vol. 22, pp. 699–734, 1980.

[10] G. Lettinga, A. de Man, A. R. M. van der Last et al., "Anaerobic treatment of domestic sewage and wastewater," *Water Science and Technology*, vol. 27, no. 9, pp. 67–73, 1993.

[11] L. Seghezzo, R. G. Guerra, S. M. González et al., "Removal efficiency and methanogenic activity profiles in a pilot-scale UASB reactor treating settled sewage at moderate temperatures," *Water Science and Technology*, vol. 45, no. 10, pp. 243–248, 2002.

[12] M. vonSperling and C. A. de Lemos Chernicharo, "Wastewater treatment in warm climates," *Water 21*, pp. 17–20, 2006.

[13] G. Lettinga, "Towards feasible and sustainable environmental protection for all," *Aquatic Ecosystem Health and Management*, vol. 11, no. 1, pp. 116–124, 2008.

[14] A. Schellinkhout and C. J. Collazos, "Full-scale application of the UASB technology for sewage treatment," *Water Science and Technology*, vol. 25, no. 7, pp. 159–166, 1992.

[15] J. T. de Sousa and E. Foresti, "Domestic sewage treatment in an upflow anaerobic sludge blanket—sequencing batch reactor system," *Water Science and Technology*, vol. 33, no. 3, pp. 73–84, 1996.

[16] A. A. Khan, *Post treatment of ABR effluent: aeration and Variant of ASP [Ph.D. thesis]*, IIT Roorkee, Uttarakhand, India, 2012.

[17] A. A. Khan, R. Z. Gaur, B. Lew, I. Mehrotra, and A. A. Kazmi, "Effect of aeration on the quality of effluent from UASB reactor treating sewage," *Journal of Environmental Engineering*, vol. 137, no. 6, pp. 464–471, 2011.

[18] M. A. El-Khateeb and A. Z. El Bahrawy, "Extensive post treatment using constructed wetland," *Life Science Journal*, vol. 10, pp. 560–568, 2013.

[19] W. Verstraete and P. Vandevivere, "New and broader applications of anaerobic digestion," *Critical Reviews in Environmental Science and Technology*, vol. 29, no. 2, pp. 151–173, 1999.

[20] N. Sato, T. Okubo, T. Onodera, A. Ohashi, and H. Harada, "Prospects for a self-sustainable sewage treatment system: a case study on full-scale UASB system in India's Yamuna River Basin," *Journal of Environmental Management*, vol. 80, no. 3, pp. 198–207, 2006.

[21] A. K. Mungray and P. Kumar, "Anionic surfactants in treated sewage and sludges: risk assessment to aquatic and terrestrial environments," *Bioresource Technology*, vol. 99, no. 8, pp. 2919–2929, 2008.

[22] M. A. El-Khateeb and F. A. El-Gohary, "Combining ABR Technology and Wetland for Domestic Wastewater Reclamation and Reuse," *Water Supply*, vol. 3, 2003.

[23] B. Hegazy, M. A. El-Khateeb, A. E.-A. Amira, and M. M. Kamel, "Low-cost wastewater treatment technology," *Journal of Applied Sciences*, vol. 7, no. 6, pp. 815–819, 2007.

[24] M. A. El-Khateeb, A. Z. Al-Herrawy, M. M. Kamel, and F. A. El-Gohary, "Use of wetlands as post-treatment of anaerobically treated effluent," *Desalination*, vol. 245, no. 1–3, pp. 50–59, 2009.

[25] V. Mudgal, N. Madaan, and A. Mudgal, "Heavy metals in plants, phytoremediation: plants used to remediate heavy metal pollution," *Agriculture and Biology Journal of North America*, vol. 1, pp. 40–46, 2010.

[26] N. Korboulewsky, R. Wang, and V. Baldy, "Purification processes involved in sludge treatment by a vertical flow wetland system: focus on the role of the substrate and plants on N and P removal," *Bioresource Technology*, vol. 105, pp. 9–14, 2012.

[27] C. Wendland, J. Behrendt, T. A. Elmitwalli et al., "ABR reactor followed by constructed wetland and UV radiation as an appropriate technology for municipal wastewater treatment in Mediterranean countries," in *Proceedings of the 7th Specialized Conference on Small Water and Wastewater Systems in Mexico*, 2006.

[28] P. Worrall, K. J. Peberdy, and M. C. Millett, "Constructed wetlands and nature conservation," *Water Science and Technology*, vol. 35, no. 5, pp. 205–213, 1997.

[29] C. M. Kao and M. J. Wu, "Control of non-point source pollution by a natural wetland," *Water Science and Technology*, vol. 43, no. 5, pp. 169–174, 2001.

[30] J. García, P. Aguirre, R. Mujeriego, Y. Huang, L. Ortiz, and J. M. Bayona, "Initial contaminant removal performance factors in horizontal flow reed beds used for treating urban wastewater," *Water Research*, vol. 38, no. 7, pp. 1669–1678, 2004.

[31] M. von Sperling and L. C. A. M. Mascarenhas, "Performance of very shallow ponds treating effluents from UASB reactors," *Water Science and Technology*, vol. 51, no. 12, pp. 83–90, 2005.

[32] M. von Sperling, R. K. X. Bastos, and M. T. Kato, "Removal of E. coli and helminth eggs in ABR: polishing pond systems in Brazil," *Water Science and Technology*, vol. 51, no. 12, pp. 91–97, 2005.

[33] C. A. L. Chernicharo, "Post-treatment options for the anaerobic treatment of domestic wastewater," *Reviews in Environmental Science and Biotechnology*, vol. 5, no. 1, pp. 73–92, 2006.

[34] American Public Health Association, *Standard Methods for the Examination of Water and Wastewater*, APHA, New York, NY, USA, 21st edition, 2005.

[35] A. Mudhoo, R. M. Pravish, and M. Romeela, "Effects of microwave heating on biogas production, chemical oxygen demand and volatile solids solubilization of food residues. world academy of science," *Engineering and Technology*, vol. 69, pp. 805–810, 2012.

[36] M. Sarioglu, S. Akkoyun, and T. Bisgin, "Inhibition effects of heavy metals (copper, nickel, zinc, lead) on anaerobic sludge," *Desalination and Water Treatment*, vol. 23, no. 1–3, pp. 55–60, 2010.

[37] K. J. Prakash, V. K. Tyagi, A. A. Kazmi, and A. Kumar, "Post-treatment of UASB reactor effluent by coagulation and flocculation process," *Environmental Progress*, vol. 26, no. 2, pp. 164–168, 2007.

[38] I. Machdar, Y. Sekiguchi, H. Sumino, A. Ohashi, and H. Harada, "Combination of a UASB reactor and a curtain type DHS (downflow hanging sponge) reactor as a cost-effective sewage treatment system for developing countries," *Water Science and Technology*, vol. 42, no. 3-4, pp. 83–88, 2000.

[39] T. V. Kumar, A. A. Khan, A. A. Kazmi, I. Mehrotra, and A. K. Chopra, "Slow sand filtration of UASB reactor effluent: a promising post treatment technique," *Desalination*, vol. 249, no. 2, pp. 571–576, 2009.

[40] A. M. Gower, *Water Quality in Catchment Ecosystems*, John Wiley & Sons, New York, NY, USA, 1980.

[41] C. S. C. Calheiros, A. F. Duque, A. Moura et al., "Substrate effect on bacterial communities from constructed wetlands planted with Typha latifolia treating industrial wastewater," *Ecological Engineering*, vol. 35, no. 5, pp. 744–753, 2009.

[42] S. Hafeznezami, J.-L. Kim, and J. Redman, "Evaluating removal efficiency of heavy metals in constructed wetlands," *Journal of Environmental Engineering*, vol. 138, no. 4, pp. 475–482, 2012.

[43] L. Marchand, M. Mench, D. L. Jacob, and M. L. Otte, "Metal and metalloid removal in constructed wetlands, with emphasis on the importance of plants and standardized measurements: a review," *Environmental Pollution*, vol. 158, no. 12, pp. 3447–3461, 2010.

[44] R. H. Kadlec and S. D. Wallace, *Treatment Wetlands*, Taylor & Francis Group, Boca Raton, Fla, USA, 2nd edition, 2008.

[45] D. J. Walker and S. Hurl, "The reduction of heavy metals in a stormwater wetland," *Ecological Engineering*, vol. 18, no. 4, pp. 407–414, 2002.

[46] R. P. Gambrell, "Trace and toxic metals in wetlands—a review," *Journal of Environmental Quality*, vol. 23, no. 5, pp. 883–891, 1994.

[47] H. Brix, "Functions of macrophytes in constructed wetlands," *Water Science and Technology*, vol. 29, no. 4, pp. 71–78, 1994.

[48] S. Cheng, W. Grosse, F. Karrenbrock, and M. Thoennessen, "Efficiency of constructed wetlands in decontamination of water polluted by heavy metals," *Ecological Engineering*, vol. 18, no. 3, pp. 317–325, 2002.

[49] J. H. Choi, S. S. Park, and P. R. Jaffé, "The effect of emergent macrophytes on the dynamics of sulfur species and trace metals in wetland sediments," *Environmental Pollution*, vol. 140, no. 2, pp. 286–293, 2006.

Hindawi Publishing Corporation
BioMed Research International
Volume 2013, Article ID 384541, 8 pages
http://dx.doi.org/10.1155/2013/384541

Research Article

Hexavalent Molybdenum Reduction to Mo-Blue by a Sodium-Dodecyl-Sulfate-Degrading *Klebsiella oxytoca* Strain DRY14

M. I. E. Halmi,[1] S. W. Zuhainis,[2] M. T. Yusof,[2] N. A. Shaharuddin,[1] W. Helmi,[3] Y. Shukor,[1] M. A. Syed,[1] and S. A. Ahmad[1]

[1] *Department of Biochemistry, Faculty of Biotechnology and Biomolecular Sciences, Universiti Putra Malaysia, 43400 Serdang, Selangor, Malaysia*
[2] *Department of Microbiology, Faculty of Biotechnology and Biomolecular Sciences, Universiti Putra Malaysia, 43400 Serdang, Selangor, Malaysia*
[3] *Department of Bioprocess Technology, Faculty of Biotechnology and Biomolecular Sciences, Universiti Putra Malaysia, 43400 Serdang, Selangor, Malaysia*

Correspondence should be addressed to S. A. Ahmad; aqlima@upm.edu.my

Received 13 July 2013; Revised 29 October 2013; Accepted 30 October 2013

Academic Editor: Chong-Jian Tang

Bacteria with the ability to tolerate, remove, and/or degrade several xenobiotics simultaneously are urgently needed for remediation of polluted sites. A previously isolated bacterium with sodium dodecyl sulfate- (SDS-) degrading capacity was found to be able to reduce molybdenum to the nontoxic molybdenum blue. The optimal pH, carbon source, molybdate concentration, and temperature supporting molybdate reduction were pH 7.0, glucose at 1.5% (w/v), between 25 and 30 mM, and 25°C, respectively. The optimum phosphate concentration for molybdate reduction was 5 mM. The Mo-blue produced exhibits an absorption spectrum with a maximum peak at 865 nm and a shoulder at 700 nm. None of the respiratory inhibitors tested showed any inhibition to the molybdenum-reducing activity suggesting that the electron transport system of this bacterium is not the site of molybdenum reduction. Chromium, cadmium, silver, copper, mercury, and lead caused approximately 77, 65, 77, 89, 80, and 80% inhibition of the molybdenum-reducing activity, respectively. Ferrous and stannous ions markedly increased the activity of molybdenum-reducing activity in this bacterium. The maximum tolerable concentration of SDS as a cocontaminant was 3 g/L. The characteristics of this bacterium make it a suitable candidate for molybdenum bioremediation of sites cocontaminated with detergent pollutant.

1. Introduction

The role of bacteria in remediation of toxic compounds has been documented over the years and would continue to be a dominant technology for the remediation of organic and inorganic compounds [1–6]. The remediation of inorganic compounds such as heavy metals remains problematic due to the indestructible property of heavy metals. Microbes, however, utilize various mechanisms such as biosorption, bioprecipitation, efflux pumping, and bioreduction to counter the toxicity of metal ions. The microorganisms involved in the process come from a variety of genera. Metals that could be detoxified include molybdenum, mercury, lead, arsenic, uranium, copper, bismuth, selenium, chromium, and tungsten [7]. Amongst these metals, molybdate reduction by microbes has been reported one hundred years ago [7, 8].

However, detailed studies on the potential mechanism of reduction were initiated only in the past 25 years in *E. coli* [9], *T. ferrooxidans* (now *Acidithiobacillus ferrooxidans*) [10, 11], and the local bacteria *Enterobacter cloacae* strain 48 or EC 48 [12–15], *Serratia* spp. [6, 11, 16], *Enterobacter* sp. [17], *Acinetobacter calcoaceticus* [18], *Pseudomonas* sp. [19], and *Klebsiella* sp. [20]. The usage of bacteria in the bioremediation of molybdenum has been documented. In Tyrol, Austria, molybdenum pollution is caused by industrial effluents and has contaminated large pasture areas, reaching

as high as 200 ppm causing scouring in ruminants [21]. Molybdate bioremediation using indigenous microbe from the contaminated site has shown positive results [21] and the works have opened the possibility of molybdenum bioremediation in other parts of the world.

The current documented reports show that metals' pollution in Malaysia is in the areas with heavy industrialization and scrap metal yards [6]. Aside from this, metal sludge, spent catalyst, spent lubricant, ink and the waste from the paint industries are also the major sources of molybdenum pollution [11]. Often cocontamination of organics and inorganics in wastes makes it difficult to remediate them. Hence, many workers have turned their attention to microbes with multiple biodegradation capacity. In this work, we report on the ability of an SDS-degrading bacterium [6] to reduce molybdenum to molybdenum blue. The characteristics of this bacterium make it a suitable candidate for molybdenum bioremediation of sites co-contaminated with detergent pollutant.

2. Materials and Methods

2.1. Isolation of Molybdenum-Reducing Bacterium. *Klebsiella oxytoca* strain DRY14 was originally isolated from an effluent of a car washing operator in Serdang, Selangor, Malaysia. The bacterium exhibits strong SDS-degrading capacity [6]. A bacterial colony grown on nutrient agar was streaked onto low phosphate (2.9 mM phosphate) agar media (pH 7.0) containing (w/v%) glucose (1.0), $(NH_4)_2SO_4$ (0.3), $MgSO_4{\cdot}7H_2O$ (0.05), NaCl (0.5), yeast extract (0.05), $Na_2MoO_4{\cdot}2H_2O$ (0.242), and $Na_2HPO_4{\cdot}2H_2O$ (0.05). Glucose was autoclaved separately. In this study, molybdenum-reducing bacterium was isolated following the method described by Shukor et al. [22].

2.2. Assay for Molybdenum-Reducing Enzyme. Molybdenum-reducing enzyme was assayed using phosphomolybdate as the electron acceptor and NADH as the electron donor [22]. Briefly, laboratory-prepared ten to four phosphomolybdate or 10 : 4 ratios of phosphomolybdate were prepared arbitrarily as a 60 mM stock solution in deionized water. This was achieved by mixing molybdate ($Na_2MoO_4{\cdot}2H_2O$) and phosphate ($Na_2HPO_4{\cdot}2H_2O$) to the final concentrations of 600 and 240 mM, respectively. The pH of the solution was adjusted to pH 5.0 using 1 M HCl. This solution is stable at this pH for several months.

2.3. Crude Enzyme Preparation. High phosphate medium was chosen as the growth media for strain DRY14 since growth on low phosphate resulted in a blue sticky culture that complicated the preparation of crude enzyme and enzyme assay. This phenomenon also prevented crude enzyme preparation from EC 48 [12]. Although the high phosphate inhibits molybdate reduction to Mo-blue, the cells contain active enzymes. Bacteria were grown in one liter of high phosphate media at 30°C for 24 hours on an orbital shaker (100 rpm). The following experiment was carried out at 4°C unless stated otherwise. Cells were harvested through centrifugation at 10000 g for 10 minutes. Cells were washed at least once with distilled water, resuspended, and recentrifuged. The pellet was reconstituted with 10 mL of 50 mM Tris HCl buffer (pH 7.5) (Tris buffer prepared at 4°C) containing 0.5 mM dithiothreitol and 0.1 mM PMSF (phenylmethanesulfonyl fluoride) as an antiproteolytic agent. Cells were sonicated for 1 minute on an ice bath with 4-minute cooling until a total sonication time of at least 20 minutes was achieved. The sonicated fraction was centrifuged at 10,000 g for 20 minutes and the supernatant consisting of the crude enzyme fraction was taken.

2.4. The Effects of Respiratory Inhibitors and Metal Ions. Respiratory inhibitors such as Antimycin A, sodium azide, rotenone, and potassium cyanide were prepared as 20 mM, 50 mM, 50 mM, and 60 mM stock solutions, respectively, in deionised water. Antimycin A and rotenone were dissolved in acetone. Metal ions such as Fe^{3+} ($FeCl_3{\cdot}6H_2O$, BDH), Fe^{2+} ($Fe(NH_4)_2(SO_4)_2{\cdot}6H_2O$, BDH), Cr^{6+} ($K_2Cr_2O_7$, BDH), Mg^{2+} ($MgCl_2$, BDH), Zn^{2+} ($ZnCl_2$, BDH), Co^{2+} ($CoCl_2{\cdot}6H_2O$, BDH), Cd^{2+} ($CdCl_2{\cdot}H_2O$, SparkChem), Ag^{+} ($AgNO_3$, JT Baker), Pb^{2+} ($PbCl_2$, JT Baker), Mn^{2+} ($MnCl_2{\cdot}4H_2O$, JT Baker), Sn^{2+} ($SnCl_2{\cdot}2H_2O$, BDH), Cu^{2+} ($CuSO_4{\cdot}5H_2O$, JT Baker), Ni^{2+} ($NiCl_2{\cdot}6H_2O$, BDH), and Hg^{2+} ($HgCl_2$, JT Baker), were dissolved in 20 mM Tris HCl buffer (pH 7.0) and added to the enzymatic reaction mixture at the final concentration of 2 mM. Inhibitors were added into the enzyme assay mixture to the final concentrations of 1.2, 10, 10, and 0.2 mM, respectively, in a volume not exceeding 20% of assay volume to prevent shifting in assay pH. Inhibitors and metal ions were preincubated with one hundred microlitres of enzyme in the reaction mixture at 4°C for 10 minutes minus NADH. The incubation mixture was then warmed to room temperature and NADH was added to start the reaction. Deionised water was added so that the total reaction mixture was 1.0 mL. As a control, 50 mL of acetone was added in the reaction mixture without inhibitors. The increase in absorbance at 865 nm was measured after a period of 5 minutes using a Shimadzu 1201 UV-Vis-NIR Spectrophotometer.

2.5. Experiment to Distinguish between Chemical and Enzymatic Reduction of Molybdenum. This experiment is a modification of the works carried out by Shukor et al. [14]. Briefly, bacteria were grown in 250 mL high phosphate media (100 mM) for 24 hours in several 250 mL conical flasks with shaking at 150 rpm on an orbital shaker (Yihder, Taiwan) at room temperature. Cells were harvested by centrifugation at 15,000 g for 10 minutes and the pellet resuspended in low phosphate solution (pH 7.0) containing (w/v) $(NH_4)_2SO_4$ (0.3%), $MgSO_4{\cdot}7H_2O$ (0.05%), NaCl (0.5%), yeast extract (0.05%), and Na_2HPO_4 (0.05%). About 8 mL of this suspension was then placed in dialysis tubing previously boiled for ten minutes (1000 molecular weight cut-off) and immersed in sterile 100 mL of low phosphate media (pH 7.0) as described previously. Aliquots (1 mL) of the media were taken at the beginning of the experiment and after a static incubation period of 4 hours at room temperature and then read at 865 nm. At the same time, 1 mL was taken out from the content of the dialysis tubing and centrifuged at 15,000 g

Table 1: Amount of molybdenum blue produced from a 24-hour static culture of strain DRY14 in comparison with other Mo-reducing bacteria [20].

Bacteria	Micromole Mo-blue
Klebsiella oxytoca strain *DRY14*	15.24 ± 0.21
Klebsiella sp. strain hkeem	32.81 ± 0.33
Serratia sp. strain Dr.Y8	10.53 ± 0.47
S. marcescens strain Dr.Y9	9.82 ± 0.24
Serratia sp. strain Dr.Y5	7.9 ± 0.12
Pseudomonas sp.strain DRY2	6.97 ± 0.78
Enterobacter sp.strain Dr.Y13	6.92 ± 0.24
Acinetobacter calcoaceticus strain Dr.Y12	5.80 ± 0.15
Serratia marcescens strain DRY6	2.88 ± 0.01
Enterobacter cloacae strain 48	2.15 ± 0.73
Escherichia coli K12	0.997 ± 0.06

for 10 minutes. The supernatant was then read at 865 nm. Experiments were carried out in triplicate.

2.6. Statistical Analysis. All replicated data are represented as means ± SE (standard error). All data were analyzed using GraphPad Prism version 3.0 and GraphPad InStat version 3.05. Comparison between groups was performed using a Student's *t*-test or a one-way analysis of variance with post hoc analysis by Tukey's test. $P < 0.05$ was considered statistically significant.

3. Results

3.1. Comparison of Mo-Blue Production among Molybdenum-Reducing Isolates. Strain DRY14 produced 1.4, 1.6, 1.9, 2.2, 2.2, 2.6, 5.3, 7.1, and 15.4 times more Mo-blue compared to *Serratia* sp. strain Dr.Y8, *S. marcescens* strainDr.Y9, *Serratia* sp. strain Dr.Y5, *Pseudomonas* sp. strain DRY2, *Enterobacter* sp. strain Dr.Y13, *Acinetobacter calcoaceticus* strain Dr.Y12, *Serratia marcescens* strain DRY6, *Enterobacter cloacae* strain 48, *and Escherichia coli* K12, respectively, with the exception of strain hkeem (Table 1). The optimum temperature supporting optimal molybdenum reduction was in between 25 and 30°C. The optimum initial pH for molybdate reduction was 7.0 (Figure 1).

3.2. The Effect of Electron Donor Sources. Different electron donor sources such as glucose, sucrose, fructose, maltose, lactose, mannitol, and starch were used at an initial concentration of 0.2% (w/v) to study their effects on the molybdate reduction efficiency of the bacterium. Previous works have shown that Mo-blue production of bacteria requires simple assimilable carbon source as electron donors [11–20], and hence these carbon sources were used in this study. Of these, only glucose, sucrose, fructose, maltose, and lactose supported molybdate reduction after 24 hours of incubation with glucose supporting significantly more Mo-blue than the rest ($P < 0.05$) (Figure 2). Optimum concentration of glucose for supporting molybdate reduction was 1.5% (w/v) after 24 hours of static incubation. Further increase in glucose concentrations had a negative effect on molybdate reduction (data not shown). During cellular reduction of molybdate to Mo-blue, it was noted that cells precipitated together with a portion of the Mo-blue product preventing accurate cellular growth kinetic determination to be carried out in the presence of different nitrogen or electron donors.

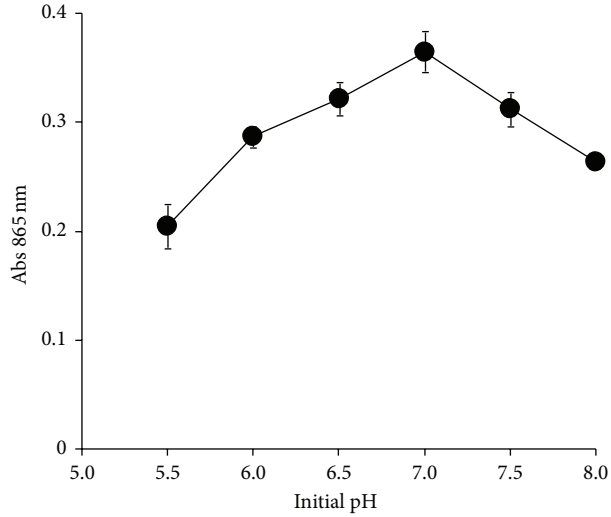

Figure 1: Molybdate reduction at various initial pH values. Strain DRY14 was grown for 24 hours in 50 mL of low phosphate liquid medium containing 10 mM molybdate at various initial pH values. Molybdate reduction was considered negligible if the absorbance at 865 nm is below 0.020. Error bars represent mean ± standard error ($n = 3$).

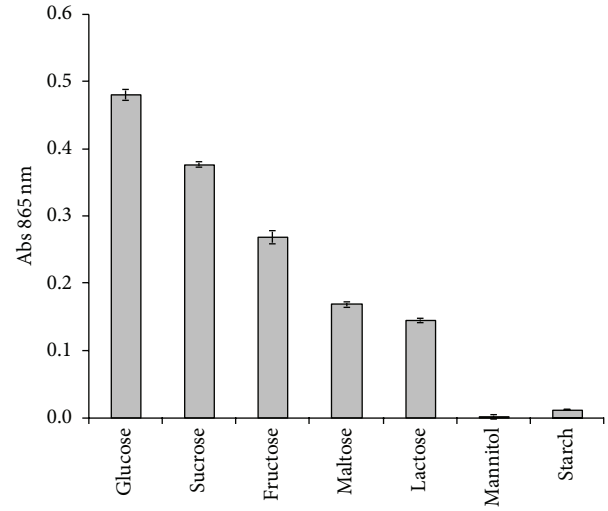

Figure 2: Molybdate reduction using various electron donors. Strain DRY14 was grown for 24 hours in 50 mL of low phosphate liquid medium containing 10 mM molybdate and various electron donors at the final concentration of 0.2% (w/v). The nitrogen source was 0.3% (w/v) ammonium sulphate. Molybdate reduction was considered negligible if the absorbance at 865 nm is below 0.020. Error bars represent mean ± standard error ($n = 3$).

3.3. The Effect of Phosphate and Molybdate Concentrations on Molybdate Reduction. The study of the effect of molybdate

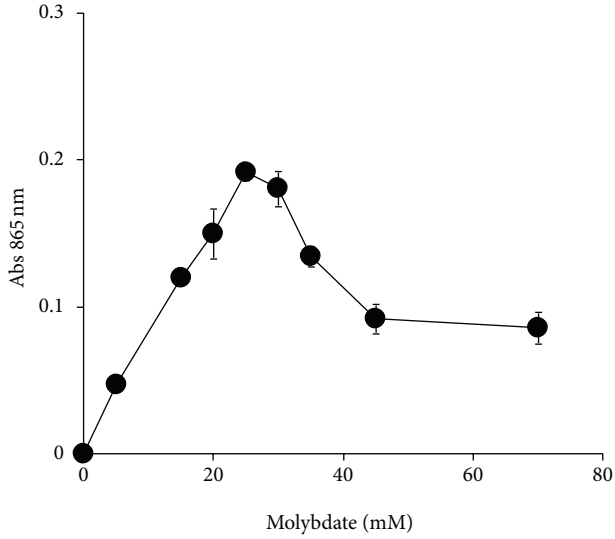

Figure 3: The effect of molybdate concentrations on molybdate reduction. Molybdate reduction was considered negligible if the absorbance at 865 nm is below 0.020. Error bars represent mean ± standard error ($n = 3$).

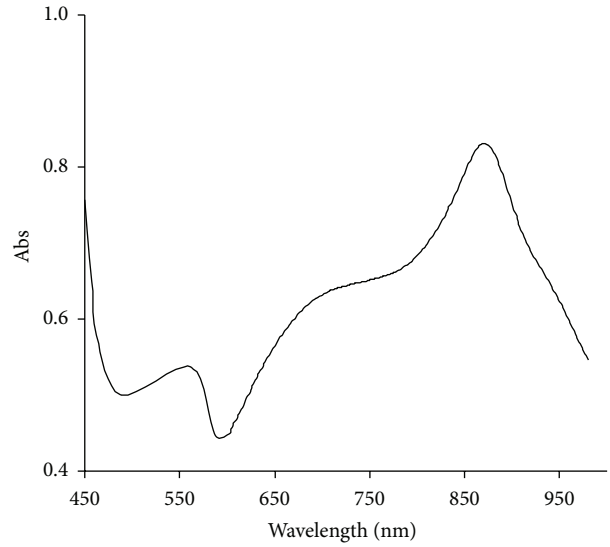

Figure 4: Scanning spectrum of Mo-blue after 24 hours of static incubation.

concentrations on molybdate reduction was carried out in an increment of 5 mM. Molybdate reduction was found to increase linearly as molybdate concentration was increased from 0 to 25 mM and reached an optimum in between the concentrations of 25 and 30 mM. At higher concentrations, molybdate reduction was inhibited (Figure 3). The optimum phosphate concentration for molybdate reduction (set at 25 mM) in this bacterium was 5 mM (data not shown).

3.4. Mo-Blue Absorbance Spectrum. The Mo-blue produced by this isolate exhibited a unique characteristics absorption profile with a maximum peak at 865 nm and a shoulder at 700 nm. There was intense absorption near the ultraviolet region (Figure 4). We observed that during the progress of molybdate reduction, there was an increase in an overall absorption profile especially at the peak maximum at 865 nm and the shoulder at 700 nm in direct correlation with the increasing blue intensity of the media.

3.5. The Effect of Respiratory Inhibitors and Metal Ions on Molybdenum-Reducing Activity. In this work, none of the respiratory inhibitors tested show any inhibition of more than 10% to the Mo-reducing activity in this bacterium (data not shown). At first, it was contemplated that the dissimilar assay composition employed in the new assay system might influence the outcome of inhibitors' results. Thus, we make use of the original assay using molybdate as the electron acceptor substrate. We observed no inhibition on the molybdenum-reducing activity (data not shown). Heavy metals could generally inactivate enzymes, and hence, elevated presence of heavy metals could be a major problem in bioremediation. In this work, it was found that chromium, cadmium, silver, copper, mercury, and lead caused approximately 77, 65, 77, 89, 80, and 80% inhibition of the molybdenum-reducing activity, respectively, while other metal ions did not show inhibition

Table 2: Effect of metal ions on molybdate reduction (mean ± standard error, $n = 3$).

Metal ions (2 mM)	Mo-blue produced (nmole/min/mg)
Control	45.01 ± 0.94
Cr^{6+}	10.19 ± 0.76
Fe^{3+}	45.50 ± 2.78
Fe^{2+}	88.20 ± 2.29
Zn^{2+}	45.58 ± 1.09
Mg^{2+}	43.92 ± 1.26
Co^{2+}	44.26 ± 1.16
Ni^{2+}	41.56 ± 1.24
Cd^{2+}	15.65 ± 0.04
Ag^{+}	10.44 ± 0.10
Mn^{2+}	43.09 ± 1.16
Cu^{2+}	5.10 ± 0.24
Hg^{2+}	9.20 ± 2.42
Pb^{2+}	9.10 ± 0.25
Sn^{2+}	94.95 ± 3.38

(Table 2). Ferrous and stannous ions markedly increased the activity of molybdenum-reducing activity in this bacterium.

3.6. Experiment to Distinguish between Chemical and Enzymatic Reduction of Molybdenum. In order to provide further confirmation on the participation of enzyme in molybdate reduction in this bacterium, we enclosed this bacterium in dialysis tubing and immersed the tubing in low phosphate media and discovered more than 95% of the Mo-blue trapped in the dialysis tubing (data not shown).

3.7. Reduction of Mo-Blue in the Presence of SDS. Figure 5 shows the effect of SDS on molybdenum reduction. The carbon source was glucose at 1.5% (w/v). Reduction was not

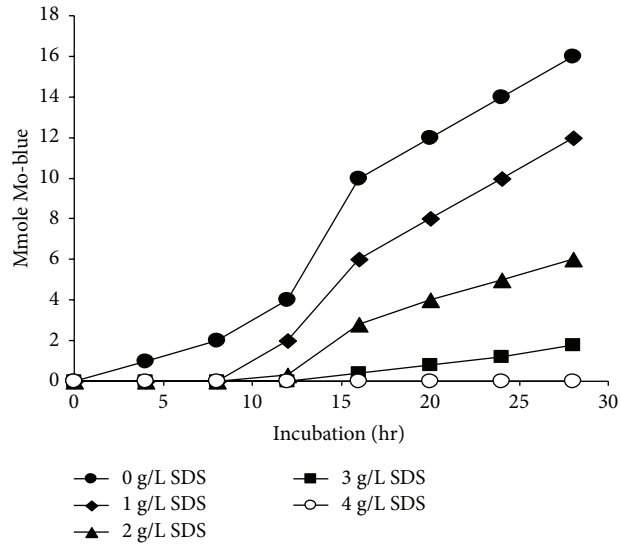

Figure 5: The effect of SDS on Mo-reduction after static incubation for 24 hours at molybdate concentration of 25 mM. Error bars represent mean ± standard error ($n = 3$).

supported when SDS was used as the sole carbon source. Production of Mo-Blue was inhibited by SDS concentration greater than 1 g/L. Production was negligible at SDS concentration higher than 4 g/L.

4. Discussion

In all of the previous studies on molybdate reduction to molybdenum blue, it was observed that the reduced products cling so tightly to the bacterial biomass that it becomes impossible to determine cellular numbers and to carry out kinetic studies [6, 11, 12, 16–19, 23]. This observation was not reported in *E. coli* K12 [9]. The study of the effect of various parameters such as source of electron donors, temperature, molybdate, and phosphate on molybdate reduction is important. This knowledge not only is important for contributing to the fundamental understanding of the mechanism of reduction but also will be beneficial in the area of bioremediation of molybdenum especially with pH and source of electron donors as these parameters can be controlled by addition of suitable compounds into the soil.

Glucose appears to be the main carbon source optimal for supporting Mo-reduction [6, 9, 17–19]. In contrast, it was reported that sucrose is the best source of electron donor for EC 48, *S. marcescens* strain DrY6, and *Serratia* sp. strain Dr.Y5 [11, 12, 16]. Fructose was the best carbon source in strain hkeem [20]. Other carbon source that support Mo-reduction were glycerol, galactose, mannose, mannitol, maltose, lactose, raffinose, and sorbitol. Attempts to use the Biolog system as carbon sources for molybdate reduction were not successful in this work and other works [6, 17–19] since the colour produced from bacterial reduction of the formazan dye was more intense than that the Mo-blue produced. Our current works include optimizing this system to exploit the 95 carbon sources available in the system. It was previously demonstrated in EC 48 that molybdate reduction is growth-associated [24] and this is also true for several other Mo-reducing bacteria [11]. Hence, it is not surprising that glucose supported the highest reduction as it is the best substrate for growth and source of carbon as well as the best substrate for producing reducing equivalents in the form of NADH or NADPH. Both reducing equivalents are needed as substrates for chromate reductase [25] and the molybdenum-reducing enzyme [22]. However, in terms of cost effectiveness, sucrose in the form of cane and sugar molasses is preferred to pure and simple carbohydrates as it is a cheaper alternative found in abundance in industrial wastes in Malaysia [26]. Molasses is regularly used in works on microbiological chromate reduction [27]. Thus, sucrose in the form of molasses would be employed for future molybdenum bioremediation.

The study of temperature optimal for the growth of microbes would be very useful for bioremediation and maximizing enzyme yield for purification purposes [28]. The optimal temperature supporting molybdenum reduction in strain DRY14 differs markedly to all of the Mo-reducing bacteria studied so far. *Escherichia coli* strain K12 reduces molybdenum optimally between 30 and 36°C [9]. Ghani et al. reported 30°C as the optimum [12]. Other Mo-reducing bacteria isolated so far have optimal pH between 30 and 37°C. Although generally it is not possible to change temperature when performing bioremediation works on the field, screening for indigenous microbes for local bioremediation works is the norm since these microbes would have an optimum temperature close to the temperature of the site chosen for bioremediation. The optimal initial pH supporting reduction is also shared by the majority of the Mo-reducing bacteria [6, 9, 11, 12, 16–20]. The obligation for neutral pH and a moderate temperature range ensures that bioremediation treatments will be economical [29] and these observable facts are also shared by many chromate-reducing bacteria [25, 30, 31]. However, most soils with active metabolic activity usually exhibited lowering in pH due to several factors such as carbohydrate fermentation and carbon dioxide production leading to the lowering of pH [32].

Campbell et al. were the first to note the inhibitory effects of elevated concentrations of both phosphate and molybdate ions on bacterial molybdenum blue production [9]. Hence, it is very important to ascertain the effects of phosphate and molybdate ions on molybdate reduction in this bacterium. A similar ratio of phosphate to molybdate is seen in *E. coli* K12 and *Klebsiella* sp. strain hkeem [20], where, at 5 mM phosphate, 80 mM molybdate is the optimum concentration for supporting molybdate reduction [9]. In EC 48, the optimum ratio is 5 mM phosphate to 20 mM molybdate. In all of the Mo-reducing bacteria studied so far, phosphate concentrations higher than 5 mM inhibited molybdate reduction. Phosphate disrupts the phosphomolybdate complex preventing reduction to Mo-blue [33–36]. The highest reported concentration of molybdenum as a pollutant is at 2000 ppm (20.8 mM molybdate) from a molybdenum mine runoff [37]. At this concentration, all of the bacteria studied so far can reduce molybdate provided that the soil phosphate concentrations do not exceed 20 mM for appreciable reduction to

take place. Fortunately, phosphate soil concentrations rarely exceeded this value in [38].

The increase at the peak maximum at 865 nm and more importantly the overall shape of the Mo-blue spectrum are the same as the majority of the Mo-reducing bacteria isolated so far [6, 11, 16–20, 23] indicating that a unique reduced phosphomolybdate species is involved in all of them. Incidentally, the spectrum is also similar to the Mo-blue spectrum produced by the ascorbic-acid-reduced phosphomolybdate in the phosphate determination method with a peak maximum at 880 nm and a shoulder around 700 nm. In a slight contrast, the Mo-blue spectrum from *E. coli* K12 showed a broad maximum peak at 820 nm and a shoulder between 600 and 700 nm [9] suggesting that a different species of phosphomolybdate probably had formed. The Mo-blue absorption spectrum is not similar to the absorption spectra of other Mo-blue products such as silicomolybdate and sulfomolybdate. This event is suggested to be an important event for phosphomolybdate formation [18, 19, 23]. Identification of phosphomolybdate by analysing the scanning spectroscopic profile is an accepted method but would not be enough to distinguish the many subtypes and lacunary species of phosphomolybdate. Identification of the exact phosphomolybdate species must be carried out using NMR and ESR. However, it would be generally enough to distinguish between phosphomolybdate and silicomolybdate or sulfomolybdate [39–42]. Based on the results above, works on the bacterial reduction of molybdenum to Mo-blue should take into account the pivotal role played by phosphomolybdate.

All of the inhibitors tested in this work show inhibition at the electron transport system at specific locations. The concentrations of inhibitors used in this assay are at least five times more than the suggested concentrations that would normally cause more than 50% inhibition of activity per mg of protein [43]. Rotenone is an inhibitor to NADH dehydrogenase while sodium azide and cyanide are inhibitors to the terminal cytochrome oxidase. Antimycin A inhibits cytochrome b [43]. The use of the respiratory inhibitor cyanide has been instrumental in locating the site of molybdenum-reducing activity in EC 48. The activity is suggested to be located at the electron transport system downstream from cytochrome b [12]. The results suggest that the electron transport system of this bacterium is not the site of molybdate reduction.

The rest of the metal ions did not have an effect on the molybdenum-reducing activity from this bacterium. Ferric ion did not enhance the activity of the molybdenum-reducing activity. Ferric, stannous, nickel, zinc, cobalt, ferrous, and silver enhanced the activity of the molybdenum-reducing enzyme in EC 48 severalfold while cupric and chromium ions strongly inhibited the activity of the enzyme [12]. Chromium also strongly inhibited Mo-blue production in *E. coli* K12 [9] while studies on the effects of metal ions on molybdate reduction were not carried out in *S. marcescens* strain DrY6 [11]. However, when we added each metal ion in the reaction mixture minus the crude extract of the enzyme, we discovered that molybdenum blue is produced by ferrous and stannous ions indicating that chemical reduction has occurred. The stimulatory effect of stannous and ferrous ions was similarly observed in this bacterium. We found out that this chemical reduction was only seen when the molybdate stock solution was adjusted to pH 7.0. When we measured the pH of the reaction mixture with the molybdate stock solution not adjusted to pH 7.0, we found the pH to be highly alkaline. Incidentally, ferrous and stannous ions have been used as reducing agents for the conversion of molybdate to Mo-blue in the phosphate determination method [33–36]. Even the stannous ions were used as a chemical reductant for the construction of the Mo-blue standard curve [12, 44]. This is likely the reason as to why ferrous irons were found to reduce molybdate to Mo-blue in the acidic media of *T. ferrooxidans* [10]. Hence, studies on the effect of metal ions on molybdate reduction and perhaps on other metal reduction works must be conducted with adequate control experiments.

We have shown recently that phosphate and arsenate are not physiological inhibitors towards Mo-blue production in EC 48 as both of these ions also inhibited the chemical production of Mo-blue. Only mercury was found to be a physiological inhibitor towards molybdate reduction in EC 48 [22]. The inhibition of molybdenum reduction to Mo-blue by copper and mercury could present a major problem for bioremediation of molybdenum polluted sites as these sites usually contain heavy metals at concentrations high enough to inhibit molybdate reduction. Both of these ions have also been reported to inhibit chromate reductase with the target of inhibition suggested as the thiol group [45]. The enormous amount of energy required for multitoxic metal resistance suggests that it would be difficult to isolate bacteria with such a capability. However, it would be important to screen and isolate bacteria with as many metal resistance capabilities as possible since the success of a bacterium to remediate a target metal would depend upon its resistance to other toxic nontarget metal ions present in the site [25].

The dialysis tubing experiment was carried out because molybdenum reduction to molybdenum blue can be carried out by many organic and inorganic reducing agents including ascorbic acid, dithionite, and metal ions. The reducing effect of stannous and ferrous ions seen in this work excellently emphasizes this point. This method is a modification of works carried out by Munch and Ottow originally to prove that the reduction of ferric to ferrous ions by bacteria is enzymatically mediated [46]. This method works because Mo-blue is colloidal and would not diffuse appreciably or slowly through dialysis tubings [35]. The dialysis tubing method was chosen since the conventional method of boiling cells (and cell fractions) to prove enzymatic reduction does not take into account that metal-reducing chemicals can be produced enzymatically. Boiling the cells denatures the enzymes responsible both for metal reduction and the enzymes that produce bioreductants that might be responsible for the reduction of metal ions. Thus, distinguishing between chemical and enzymatic reduction will not be possible. The results obtained reiterate the fact that molybdenum reduction, at least in the heterotrophic bacteria, is enzyme-driven and not due to biotic or abiotic reducing agents. The remaining 5%–10% of Mo-blue seen in the external side of the dialysis tubing

is due to slow diffusion of the colloidal Mo-blue [6, 11, 16–19, 23].

Strain DRY14 can utilize SDS as the sole carbon source. However, reduction was not supported by SDS. Our results showed that reduction using glucose was inhibited by SDS. Previously this strain exhibited optimal growth on SDS at 2 g/L. As molybdenum reduction is growth-associated, the inhibitory effect of SDS on reduction is probably a result of growth retardation due to the toxicity of SDS.

In conclusion, the work carried out in this study is the continuation of the works reported more than one hundred years ago. The bacterium shows similar and differential Mo-reducing characteristics to previously reported Mo-reducing bacteria but with an added advantage—its ability to degrade SDS. More Mo-reducing bacteria should be reported to suit the various environmental conditions needed for remediation. Unfortunately, very few molybdenum-reducing microbes have been reported unlike works on chromate. Molybdenum is very toxic to ruminant and its remediation in contaminated aquatic bodies and soils of agricultural importance is highly sought. We are purifying the molybdenum-reducing enzyme from this bacterium to answer some of the questions pertaining to molybdate reduction to Mo-blue.

Acknowledgment

This project was supported by fund from The Ministry of Science, Technology and Innovation (MOSTI), Malaysia, under IRPA-EA Grant no. 09-02-04-0854-EA001.

References

[1] A. B. Moldes, R. Paradelo, X. Vecino et al., "Partial characterization of biosurfactant from lactobacillus pentosus and comparison with sodium dodecyl sulphate for the bioremediation of hydrocarbon contaminated soil," *BioMed Research International*, vol. 2013, Article ID 961842, 6 pages, 2013.

[2] M. B. H. Rahim, M. A. Syed, and M. Y. Shukor, "Isolation and characterization of an acrylamide-degrading yeast *Rhodotorula* sp. strain MBH23 KCTC, 11960BP," *Journal of Basic Microbiology*, vol. 52, no. 5, pp. 573–581, 2012.

[3] J. Cheriaa, M. Khaireddine, M. Rouabhia, and A. Bakhrouf, "Removal of triphenylmethane dyes by bacterial consortium," *The Scientific World Journal*, vol. 2012, Article ID 512454, 9 pages, 2012.

[4] Y. N. Suhaila, M. Rosfarizan, S. A. Ahmad, I. B. Latif, and A. B. Ariff, "Nutrients and culture conditions requirements for the degradation of phenol by Rhodococcus UKMP-5M," *Journal of Environmental Biology*, vol. 34, pp. 635–643, 2013.

[5] N. Das and P. Chandran, "Microbial degradation of petroleum hydrocarbon contaminants: an overview," *Biotechnology Research International*, vol. 2011, Article ID 941810, 13 pages, 2011.

[6] M. Y. Shukor, W. S. W. Husin, M. F. A. Rahman, N. A. Shamaan, and M. A. Syed, "Isolation and characterization of an SDS-degrading *Klebsiella oxytoca*," *Journal of Environmental Biology*, vol. 30, no. 1, pp. 129–134, 2009.

[7] E. M. Bautista and M. Alexander, "Reduction of inorganic compounds by soil microorganisms," *Soil Science Social of American Journal*, vol. 36, no. 6, pp. 918–920, 1972.

[8] V. E. Levine, "The reducing properties of microorganisms with special reference to selenium compounds," *Journal of Bacteriology*, vol. 10, pp. 217–263, 1925.

[9] A. M. Campbell, A. Del Campillo-Campbell, and D. B. Villaret, "Molybdate reduction by *Escherichia coli* K-12 and its chl mutants," *Proceedings of the National Academy of Sciences of the United States of America*, vol. 82, no. 1, pp. 227–231, 1985.

[10] N. K. Yong, M. Oshima, R. C. Blake II, and T. Sugio, "Isolation and some properties of an iron-oxidizing bacterium *Thiobacillus ferrooxidans* resistant to molybdenum ion," *Bioscience, Biotechnology and Biochemistry*, vol. 61, no. 9, pp. 1523–1526, 1997.

[11] M. Y. Shukor, S. H. M. Habib, M. F. A. Rahman et al., "Hexavalent molybdenum reduction to molybdenum blue by *S. Marcescens* strain DrY6," *Applied Biochemistry and Biotechnology*, vol. 149, no. 1, pp. 33–43, 2008.

[12] B. Ghani, M. Takai, N. Z. Hisham et al., "Isolation and characterization of a Mo^{6+}-reducing bacterium," *Applied and Environmental Microbiology*, vol. 59, no. 4, pp. 1176–1180, 1993.

[13] M. Y. Shukor, N. A. Shamaan, M. A. Syed, C. H. Lee, and M. I. A. Karim, "Characterization and quantification of Mo-blue production in *Enterobacter cloacae* strain 48 using 12-phosphomolybdate as the reference compound," *Asia-Pacific Journal of Molecular Biology and Biotechnology*, vol. 8, no. 2, pp. 167–172, 2000.

[14] M. Y. Shukor, M. A. Syed, C. H. Lee, M. I. A. Karim, and N. A. Shamaan, "A method to distinguish between chemical and enzymatic reduction of molybdenum in *Enterobacter cloacae* strain 48," *Malaysian Journal of Biochemistry*, vol. 7, pp. 71–72, 2002.

[15] M. Y. Shukor, C. H. Lee, I. Omar, M. I. A. Karim, M. A. Syed, and N. A. Shamaan, "Isolation and characterization of a molybdenum-reducing enzyme in *Enterobacter cloacae* strain 48," *Pertanika Journal of Science and Technology*, vol. 11, no. 2, pp. 261–272, 2003.

[16] M. F. A. Rahman, M. Y. Shukor, Z. Suhaili, S. Mustafa, N. A. Shamaan, and M. A. Syed, "Reduction of Mo(VI) by the bacterium *Serratia* sp. strain DRY5," *Journal of Environmental Biology*, vol. 30, no. 1, pp. 65–72, 2009.

[17] M. Y. Shukor, M. F. Rahman, Z. Suhaili, N. A. Shamaan, and M. A. Syed, "Bacterial reduction of hexavalent molybdenum to molybdenum blue," *World Journal of Microbiology and Biotechnology*, vol. 25, no. 7, pp. 1225–1234, 2009.

[18] M. Y. Shukor, M. F. Rahman, Z. Suhaili, N. A. Shamaan, and M. A. Syed, "Hexavalent molybdenum reduction to Mo-blue by *Acinetobacter calcoaceticus*," *Folia Microbiologica*, vol. 55, no. 2, pp. 137–143, 2010.

[19] M. Y. Shukor, S. A. Ahmad, M. M. M. Nadzir, M. P. Abdullah, N. A. Shamaan, and M. A. Syed, "Molybdate reduction by *Pseudomonas* sp. strain DRY2," *Journal of Applied Microbiology*, vol. 108, no. 6, pp. 2050–2058, 2010.

[20] H. K. Lim, M. A. Syed, and M. Y. Shukor, "Reduction of molybdate to molybdenum blue by *Klebsiella* sp. strain hkeem," *Journal of Basic Microbiology*, vol. 52, no. 3, pp. 296–305, 2012.

[21] C. Neunhäuserer, M. Berreck, and H. Insam, "Remediation of soils contaminated with molybdenum using soil amendments and phytoremediation," *Water, Air, and Soil Pollution*, vol. 128, no. 1-2, pp. 85–96, 2001.

[22] M. Y. Shukor, M. F. A. Rahman, N. A. Shamaan, C. H. Lee, M. I. A. Karim, and M. A. Syed, "An improved enzyme assay for molybdenum-reducing activity in bacteria," *Applied*

Biochemistry and Biotechnology, vol. 144, no. 3, pp. 293–300, 2008.

[23] M. Y. Shukor, H. Adam, K. Ithnin, I. Yunus, N. A. Shamaan, and A. Syed, "Molybdate reduction to molybdenum blue in microbe proceeds via a phosphomolybdate intermediate," *Journal of Biological Sciences*, vol. 7, no. 8, pp. 1448–1452, 2007.

[24] A. B. Ariff, M. Rosfarizan, B. Ghani, T. Sugio, and M. I. A. Karim, "Molybdenum reductase in *Enterobacter cloacae*," *World Journal of Microbiology and Biotechnology*, vol. 13, no. 6, pp. 643–647, 1997.

[25] R. K. Upreti, V. Sinha, R. Mishra, and A. Kannan, "In vitro development of resistance to arsenite and chromium-VI in *Lactobacilli* strains as perspective attenuation of gastrointestinal disorder," *Journal of Environmental Biology*, vol. 32, no. 3, pp. 325–332, 2011.

[26] G. D. Najafpour and C. P. Shan, "Enzymatic hydrolysis of molasses," *Bioresource Technology*, vol. 86, no. 1, pp. 91–94, 2003.

[27] J. V. Bhide, P. K. Dhakephalkar, and K. M. Paknikar, "Microbiological process for the removal of Cr(VI) from chromate-bearing cooling tower effluent," *Biotechnology Letters*, vol. 18, no. 6, pp. 667–672, 1996.

[28] W. Fritsche and M. Hofrichter, "Aerobic degradation by microorganisms," in *Biotechnology, a Multi-Volume Comprehensive Treatise*, J. Klein, Ed., pp. 147–154, Wiley-VCH, Weinheim, Germany, 1999.

[29] A. Tripathi, R. C. Upadhyay, and S. Singh, "Mineralization of mono-nitrophenols by *Bjerkandera adusta* and *Lentinus squarrosulus* and their extracellular ligninolytic enzymes," *Journal of Basic Microbiology*, vol. 51, no. 6, pp. 635–649, 2011.

[30] L. Xu, M. Luo, C. Jiang et al., "In vitro reduction of hexavalent chromium by cytoplasmic fractions of *Pannonibacter phragmitetus* LSSE-09 under aerobic and anaerobic conditions," *Applied Biochemistry and Biotechnology*, vol. 166, no. 4, pp. 933–941, 2012.

[31] B. Poljsak, I. Pócsi, P. Raspor, and M. Pesti, "Interference of chromium with biological systems in yeasts and fungi: a review," *Journal of Basic Microbiology*, vol. 50, no. 1, pp. 21–36, 2010.

[32] B. A. Wrenn, J. R. Haines, A. D. Venosa, M. Kadkhodayan, and M. T. Suidan, "Effects of nitrogen source on crude oil biodegradation," *Journal of Industrial Microbiology*, vol. 13, no. 5, pp. 279–286, 1994.

[33] J. L. Glenn and F. L. Crane, "Studies on metalloflavoproteins. V. The action of silicomolybdate in the reduction of cytochrome c by aldehyde oxidase," *Biochimica et Biophysica Acta*, vol. 22, no. 1, pp. 111–115, 1956.

[34] J. D. Lee, *Concise Inorganic Chemistry*, Van Reinhold Company, New York, NY, USA, 1977.

[35] N. V. Sidgwick, *The Chemical Elements and Their Compounds*, Clarendon Press, Oxford, UK, 1984.

[36] L. S. Clesceri, A. E. Greenberg, and R. R. Trussel, *Standard Methods for the Examination of Wastewater*, American Public Health Association, Port City Press, Baltimore, Md, USA, 17th edition, 1989.

[37] D. D. Runnells, D. S. Kaback, and E. M. Thurman, "Geochemistry and sampling of molybdenum in sediments, soils, and plants in Colorado," in *Molybdenum in the Environment*, W. R. Chappel and K. K. Peterson, Eds., Marcel Dekker, New York, NY, USA, 1976.

[38] B. Chai, Y. Wu, P. Liu, B. Liu, and M. Gao, "Isolation and phosphate-solubilizing ability of a fungus, *Penicillium* sp. from soil of an alum mine," *Journal of Basic Microbiology*, vol. 51, no. 1, pp. 5–14, 2011.

[39] R. P. A. Sims, "Formation of heteropoly blue by some reduction procedures used in the micro-determination of phosphorus," *The Analyst*, vol. 86, no. 1026, pp. 584–590, 1961.

[40] L. P. Kazansky and M. A. Fedotov, "Phosphorus-31 and oxygen-17 N.M.R. evidence of trapped electrons in reduced 18-molybdodiphosphate(V), $P_2Mo_{18}O_6^{28-}$," *Journal of the Chemical Society, Chemical Communications*, no. 14, pp. 644–647, 1980.

[41] K. Yoshimura, M. Ishii, and T. Tarutani, "Micro determination of phosphate in water by gel-phase colorimetry with molybdenum blue," *Analytical Chemistry*, vol. 58, no. 3, pp. 591–594, 1986.

[42] T. Hori, M. Sugiyama, and S. Himeno, "Direct spectrophotometric determination of sulphate ion based on the formation of a blue molybdosulphate complex," *The Analyst*, vol. 113, no. 11, pp. 1639–1642, 1988.

[43] R. M. C. Dawson, D. C. Elliott, W. H. Elliott, and K. M. Jones, *Data for Biochemical Research*, Oxford University Press, London, UK, 1969.

[44] T. Sugio, Y. Tsujita, T. Katagiri, K. Inagaki, and T. Tano, "Reduction of Mo^{6+} with elemental sulfur by *Thiobacillus ferrooxidans*," *Journal of Bacteriology*, vol. 170, no. 12, pp. 5956–5959, 1988.

[45] R. Elangovan, L. Philip, and K. Chandraraj, "Hexavalent chromium reduction by free and immobilized cell-free extract of *Arthrobacter rhombi*-RE," *Applied Biochemistry and Biotechnology*, vol. 160, no. 1, pp. 81–97, 2010.

[46] J. C. Munch and J. C. G. Ottow, "Reductive transformation mechanism of ferric oxides in hydromorphic soils," *Environmental Biogeochemistry*, vol. 35, pp. 383–394, 1983.

Hindawi Publishing Corporation
BioMed Research International
Volume 2013, Article ID 969135, 10 pages
http://dx.doi.org/10.1155/2013/969135

Research Article

Bioleaching of Arsenic-Rich Gold Concentrates by Bacterial Flora before and after Mutation

Xuehui Xie, Xuewu Yuan, Na Liu, Xiaoguang Chen, Awad Abdelgadir, and Jianshe Liu

College of Environmental Science and Engineering, Donghua University, 2999 North Renmin Road, Shanghai 201620, China

Correspondence should be addressed to Jianshe Liu; liujianshe@dhu.edu.cn

Received 20 September 2013; Accepted 30 October 2013

Academic Editor: Chong-Jian Tang

In order to improve the bioleaching efficiency of arsenic-rich gold concentrates, a mixed bacterial flora had been developed, and the mutation breeding method was adopted to conduct the research. The original mixed bacterial flora had been enrichedin acid mine drainage of Dexing copper mine, Jiangxi Province, China. It was induced by UV (ultraviolet), ultrasonic, and microwave, and their combination mutation. The most efficient bacterial flora after mutation was collected for further bioleaching of arsenic-rich gold concentrates. Results indicated that the bacterial flora after mutation by UV 60 s combined with ultrasonic 10 min had the best oxidation rate of ferrous, the biggest density of cells, and the most activity of total protein. During bioleaching of arsenic-rich gold concentrates, the density of the mutant bacterial cells reached to 1.13×10^8 cells/mL at 15 days, more than 10 times compared with that of the original culture. The extraction of iron reached to 95.7% after 15 days, increased by 9.9% compared with that of the original culture. The extraction of arsenic reached to 92.6% after 12 days, which was increased by 46.1%. These results suggested that optimum combined mutation could improve leaching ability of the bacterial flora more significantly.

1. Introduction

With the development of economy, high-grade gold ores are almost processed, low-grade gold ores and concentrates are becoming the main gold resources. Thus, it is increasingly necessary to process ores of lower grade to meet demand, especially on arsenic-rich gold concentrates [1, 2]. In arsenic-rich gold concentrates, gold grain is always occluded by sulfide minerals such as arsenopyrite (FeAsS), pyrite (FeS_2), realgar (As_2S_2), or orpiment (As_2S_3), which severely cut off the cyanide from gold grain [3, 4]. To achieve a satisfactory extraction of gold grain, an oxidative treatment is required to break down the blockade of sulfide minerals before cyanide leaching [5]. Bacteria oxidation has the advantages of low cost, low energy consumption and environmental protection, which shows the broad prospects for development on the treatment of low-grade gold ores and concentrates [6, 7]. However, bioleaching bacteria have some drawbacks such as long growth cycle and slow oxidation activity, which lead to poor effect on bioleaching [8].

Due to the major drawbacks of bioleaching bacteria, selecting and breeding the efficient bacteria for gold concentrates bioleaching are becoming more and more important. Mutation breeding is a frequently-used and effective method of obtaining excellent leaching microorganism. Xu et al. [9] used UV mutation to treat strains *Acidithiobacillus ferrooxidans* GF and *Acidiphilium cryptum* DX1-1 for chalcopyrite bioleaching, which obtained excellent leaching bacteria and increased the dissolution of copper. Kang et al. [10] treated mixed microorganisms with mutagens NO_2^-, diethyl sulfate (DES), UV, and their combinations, and the best one increased the content of Cu^{2+} by 101.4% in 20 days of leaching compared with the control culture on chalcocite-leaching.

Many studies on mutation breeding of bioleaching bacteria have been done all over the world, but few focused on the bacteria for arsenic-rich gold concentrates bioleaching [11, 12]. In this paper, the bacterial flora enriched in acid mine drainage of Dexing copper mine, Jiangxi Province, China, was used to be mutated and for arsenic-rich gold concentrates bioleaching. UV, ultrasonic, and microwave were major mutation methods and were adopted alone or combined to obtain excellent bioleaching bacteria. The effects of mutation on bacterial growth, activity and arsenic-rich

Table 1: Elemental composition of arsenic-rich gold concentrates.

Element	Content (%)
Fe	19.3
As	9.3
S	20.4
Ni	0.024
Zn	0.266
Pb	0.08
Cu	0.086
Ca	2.9
Ag	0.006
Au	<0.001

gold concentrates bioleaching were the main contents in this study.

2. Material and Method

2.1. Bacterial Flora. Original bacterial flora was enriched in acid mine drainage of Dexing copper mine, Jiangxi Province, China. Microbial diversity of the bacterial flora had been analyzed by RFLP analysis [13, 14]. Results indicated that the bacterial flora was dominated by moderate thermophilic microbes, including *Leptospirillum* sp. and *Sulfobacillus* sp. two putative divisions. Especially, *Leptospirillum* sp. was the most dominant division, which represented 52.5% of the total clones in the 16S rDNA cloning library of the bacterial flora (data not shown).

2.2. Mineral Sample. In this study, the arsenic-rich gold concentrates were obtained from Shandong province, China. The element analysis results of the sample were shown in Table 1.

It could be seen that the sample was rich of arsenic (As 9.3%) and belonged to arsenic-rich gold concentrates. X-ray diffraction (XRD) patterns of arsenic-rich gold concentrates showed that the main mineral phases were arsenopyrite (FeAsS), pyrite (FeS_2), quartz (SiO_2), and gypsum ($CaSO_4{\cdot}2H_2O$). The mineral sample was grounded and the particle size was <74 μm for bioleaching experiments.

2.3. Culture Medium. The bacterial flora was cultivated in 9 K liquid medium. 9 K liquid medium: $(NH_4)_2SO_4$ 3.0 g/L; $MgSO_4{\cdot}7H_2O$ 0.5 g/L; K_2HPO_4 0.5 g/L; KCl 0.1 g/L; $Ca(NO_3)_2$ 0.01 g/L, and $FeSO_4{\cdot}7H_2O$ was the energy source for bacterial growth. pH value of culture was modulated to 1.5 with 5 mol/L H_2SO_4. The liquid medium was sterilized at 121°C for 20 min before use. Bacteria were inoculated in 250 mL flasks containing 100 mL 9 K medium. Flasks were incubated at 40°C in a rotary shaker at 160 rpm.

2.4. Mutation. Cells in the logarithmic phase were centrifuged for 20 min (10000 rpm) and suspended in 9 K basic salts medium without Fe^{2+}, and the density of cells was adjusted to about 1.8×10^8 cells/mL.

Mutation experiments were performed under the following conditions. For UV mutation, the power of UV lamp was 15 W. The suspended cells were taken into a plate and at a distance of 30 cm to the UV lamp, and the radiation time was 60, 120, and 180 s, respectively. After mutation, the sample was kept away from light and stored in the refrigerator at 4°C for 12 hours to prevent the bacteria from recovery with light. For microwave mutation, the bacterial suspension was treated in a microwave oven (2450 MHz, 700 W) for 10, 20 and 30 s, respectively. Bacterial mutant were transferred on the ice to remove thermal radiation, and protect enzyme from inactivation. For ultrasonic mutation, ultrasonic cells crusher was used to treat the suspended cells. The power was 500 W and frequency was 40 KHz; the treatment time was 10, 20, and 30 min, respectively. For combination mutation, UV, ultrasonic, and microwave were used, respectively, to two combinations and three combinations for composite mutagenesis. After mutation, the bacterial mutants were cultivated in 9 K liquid medium under optimal growth conditions, and the density of cells and rate of Fe^{2+} oxidation were measured every 12 hours. The bacterial mutants with good oxidation activity on Fe^{2+} were selected in gold concentrates bioleaching experiments.

Total protein activity detection. The bacterial mutants selected growing at the stationary growth stage in 9 K medium were collected by centrifugation (10,000 rpm for 20 min), washed with distilled water, and suspended in the acetate buffer. pH value of suspension was adjusted to about 5.8. Cells obtained were crushed by biological cell disruption of AH-100B (ATS Engineering Inc. Canada) and centrifuged at 10,000 rpm for 30 min (4°C) to collect total protein. The total protein activity was determined by two-point inverse calibration method [15]. In this study, the amount of ferrous ions oxidation in unit time was used to weigh the activity of total protein, and a purple coordination compound was formed by combining ferrous ions nonoxidized with ferrozine. Total protein activity was monitored by measuring the absorbance of the compound in 570 nm wavelength using a UV-vis spectrophotometer (Hitachi Model U-2910). The less absorbance of the compound, the more activity of bacterial total protein.

2.5. Bioleaching Experiments. Bioleaching experiments were conducted in 250 mL flasks containing 100 mL 9 K liquid medium and 10% (v/v) of bacterial flora. The pulp density of arsenic-rich gold concentrates was 5% (w/v), and the initial pH of the culture was adjusted to 2.0 with 5 mol/L H_2SO_4. Flasks were incubated at 40°C and 160 rpm in a rotary shaker. During bioleaching process, the density of cells, pH values, concentration of total arsenic, and total iron in the solution were determined at certain intervals. The medium in flasks taken out must be compensated with 9 K medium, and the evaporation of water in flasks was supplemented with distilled water. All experiments were performed in triplicate and the average values were reported.

The density of cells was determined by hemacytometer counting method under the optical microscope (Olympus CX31). Potassium dichromate titration was used to calculate

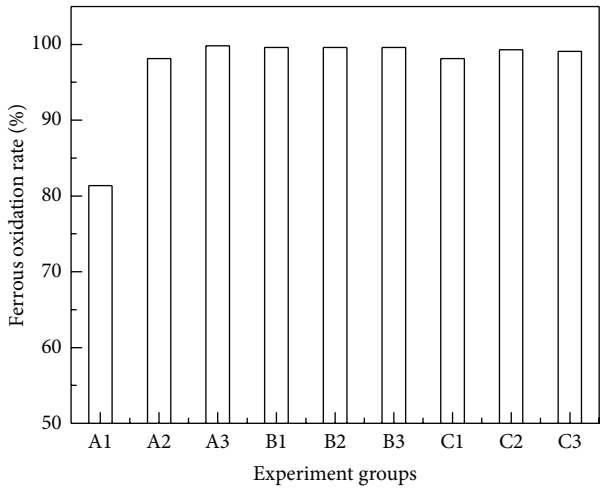

Figure 1: Mutation experiments with single factors. A1: UV 60 s, A2: UV 120 s, and A3: UV 180 s; B1: ultrasonic 10 min, B2: ultrasonic 20 min, and B3: ultrasonic 30 min; C1: microwave 10 s, C2: microwave 20 s, and C3: microwave 30 s.

ferrous iron oxidation rate. Concentrations of total arsenic and total iron were determined by ultraviolet spectrophotometry. pH values of the solution were measured by multifunctional water quality analyzer (WTW, Germany).

3. Results and Discussion

3.1. Mutation Results. Considering that bioleaching bacteria was strictly chemoautotrophy bacterium, the existence of organic matter would inhibit its growth [16]. And furthermore, the majority of chemical mutagens play the best mutation effect only in the near-neutral environment, but decompose into a variety of harmful organic compounds in the acidic environment, so, physical mutagens such as UV, ultrasonic, and microwave were preferred to be selected in this mutation experiment.

3.1.1. Mutation with Single Factors. Bacterial flora after mutation with single mutation factors were cultured in 250 mL flasks containing 100 mL 9 K liquid medium with ferrous iron. The initial density of cells was adjusted to about 1.0×10^7 cells/mL. The results of ferrous iron oxidation rate were shown in Figure 1.

Most experimental groups had good effects. Especially, the mutation group A3 (UV 180 s) had the greatest effects on improving the rate of ferrous iron oxidation, which reached to 99.8% at 36 hours.

3.1.2. Mutation with Combination of Mutation Factors. A problem that suffered in mutation process is repeated when using single mutagenic agents. It may cause bacteria to produce passive phenomenon and be hard to acquire the best mutation effect. Some researches revealed that several combined mutation techniques can increase mutation effect more efficiently than single mutation factors. El-Bestawy et al. [17] used ultraviolet irradiation combined ethidium bromide to obtain bacterial strains with capability of removing heavy metals at high efficiency, such as Cd (89.9–100%), Cr (87.3–99.7%) and Zn (47.7–100%). In this study, bacterial flora processed by combination of mutation factors were also conducted.

Processed with two combined mutation factors. Bacterial flora after mutation with two combined mutation factors were cultured in 250 mL flasks containing 100 mL 9 K liquid medium with ferrous iron. The initial density of cells was adjusted to about 1.0×10^7 cells/mL. The results of ferrous iron oxidation were shown in Figure 2.

It was obvious that there were big fluctuations on mutation effects among different compound mutation groups. Figure 2(a) showed ferrous iron oxidation results with combined mutation factors of UV and ultrasonic. Experimental groups from D1 to D9 indicated different mutation conditions. The best experimental group was D1 (UV 60 s + ultrasonic 10 min), which indicated that the bacterial flora had been processed by UV for 60 s, and then by ultrasonic for 10 min, the rate of ferrous iron oxidation could reach to 100% at 36 hours. Figure 2(b) showed ferrous iron oxidation results with combined mutation factors of UV and microwave. The best experimental group was E6 (UV 180 s + microwave 20 s), the rate of ferrous iron oxidation could reach to 99.6% at 36 hours. Figure 2(c) showed ferrous iron oxidation results with combined mutation factors of ultrasonic and microwave. The best experimental group was F8 (ultrasonic 20 min + microwave 30 s), the rate of ferrous iron oxidation could reach to 99.6% at 36 hours. Therefore, from Figure 3, it could be deduced that the experimental group D1 (UV 60 s + ultrasonic 10 min) had the greatest effect on improving the ferrous iron oxidation rate of bacterial flora.

Processed with three combined mutation factors. Bacterial flora after mutation with three combined mutation factors were cultured in 250 mL flasks, containing 100 mL 9 K liquid medium with ferrous iron. The initial density of cells was adjusted to about 1.0×10^7 cells/mL. The results of ferrous iron oxidation were shown in Figure 3.

It showed that group G6 (UV 120 s + ultrasonic 30 min + microwave 10 s) had the best effect on improving the ferrous iron oxidation rate of bacterial flora, and it could reached to 99.8% at 36 hours.

3.2. Influences of Mutation on Bacterial Flora's Growth and Activity. Mutation technique had been wildly used to increase the production of industrially valuable compounds with microbial mutants [18]. And other researches had focused on adopting mutation technique to obtain microbial mutants owning more resistibility for heavy metals [19]. In this study, mutation was mainly adopted to improve the bacterial flora's growth and activity.

Bacterial flora mutants, which were processed by three different mutation experimental groups such as A3 (UV 180 s), D1 (UV 60 s + ultrasonic 10 min), and G6 (UV 120 s + microwave 10 s + ultrasonic 30 min), respectively, were selected for further study. The untreated original culture and the mutants were cultivated in 250 mL flasks containing 100 mL 9 K liquid medium with ferrous iron, and the initial density of cells was adjusted to about 1.0×10^7 cells/mL. The

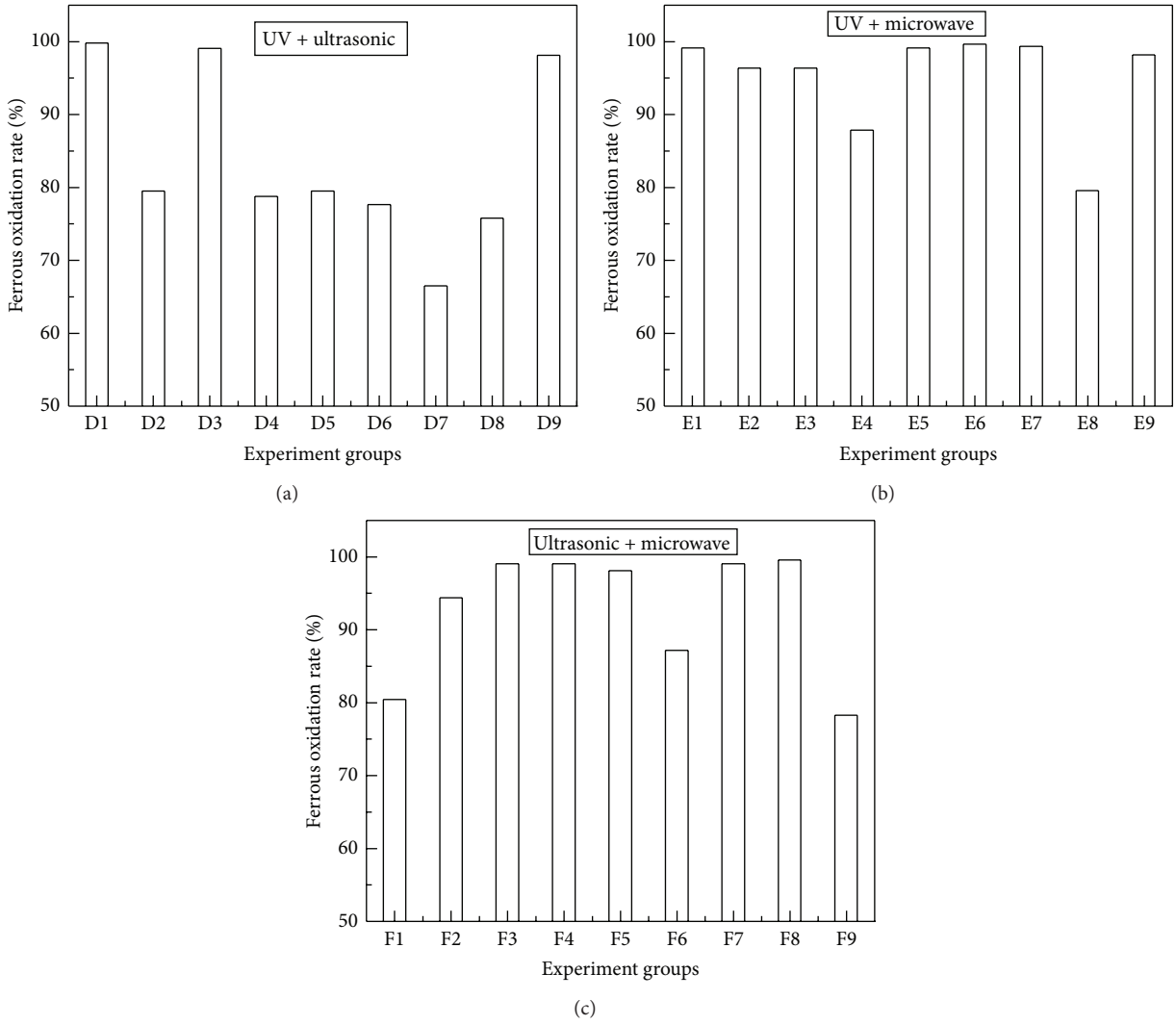

Figure 2: Mutation experiments with two combined mutation factors. (a) UV+ultrasonic (D1: UV 60 s + ultrasonic 10 min, D2: UV 60 s + ultrasonic 20 min, D3: UV 60 s + ultrasonic 30 min, D4: UV 120 s + ultrasonic 10 min, D5: UV 120 s + ultrasonic 20 min, D6: UV 120 s + ultrasonic 30 min, D7: UV 180 s + ultrasonic 10 min, D8: UV 180 s + ultrasonic 20 min, and D9: UV 180 s + ultrasonic 30 min), (b) UV + microwave (E1: UV 60 s + microwave 10 s, E2: UV 120 s + microwave 10 s, E3: UV 180 s + microwave 10 s, E4: UV 60 s + microwave 20 s, E5: UV 120 s + microwave 20 s, E6: UV 180 s + microwave 20 s, E7: UV 60 s + microwave 30 s, E8: UV 120 s + microwave 30 s, and E9: UV 180 s + microwave 30 s), (c) ultrasonic + microwave (F1: ultrasonic 10 min + microwave 10 s, F2: ultrasonic 20 min + microwave 10 s, F3: ultrasonic 30 min + microwave 10 s, F4: ultrasonic 10 min + microwave 20 s, F5: ultrasonic 20 min + microwave 20 s, F6: ultrasonic 30 min + microwave 20 s, F7: ultrasonic 10 min + microwave 30 s, F8: ultrasonic 20 min + microwave 30 s, and F9: ultrasonic 30 min + microwave 30 s).

initial pH value of the culture was adjusted to 2.0 with 5 mol/L H_2SO_4. All flasks were performed at 40°C and 160 rpm in a rotary shaker. Various growth patterns of bacterial flora untreated and mutated growing in 9 K medium with ferrous iron were shown in Figure 4.

Figure 4(a) showed the results of ferrous iron oxidation of bacterial flora before and after mutation at 36 hours. For bacterial mutants, ferrous iron was almost oxidized completely within 36 hours. However, for the original culture, ferrous iron oxidation rate was only 70.21% at 36 hours. These results indicated that mutation could significantly improve the ferrous oxidation activity of this bacterial flora.

The growth curves of bacterial flora before and after mutation were shown in Figure 4(b). Results indicated that the growth of bacterial mutants was better than that of the original culture. And mutation treatments could obviously increase the density of cells in sequence of group D1 > G6 > A3. The density of cells reached to 1.2×10^8, 1.15×10^8, and 1.1×10^8 cells/mL, increased by 20%, 15%, and 10% after mutation with group D1, G6, and A3, respectively. From this result, it could be known mutation could improve bacterial growth activity.

Furthermore, the activity of protein plays a key role in bacterial oxidation activity [20]. During autotrophic growth on iron, bacteria obtain energy through the oxidation of ferrous ion to ferric ion, and energy transduction is catalyzed by protein, such as rusticyanin, which participates in the ferrous oxidation pathway [21, 22]. In this study,

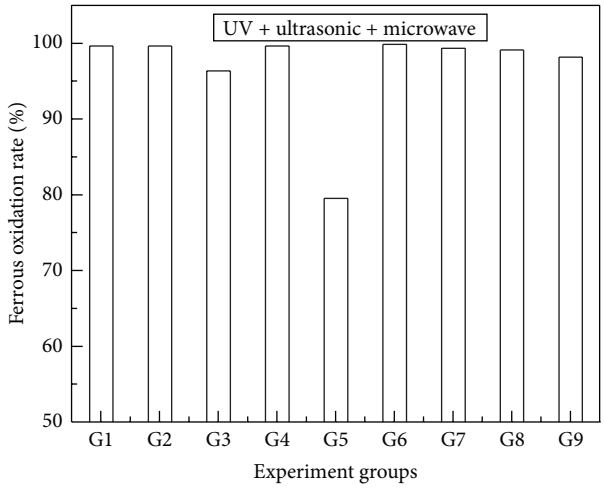

Figure 3: Mutation experiments with three combined mutation factors. (G1: UV 60 s + ultrasonic 10 min + microwave 10 s, G2: UV 60 s + ultrasonic 20 min + microwave 20 s, G3: UV 60 s + ultrasonic 30 min + microwave 30 s, G4: UV 120 s + ultrasonic 10 min + microwave 20 s, G5: UV 120 s + ultrasonic 20 min + microwave 30 s, G6: UV 120 s + ultrasonic 30 min + microwave 10 s, G7: UV 180 s + ultrasonic 10 min + microwave 30 s, G8: UV 180 s + ultrasonic 20 min + microwave 10 s, G9: UV 180 s + ultrasonic 30 min + microwave 20 s).

the total protein activity was determined by a two-point inverse calibration method, and the results were shown in Figure 4(c). It could be seen that all the absorbance of the purple coordination compound continuously decreased as time increased. The absorbance values of bacterial mutants were always lower than that of the original culture and the blank (without bacteria) during the measuring time, which could indicate the total protein activity of bacterial flora mutants was improved. Meanwhile, the value of absorbance of different bacterial mutants was in sequence of group A3 > G6 > D1, which suggested that bacterial flora processed by mutation group D1 had the best total protein activity.

From these results, it could be deduced that the bacterial flora after mutation process with group D1 had the best ferrous oxidation activity, growth activity, and the total protein activity. It was selected as the experimental bacteria in further study of arsenic-rich gold concentrates bioleaching.

3.3. Bioleaching of Arsenic-Rich Gold Concentrates. The original bacterial flora and the bacterial flora after mutation by method group D1 (UV 60 s + ultrasonic 10 min) were used for arsenic-rich gold concentrates bioleaching. The results in terms of changes in the density of cells, pH value, and extraction of elements Fe and As were shown in Figure 5.

As shown in Figure 5(a), bacterial mutants always grew better than the original bacteria during the whole bioleaching process, which was in accordance with the result of Dong et al. [23]. For the original bacteria, the density of cells was 9.7×10^7 cells/mL at 15 days. While for bacterial mutant, the density of cells reached to 1.13×10^8 cells/mL at 15 days. However, the maximum concentration of cells was smaller than that growing in 9 K medium without arsenic-rich gold concentrates, because of high arsenic concentration inhibiting the bacterial growth.

Figure 5(b) showed pH values' variation during arsenic-rich gold concentrates bioleaching by the original bacteria and bacterial mutant. It indicated that pH value was fluctuating among the whole bioleaching process. At an earlier stage, pH value was uptrend. Then pH value continuously decreased as time increased both of the original bacteria and the bacterial mutant, down to 1.54 and 1.39 at 18 days, respectively. These results may attribute to that bacteria uses acid for its growth and reproduction at the beginning process (1) [24]. And then, the gold ore bioleaching involves in sulfur and sulfide minerals oxidation (2) to (4) [25, 26], which leads to a decrease in pH value [27]. These results were similar to the study of Zhou et al. [28]. Consider

$$4Fe^{2+} + 4H^+ + O_2 \xrightarrow{\text{bacteria}} 4Fe^{3+} + 2H_2O \quad (1)$$

$$2FeAsS + 2Fe^{3+} + 4H_2O + 6O_2 \longrightarrow 2H_3AsO_4 + 4Fe^{2+} + 2H^+ + 2SO_4^{2-} \quad (2)$$

$$FeS_2 + 14Fe^{3+} + 8H_2O \longrightarrow 2SO_4^{2-} + 15Fe^{2+} + 16H^+ \quad (3)$$

$$2S + 2H_2O + 3O_2 \xrightarrow{\text{bacteria}} 4H^+ + 2SO_4^{2-} \quad (4)$$

The extraction of total iron and arsenic leached by the original bacteria and bacterial mutant were shown in Figures 5(c) and 5(d). Firstly, all the figures indicated that arsenic-rich leaching by bacteria had better effect than that of leaching by acid. Then, bacterial mutant had better effect on the solubilization of total iron and total arsenic than that of the original bacteria. For leaching by the bacterial mutant, the extraction of total iron reached to 95.7% after 15 days. While, leaching by the original bacteria, the extraction of total iron was 85.8% after 15 days. A total of 9.9% extraction was improved by the bacterial mutant compared with original bacteria (Figure 5(c)). During the whole bioleaching process, the extraction of total arsenic by bacterial mutant was always higher than that by the original bacteria. For leaching by the bacterial mutant, the maximum leaching of arsenic reached to 92.6% after 12 days. When leaching by the original bacteria, the extraction of total arsenic was only 46.5% after 12 days. 46.1% of improvement was obtained by the bacterial mutant compared with that of the original bacteria (Figure 5(d)). At the later stage of bioleaching, the extraction of total iron and arsenic had a decrease trend, which might be due to the formation of secondary minerals such as jarosite and scorodite. Many researches indicated that in the process of mineral bioleaching the passivation layer was formed, adsorbed on the surface of mineral, and hindered the continuous bioleaching of mineral [25, 29–32].

3.4. XRD Analysis. In order to verify the formation of secondary minerals such as jarosite and scorodite on the surface of the arsenic-rich gold concentrates after bioleaching and oxidation, the X-ray diffraction (XRD) patterns of the

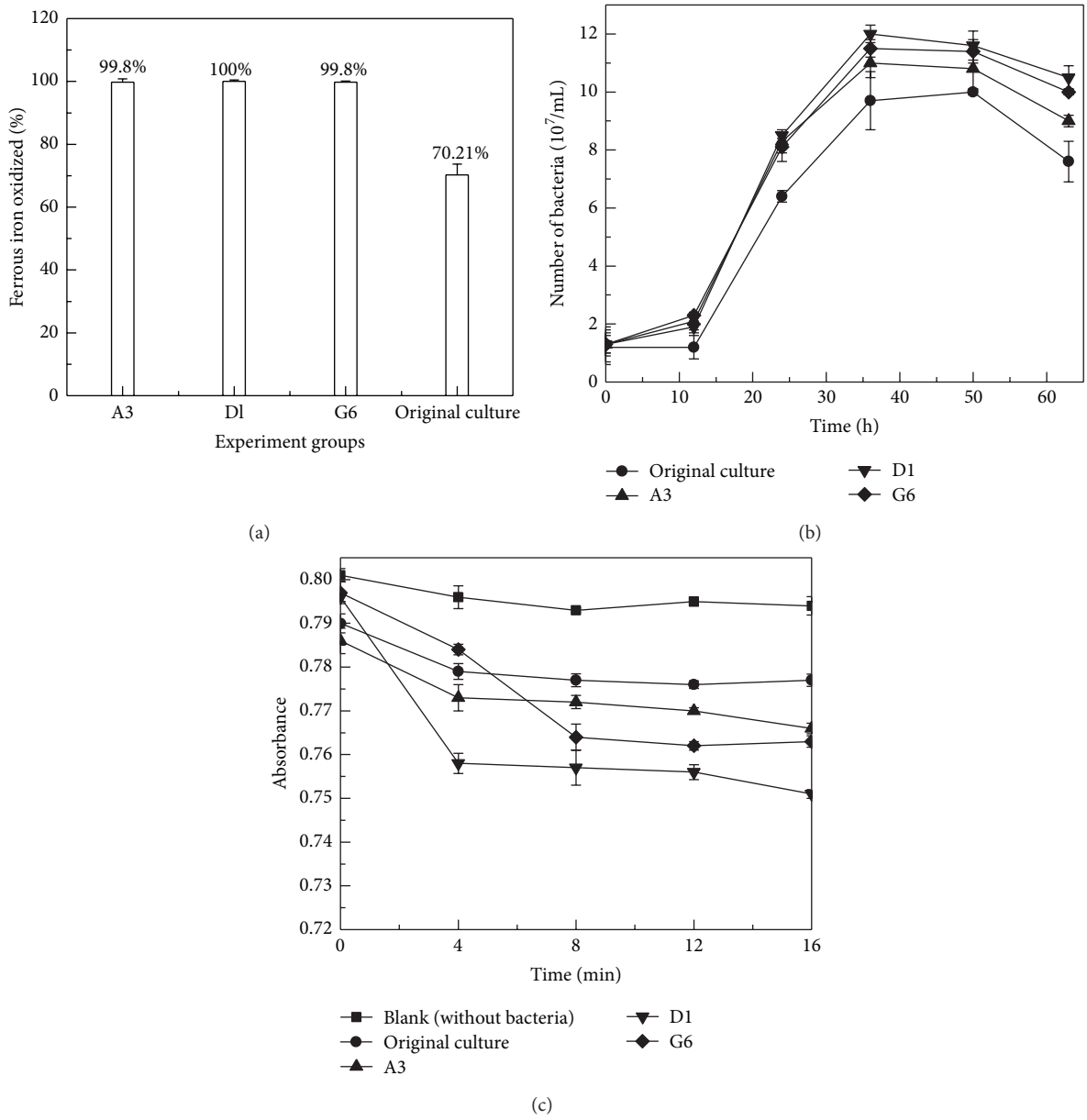

Figure 4: Various growth patterns of bacterial flora before and after mutation growing in 9 K medium with ferrous iron. (a) Ferrous oxidation rate, (b) growth curve, (c) total protein activity (A3: UV 180 s; D1: UV 60 s + Ultrasound 10 min; G6: UV 120 s + Microwave 10 s + Ultrasound 30 min).

original material and leached residues were further analyzed. The results were seen in Figure 6.

It showed that the main mineral phases were quartz (SiO_2), sulfur (S_8), jarosite ($Fe_3(SO_4)_2(OH)_6$), gypsum ($CaSO_4{\cdot}2H_2O$), and scorodite ($FeAsO_4(H_2O)_2$) in the residues (Figure 6(b)). Compared with the XRD patterns of the original concentrates (seen in Figure 6(a)), it could be deduced that arsenopyrite (FeAsS) and pyrite (FeS_2) in the original mineral had been oxidized completely, and new materials such as sulfur (S_8), jarosite ($Fe_3(SO_4)_2(OH)_6$), and scorodite ($FeAsO_4(H_2O)_2$) had generated, which were substances that often form a passivation layer [25, 31, 32].

On the base of XRD analysis results, the generation process of the passivation layer during bioleaching of the arsenic-rich gold concentrates was further derived, and a model was built in this study (seen in Figure 7).

From Figure 7, it could be seen that the gold concentrates were oxidized and generated $H_2AsO_4^-$, Fe^{3+}, S and SO_4^{2-}, which formed jarosite, scorodite, sulfur, and other substances covering in the mineral surface to form a passivation layer, wherein S layer was formed in the case of elemental sulfur which is excessive and not oxidized. The process might mainly refer to the following reactions [33–35]:

$$3Fe^{3+} + 2HSO_4^- + K^+ + 6H_2O \longrightarrow KFe_3(SO_4)_2(OH)_6 + 8H^+$$

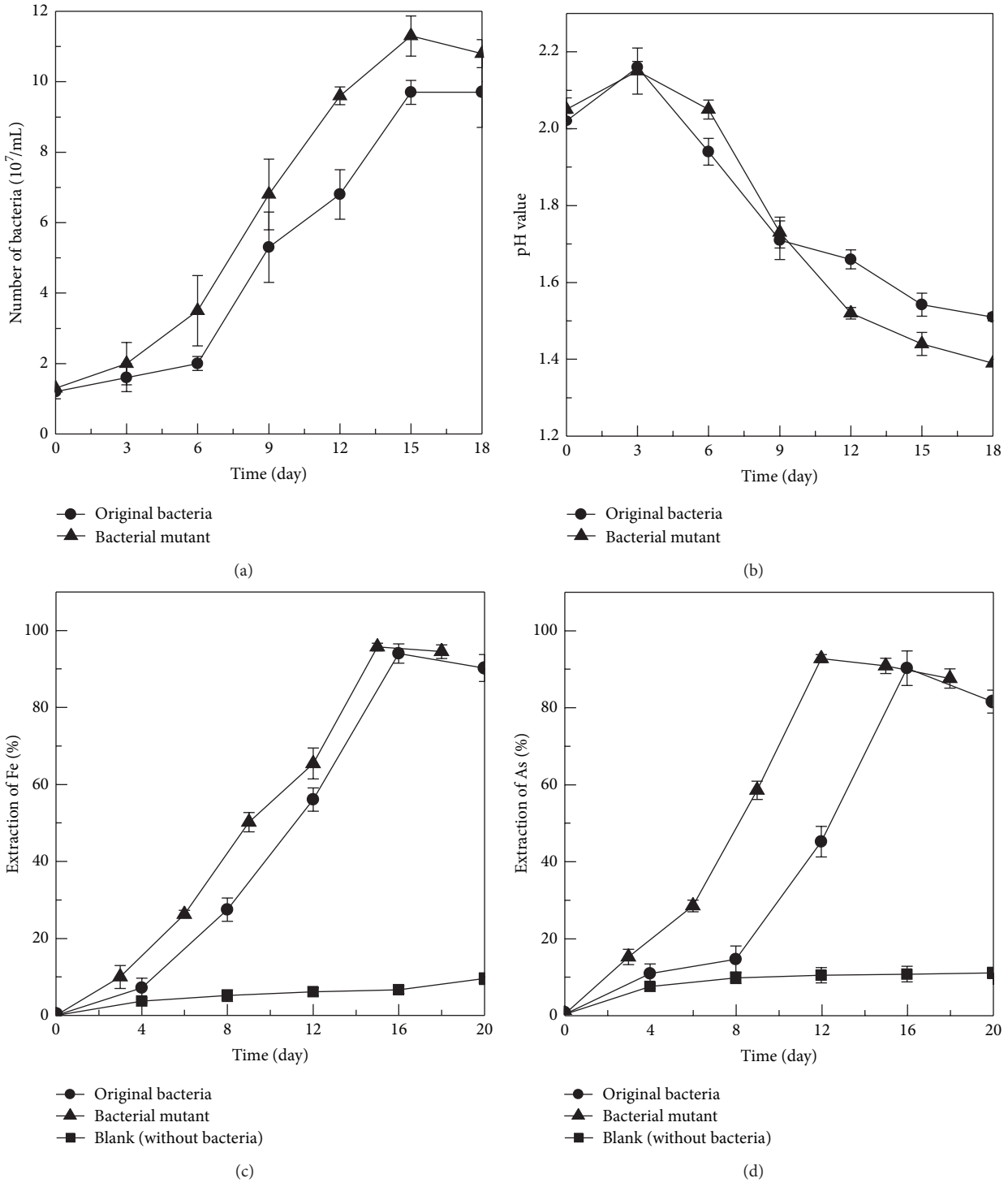

FIGURE 5: Various growth patterns of the original bacteria and bacterial mutant during arsenic-rich gold concentrates bioleaching. (a) Growth curve, (b) pH value, (c) extraction of Fe, and (d) extraction of As.

$$\begin{gathered} H_3AsO_4 + Fe^{3+} + 2H_2O \longrightarrow FeAsO_4 \cdot 2H_2O + 3H^+ \\ FeS_2 + 2Fe^{3+} \longrightarrow 3Fe^{2+} + 2S \\ FeAsS + 5Fe^{3+} + 3H_2O \longrightarrow 6Fe^{2+} + 3H^+ + H_3AsO_3 + S \end{gathered} \tag{5}$$

From the results it could be known that, for original bacteria and the mutant bacteria, the leaching process may be the same, and the leached residues may have the similar characteristics, but their leaching efficiency is different. Bacterial mutant could increase the extraction of iron and arsenic significantly and could shorten the leaching time.

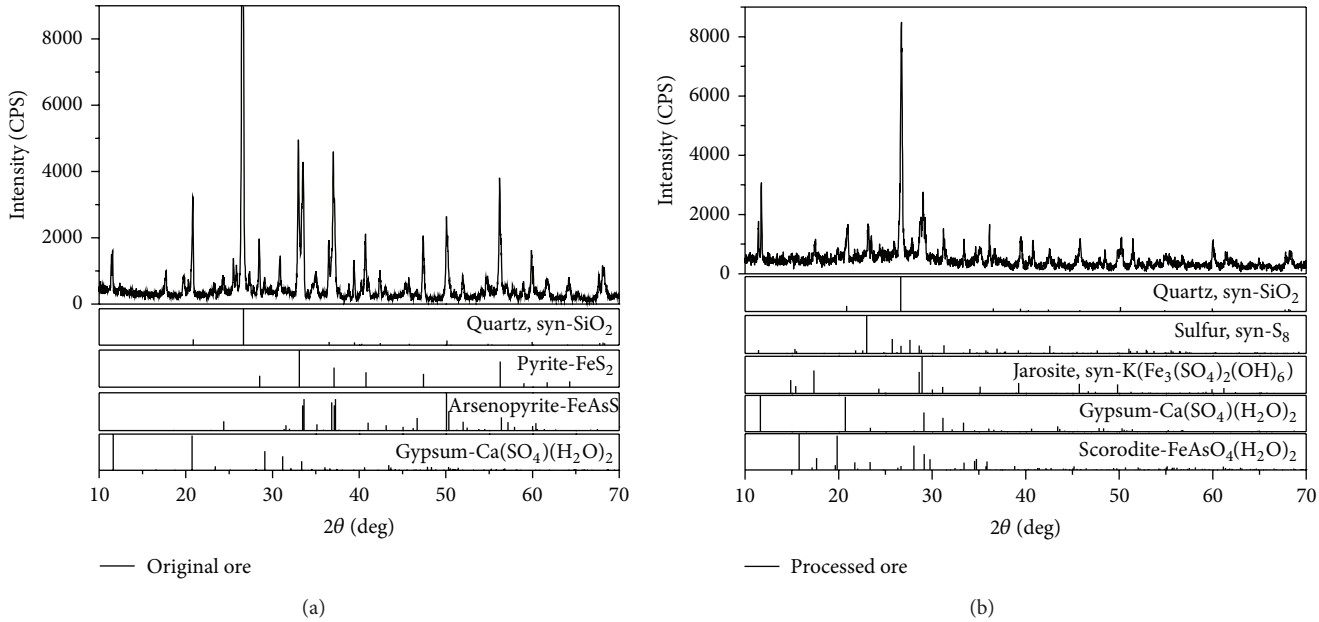

Figure 6: XRD patterns of the arsenic-rich gold concentrates' sample before and after bioleaching. (a) Original mineral sample, (b) leached residues.

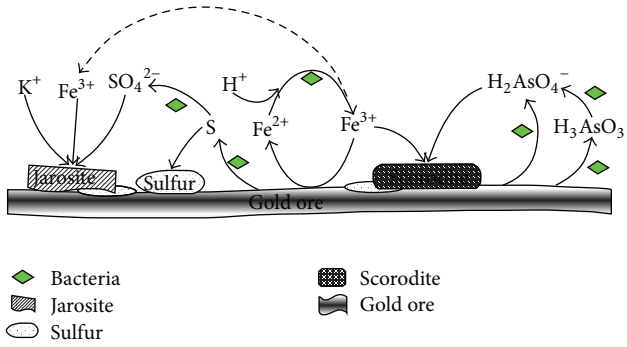

Figure 7: The formation of passivation layer on arsenic-rich gold concentrates surface.

4. Conclusion

In conclusion, the bacterial flora after mutation processed by combined mutation group D1 (UV 60 s + ultrasonic 10 min) had the best ferrous oxidation rate, the maximum density of cells, and the most total protein activity, and it had been selected for the further study of arsenic-rich gold concentrates bioleaching. Bioleaching results showed that the bacterial mutant could increase the extraction of iron and arsenic significantly and could shorten the leaching time. At the same time, XRD analysis results revealed the generation of new materials such as sulfur, jarosite, and scorodite covering in the gold concentrates' surface, which might form a passivation layer and hindered the continuous bioleaching of the gold concentrates. Further study focused on the community structure of the flora before and after mutation would be conducted. Succession of communities during the bioleaching process of the arsenic-rich gold concentrates will be the main study contents.

Conflict of Interests

The author(s) declare(s) that there is no conflict of interests regarding the publication of this paper.

Acknowledgments

This work was supported by the National Natural Science Foundation of China (no. 41073060), Ph.D. Programs Foundation of Ministry of Education of China Young Scholars (no. 20120075120014), Shanghai Natural Science Foundation of Youth Project (no. 12ZR1440400), Shanghai Leading Academic Discipline Project (B604), and the State Environmental Protection Engineering Center for Pollution Treatment and Control in Textile Industry.

References

[1] G. Gao, D. Li, Y. Zhou, X. Sun, and W. Sun, "Kinetics of high-sulphur and high-arsenic refractory gold concentrate oxidation by dilute nitric acid under mild conditions," *Minerals Engineering*, vol. 22, no. 2, pp. 111–115, 2009.

[2] Q. Li, D. Li, and F. Qian, "Pre-oxidation of high-sulfur and high-arsenic refractory gold concentrate by ozone and ferric ions in acidic media," *Hydrometallurgy*, vol. 97, no. 1-2, pp. 61–66, 2009.

[3] P. A. Schmitz, S. Duyvesteyn, W. P. Johnson, L. Enloe, and J. McMullen, "Adsorption of aurocyanide complexes onto carbonaceous matter from preg-robbing Goldstrike ore," *Hydrometallurgy*, vol. 61, no. 2, pp. 121–135, 2001.

[4] C. L. Zhu, H. Y. Yang, X. G. Tang, Y. J. Fan, and L. L. Tong, "Current status of studies on bacterial pre-oxidation and leaching of refractory gold ores with as," *Precious Metals*, vol. 31, pp. 48–52, 2010 (Chinese).

[5] P. Miller and A. Brown, "Bacterial oxidation of refractory gold concentrates," *Developments in Mineral Processing*, vol. 15, pp. 371–402, 2005.

[6] R.-C. Cui, H.-Y. Yang, S. Chen, S. Zhang, and K.-F. Li, "Valence variation of arsenic in bioleaching process of arsenic-bearing gold ore," *Transactions of Nonferrous Metals Society of China*, vol. 20, no. 6, pp. 1171–1176, 2010.

[7] J. J. Plumb, R. Muddle, and P. D. Franzmann, "Effect of pH on rates of iron and sulfur oxidation by bioleaching organisms," *Minerals Engineering*, vol. 21, no. 1, pp. 76–82, 2008.

[8] Y.-D. Liu, X.-B. Wang, W.-T. Shi, Y. Yang, and X. Zhang, "Experimental research into the mutagenic mechanism of *Thiobacillus ferrooxidans*," *Transaction of Beijing Institute of Technology*, vol. 30, no. 7, pp. 869–872, 2010 (Chinese).

[9] A.-L. Xu, J.-L. Xia, S. Zhang, Y. Yang, Z.-Y. Nie, and G.-Z. Qiu, "Bioleaching of chalcopyrite by UV-induced mutagenized *Acidiphilium cryptum* and *Acidithiobacillus ferrooxidans*," *Transactions of Nonferrous Metals Society of China*, vol. 20, no. 2, pp. 315–321, 2010.

[10] J. Kang, G.-Z. Qiu, J. Gao, H.-H. Wang, X.-L. Wu, and J.-N. Ding, "Bioleaching of chalcocite by mixed microorganisms subjected to mutation," *Journal of Central South University of Technology*, vol. 16, no. 2, pp. 218–222, 2009.

[11] C. Meng, X. Shi, H. Lin, J. Chen, and Y. Guo, "UV induced mutations in *Acidianus brierleyi* growing in a continuous stirred tank reactor generated a strain with improved bioleaching capabilities," *Enzyme and Microbial Technology*, vol. 40, no. 5, pp. 1136–1140, 2007.

[12] L. Xia, J. Zeng, J. Ding et al., "Comparison of three induced mutation methods for *Acidiothiobacillus caldus* in processing sphalerite," *Minerals Engineering*, vol. 20, no. 14, pp. 1323–1326, 2007.

[13] L.-X. Xia, L. Tang, J.-L. Xia et al., "Relationships among bioleaching performance, additional elemental sulfur, microbial population dynamics and its energy metabolism in bioleaching of chalcopyrite," *Transactions of Nonferrous Metals Society of China*, vol. 22, no. 1, pp. 192–198, 2012.

[14] X. W. Yuan, *Bioleaching of arsenic-rich gold ores with bacterial mixture before and after mutation and study of community shift [M.S. thesis]*, Donghua University, Shanghai, China, 2013, (Chinese).

[15] Y. S. Xiao and X. Y. Zhang, "Dotection of serum ferroxidase activity by two-point inverse calibration," *Jiangxi Journal of Medical Laboratory Sciences*, vol. 19, pp. 343–346, 2001 (Chinese).

[16] D. B. Johnson, "Selective solid media for isolating and enumerating acidophilic bacteria," *Journal of Microbiological Methods*, vol. 23, no. 2, pp. 205–218, 1995.

[17] E. El-Bestawy, E. Abou El-KHeir, H. I. Abd El-Fatah, and S. M. Hassouna, "Enhancement of bacterial efficiency for metal removal using mutation techniques," *World Journal of Microbiology and Biotechnology*, vol. 14, no. 6, pp. 853–856, 1998.

[18] N. Mollania, K. Khajeh, B. Ranjbar, and S. Hosseinkhani, "Enhancement of a bacterial laccase thermostability through directed mutagenesis of a surface loop," *Enzyme and Microbial Technology*, vol. 49, no. 5, pp. 446–452, 2011.

[19] X. W. Zhao, M. H. Zhou, Q. B. Li et al., "Simultaneous mercury bioaccumulation and cell propagation by genetically engineered *Escherichia coli*," *Process Biochemistry*, vol. 40, no. 5, pp. 1611–1616, 2005.

[20] J. Zeng, M. Geng, Y. Liu et al., "Expression, purification and molecular modelling of the Iro protein from *Acidithiobacillus ferrooxidans* Fe-1," *Protein Expression and Purification*, vol. 52, no. 1, pp. 146–152, 2007.

[21] C. Ida, K. Sasaki, A. Ando, R. C. Blake II, H. Saiki, and N. Ohmura, "Kinetic rate constant for electron transfer between ferrous ions and novel rusticyanin isoform in *Acidithiobacillus ferrooxidans*," *Journal of Bioscience and Bioengineering*, vol. 95, no. 5, pp. 534–537, 2003.

[22] A. Yarzábal, K. Duquesne, and V. Bonnefoy, "Rusticyanin gene expression of *Acidithiobacillus ferrooxidans* ATCC 33020 in sulfur- and in ferrous iron media," *Hydrometallurgy*, vol. 71, no. 1-2, pp. 107–114, 2003.

[23] Y. Dong, H. Lin, H. Wang, X. Mo, K. Fu, and H. Wen, "Effects of ultraviolet irradiation on bacteria mutation and bioleaching of low-grade copper tailings," *Minerals Engineering*, vol. 24, no. 8, pp. 870–875, 2011.

[24] J. Vilcáez, K. Suto, and C. Inoue, "Response of *thermophiles* to the simultaneous addition of sulfur and ferric ion to enhance the bioleaching of chalcopyrite," *Minerals Engineering*, vol. 21, no. 15, pp. 1063–1074, 2008.

[25] A. Ahmadi, M. Schaffie, J. Petersen, A. Schippers, and M. Ranjbar, "Conventional and electrochemical bioleaching of chalcopyrite concentrates by moderately thermophilic bacteria at high pulp density," *Hydrometallurgy*, vol. 106, no. 1-2, pp. 84–92, 2011.

[26] H. Ciftci and A. Akcil, "Effect of biooxidation conditions on cyanide consumption and gold recovery from a refractory gold concentrate," *Hydrometallurgy*, vol. 104, no. 2, pp. 142–149, 2010.

[27] J. J. Plumb, N. J. McSweeney, and P. D. Franzmann, "Growth and activity of pure and mixed bioleaching strains on low grade chalcopyrite ore," *Minerals Engineering*, vol. 21, no. 1, pp. 93–99, 2008.

[28] H.-B. Zhou, W.-M. Zeng, Z.-F. Yang, Y.-J. Xie, and G.-Z. Qiu, "Bioleaching of chalcopyrite concentrate by a moderately thermophilic culture in a stirred tank reactor," *Bioresource Technology*, vol. 100, no. 2, pp. 515–520, 2009.

[29] M. Fantauzzi, C. Licheri, D. Atzei et al., "Arsenopyrite and pyrite bioleaching: evidence from XPS, XRD and ICP techniques," *Analytical and Bioanalytical Chemistry*, vol. 401, no. 7, pp. 2237–2248, 2011.

[30] R. L. Flemming, K. A. Salzsauler, B. L. Sherriff, and N. V. Sidenko, "Identification of scorodite in fine-grained, high-sulfide, arsenopyrite mine-waste using micro x-ray diffraction (μXRD)," *Canadian Mineralogist*, vol. 43, no. 4, pp. 1243–1254, 2005.

[31] H. He, J.-L. Xia, F.-F. Hong, X.-X. Tao, Y.-W. Leng, and Y.-D. Zhao, "Analysis of sulfur speciation on chalcopyrite surface bioleached with *Acidithiobacillus ferrooxidans*," *Minerals Engineering*, vol. 27-28, pp. 60–64, 2012.

[32] L. Chang-Li, X. Jin-Lan, N. Zhen-Yuan, Y. Yi, and M. Chen-Yan, "Effect of sodium chloride on sulfur speciation of chalcopyrite bioleached by the extreme thermophile *Acidianus manzaensis*," *Bioresource Technology*, vol. 110, pp. 462–467, 2012.

[33] A. Ahmadi, M. Ranjbar, and M. Schaffie, "Catalytic effect of pyrite on the leaching of chalcopyrite concentrates in chemical, biological and electrobiochemical systems," *Minerals Engineering*, vol. 34, pp. 11–18, 2012.

[34] A. Hol, R. D. van der Weijden, G. van Weert, P. Kondos, and C. J. N. Buisman, "Processing of arsenopyritic gold concentrates by partial bio-oxidation followed by bioreduction," *Environmental Science and Technology*, vol. 45, no. 15, pp. 6316–6321, 2011.

[35] K. Takatsugi, K. Sasaki, and T. Hirajima, "Mechanism of the enhancement of bioleaching of copper from enargite by thermophilic iron-oxidizing archaea with the concomitant precipitation of arsenic," *Hydrometallurgy*, vol. 109, no. 1-2, pp. 90–96, 2011.

Hindawi Publishing Corporation
BioMed Research International
Volume 2013, Article ID 134914, 21 pages
http://dx.doi.org/10.1155/2013/134914

Review Article

The Increasing Interest of ANAMMOX Research in China: Bacteria, Process Development, and Application

Mohammad Ali,[1,2] Li-Yuan Chai,[1,2] Chong-Jian Tang,[1,2] Ping Zheng,[3] Xiao-Bo Min,[1,2] Zhi-Hui Yang,[1,2] Lei Xiong,[1,2] and Yu-Xia Song[1,2]

[1] *Department of Environmental Engineering, School of Metallurgy and Environment, Central South University, Lushan South Road 932, Changsha, Hunan 410083, China*
[2] *National Engineering Research Centre for Control and Treatment of Heavy Metal Pollution, Changsha 410083, China*
[3] *Department of Environmental Engineering, Zhejiang University, Hangzhou 310058, China*

Correspondence should be addressed to Chong-Jian Tang; chjtang@csu.edu.cn

Received 20 September 2013; Accepted 19 October 2013

Academic Editor: Qaisar Mahmood

Nitrogen pollution created severe environmental problems and increasingly has become an important issue in China. Since the first discovery of ANAMMOX in the early 1990s, this related technology has become a promising as well as sustainable bioprocess for treating strong nitrogenous wastewater. Many Chinese research groups have concentrated their efforts on the ANAMMOX research including bacteria, process development, and application during the past 20 years. A series of new and outstanding outcomes including the discovery of new ANAMMOX bacterial species (Brocadia sinica), sulfate-dependent ANAMMOX bacteria (Anammoxoglobus sulfate and *Bacillus benzoevorans*), and the highest nitrogen removal performance (74.3–76.7 kg-N/m^3/d) in lab scale granule-based UASB reactors around the world were achieved. The characteristics, structure, packing pattern and floatation mechanism of the high-rate ANAMMOX granules in ANAMMOX reactors were also carefully illustrated by native researchers. Nowadays, some pilot and full-scale ANAMMOX reactors were constructed to treat different types of ammonium-rich wastewater including monosodium glutamate wastewater, pharmaceutical wastewater, and leachate. The prime objective of the present review is to elucidate the ongoing ANAMMOX research in China from lab scale to full scale applications, comparative analysis, and evaluation of significant findings and to set a design to usher ANAMMOX research in culmination.

1. Introduction

Anaerobic ammonia oxidation (ANAMMOX) process is a novel and promising biological nitrogen removal biotechnology that has been successfully applied from the beginning of this century [1–3]. ANAMMOX bacteria convert ammonium directly to nitrogen gas with nitrite as the electron acceptor under anoxic conditions. From the discovery of the ANAMMOX process in mid 1990s [1], it has been regarded as a cost-effective and environment-friendly way to treat wastewater containing high ammonium concentrations [4].

By smart application of ANAMMOX in municipal treatment, wastewater treatment plants could be converted from energy-consuming into energy-producing systems [5]. It becomes a hot topic in the fields of microbiology and environmental science and engineering due to its merits of effective removal of both ammonium and nitrite under anaerobic conditions with high removal rate, little sludge production, and low operational cost [5–8].

The drawback of this new and cost-effective process is the low growth rate of involved bacteria (0.0027 h^{-1} reported by Strous et al. [2]; 0.016 h^{-1} reported by Isaka et al. [9]). So, the ANAMMOX reactors are often operated at a long solids retention time (SRT) in order to accumulate the necessary biomass in the system [2, 10, 11]. Till now 5 genera of ANAMMOX bacteria including 13 species [12] have been identified and, among these, *Candidatus* Brocadia sinica has been discovered in China [13]. On the other hand, the existence of sulfate-dependent anaerobic ammonium oxidation has been recognized so far, but the involved microorganisms have been isolated infrequently. Recently new species of sulfate-dependent ANAMMOX bacteria Anammoxoglobus sulfate

[14] and *Bacillus benzoevorans* [15] have been discovered in China which are the functional community to remove ammonium and sulfate simultaneously.

High rate is one of the prime objectives for ANAMMOX process. Within the last decades some specialized reactor systems such as sequencing batch reactor (SBR) [2, 16–19], rotating biological contactor (RBC) [18], trickling filter [19], UBF reactor [20], granular sludge bed reactor [21], and membrane bioreactor [3, 22] have been introduced in both laboratory and full scale to obtain high removal rate, and finally noticed that these reactors played an important role in securing high rate performance for ammonium and nitrite removal. The NRR of conventional nitrogen removal biotechnologies was less than 0.5 kg-N/m^3/d [20] while, for ANAMMOX process, it was higher than 5 kg-N/m^3/d as obtained by a number of researchers using different reactors such as upflow biofilter, upflow anaerobic sludge blanket (UASB) reactor, and gas-lift reactor [3, 23–26].

Nitrogen pollution (N-pollution) causes serious environmental problems. N-pollution not only hampers the sustainable development of agriculture, fishery, tourism, and so forth but also threatens the living environment of human beings. According to the report of "the state of the environment in China (2009)," the ammonium emission was up to 1.23 million tons per year [27]. Thus, it was necessary to remove nitrogen from different ammonium wastewater in China. To fulfill the demand, the research groups in China started to carry out ANAMMOX research and obtained significant outcomes. As a part of continuation of ANAMMOX research, nitrogen removal rate higher than 10 kg-N/m^3/d was obtained by a significant number of researchers in China [26, 28–30]. Till now, the highest NRR in the world was reported by Chinese research group which was 74.3–76.7 kg-N/m^3/d at hydraulic retention time (HRT) of 0.16 h [28]. Besides nitrogen, sulfur is another necessary nutrient for all living creatures, which means that no one can grow and reproduce without them [31, 32]. Ammonium and sulfate are coexistent in seawater and sediments with the average concentrations of 100 mM and 20 mM, respectively, and this coexistence offers a basic condition for sulfate-dependent anaerobic ammonium oxidation [33]. Using this basic condition, simultaneous removal of ammonium and sulfate was discovered in 2001 in an anaerobic fluidized-bed reactor by Fdz-Polanco et al. [34] and they reported that 80% sulfate was converted to elemental sulfur accompanied by ammonium oxidation to dinitrogen gas. Subsequently, the existence of sulfate-dependent anaerobic ammonium oxidation has been confirmed by other researchers [14, 35–38]. Sulfate-dependent ANAMMOX process was also reported by a number of researchers in China [14, 15, 37–39].

The research groups from the mainland, Taiwan, and Hong Kong of China have conducted a lot of investigations on ANAMMOX process including density and settleability mechanism of sludge, modeling of packing pattern, control mechanism for floating sludge, sequential biocatalyst addition for inhibition recovery, process recovery mechanisms illustration, and so on to enhance the ANAMMOX process performance and stability of the process. After nearly 20 years of hard work, the full-scale application of the ANAMMOX has been successfully implemented for treatment of monosodium glutamate wastewater, pharmaceutical wastewater, and landfill leachate [40–44]. A series of progress in bacteria and process development were also forwarded, which contributed significantly to help us understand the process, and finally instigated researchers to operate and control the novel autotrophic process. The objective of this review is to present a detailed comparative summary of previous and current researches on the progress in ANAMMOX bacteria discovery, process development, and the full-scale application in China.

2. Recent Progress of ANAMMOX Bacteria in China

The ANAMMOX process is carried out by a group of ANAMMOX bacteria which are monophyletic group of bacteria under Planctomycetes phylum, Brocadiales order, and *Candidatus* taxonomic component [12]. Till now at least 5 genera and 13 species have been identified using culture-independent molecular techniques [12] including *Candidatus* "Brocadia" (*Ca.* "Brocadia anammoxidans", *Ca.* "Brocadia fulgida," and *Ca.* "Brocadia sinica"); *Candidatus* "Kuenenia stuttgartiensis"; *Candidatus* "Scalindua" (*Ca.* "Scalindua brodae", *Ca.* "Scalindua wagneri", *Ca.* "Scalindua sorokinii", *Ca.* "Scalindua arabica", *Ca.* "Scalindua sinooilfield," and *Ca.* "Scalindua zhenghei"); *Candidatus* "Anammoxoglobus" (*Ca.* "Anammoxoglobus propionicus" and *Ca.* "Anammoxoglobus sulfate"); *Candidatus* "Jettenia asiatica".

Candidatus Brocadia, Kuenenia, Scalindua, Anammoxoglobus, Jettenia genera have been isolated from different wastewater treatment systems [6, 17, 19, 45–47]; only one genus (*Candidatus* Scalindua) seems to be predominant in marine ecosystems ranging from arctic to tropical regions [48–50]. K. stuttgartiensis is fresh water ANAMMOX bacterium but could adapt to high salinity (up to 3%) [51]. Addition of organic acids like propionate or acetate favored to proliferate the Brocadia fulgida or Anammoxoglobus propionicus species with low fluxes of organic matter [17, 46].

Three new species of ANAMMOX bacteria (*Candidatus* Brocadia sinica, *Candidatus* Anammoxoglobus sulfate, and *Bacillus benzoevorans*) have been discovered in China. Among these three species *Candidatus* Brocadia sinica was isolated from ANAMMOX reactors and other two species (Anammoxoglobus sulfate and *Bacillus benzoevorans*) were identified in sulfate removal reactors.

2.1. Candidatus Brocadia sinica. Hu et al. [13] operated 8 bioreactors with highly compact granulated sludge in different physicochemical conditions. Although the reactors were operated in distinct variations in temperature (9–27°C) or influent wastewater (inorganic medium, glucose, or glutamate addition), these variations did not influence the inhibition of ANAMMOX bacteria in reactor. Vice-versa, these changing conditions play an important role to grow up large population of the species which only can adapt to this changing situation. Especially, a new ANAMMOX bacterial

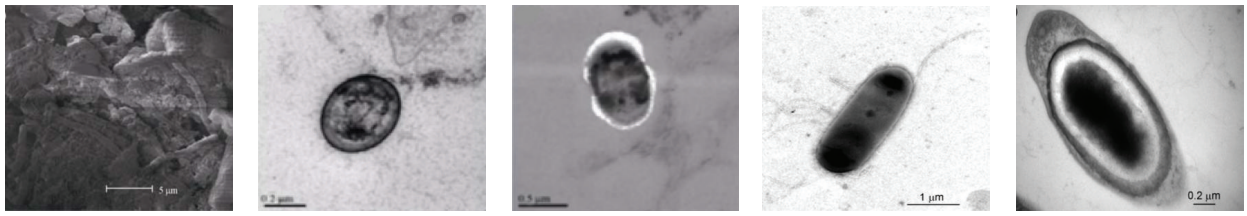

(a) (b) (c) (d) (e)

Figure 1: Morphology of sulfate-dependent sludge: (a) SEM, ((b)–(e)) TEM ((a) sludge microbes, (b) Cocci, (c) Bacilli, (d) morphological characteristics of *Bacillus benzoevorans* (×30000), and (e) structural characteristics of *Bacillus benzoevorans* (×70000)) [15, 37].

species was enriched in five reactors among operated eight reactors, which was then provisionally identified as "*Candidatus* Brocadia sinica" according to the taxonomic guidelines. This indicated that ANAMMOX bacteria were found to be adapted to varying seeding influent conditions [51, 52].

2.2. Sulfate-Dependent ANAMMOX Bacteria. The research groups in China have discovered two novel species which are inevitable for sulfate removal and conducive for simultaneous ammonium and sulfate removal process. Liu et al. [14] discovered a new species called "Anammoxoglobus sulfate" which was the functional community in reactor to remove ammonium and sulfate concomitantly. Anammoxoglobus sulfate mainly complete the conversion of ammonium and sulfate producing nitrite as intermediate product and then the nitrite diffused from cell to reactor solution across the biological membrane. At the same time, other functional Planctomycetes bacteria performed the traditional ANAMMOX process because both nitrite and ammonium were available in the reactor due to diffusion. Another report showed that Cai et al. [15] conducted the isolation, identification, and characterization of an autotrophic bacterial strain for simultaneous anaerobic ammonium and sulfate removal and identified a new species. The newly discovered species of ANAMMOX bacteria was identified as "*Bacillus benzoevorans*" which was able to use sulfate for anaerobic ammonia oxidation. The identified species will be conducive to the understanding of microbial metabolism of sulfate-dependent ANAMMOX and will enrich microbial resources.

The sulfate-dependent ANAMMOX bacteria are rod-shaped with flagellum and spore, having a size of (0.7–1.0) × (2.4–3.5) μm. The colony on the plate appeared light yellow, round with a diameter about 1 mm, whose surface was wet and smooth. Scan electron microscopy (SEM) displayed that the sulfate-dependent sludge was dominated by chains of Bacilli and Cocci. The diameter of Cocci was around 0.9 μm and Bacilli diameter was around 0.8 μm, but length varied from 1 to 1.2 μm. Bacterial cells were with inclusions (Figures 1(a)–1(c)) [37]. Another report agreed that sulfate removal *Bacillus benzoevorans* was rod-shaped, spore forming with flagellum which was discovered (Figures 1(d)–1(e)) by Cai et al. [15].

2.3. Natural Distribution of ANAMMOX Bacteria in China. ANAMMOX bacteria have been detected in various natural habitats such as anoxic marine sediments and water columns, freshwater sediments and water columns, terrestrial ecosystems, some special ecosystems (e.g., petroleum reservoirs, leachate, pharmaceutical waste, and mangrove), and wastewater treatment systems. ANAMMOX bacteria enumerated, isolated, and identified from different ecosystems in different areas of China have been illustrated in Table 1.

The aforementioned data (Table 1) showed that ANAMMOX bacteria were frequently identified from different ecosystems of different regional areas including terrestrial (soil, wetland) ecosystem, aquatic ecosystem (lake, estuary, river, sea, etc.), and some specialized ecosystem (oil reservoir, MSG wastewater and pharmaceutical waste, landfill leachate, etc.). In most cases, Scalindua and Brocadia were frequently isolated and identified while another genus of ANAMMOX bacteria was identified randomly. So, it is clear that ANAMMOX bacteria were widely distributed in China and, among them, Brocadia was predominant in fresh water and Scalindua in sea water.

3. Development of ANAMMOX Process in China

Most of the researchers used synthetic waste waters as influent and other researchers used natural waste (monosodium glutamate waste water, sea, lake, river water, etc.) as influent. Synthetic wastewater was mostly prepared as influent with the addition of ammonium and nitrite in the form of $NH_4Cl/(NH_4)_2SO_4$ and $NaNO_2$. A variety of reactor types including sequencing batch reactor (SBR) [77], upflow anaerobic sludge blanket (UASB) [78], continuous stirred tank reactor (CSTR) [79], and membrane bioreactor (MBR) [80] have been tested for ANAMMOX startup and all show advantages and disadvantages. Usually 20 days matured sludges are better for the reactor start up. The carmine color or bright red color settled sludge was more active than the floating sludge.

Reactors startup occurred by depositing the seeding sludge in reactor and subsequent addition of natural or synthetic waste waters in reactors. During the reactor startup influent concentrations below 100 mg/L of nitrite, long HRT (few days to few hours), and completely anaerobic and dark conditions are conducive for quick and effective reactor startup. During reactor startup most of the researchers maintained NH_4–N : NO_2–N at 1 : 1.1 to 1 : 1.32 and outflow

Table 1: Natural distribution, abundance, and identification of ANAMMOX bacteria from different ecosystems in China.

Ecosystem	Abundance	ANAMMOX Bacteria	Area	Reference
South China Sea, Tai Lam Chung Water Reservoir and Mai Po Nature Reserve	N.A.	Scalindua, Jettenia, Kuenenia, Anammoxoglobus, and Brocadia	South China	[53]
South China Sea	1.19×10^4 to 7.17×10^4	Scalindua	South China	[54]
Jiaozhou Bay	3.89×10^1 to 3.89×10^6	Scalindua, Jettenia, Brocadia, Anammoxoglobus, and Kuenenia	East China	[55]
Shengli Oilfield at Yellow River Delta	4.4×10^6 copies/g of soil	Brocadia, Kuenenia, Scalindua, Jettenia, and Anammoxoglobus	East China	[56]
Paddy field	N.A.	Kuenenia, Anammoxoglobus, Jettenia, and Brocadia	North China	[57]
Freshwater sediments of the Xinyi River	N.A.	Scalindua	East China	[58]
Different natural ecosystems	N.A.	Brocadia, Kuenenia, Scalindua, and Jettenia	East China	[12]
Pharmaceutical wastewater	N.A.	Photobacterium phosphoreum	East China	[40]
Monosodium glutamate (MSG) wastewater	N.A.	Kuenenia	East China	[59]
Qiantang River	N.A.	Brocadia, Kuenenia and Scalindua	East China	[13]
Honghe State Farm soil	N.A.	Scalindua	Northeast China	[60]
Wetland	10^5 copies/g	Scalindua, Kuenenia, Brocadia, and Jettenia	South China	[61]
Qiantang River	N.A.	AOA and AOB	East China	[62]
Paddy soil	N.A.	Anammoxoglobus, Jettenia, and Anammoxoglobus propionicus	East China	[63]
Qiantang River	N.A.	Brocadia, Kuenenia and Scalindua	East China	[64]
Paddy Soil Column	N.A.	Nitrososphaera, Nitrosotalea and Nitrosopumilus	East China	[65]
Jiaojiang Estuary	N.A.	Brocadia, Kuenenia, Scalindua, and Jettenia	East China	[66]
Agricultural soils	$6.38 \pm 0.42 \times 10^4$ to $3.69 \pm 0.25 \times 10^6$	Brocadia, Kuenenia, Jettenia, and Anammoxoglobus	East China	[67]
Mai Po Nature Reserve	N.A.	Scalindua, Kuenenia, Scalindua, and Anammoxoglobus	South China	[68]
Paddy soil	6.5×10^3 to 7.5×10^4	Brocadia and Jettenia	North China	[69]
Waste Lake	N.A.	Brocadia, Kuinenia, and Scalindua	East China	[70]

N.A.: not available; AOA: ammonia-oxidizing archaea, AOB: ammonia-oxidizing bacteria.

concentration below 30 mg/L. The temperature was set at 35 ± 1°C according to Tsushima et al. [8], and the influent pH was controlled within the range of 6.8–7.0 [81].

3.1. High-Rate Nitrogen Removal Performance. ANAMMOX research is promising and booming in China. Many researchers focused on high performance of ANAMMOX activity, some researchers emphasized high loading rate, and some other researchers plunged to discover something new and promising for ANAMMOX development. As a result, different kinds of ANAMMOX activity in lab scale to full scale have been carried out and a lot of findings have been achieved in China. The significant findings and crucial development in ANMMOX research have been highlighted in Table 2.

Tabular data showed that many research groups obtained NRR more than 10 kg-N/m^3/d which was significantly higher than the reported values all over the world. Chen et al. [29] obtained 57 kg-N/m^3/d nitrogen removal rate which was significantly a higher value compared to most of the reported values. Tang et al. [28] obtained a super high rate performance with nitrogen removal rate (NRR) of 74.3–76.7 kg-N/m^3/d at 0.16–0.11 h HRT which was 3 times higher than the previously reported highest value by Tsushima et al. [8]. This was not only top value in China but also in the whole world for laboratory scale reactor performance. Tang et al. [28] also obtained maximum sludge concentration in reactor (42.0–57.7 g-VSS/L) which was 2-3 times higher than previously reported values (0.07 g-VSS/g-NH_4^+–N, Trigo et al. [22]; 0.088 g-VSS/g-NH_4^+–N, Strous et al. [2] and 0.11 g-VSS/g-NH_4^+–N, van Dongen et al. [82]), and the biomass

Table 2: Overview of high ANAMMOX performance in China.

Reactor	HRT	Influent conc. mg/L		Removal efficiency (%)		NLR kg-N/m^3/d	NRR kg-N/m^3/d	Reference
		NH_4–N	NO_2–N	NH_4–N	NO_2–N			
UASB reactor	0.2 h	300	360	90	N.A.	89.1	74.3–76.7	[28]
EGSB reactor	6–0.3 h	494	522	94.68	99.84	77.84	57.14	[29]
EGSB reactor	1.5 h	661.9	767.2	71.7	94.1	22.87	18.65	[30]
AGSB reactor	1.1 h	400	500	N.A.	N.A.	N.A.	15.40	[26]
UASB reactor	N.A.	320–340	350–380	96.1	95.2	7.2	6.2	[27]
Upflow filter system	1.99 h	305	304	74.2	92.4	7.34	6.11	[71]
UASB reactor	0.12 h	16.87 ± 2.09	20.57 ± 2.31	92.81	94.35	N.A.	5.72	[72]
ALR reactor	5.4 h	546	N.A.	94.4	N.A.	2.37	2.29	[73]
UASB reactor	0.28 h	16.87 ± 2.09	20.57 ± 2.31	78.45	92.31	N.A.	2.28	[72]
UBF reactor	1.54 h	976.0	1280	88.84	98.1	34.5	N.A.	[74]
SBR reactor	0.18 d	500	580	97	97	0.156	N.A.	[75]
SBR reactor	3 d	268	345	83.6	100	N.A.	N.A.	[76]
SBR reactor	1.5 h	N.A.	N.A.	80.9	88	N.A.	N.A.	[77]

N.A.: not available.

doubling times were also shorter than the value reported in 11 days by Strous et al. [2]. The research reports clarified that the highest performance was directly related to high settling velocity of sludge, high specific ANAMMOX activity (SAA), and high ECP and Heme *c* contents. So, it could be assumed that high reactor performance would be obtained with the following strategies.

(i) The biomass concentrations in the reactors more than 37 g-VSS/L lead to compact packing of sludge which directly favored the high reactor performance.

(ii) The well-settled granules accumulation in reactor contributes to the super high volumetric nitrogen removal rates even at extremely high NLRs and short HRTs.

(iii) The high value of specific ANAMMOX activity (up to 5.6 kg-N/kg-VSS/d) and short doubling time of bacteria (below 11 days) could be regarded as the key factors to obtain the super high rate performance.

(iv) Relatively high ECP and Heme *c* content and low PN/PS ratios contributed to the ANAMMOX granulation which leads to high performance.

3.2. Sulfate-Dependent ANAMMOX Process. Simultaneous removal of sulfate and ammonium by ANAMMOX process is a new biotechnology in wastewater treatment in which ammonium is oxidized with sulfate as electron acceptor under anoxic conditions. The new anaerobic ammonium and sulfate removal process can offer a great future potential for an energy-saving and environment-friendly alternative for simultaneous nitrogen and sulfate removal from wastewater. In 2001, the simultaneous ammonium and sulfate removal process was firstly discovered in an anaerobic fluidized-bed reactor by Fdz-Polanco et al. [34]. According to the report 80% sulfate was converted to elemental sulfur accompanied by ammonium oxidation to dinitrogen gas.

3.2.1. Possible Reaction Mechanisms for Sulfate-Dependent ANAMMOX. Anaerobic ammonium oxidation with sulfate is a microbiological sulfate reducing reaction. The sulfate-dependent isolate used carbonate as carbon source, ammonium as energy and nitrogen source, and sulfate as electron acceptor. Both SO_4^{2-} and NH_4^+ were chemically stable under anaerobic conditions, but the reaction could be possible in the presence of biological catalyst (sludge). The spontaneity of a chemical reaction is associated with its free energy change (ΔG) [83]. Free energy for NH_4^+ is −79.37 KJ/mol and for SO_4^{2-} is −744.63 KJ/mol, respectively. ΔG^θ of the sulfate and ammonium reaction ($2NH_4^+ + SO_4^{2-} \rightarrow N_2 + S + 4H_2O$ ($\Delta G^\theta = -45.35$ KJ/mol)) is −45.35 KJ/mol. So, it indicated that the simultaneous reaction could occur. Practically the spontaneity of chemical processes is conducted by ΔG if the absolute value of its ΔG^θ is less than 46 KJ/mol [20]. Thus, ΔG at different substrate concentrations is calculated according to the equation $\Delta G = \Delta G^\theta + RT \ln Q$ (Q is reaction quotient). If the ΔG value under tested conditions changed from positive to negative by increasing the substrate concentrations, the reactions between NH_4^+–N and SO_4^{2-} were therefore enhanced based on this principle. On the other hand, optimal nutrient and environmental conditions ΔG also play an important role in the process realization. Sulfate reducing ANAMMOX bacteria (SRB) are a kind of obligate anaerobic bacteria and only viable when the oxidation reduction potential (ORP) is below −100 mV, which was fulfilled by flushing the reactor with N_2 [84]. This higher substrate concentration and lower (below −100 mV) oxidation reduction potential (ORP) phenomenon contributed to the simultaneous sulfate and ammonium removal.

Fdz-Polanco et al. [34] explanation showed that autotrophic anaerobic ammonium oxidation and sulfate deoxidation occurred by three consecutive biochemical reactions: (1), (2), and (3).

(i) Ammonium was partly oxidized by sulfate and vice versa sulfate was deoxidized to produce nitrite and sulfide.

(ii) Then part of the produced nitrite was reduced by sulfide and was converted to dinitrogen gas and elemental sulfur.

(iii) Finally, nitrite-dependant anaerobic ammonium oxidation (ANAMMOX) took place.

(iv) Being in a reduced form, sulfide can be oxidized into either elemental sulfur or sulfate, depending on the initial ratio between sulfide and nitrite [85]. The main products are likely to be elemental sulfur and sulfate at a ratio of 3 : 4 (4). Sulfide and nitrite molecular ratio must be critically controlled to prevent sulfate production:

$$3SO_4^{2-} + 4NH_4^+ \longrightarrow 3S_2^- + 4NO_2^- + 4H_2O + 8H^+ \quad \text{(ammonium oxidation process)} \tag{1}$$

$$3S_2^- + 2NO_2^- + 8H^+ \longrightarrow N_2 + 3S + 4H_2O \quad \text{(nitrite reduction process)} \tag{2}$$

$$2NO_2^- + 2NH_4^+ \longrightarrow 2N_2 + 4H_2O \quad \text{(ANAMMOX process)} \tag{3}$$

$$3S_2^- + 4NO_2^- + 4H_2O \longrightarrow SO_4^{2-} + 2S + 8OH^- + 2N_2 \tag{4}$$

$$NH_4^+ + \frac{1}{2}SO_4^{2-} \longrightarrow \frac{1}{2}N_2 + \frac{1}{2}S + 2H_2O \tag{5}$$

The experimental data revealed that high substrate concentrations and low oxidation-reduction potential (ORP) enhanced the biological reaction. From the above reactions we can conclude that ammonium reacted with sulfate and was oxidized to nitrite (intermediate product) inside sludge granule (bacterial cell) by oxidation process and concomitantly sulfate is deoxidized. Then, the produced nitrite diffused from sludge (bacterial cell) to reactor and reacted with ammonium in the reactor by ANAMMOX process and eventually produced nitrogen gas. In the terminal stage ammonium and sulfate reacted with each other and were converted to nitrogen gas and solid sulfur.

3.2.2. Sulfate-Dependent ANAMMOX Researches in China. Most of the research groups had used $(NH_4)_2SO_4$ and $NaNO_2$ substrates as influent in reactor for N and S source, respectively [15, 37, 38]. Vice versa some researchers used only $(NH_4)_2SO_4$ as sole substrate in influent for N and S source [14].

Sulfate-dependent ANAMMOX bacterial growth is too slow or the doubling time is too long, and thus it takes more time to start up the reactor. The anaerobic digested sludge was cultivated in an anaerobic reactor for three years, and then the sludge became capable to oxidize ammonium with sulfate anaerobically. The sludge volume increase of sulfate reducing ANAMMOX was trivial because a little bit biomass development was achieved after a long-term reactor operation. Reaction between sulfate and ammonium that occurred rarely was difficult to observe, but it became possible only with the coexisting of sulfate reducing and ANAMMOX bacteria. Although some research groups revealed the reaction mechanisms for simultaneous removal of ammonium and sulfate, only very few researches on this topic were carried out due to requirement of long-term operation and minuscule success probability. It is found that some research groups conducted research on this and disclosed promising idea and application. The reports of recent researches have been presented in Table 3.

Cai et al. [15] investigated simultaneous ammonium and sulfur removal ANAMMOX process and phylogenetically analyzed a sulfate reducing strain which was related to *Bacillus benzoevorans*. The investigation also revealed that the maximum 44.4% and 40% ammonia and sulfate removal rates even at pH 8.5 and stoichiometric ratio 2.01 : 1 developed by Fdz-Polanco et al. [34] were obtained, respectively. Yang et al. [38] also reported 40% and 30% removal efficiencies of ammonium and sulfate at molar ratio of ammonium to sulfate consumption of 2 : 1, respectively, in an anaerobic bioreactor filled with granular activated carbon. Another report of Liu et al. [14] disclosed that a new species of Brocadia genus, namely, "Anammoxoglobus sulfate" which was discovered from a ammonium and sulfate enriched niche and revealed that this species played a critical role in the ammonium oxidization and sulfate reduction. The species mainly completed the conversion of ammonium and sulfate and then produced an intermediate product nitrite which diffused from bacteria (sludge) to reactor solution across the biological membrane. Then some other functional Planctomycetes bacteria perform the traditional ANAMMOX process due to presence of ammonium and nitrite. So, the investigation indicated that the full conversion of ammonium and sulfate occurred with the coexistence of ANAMMOX and sulfate reducing bacteria. In this investigation nonwoven rotating biological contactor reactor was preferred over some other types of reactors because it combines the advantages of a biofilm reactor (large specific surface area) and adsorption characteristics with the improvement of the gas-liquid transfer rate (good mixture of substrates and flux). Zhang et al. [37] cultivated the anaerobic digested sludge in an anaerobic reactor for three years and found that after long-term operation the sludge became capable to oxidize ammonium with sulfate anaerobically. The obtained results significantly contributed to the sulfate-dependent ANAMMOX research in the world.

Sulfate reducing ANAMMOX process was sensitive to pH and temperature, and it is reported that reactor performance was inhibited at pH and temperature higher than 8.5 and 30°C [15], respectively. Liu et al. [14] reported that simultaneous removal process might be hindered if there is no coexistence of sulfate reducing bacteria and autotrophic ANAMMOX bacteria. According to Yang et al. [38] ammonium and sulfate removal efficiencies might be affected by some middle medium, such as nitrite, H_2S, and sulfur. Supporting to this report, Fdz-Polanco et al. [34] reported a complete loss of ANAMMOX activity when the nitrite concentration

Table 3: Overview of the sulfate-dependent ANAMMOX process investigation in China.

Source	pH	Reactor	VSS g/L	HRT	Influent mg/L		Removal ratio	Average removal efficiency (%)		Reference
					NH_4–N	SO_4–S	$NH_4 : SO_4$	NH_4–N	SO_4–S	
K_2SO_4 NH_4Cl	8.5	Lab-scale reactor	N.A.	1 d	229	163	2.01 : 1	44.4	40	[15]
$NaNO_2$ $(NH_4)_2SO_4$ $(NH_4)_2SO_4$	8–8.2	NRBC reactor	0.32–0.054	4–24 h	288[b]	N.A.	1.71 : 1.75	50[b]	N.A.	[14]
NH_4Cl $NaNO_2$ $NaSO_4$	7.5–8.5	UASB reactor	N.A.	1.5 d	60	240	2 : 1	40	30	[38]
$(NH_4)_2SO_4$ $NaNO_2$	7.5	Expanded bed reactor	14.9	1 d	843	130	2 : 1	56.82[a]	71.67[a]	[37]
$Na_2S{\cdot}9H_2O$	8.33 ± 0.18	UASB reactor	35.7	0.8 h	350	264	N.A.	94.7	N.A.	[39]

[a]Concentration in mg/L, [b]concentration in mmol/L/D, N.A.: not Available.

remained above 5 mM (70 g NO_2^-–N/m^3) for a long period (12 h). Another report surmised that sulfide might toxic to microorganisms [86].

3.2.3. Future Prospect of Sulfate-Dependent ANAMMOX Process in China. It can be proposed that sulfate-dependent ANAMMOX researches have an inspiring future and development and application in China with the following prospects.

(i) Comparing to ANAMMOX bacteria, the biomass production or doubling time of sulfate-dependent ANAMMOX is too slow. This limitation could be overcome by enrichment of reactor with special care.

(ii) Newly discovered two species, *Bacillus benzoevorans* and Brocadia "Anammoxoglobus sulfate," could be used ubiquitous for simultaneous removal of sulfate and ammonium.

(iii) Pure chemical reaction between ammonium and sulfate without microorganisms was not possible. So, massive biomass production could open a new way for vigorous application.

(iv) Sulfate-dependent ANAMMOX performed good in coexistence condition of biomass which could play an important role in extensive reactor performance improvement.

3.3. ANAMMOX Process with Sequential Biocatalysts Addition. Tang et al. [40] observed that the pharmaceutical wastewater possessed severe acute toxicity with a relative luminosity value of 3.46 ± 0.45% and the conventional ANAMMOX process was not suitable for nitrogen removal from this wastewater due to cumulative toxicity. Finally, the toxicity of the pharmaceutical wastewater was successfully avoided with the introduction of a novel SBA-ANAMMOX process (ANAMMOX process with sequential biocatalyst addition) and the nitrogen removal rate was also significantly enhanced to 9.4 kg-N/m^3/d (by adding 0.025 g VSS/d fresh seeding sludge in reactor) [40]. So, the application of SBA-ANAMMOX process in refractory ammonium-rich wastewater is encouraging.

There may be a question of how the sequential addition of fresh sludge improves the reactor performance. Exogenous addition of high-activity ANAMMOX biomass into the reactor system can supplement the required bacterial amount and also can increase the density of sludge in reactor which eventually enhanced the nitrogen removal performance. Deliberate addition of high-activity ANAMMOX seeding sludge into reactor led to the addition of some unknown growth factors contained in the granules which showed stronger resistance to toxic substances and eventually enhanced the growth of ANAMMOX bacteria [40]. The granules addition subsequently contributed to the high-rate nitrogen removal performance at the low biocatalyst addition rate. So, the answer is that addition of fresh sludge in the reactor increased the settleability, density, and growth conditions of the existing sludge which help to rejuvenate the existing sludge activity and thus improve the reactor performance.

Li et al. [27] disclosed that the returning of washout sludge to the reactor played an important role in prompt recovery of ANAMMOX performance. Yang et al. [87] proposed that addition of fresh ANAMMOX sludge to reactor may improve the living conditions of ANAMMOX bacteria, and, by adding 20.1 g/L (VSS) sludge (on day 135) and 21.0 g/L (VSS) sludge (on day 170) in the inhibited reactor, they obtained increasing nitrogen removal rate from 0.025 to 0.069 kg-N/m^3/d (on day 135) and from 0.069 to 0.323 kg-N/m^3/d (on day 170), respectively. By operating the conventional ANAMMOX reactor and SBA-ANAMMOX reactor in parallel, Tang et al. [40] found that the ammonium and nitrite removal efficiencies for SBA-ANAMMOX reactor were 80.4–86.2% and 92.6–94.8%, respectively, while the removal efficiencies for conventional reactor were only 1.9–13.8% and 14.5–34.2%, respectively. This indicated that SBA-ANAMMOX process could successfully overcome the toxic effects of refractory ammonium-rich pharmaceutical wastewater. From different research reports, it could be concluded that sequential sludge addition is an effective and sustainable way to improve the reactor performance. Thus, the cost-effective and high-rate SBA-ANAMMOX process is a promising biotechnology with enormous advantages that could treat ammonium-rich wastewaters effectively.

4. Morphological Study of ANAMMOX Granules

4.1. General Characteristics of ANAMMOX Granules

Color. The color of high performing fresh seeding ANAMMOX sludge tended to be bright red or carmine (Figure 2). Sludge color is an indicator of sludge viability and performance. If the sludge color changed from carmine to pale red or black, it indicated that the sludge activity reduced.

After a long-term reactor operation the sludge became pale red due to a decrease of Heme *c* and became black because the sludge did not get a substrate for a long time.

Size. The average diameter of ANAMMOX sludge granule varied from 2.2 to 2.5 mm with VSS/TSS at 87% and among them the larger than 2 mm granules were predominant (68–71%) [28]. Sludge size is also an indicator of reactor performance. Large sludge has low settleability and small sludge has high settleability. High settleability is a good indicator for effective reactor performance. The diameter of the floating granules was 2.31–6.96 mm with an average of 4.58 ± 1.22 mm, while that of the settling granules was 0.86–6.98 mm with an average of 2.96 ± 0.99 mm [89]. Large sludge has more gas pockets and gas volume than small sludge [89]. It implied that the ANAMMOX granules with a diameter larger than 4 mm had a strong trend to float in high rate reactors due to accumulation of dinitrogen gas in gas pockets [28]. At high removal rate more gas produced inside the sludge which lead to decrease the settleability of sludge, and thus larger sludge became floating and smaller sludge

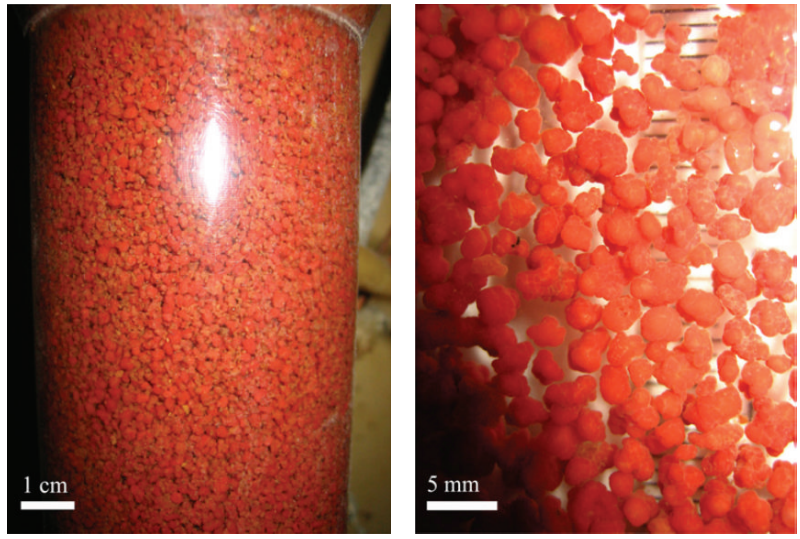

(a) (b)

Figure 2: The granules in high-rate ANAMMOX UASB reactor (a) and the image of ANAMMOX granules (b) [88].

remained settled [89]. Floating behaviors of sludge decrease the reactor performance.

Density. Sludge density is another indicator of high activity reactor performance. The density of ANAMMOX granules in reactors was measured by Tang et al. [28], and it was about 1.03 g/mL; the specific density of the ANAMMOX granules (91 to 120 g-VSS/L-granules) was also comparable to aerobic granules (40 to 70 g-VSS/L-granules) and high-loaded denitrifying granules (128 to 136 g-VSS/L-granules, Franco et al. [90]). Sludge density is proportional to reactor performance, and alternatively sludge size is disproportional to sludge density.

Settling Velocity of ANAMMOX Granules. According to the well-known Stokes equation, the settling velocity of ANAMMOX granules is closely related to their size and density. The increasing size and density might result in a significant increase of settling velocity of granules [91]. The floating ANAMMOX granules did not settle, so only the settling velocity of settling ANAMMOX granules was determined. The settling velocity increased with the increase of sludge diameter and high settling velocity (73 to 88 m/h) was obtained by Lu et al. [92].

Relationship of Settleability with Structure and Density. The diameter and the density were two key factors for the settleability of ANAMMOX granules in the reactors. The settling velocity of ANAMMOX granules increased with the increasing diameter, while the density of ANAMMOX granules decreased with the increasing diameter. Mature ANAMMOX granules settled very well at velocities of 41 to 79 m/h, which were similar to the settling velocities of the methanogenic granules (e.g., 52.9 m/h) and at least two times greater than those of the flocculated ANAMMOX sludge [41]. The significant increase in settling velocities indicated that the ANAMMOX granules had a highly dense and compact structure which is more effective for sludge-effluent separation in the treatment system.

4.2. Morphology of ANAMMOX Granules. The structure of the microbial granules developed in reactors was observed by means of SEM and TEM. The scanning electron micrographs (SEM) showed typical coccoid-shaped cells as the dominant microorganisms on the granule surface embedded in an extracellular polysaccharide (EPS) matrix (Figure 3(a)), very similar to those reported by others [53, 93, 94]. Figure 3(b) showed the typical crescent-shaped ANAMMOX cells obtained via transmission electron micrograph of chemically fixed ANAMMOX cells [95]. The scanning electron micrographs represented by Tang et al. [28] showed that a red-colored mature ANAMMOX granule was characterized by a cauliflower-like shape. The granular surface mainly consisted of spherical and elliptical bacteria; few or even no bacilli and filamentous bacteria were observed in the two reactor enrichments, suggesting that the ANAMMOX bacteria dominated after enrichment [28].

4.3. Chemical Properties of ANAMMOX Granules

4.3.1. Extracellular Polymers. Before discovery of granulation mechanism, researchers used single ANAMMOX bacterial cells for reactor operation. After discovery of sludge granulation process, plenty of researchers operated reactors with sludge and pointed out that sludge mediated reactor performances were obviously higher than bacterial mediated reactor performance. So, it was of a great demand to the researchers to explore the possibility of granulation of ANAMMOX biomass and its application for high performance. The EPS containing bacteria played vital role in the formation of granules in bioreactors [96–99]. ECPs

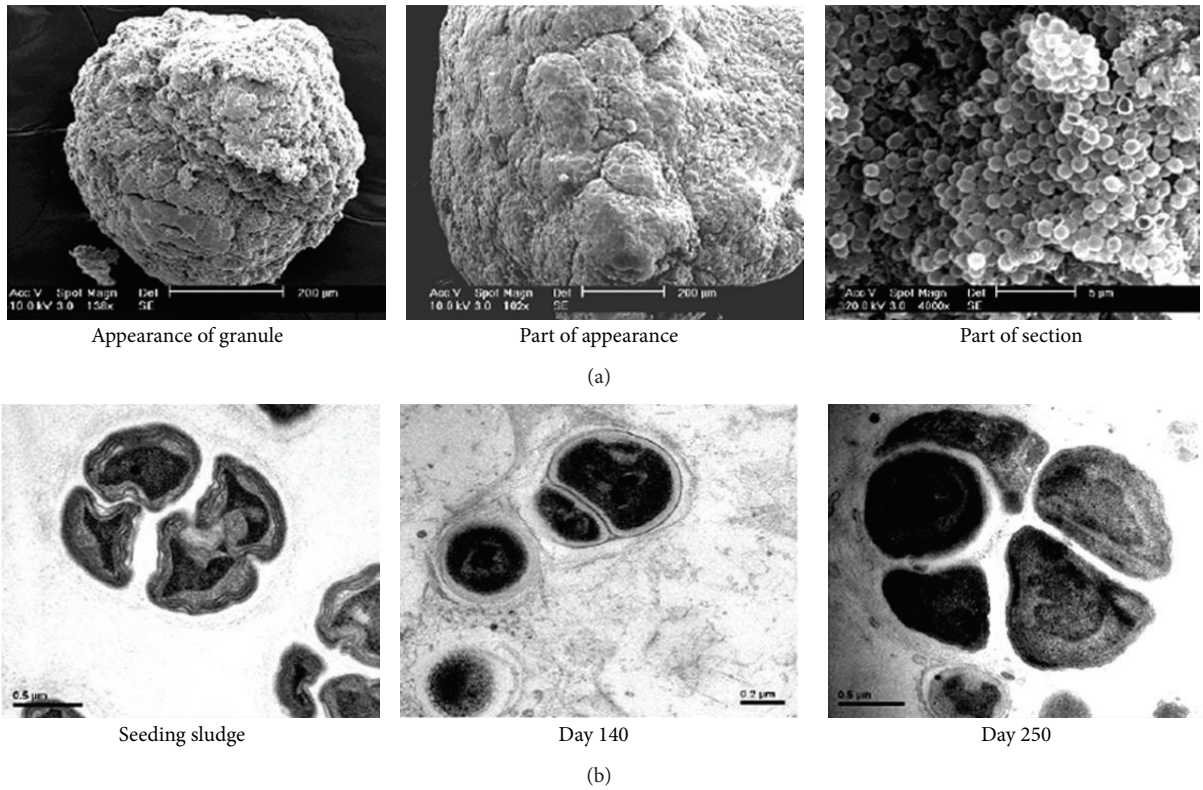

Figure 3: (a) SEM images of the ANAMMOX granular sludge. (b) TEM images of the ANAMMOX bacteria in sludge in the granulation process [41].

could physically bridge neighboring cells by altering the negative charges on bacterial surface [99], and thus granulation may be facilitated by large secretion of ECP. EPSs are distributed throughout the ANAMMOX bacterial surface which attracted scientists to study it with a view of obtaining an efficient, sustainable, and stable sludge granulation for high rate reactor operation.

The microbial ECPs are a rich matrix of polymers which mainly constituted of polysaccharides and proteins [98]. The EPS of each gram of ANAMMOX granule (in VSS) contained 83.2 ± 7.9 mg carbohydrates and 42.7 ± 6.5 mg proteins granules [41]. The EPS content of autotrophic ANAMMOX granules (125 mg EPS/g-VSS) is significantly higher than EPS content (10–91 mg EPS/g-VSS) of heterotrophic methanogenic granules [41]. The protein/carbohydrate ratio (0.51) of autotrophic ANAMMOX granule is lower than heterotrophic methanogenic granules (1.2–4.0) [41]. This indicated that protein might be the key constituent for methanogenic granules and contrarily carbohydrate might be the major constituent for ANAMMOX granules. This information postulated that carbohydrate might play more important role than protein in the formation of ANAMMOX granules. The large amount of glycosylation proteins encoded by the "*Candidatus* Kuenenia" genome is supportive of this suggestion [17]. Tang et al. [28] determined the ECP content at different nitrogen removal levels and summarized that both polysaccharide and protein contents increased with the increasing nitrogen removal rate (NRR). The investigation also revealed that the polysaccharide contents (71.8 ± 2.3 mg/g-VSS) increased slowly as compared to the protein contents (164.4 ± 9.3 mg/g-VSS). The CLSM analysis (Figure 4) showed mixed patterns of cells and EPS distributions in the ANAMMOX granules [41]. The EPSs were distributed throughout the granules, while the bacteria were mainly situated in the outer layer of the granule.

The proteins to polysaccharides ratio (PN/PS) was generally used to assess the granular settleability and strength [90, 100–104]. Various researchers investigated EPS and pointed out that the higher PN/PS ratio of microbial granules led to lower strength and weaker settleability [100–103]; thus the sludge floating or foaming would occurr easily [90, 104]. The PN/PS ratio of the ANAMMOX granules (0.51) was also low in contrast to other microbial granules (1.2–4.0), recommending a greater granular stability [90]. Tang et al. [28] determined the ECP contents of the floated granules and found that extracellular proteins and PN/PS ratios of the floated ANAMMOX granules (3.88–4.09) at high NRRs and HLRs were significantly higher than the counterparts of well-settled (2.40–2.65) granules. The overproduction of extracellular proteins might be a potential cause resulting in the severe sludge washout from the UASB reactors.

4.3.2. Heme c Content. Sludge color is an indicator of high activity ANAMMOX granule, and the sludge color varied

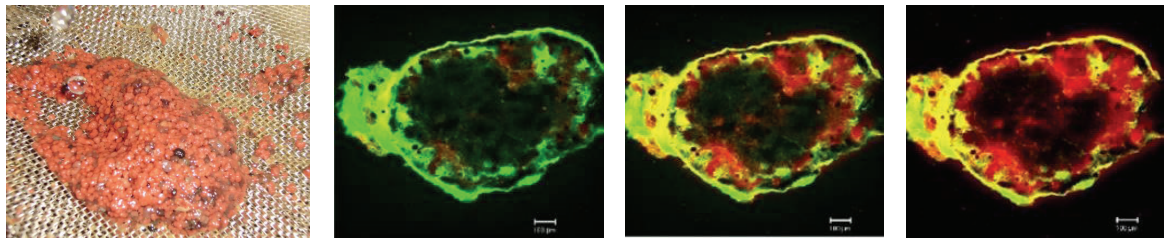

Figure 4: (a) EPSs at outer surface of carmine red ANAMMOX sludge, (b) CLSM images of the 50 μm cryosections of the ANAMMOX granule from surface to center. Cells were stained with SYTO9 (green) and polysaccharides were stained with concanavalin A (red) [28, 41].

from carmine red to pale red, brownish, or black. High-load ANAMMOX granules are uniquely carmine (Figure 4) in color. It was well accepted that Heme *c* played a vital role to develop carmine color in sludge granule. Sludge color was directly related to reactor performance, and thus researchers penetrated their concentration to reveal the role of Heme *c* and its evaluation.

ANAMMOX bacteria have some vital enzymes such as hydrazine synthase (HZS), hydroxylamine oxidoreductase (HAO), and hydrazine oxidase [105] which are rich in ANAMMOX bacteria cell and involved in substance and energy metabolism. Recent researches report postulated that Heme *c* is the indispensible part of these key enzymes of ANAMMOX bacteria [106, 107] and the content of Heme *c* might be involved in ANAMMOX activity and other relative activities [108]. Heme *c* also plays an important role for the development of carmine color of ANAMMOX sludge. It is assumed that the content of heme *c* might be changed with the fluctuation of nitrogen removal rates (NRR), and Tang et al. [28] disclosed that the content of Heme *c* increased significantly with the increasing NRR. Tang et al. [28] showed that the Heme *c* content was 0.7–1.4 mmol/g-VSS at NRR lower than 10 kg-N/m^3/d and the content dramatically reached 9.7–10.8 mmol/g VSS at NRR higher than 70 kg-N/m^3/d. Thus the increase of Heme *c* content was associated with the increase of ANAMMOX bacterial numbers, resulting in high specific ANAMMOX activity (SAA). Finally it could be concluded that the changes of Heme *c* content could represent the growth status of ANAMMOX consortia and Heme *c* level could be used to evaluate the relative activity of ANAMMOX microorganisms and to imply the recovery of ANAMMOX reactor performance. Carmine red, grey, and black color sludges are presented in Figure 4(a). The red colored is due to high Heme *c* content, grey color due to low content, and back is due to absence of Heme *c* that occurred by blockage of sludge.

4.4. Structure of ANAMMOX Granules and Granulation of ANAMMOX Biomass

4.4.1. Structure of ANAMMOX Granules. According to the observation of Lu et al. [92] under light microscope and electron microscope, the structure of ANAMMOX granules included granule, subunit, microbial cell cluster, and single cell (Figure 5).

(i) Granule. Anammox granules were irregular in shape with a diameter of 2.96 ± 0.99 mm [92] and the surface of granule was rough. The granule was broken along the furrow and the broken parts were known as subunits. Subunits were linked to each other by EPS and filamentous bacteria.

(ii) Subunit. SEM and TEM micrographs of different researches mentioned that filamentous bacteria were predominant both in inner and outer surface of ANMMOX subunits. Subunit or "EPS-filamentous bacteria" bands were segmented into several compartments which were called cell clusters.

(iii) Microbial Cell Cluster. In cell clusters microbial cells were aggregated close to each other by EPSs and filamentous bacteria, and the cluster size varied from few to 200 μm. The microbial cell clusters were composed of ANAMMOX bacteria-like cells.

(iv) Interstitial Voids. Subunits, microbial cell clusters, or microbial cells were separated from each other by interstitial space which was known as interstitial voids. Interstitial voids were surrounded by EPSs and were filled with water or dinitrogen gas. The sizes of interstitial voids were proportional to granular size and voids could serve as water channel and gas tunnel. In the beginning interstitial voids were filled with water and worked as water channel to transport substrates (NH_4^+ and NO_2^-) and products and they were 80 nm in diameter [109, 110]. With the activities of microbial cells the transported substrates were converted to dinitrogen gas and this gas accumulated inside the ANAMMOX granules, and the interstitial voids were finally used as gas tunnels for release of dinitrogen gas.

4.4.2. Granulation of ANAMMOX Biomass. In the beginning of ANAMMOX process discovery the low influent loading rate or moderate influent loading reactors were operated with single ANAMMOX bacteria and there were no problem in reactor operation. But when high loading rate reactors operation started with an extremely high upflow velocity,

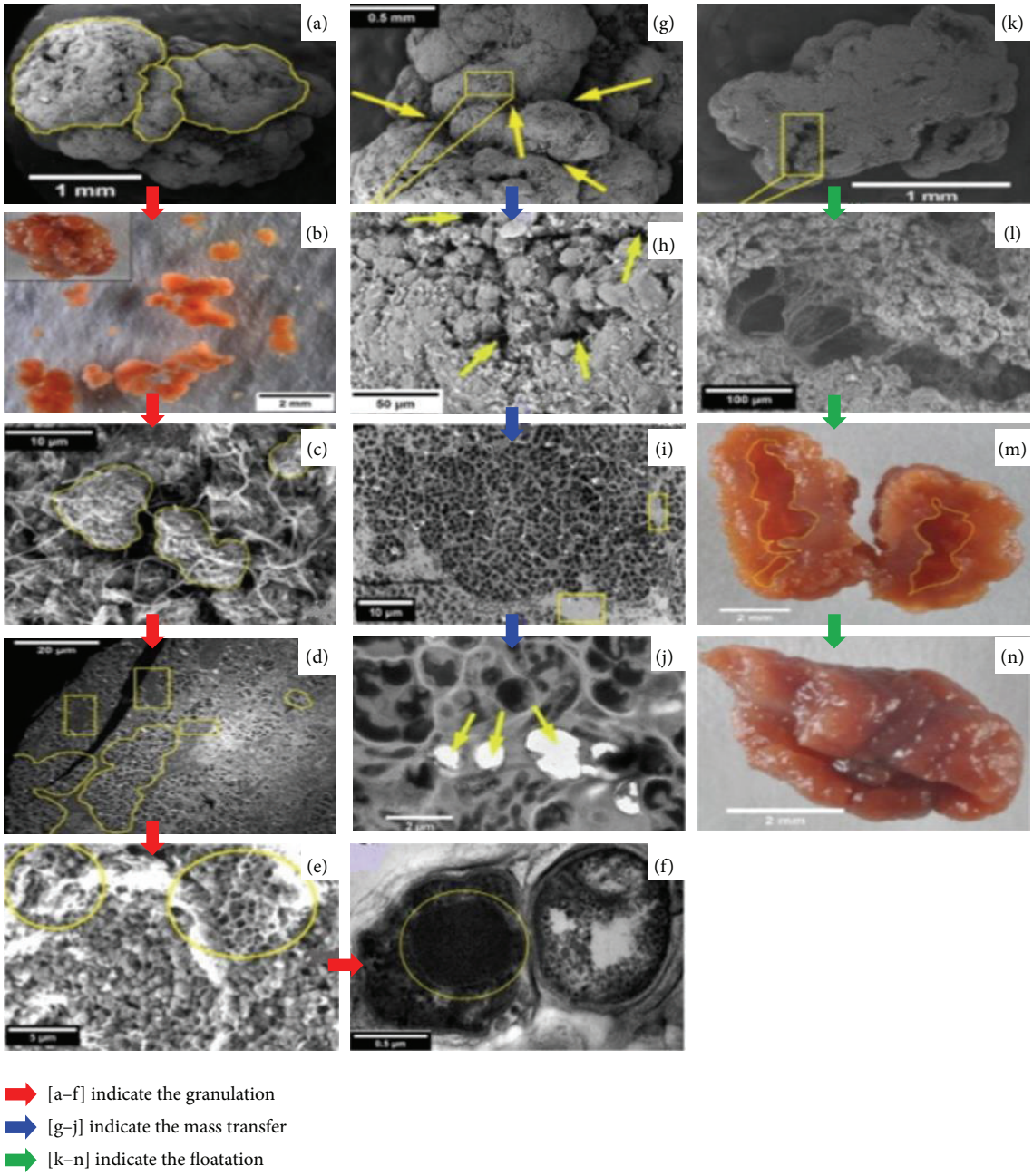

Figure 5: Structures of ANAMMOX granules DMP ((b), (m)-(n)), SEM ((a), (c), (e)–(h), (k), and (l)), and TEM ((d), (f), and (i)-(j)). (a) One ANAMMOX granule composed of subunits (marked with closed curve) and ditches (indicated with arrows) separating the subunits. (b) An ANAMMOX granule (on the top left corner) broken into several subunits. (c) Microbial cell clusters (marked with closed curve) connected by the filamentous bacteria and (d) separated by filamentous bacteria-EPS bands (indicated with rectangles). (e) Interstitial space: the honeycomb-like structures (indicated with circles). (f) ANAMMOX bacteria-like cells (marked with a circle). (g) Ditches (indicated with yellow arrows) between subunits in the exterior of granules. (h) Interstitial voids (indicated with yellow arrows) between microbial cell clusters in the exterior of granules and (i) in the interior of granules (indicated with rectangles). (j) Gas tunnels between microbial cells (indicated with arrows). (k) Small gas pocket (marked with rectangle). (l) Gas pocket of a settling granule formed by inflation of dinitrogen gas. (m) Gas pocket of a floating granule (indicated with closed curve). (n) A broken floating ANAMMOX granule formed by the burst of dinitrogen gas [92].

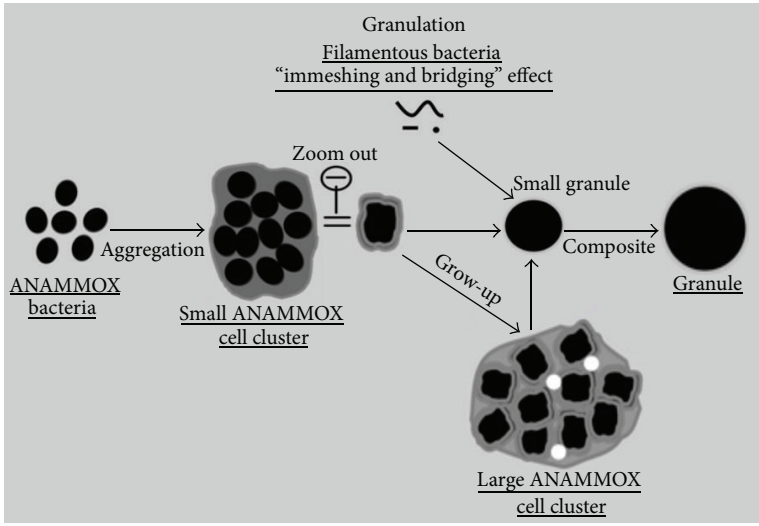

Figure 6: The hypothesized mechanism for granulation and floatation of ANAMMOX biomass. Underlined are the microbial structures observed in this study [92].

large influent loading rate and large gas production of the ANAMMOX biomass were washed out with effluent due to poor settleability [111]. So, granulation of ANAMMOX biomass was inevitable to overcome the biomass washout and to enhance reactor performance. Thus researchers emphasized this and their microscopic observations assumed that granulation process accomplished with the sequential aggregation of microbial cells, cell clusters, and subunit.

ANAMMOX sludge granulation started from ANAMMOX bacterial cell. With an extremely slow growth rate the ANAMMOX bacteria have an affinity to accumulate EPSs [28] and this leads to granulation [22, 112]. ANAMMOX granule has been investigated thoroughly in various bioreactors [22, 82, 113–116], but there is very few studies and findings about the granulation mechanism. According to microscopic observation of Lu et al. [92] the granulation of ANAMMOX biomass granulation (Figure 6) in high-rate reactors could be accomplished in three consecutive steps.

(i) Formation of Microbial Cell Cluster. In a high influent loading reactor the bacteria collide with each other due to high flow rate and high shear force. At the time of collision, the bacteria are entrapped with each other by their immobilized sticky EPSs and form an aggregate of bacterial cell called cell cluster.

(ii) Formation of ANAMMOX Subunit. Then the microbial cell clusters were assembled together with the help of filamentous bacteria to form an aggregate of cell cluster which is called ANAMMOX subunits. The filamentous bacteria departed from ANAMMOX subunits, and then gas tunnel developed in the interstitial space among microbial cell clusters.

(iii) Formation of ANAMMOX Granule. The ANAMMOX subunits in the reactors collided with each other due to the high inflow rate and high gas production and then assembled together with immobilized EPSs and finally produced ANMMOX granules (Figure 6).

4.5. Floatation and Control of ANAMMOX Granule

4.5.1. Floatation of ANAMMOX Biomass. All of the ANAMMOX granules have gas tunnels and gas pockets. In high loading reactors with high activity of ANAMMOX bacteria, the gas bubbles are produced in gas tunnels and gas pockets. The gas bubbles entrapped in gas pockets were supposed to be the key factor to cause sludge floatation. After the hollows were filled with gas bubbles, the ANAMMOX granules would float and be washed out of reactor, leading to failure of ANAMMOX process. The granule floatation was found to be an important factor that causes instability or even collapse of ANAMMOX reactor. Facing these problems some Chinese research groups [92, 113] conducted research and revealed the effective strategy to overcome the floatation and to restore reactor performance.

Inside the floating granules the gas tunnels were closed and inside settled sludge the tunnels were opened. This phenomenon suggested that the gas inside settled sludge could be released easily but the gas inside floating sludge could not be released due to clogging of the gas tunnels. As a result the sludges were floated at high dinitrogen releasing stage and these floatings declined the reactor performances. So, there was a necessity to find out the reason of sludge floatation and control mechanism of floatation for restoration of reactor performance. The floatation of ANAMMOX biofilm was extensively investigated and mechanism of sludge floatation (Figure 7) could be explained in three sequential phases [92] such as (i) formation of gas tunnel, (ii) formation of gas pocket and (iii) floatation of sludge granule.

(i) Formation of Gas Tunnel. It has been reported that the ANAMMOX bacteria tend to grow together [22] and thus

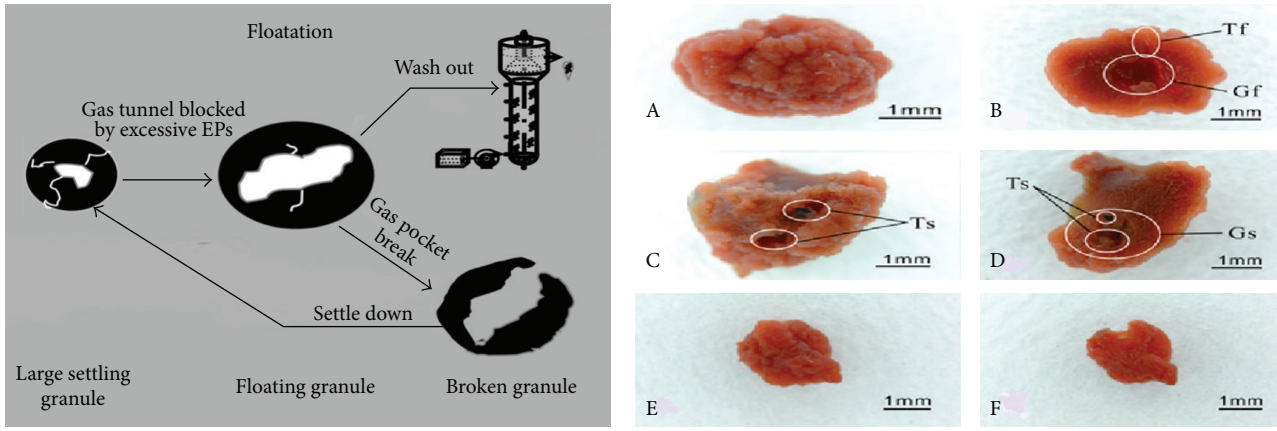

(a) (b)

FIGURE 7: (a) The hypothesized mechanisms for floatation of ANAMMOX sludge, (b) granules in different operation phases: floating granules (A, B), settling granules (C, D), and mechanically broken granules (E, F) in reactor. Both the floating and settling granules contained gas pockets marked G_f and G_s and gas tunnels marked T_f and T_s, respectively [92, 113].

the ANAMMOX granules were supposed to develop from small sludge granules by adhering to each other, and hollow space inside granules was supposed to develop from the gaps between small sludge granules. The substrates were (ammonia and nitrite) diffused into the bacterial cells from reactor, and subsequently dinitrogen gas was produced inside the sludge due to bacteria activities and accumulated as gas bubbles. Then the gas bubbles tend to be released from sludge through the interstitial gaps between small sludge granules and thus create gas tunnels. Microscopic observation reported that a lot of gas tunnels developed for releasing gas outside of the sludge through these tunnels. The gas tunnels inside settled sludge were open, but inside floating sludge were closed.

(ii) Formation of Gas Pocket. With increasing influent rate and high reactor performance, extensive dinitrogen gas was produced. The produced dinitrogen gas entrapped with ANAMMOX granules for maintaining a balance of production and release [114]. The excessive dinitrogen gas inside the granules moved to and fro which created a larger resistance and higher pressure. These larger resistance and higher pressure were forced to enlarge the loose of interstitial voids between cell clusters of subunit and thus led to develop gas pocket. The gas pockets inside the granules were connected to outside environment through gas tunnels.

(iii) Floatation of ANAMMOX Granules. According to research reports EPSs production increased with the increasing loading rates [28] and thus extensive EPSs were produced at high loading rates which led to clog the gas tunnels. High loading rate favored the ANAMMOX sludge to produce huge amount of dinitrogen gas which could not be released outside of sludge through the tunnels due to clogging of gas tunnels [113]. As a result, the excessive gas bubbles were entrapped inside gas tunnels. The entrapped dinitrogen gas surpassed a critical value (5.7%, V/V) and thus the density of granules would be lower than that of water, which led to the floatation of ANAMMOX granules.

4.5.2. Control Strategy for Granule Floatation. Chen et al. [113] assumed that the floating granules have blocked gas tunnels and gas pockets and thus the dinitrogen gas could not be released from sludge which caused floating of the sludges. Then the floating sludges were washed out with effluent from reactor which caused deterioration of reactor performance and thus lead to failure of ANAMMOX process. This washout obstacle compelled the researchers to find out the possible way to overcome this obstacle.

The floating granules were taken out of the reactor and broken into small pieces and returned into reactor to overcome the frequent floating problem of ANAMMOX sludge. After the reactor was operated with the control strategy, the floatation and washout of ANAMMOX sludge became constrained and the performance improved. The broken granules (BGs) had various size with diameters mainly of 0.5–2.6 mm and the wet density of broken granules was higher than that of settled granules, reaching 1047.7 ± 5.1 mg/L [113]. The control strategy improved the performance of ANAMMOX reactor. So, "collecting-breaking-returning" procedure (Figure 7) was suggested to be an effective control strategy to solve granule floatation and improve reactor performance. Alternatively the collecting-breaking-returning procedure in some cases might disturb the microbial ecology (death of bacteria, reduction of ANAMMOX activity, loss of biomass particles, etc.) inside granules and impair the ANAMMOX activity. Furthermore, the recovery of the reactor performance might be a bit long since the reformation of ANAMMOX granules was needed.

4.6. Packing Pattern and Packing Density of ANAMMOX Sludge. The pore volume and sludge concentration inside ANAMMOX reactors are related to the packing patterns of

(a) (b)

Figure 8: Images of the pilot-scale ANAMMOX reactor (a) and packing materials (b) [117].

ANAMMOX granules. The packing patterns are characterized with the coordination number, and packing pattern varied depending on coordination numbers. Previous research reports explained that packing patterns were responsible for pore volume and sludge density, and subsequently sludge density directly led to reactor performance. According to the reports the sludge density 52–55% [88] showed the maximum reactor performance. Different types of packing patterns represent different sludge density and variable reactor performance. So, there was a need to find out the appropriate packing pattern for optimum reactor performance.

Tang et al. [88] initially developed the packing pattern of granular sludge following the principles and theories of crystal lattice patterns [118]. A series of relationships among packing density, sludge concentration, coordination number, nitrogen removal performance, and HRT were evaluated. Finally, the mathematic equation of the packing pattern concerning the nitrogen removal rate (R), sludge concentration (C_X), and the substrate loading (c) was constructed, as shown in (6). Depending on this packing pattern, the nitrogen removal performance could be illustrated by the sludge concentration and substrate load:

$$R = 0.527 C_X q \left(1 - \frac{C_X}{\rho\,\text{granule}}\right)^{25.0} \left(\frac{C_X}{\rho\,\text{granule} \cdot \text{SV}}\right)^{0.16} C^{0.23}, \quad (6)$$

where q is specific activity of the sludge, ρ granule is the density of granular sludge, and SV is the sludge volume.

The reactor performance could be evaluated with the developed packing pattern. Sludge density, pore volume, and sludge concentration in reactor could be investigated with the help of packing pattern. Based on the sensitivity analysis, the following conclusions could be drawn. When C_X is equal to 37.8 g/L, the sludge concentration and substrate loading rate were equally important in contributing to the high conversion capacity of the ANAMMOX UASB reactor. When C_X was less than 37.8 g/L, C_X was more sensitive than c, indicating that it was more effective to enhance sludge concentration for improvement of conversion capacity while, when C_X was higher than 37.8 g/L, c was more sensitive, which meant that elevating substrate loading was an advisable strategy for ANAMMOX reactor operation.

5. Application of ANAMMOX Process in China

In China, ANAMMOX research area is growing day by day. Most of the researches have been conducted in laboratory scale. Some ANAMMOX research groups also carried out ANAMMOX research in pilot-scales and found significant outcomes. Different research groups are operating pilot-scale ANAMMOX process to treat different types of waste and finally succeeded to protect the ecosystem with their maximum capability. The pilot-scale operation is at the point from where the researchers opted to devise for full scale operation. Some pilot-scale ANAMMOX applications have been highlighted in Table 4 and Figure 8.

The above-mentioned data (Table 4) showed that pilot scale reactors were operated with working volume that ranged between 0.020 and 22.5 m^3, and different types of waste water were treated by applying this process. This implied that pilot-scale reactor operation in China is significant in the transitional point from the development point of view. An et al. [117] successfully operated a pilot-scale ANAMMOX reactor to treat dry-spun acrylic fiber wastewater (DAFW) which is depicted in Figure 8. By controlling the reactor temperature and SS in influent, the removal efficiencies of ammonium and nitrite were 85% and 90%, respectively.

Nitrogen waste is one of the vital pollution problems in China. With the increase of Chinese economy the ANMMOX researches tend to move in full-scale treatment plant. So, China is the promising and largest market for ANAMMOX waste treatments. In the Netherlands, the first full-scale granular ANAMMOX reactor was commenced at the wastewater treatment plant of Water board Holland se Delta in Rotterdam in 2006 [16, 99]. This full-scale ANMMOX treatment plant was the milestone for commercial application of ANAMMOX process. The first full-scale reactor volume was 70 m^3 which was 7000-fold from 10 L lab-scale experiment. So far, more than 30 full-scale divergent plants are in operation throughout the world, mostly in Austria, China, Japan, the Netherlands, and USA. All of these plants were established emphasizing ANAMMOX process and finally has become a commercial technique. In 2009 Environmental Technology (Shanghai) released the news that an agreement had been reached to build the world's largest ANAMMOX based wastewater treatment plant in China [44].

Table 4: Brief description of pilot-scale application of ANAMMOX process in China.

Wastewater	Reactor	Working volume	VSS g/L	pH	Temp °C	Influent mg/L		Ratio	Removal efficiency (%)		NRR kg/m^3/d	Reference
						NH_4–N	NO_2–N	$NH_4 : NO_2$	NH_4–N	NO_2–N		
Synthetic wastewater	UASB	2.5 m^3	43.5	6.8	5–27	299	336	1 : 1.12	84	98	1.30	[119]
Synthetic wastewater	UASB reactor	50 L	3.78	7.5–8.0	37	448	575	1 : 1 ± 0.26	93	99	27.8	[78]
DAFW	UASB reactor	68 L	2.2	6.8–7.0	35 ± 1	150–180	120–150	1 : 1.26	85	90	N.A.	[117]
Synthetic wastewater	UASB reactor	20 L	7.2	7.5–8.0	35	377	557	1 : 1	85.5	91.4	640 TN	[120]
PW	MABR reactor	22.5 m^3	10	7.2–8.5	12–26	N.A.	N.A.	N.A.	98	N.A.	N.A.	[42]

DAFW: dry-spun acrylic fiber wastewater, PW: pharmaceutical waste, N.A.: not available.

Table 5: Brief description of full scale ANAMMOX plants in China.

Company/Institution	Area	Substrate	Reactor volume m^3	Designed load kg-N/d	Year	Reference
Zhejiang University	Zhejiang	Pharmaceutical waste	10	5	2010	[40]
Zhejiang University	Zhejiang	Monosodium glutamate wastewater	60	5	2008	Personal communication
National Chiao Tung University	Taiwan	Landfill leachate	384	304 m^3/d*	2006	[43]
Angel Yeast	Yichang	Yeast production	500	1000	2009	Paque [44]
Meihua I	Tongliao	Monosodium glutamate (MSG)	6600	11000	2009	
Meihua II	Tongliao	MSG	4100	9000	2010	
Shandong Xiangrui	Shandong	Corn starch and MSG	4300	6090	2011	
Jiangsu Hangguang Bio-engineering	Wuxi	Sweetener	1600	2180	2011	
Xinjiang Meihua Amino Acid	Wujiaqu	MSG	5400	10710	2011	
Kuaijishan hoaxing Winery	Shaoxing	Distillery	560	900	2011	

* Average leachate flow of 304 m^3/d with a sludge retention time between 12 and 18 d.

Figure 9: Full-scale 11,000 kg-N/d one-step ANAMMOX installation at the Tongliao Meihua Company in China, Courtesy Paques [121].

At the Tongliao Meihua industrial complex, one step ANAMMOX reactor with design capacity of 11,000 kg-N/d has been implemented by Paque which could treat the effluent from monosodium glutamate production (Figure 9) [121]. This is one of the largest treatment plants and is ten times larger than the largest plant built before in 2008 in China. Another 11 ANAMMOX plants were implemented by Paques, seven of which are located in China (Table 5). As the world's biggest developing market, China contributes significantly towards commercialization of ANAMMOX process.

Besides imported technology, some research groups in China were set to operate with full scale ANAMMOX process with their own possessed sludge, expertise, and technology. It came to know that Zhejiang University ANAMMOX research group have succeeded in implementing two full scale ANAMMOX treatment plants for treatment of monosodium glutamate wastewater (60 m^3) in Yiwu City and pharmaceutical wastewater (10 m^3) in Dongyang City, Zhejiang Province, China. Some other research groups also opted to set up full scale application. These initiatives are the clear indication that China already have achieved dramatic progress in ANAMMOX research and very near to be one of the leading group in ANAMMOX technology.

6. Conclusion

ANAMMOX process was considered to be one of the most sustainable pathways for nitrogen removal from ammonium-rich wastewater. During the past decades, many Chinese groups have dedicated their efforts on the ANAMMOX research. The highest nitrogen removal rate in laboratory scale has been obtained from a research group in China which is a strong evidence of development in ANAMMOX research. Three new species of ANAMMOX bacteria have been identified, among them two species are responsible for simultaneous ammonium and sulfate removal which is a new addition in ANAMMOX process for simultaneous treatment. Pilot-scale operations are expanding and using domestic expertise, technology, manpower, and so forth, full scale application with domestic expertise and technology is beckoning for commencement. Overall China's progress in ANAMMOX process is appreciating and time befitting.

6.1. Highlights. Discovery of ANAMMOX and sulfate-dependent ANAMMOX bacteria, ANAMMOX process and sulfate-dependent ANAMMOX process development for simultaneous removal, and pilot scale to full scale ANAMMOX process application were reviewed.

Conflict of Interests

The authors declare that there is no conflict of interests.

Acknowledgments

The financial support of this work by the National Natural Science Foundation of China (51204213), the Key Project

of Science and Technology program of Hunan Province (2013WK2007), the Special National Post-doctoral Science Foundation of China (2013T60782), the National Funds for Distinguished Young Scientists of China (50925417), the National Post-doctoral Science Foundation of China (2012M511769), and the Post-doctoral Foundation of Central South University, China is gratefully acknowledged. The authors also want to appreciate the anonymous reviewers and editor for their pertinent contribution to improve the paper.

References

[1] A. Mulder, A. A. van de Graaf, L. A. Robertson, and J. G. Kuenen, "Anaerobic ammonium oxidation discovered in a denitrifying fluidized bed reactor," *FEMS Microbiology Ecology*, vol. 16, no. 3, pp. 177–184, 1995.

[2] M. Strous, J. J. Heijnen, J. G. Kuenen, and M. S. M. Jetten, "The sequencing batch reactor as a powerful tool for the study of slowly growing anaerobic ammonium-oxidizing microorganisms," *Applied Microbiology and Biotechnology*, vol. 50, no. 5, pp. 589–596, 1998.

[3] W. R. L. van der Star, W. R. Abma, D. Blommers et al., "Startup of reactors for anoxic ammonium oxidation: experiences from the first full-scale anammox reactor in Rotterdam," *Water Research*, vol. 41, no. 18, pp. 4149–4163, 2007.

[4] M. S. M. Jetten, S. Logemann, G. Muyzer et al., "Novel principles in the microbial conversion of nitrogen compounds," *Antonie van Leeuwenhoek, International Journal of General and Molecular Microbiology*, vol. 71, no. 1-2, pp. 75–93, 1997.

[5] B. Kartal, J. G. Kuenen, and M. C. M. van Loosdrecht, "Sewage treatment with anammox," *Science*, vol. 328, no. 5979, pp. 702–703, 2010.

[6] M. Strous, J. A. Fuerst, E. H. M. Kramer et al., "Missing lithotroph identified as new planctomycete," *Nature*, vol. 400, no. 6743, pp. 446–449, 1999.

[7] Y. Tao, D.-W. Gao, Y. Fu, W.-M. Wu, and N.-Q. Ren, "Impact of reactor configuration on anammox process start-up: MBR versus SBR," *Bioresource Technology*, vol. 104, pp. 73–80, 2012.

[8] I. Tsushima, Y. Ogasawara, T. Kindaichi, H. Satoh, and S. Okabe, "Development of high-rate anaerobic ammonium-oxidizing (anammox) biofilm reactors," *Water Research*, vol. 41, no. 8, pp. 1623–1634, 2007.

[9] K. Isaka, Y. Date, T. Sumino, S. Yoshie, and S. Tsuneda, "Growth characteristic of anaerobic ammonium-oxidizing bacteria in an anaerobic biological filtrated reactor," *Applied Microbiology and Biotechnology*, vol. 70, no. 1, pp. 47–52, 2006.

[10] I. Fernández, J. R. Vázquez-Padín, A. Mosquera-Corral, J. L. Campos, and R. Méndez, "Biofilm and granular systems to improve Anammox biomass retention," *Biochemical Engineering Journal*, vol. 42, no. 3, pp. 308–313, 2008.

[11] H. López, S. Puig, R. Ganigué, M. Ruscalleda, M. D. Balaguer, and J. Colprim, "Start-up and enrichment of a granular anammox SBR to treat high nitrogen load wastewaters," *Journal of Chemical Technology and Biotechnology*, vol. 83, no. 3, pp. 233–241, 2008.

[12] B.-L. Hu, L.-D. Shen, X.-Y. Xu, and P. Zheng, "Anaerobic ammonium oxidation (anammox) in different natural ecosystems," *Biochemical Society Transactions*, vol. 39, no. 6, pp. 1811–1816, 2011.

[13] B.-L. Hu, P. Zheng, C.-J. Tang et al., "Identification and quantification of anammox bacteria in eight nitrogen removal reactors," *Water Research*, vol. 44, no. 17, pp. 5014–5020, 2010.

[14] S. Liu, F. Yang, Z. Gong et al., "Application of anaerobic ammonium-oxidizing consortium to achieve completely autotrophic ammonium and sulfate removal," *Bioresource Technology*, vol. 99, no. 15, pp. 6817–6825, 2008.

[15] J. Cai, J. X. Jiang, and P. Zheng, "Isolation and identification of bacteria responsible for simultaneous anaerobic ammonium and sulfate removal," *Science China Chemistry*, vol. 53, no. 3, pp. 645–650, 2010.

[16] B. L. Hu, P. Zheng, Q. Mahmood, H. F. Qian, and D. L. Wu, "Cultivation, granulation and characteristics of anaerobic ammonium-oxidizing sludge in sequencing batch reactor," *Water Science and Technology*, vol. 6, no. 6, pp. 71–79, 2006.

[17] B. Kartal, L. van Niftrik, J. Rattray et al., "*Candidatus* "Brocadia fulgida": an autofluorescent anaerobic ammonium oxidizing bacterium," *FEMS Microbiology Ecology*, vol. 63, no. 1, pp. 46–55, 2008.

[18] K. Pynaert, B. F. Smets, S. Wyffels, D. Beheydt, S. D. Siciliano, and W. Verstraete, "Characterization of an autotrophic nitrogen-removing biofilm from a highly loaded lab-scale rotating biological contactor," *Applied and Environmental Microbiology*, vol. 69, no. 6, pp. 3626–3635, 2003.

[19] M. Schmid, U. Twachtmann, M. Klein et al., "Molecular evidence for genus level diversity of bacteria capable of catalyzing anaerobic ammonium oxidation," *Systematic and Applied Microbiology*, vol. 23, no. 1, pp. 93–106, 2000.

[20] R.-C. Jin, P. Zheng, A.-H. Hu, Q. Mahmood, B.-L. Hu, and G. Jilani, "Performance comparison of two anammox reactors: SBR and UBF," *Chemical Engineering Journal*, vol. 138, no. 1–3, pp. 224–230, 2008.

[21] P. Zheng, F.-M. Lin, B.-L. Hu, and J.-S. Chen, "Start-up of anaerobic ammonia oxidation bioreactor with nitrifying activated sludge," *Journal of Environmental Sciences*, vol. 16, no. 1, pp. 13–16, 2004.

[22] C. Trigo, J. L. Campos, J. M. Garrido, and R. Méndez, "Start-up of the Anammox process in a membrane bioreactor," *Journal of Biotechnology*, vol. 126, no. 4, pp. 475–487, 2006.

[23] A. O. Sliekers, K. A. Third, W. Abma, J. G. Kuenen, and M. S. M. Jetten, "CANON and Anammox in a gas-lift reactor," *FEMS Microbiology Letters*, vol. 218, no. 2, pp. 339–344, 2003.

[24] U. Imajo, T. Tokutomi, and K. Furukawa, "Granulation of Anammox microorganisms in up-flow reactors," *Water Science and Technology*, vol. 49, no. 5-6, pp. 155–163, 2004.

[25] K. Isaka, T. Sumino, and S. Tsuneda, "High nitrogen removal performance at moderately low temperature utilizing anaerobic ammonium oxidation reactions," *Journal of Bioscience and Bioengineering*, vol. 103, no. 5, pp. 486–490, 2007.

[26] C.-J. Tang, P. Zheng, and Q. Mahmood, "The shear force amendments on the slugging behavior of upflow Anammox granular sludge bed reactor," *Separation and Purification Technology*, vol. 69, no. 3, pp. 262–268, 2009.

[27] H. Li, S. Zhou, W. Ma, G. Huang, and B. Xu, "Fast start-up of ANAMMOX reactor: operational strategy and some characteristics as indicators of reactor performance," *Desalination*, vol. 286, pp. 436–441, 2012.

[28] C.-J. Tang, P. Zheng, C.-H. Wang et al., "Performance of high-loaded ANAMMOX UASB reactors containing granular sludge," *Water Research*, vol. 45, no. 1, pp. 135–144, 2011.

[29] T. Chen, P. Zheng, C. Tang, S. Wang, and S. Ding, "Performance of ANAMMOX-EGSB reactor," *Desalination*, vol. 278, no. 1–3, pp. 281–287, 2011.

[30] T. Chen, P. Zheng, L. Shen, S. Ding, and Q. Mahmood, "Kinetic characteristics and microbial community of Anammox-EGSB reactor," *Journal of Hazardous Materials*, vol. 190, no. 1–3, pp. 28–35, 2011.

[31] P. Zheng, X. Y. Xu, and B. L. Hu, *New Theory and Technology For Biological Nitrogen Removal*, Science Press, Beijing, China, 2004.

[32] Y. Q. Miu, *Theory and Technology of Wastewater Desulfurization*, Chemical Industry Press, Beijing, China, 2004.

[33] M. M. M. Kuypers, A. O. Silekers, G. Lavik et al., "Anaerobic ammonium oxidation by anammox bacteria in the Black Sea," *Nature*, vol. 422, no. 6932, pp. 608–611, 2003.

[34] F. Fdz-Polanco, M. Fdz-Polanco, N. Fernandez, M. A. Urueña, P. A. Garcia, and S. Villaverde, "New process for simultaneous removal of nitrogen and sulphur under anaerobic conditions," *Water Research*, vol. 35, no. 4, pp. 1111–1114, 2001.

[35] L. X. Dong, Y. T. Lu, Q. Y. Han, and Z. Y. Wang, "The effect of sulfate reduction on ammonium oxidation and its inhibitory properties," *Journal of Xi'An University of Architecture And Technology*, vol. 38, no. 3, pp. 425–428, 2006.

[36] Q.-I. Zhao, W. Li, and S.-J. You, "Simultaneous removal of ammonium-nitrogen and sulphate from wastewaters with an anaerobic attached-growth bioreactor," *Water Science and Technology*, vol. 54, no. 8, pp. 27–35, 2006.

[37] L. Zhang, P. Zheng, Y. He, and R. Jin, "Performance of sulfate-dependent anaerobic ammonium oxidation," *Science in China B*, vol. 52, no. 1, pp. 86–92, 2009.

[38] Z. Yang, S. Zhou, and Y. Sun, "Start-up of simultaneous removal of ammonium and sulfate from an anaerobic ammonium oxidation (anammox) process in an anaerobic up-flow bioreactor," *Journal of Hazardous Materials*, vol. 169, no. 1–3, pp. 113–118, 2009.

[39] R. C. Jin, G. F. Yang, Q. Q. Zhang, C. Ma, J. J. Yu, and B. S. Xing, "The effect of sulfide inhibition on the ANAMMOX process," *Water Research*, vol. 47, no. 3, pp. 1459–1469, 2013.

[40] C.-J. Tang, P. Zheng, T.-T. Chen et al., "Enhanced nitrogen removal from pharmaceutical wastewater using SBA-ANAMMOX process," *Water Research*, vol. 45, no. 1, pp. 201–210, 2011.

[41] B.-J. Ni, B.-L. Hu, F. Fang et al., "Microbial and physicochemical characteristics of compact anaerobic ammonium-oxidizing granules in an upflow anaerobic sludge blanket reactor," *Applied and Environmental Microbiology*, vol. 76, no. 8, pp. 2652–2656, 2010.

[42] B. L. X. Wei, S. Zhao, L. Wang, H. Zhang, C. Li, and S. Wang, "Mixed pharmaceutical wastewater treatment by integrated membrane-aerated biofilm reactor (MABR) system—a pilot-scale study," in *Bioresource Technology*, vol. 122, pp. 189–195, 2012.

[43] C.-C. Wang, P.-H. Lee, M. Kumar, Y.-T. Huang, S. Sung, and J.-G. Lin, "Simultaneous partial nitrification, anaerobic ammonium oxidation and denitrification (SNAD) in a full-scale landfill-leachate treatment plant," *Journal of Hazardous Materials*, vol. 175, no. 1–3, pp. 622–628, 2010.

[44] M. C. M. van Loosdrecht, "Environmental Biotechnologist wins Lee Kuan Yew Water Prize 2012," Fact Sheet, 2012, http://www.siww.com.sg/media/environmental-biotechnologist-wins-lee-kuan-yew-water-prize-2012.

[45] M. Schmid, K. Walsh, R. Webb et al., "*Candidatus* "Scalindua brodae", sp. nov., *Candidatus* "Scalindua wagneri", sp. nov., Two New Species of Anaerobic Ammonium Oxidizing Bacteria," *Systematic and Applied Microbiology*, vol. 26, no. 4, pp. 529–538, 2003.

[46] B. Kartal, J. Rattray, L. A. van Niftrik et al., "*Candidatus* "Anammoxoglobus propionicus" a new propionate oxidizing species of anaerobic ammonium oxidizing bacteria," *Systematic and Applied Microbiology*, vol. 30, no. 1, pp. 39–49, 2007.

[47] Z.-X. Quan, S.-K. Rhee, J.-E. Zuo et al., "Diversity of ammonium-oxidizing bacteria in a granular sludge anaerobic ammonium-oxidizing (anammox) reactor," *Environmental Microbiology*, vol. 10, no. 11, pp. 3130–3139, 2008.

[48] M. M. M. Kuypers, G. Lavik, D. Woebken et al., "Massive nitrogen loss from the Benguela upwelling system through anaerobic ammonium oxidation," *Proceedings of the National Academy of Sciences of the United States of America*, vol. 102, no. 18, pp. 6478–6483, 2005.

[49] M. C. Schmid, N. Risgaard-Petersen, J. van de Vossenberg et al., "Anaerobic ammonium-oxidizing bacteria in marine environments: widespread occurrence but low diversity," *Environmental Microbiology*, vol. 9, no. 6, pp. 1476–1484, 2007.

[50] C. R. Penton, A. H. Devol, and J. M. Tiedje, "Molecular evidence for the broad distribution of anaerobic ammonium-oxidizing bacteria in freshwater and marine sediments," *Applied and Environmental Microbiology*, vol. 72, no. 10, pp. 6829–6832, 2006.

[51] B. Kartal, M. Koleva, R. Arsov, W. van der Star, M. S. M. Jetten, and M. Strous, "Adaptation of a freshwater anammox population to high salinity wastewater," *Journal of Biotechnology*, vol. 126, no. 4, pp. 546–553, 2006.

[52] K. Windey, I. de Bo, and W. Verstraete, "Oxygen-limited autotrophic nitrification-denitrification (OLAND) in a rotating biological contactor treating high-salinity wastewater," *Water Research*, vol. 39, no. 18, pp. 4512–4520, 2005.

[53] P. Han and J. D. Gu, "More refined diversity of anammox bacteria recovered and distribution in different ecosystems," *Applied Microbiology and Biotechnology*, vol. 97, pp. 3653–3663, 2013.

[54] Y.-G. Hong, M. Li, H. Cao, and J.-D. Gu, "Residence of habitat-specific anammox bacteria in the deep-sea subsurface sediments of the south china sea: analyses of marker gene abundance with physical chemical parameters," *Microbial Ecology*, vol. 62, no. 1, pp. 36–47, 2011.

[55] H. Dang, R. Chen, L. Wang et al., "Environmental factors shape sediment anammox bacterial communities in hypernutrified Jiaozhou Bay, China," *Applied and Environmental Microbiology*, vol. 76, no. 21, pp. 7036–7047, 2010.

[56] H. Li, S. Chen, B.-Z. Mu, and J.-D. Gu, "Molecular detection of anaerobic ammonium-oxidizing (Anammox) bacteria in high-temperature petroleum reservoirs," *Microbial Ecology*, vol. 60, no. 4, pp. 771–783, 2010.

[57] G. Zhu, S. Wang, Y. Wang et al., "Anaerobic ammonia oxidation in a fertilized paddy soil," *International Society for Microbial Ecology*, vol. 5, no. 12, pp. 1905–1912, 2011.

[58] Y. Zhang, X.-H. Ruan, H. J. M. Op Den Camp, T. J. M. Smits, M. S. M. Jetten, and M. C. Schmid, "Diversity and abundance of aerobic and anaerobic ammonium-oxidizing bacteria in freshwater sediments of the Xinyi River (China)," *Environmental Microbiology*, vol. 9, no. 9, pp. 2375–2382, 2007.

[59] L.-D. Shen, A.-H. Hu, R.-C. Jin et al., "Enrichment of anammox bacteria from three sludge sources for the startup of

monosodium glutamate industrial wastewater treatment system," *Journal of Hazardous Materials*, vol. 199-200, pp. 193–199, 2012.

[60] J. Wang and J.-D. Gu, "Dominance of *Candidatus* Scalindua species in anammox community revealed in soils with different duration of rice paddy cultivation in Northeast China," *Applied Microbiology and Biotechnology*, vol. 97, no. 4, pp. 1785–1798, 2013.

[61] M. Li and J.-D. Gu, "Advances in methods for detection of anaerobic ammonium oxidizing (anammox) bacteria," *Applied Microbiology and Biotechnology*, vol. 90, no. 4, pp. 1241–1252, 2011.

[62] S. Liu, L. D. Shen, L. Lou, G. Tian, P. Zheng, and B. L. Hu, "Spatial distribution and factors shaping the niche segregation of Ammonia-oxidizing microorganisms in the Qiantang river, China," *Applied and Environmental Microbiology*, vol. 79, no. 13, pp. 4065–4071, 2013.

[63] B. L. Hu, L. D. Shen, S. Liu et al., "Enrichment of an anammox bacterial community from a flooded paddy soil," *Environmental Microbiology Reports*, vol. 5, no. 3, pp. 483–489, 2013.

[64] B. L. Hu, L. D. Shen, P. Zheng et al., "Distribution and diversity of anaerobic ammonium-oxidizing bacteria in the sediments of the Qiantang River," *Environmental Microbiology Reports*, vol. 4, no. 5, pp. 540–547, 2012.

[65] H. L. Baolan, S. Liu, L. D. Shen, P. Zheng, X. Y. Xu, and L. P. Lou, "Effect of different Ammonia concentrations on community succession of Ammonia-oxidizing microorganisms in a simulated paddy soil column," *PloS One*, vol. 7, no. 8, Article ID e44122, 2012.

[66] B. Hu, L. Shen, P. Du, P. Zheng, X. Xu, and J. Zeng, "The influence of intense chemical pollution on the community composition, diversity and abundance of anammox bacteria in the Jiaojiang Estuary (China)," *PLoS ONE*, vol. 7, no. 3, Article ID e33826, 2012.

[67] L. D. Shen, S. Liu, L. P. Lou et al., "Broad distribution of diverse anaerobic ammonium-oxidising bacteria in Chinese agricultural soils," *Applied and Environmental Microbiology*, vol. 79, no. 19, pp. 6167–6172, 2013.

[68] M. Li, H. Cao, Y.-G. Hong, and J. D. Gu, "Seasonal dynamics of anammox bacteria in estuarial sediment of the mai po nature reserve revealed by analyzing the 16s rRNA and hydrazine oxidoreductase (hzo) genes," *Microbes and Environments*, vol. 26, no. 1, pp. 15–22, 2011.

[69] Y. Wang, G. Zhu, H. R. Harhangi et al., "Co-occurrence and distribution of nitrite–dependent anaerobic ammonium and methane-oxidizing bacteria in a paddy soil," *FEMS Microbiology Letters*, vol. 336, no. 2, pp. 79–88, 2012.

[70] L. D. Shen, B. L. Hu, P. Zheng et al., "Molecular detection of anammox bacteria in the sediment of West Lake," *Acta Scientiae Circumstantiae*, vol. 31, no. 8, pp. 1609–1615, 2011.

[71] R.-C. Jin and P. Zheng, "Kinetics of nitrogen removal in high rate anammox upflow filter," *Journal of Hazardous Materials*, vol. 170, no. 2-3, pp. 652–656, 2009.

[72] Y. P. B. Ma, S. Zhang, J. Wang et al., "Performance of anammox UASB reactor treating low strength wastewater under moderate and low temperatures," *Bioresource Technology*, vol. 129, pp. 606–611, 2013.

[73] R.-C. Jin, P. Zheng, Q. Mahmood, and L. Zhang, "Performance of a nitrifying airlift reactor using granular sludge," *Separation and Purification Technology*, vol. 63, no. 3, pp. 670–675, 2008.

[74] J. Chen, P. Zheng, Y. Yu, C. Tang, and Q. Mahmood, "Promoting sludge quantity and activity results in high loading rates in Anammox UBF," *Bioresource Technology*, vol. 101, no. 8, pp. 2700–2705, 2010.

[75] Y. Yuan, Y. Huang, H. Deng, Y. Li, and Y. Pan, "Research on enrichment for anammox bacteria inoculated via enhanced endogenous denitrification," in *Life System Modeling and Intelligent Computing*, vol. 6330, pp. 700–707, Springer, Berlin, Germany, 2010.

[76] D. Liao, X. Li, Q. Yang, G. Zeng, L. Guo, and X. Yue, "Effect of inorganic carbon on anaerobic ammonium oxidation enriched in sequencing batch reactor," *Journal of Environmental Sciences*, vol. 20, no. 8, pp. 940–944, 2008.

[77] T. Wang, H. Zhang, D. Gao et al., "Enrichment of Anammox bacteria in seed sludges from different wastewater treating processes and start-up of Anammox process," *Desalination*, vol. 271, no. 1–3, pp. 193–198, 2011.

[78] S.-Q. Ni, B.-Y. Gao, C.-C. Wang, J.-G. Lin, and S. Sung, "Fast start-up, performance and microbial community in a pilot-scale anammox reactor seeded with exotic mature granules," *Bioresource Technology*, vol. 102, no. 3, pp. 2448–2454, 2011.

[79] S. Bagchi, R. Biswas, and T. Nandy, "Start-up and stabilization of an Anammox process from a non-acclimatized sludge in CSTR," *Journal of Industrial Microbiology and Biotechnology*, vol. 37, no. 9, pp. 943–952, 2010.

[80] T. Wang, H. Zhang, F. Yang, S. Liu, Z. Fu, and H. Chen, "Start-up of the Anammox process from the conventional activated sludge in a membrane bioreactor," *Bioresource Technology*, vol. 100, no. 9, pp. 2501–2506, 2009.

[81] C.-J. Tang, P. Zheng, Q. Mahmood, and J.-W. Chen, "Start-up and inhibition analysis of the Anammox process seeded with anaerobic granular sludge," *Journal of Industrial Microbiology and Biotechnology*, vol. 36, no. 8, pp. 1093–1100, 2009.

[82] U. van Dongen, M. S. M. Jetten, and M. C. M. van Loosdrecht, "The SHARON-Anammox process for treatment of ammonium rich wastewater," *Water Science and Technology*, vol. 44, no. 1, pp. 153–160, 2001.

[83] W. S. H. R. H. Petrucci and F. G. Herring, *General Chemistry: Principles and Modern Applications*, Higher Education Press, Beijing, China, 8th edition, 2004.

[84] H. Min, M. C. Chen, Y. H. Zhao, and Z. S. Qian, *Anaerobic Microbiology*, Zhejiang University Press, Hangzhou, China, 1993.

[85] Q. Mahmood, *Process performance, optimization and microbiology of anoxic sulfide biooxidation using nitrite as electron acceptor [Ph.D. Dissertation]*, Zhejiang University, Hangzhou, China, 2007.

[86] A. Wiessner, U. Kappelmeyer, P. Kuschk, and M. Kästner, "Sulphate reduction and the removal of carbon and ammonia in a laboratory-scale constructed wetland," *Water Research*, vol. 39, no. 19, pp. 4643–4650, 2005.

[87] G. F. Yang, Q. Q. Zhang, and R. C. Jin, "Changes in the nitrogen removal performance and the properties of granular sludge in an Anammox system under oxytetracycline (OTC) stress," *Bioresource Technology*, vol. 129, pp. 65–71, 2013.

[88] C. J. Tang, R. He, P. Zheng, L. Y. Chai, and X. B. Min, "Mathematical modelling of high-rate Anammox UASB reactor based on granular packing patterns," *Journal of Hazardous Materials*, vol. 250-251, pp. 1–8, 2013.

[89] H. F. Lu, Q. X. Ji, S. Ding, and P. Zheng, "The morphological and settling properties of ANAMMOX granular sludge in high-rate reactors," *Bioresource Technology*, vol. 143, pp. 592–597, 2013.

[90] A. Franco, E. Roca, and J. M. Lema, "Granulation in high-load denitrifying upflow sludge bed (USB) pulsed reactors," *Water Research*, vol. 40, no. 5, pp. 871–880, 2006.

[91] K. Z. Su, B. J. Ni, and H. Q. Yu, "Modeling and optimization of granulation process of activated sludge in sequencing batch reactors," *Biotechnology and Bioengineering*, vol. 110, pp. 1312–1322, 2013.

[92] H. F. Lu, P. Zheng, Q. X. Ji et al., "The structure, density and settlability of anammox granular sludge in high-rate reactors," *Bioresource Technology*, vol. 123, pp. 312–317, 2012.

[93] M. S. M. Jetten, M. Wagner, J. Fuerst, M. van Loosdrecht, G. Kuenen, and M. Strous, "Microbiology and application of the anaerobic ammonium oxidation ('anammox') process," *Current Opinion in Biotechnology*, vol. 12, no. 3, pp. 283–288, 2001.

[94] A. A. van de Graaf, P. de Bruijn, L. A. Robertson, M. S. M. Jetten, and J. G. Kuenen, "Autotrophic growth of anaerobic ammonium-oxidizing micro-organisms in a fluidized bed reactor," *Microbiology*, vol. 142, no. 8, pp. 2187–2196, 1996.

[95] L. van Niftrik, W. J. C. Geerts, E. G. van Donselaar et al., "Combined structural and chemical analysis of the anammoxosome: a membrane-bounded intracytoplasmic compartment in anammox bacteria," *Journal of Structural Biology*, vol. 161, no. 3, pp. 401–410, 2008.

[96] Y. Liu and J.-H. Tay, "The essential role of hydrodynamic shear force in the formation of biofilm and granular sludge," *Water Research*, vol. 36, no. 7, pp. 1653–1665, 2002.

[97] L. W. Hulshoff Pol, S. I. de Castro Lopes, G. Lettinga, and P. N. L. Lens, "Anaerobic sludge granulation," *Water Research*, vol. 38, no. 6, pp. 1376–1389, 2004.

[98] X.-W. Liu, G.-P. Sheng, and H.-Q. Yu, "Physicochemical characteristics of microbial granules," *Biotechnology Advances*, vol. 27, no. 6, pp. 1061–1070, 2009.

[99] Y.-Q. Liu, Y. Liu, and J.-H. Tay, "The effects of extracellular polymeric substances on the formation and stability of biogranules," *Applied Microbiology and Biotechnology*, vol. 65, no. 2, pp. 143–148, 2004.

[100] J. Quarmby and C. F. Forster, "An examination of the structure of UASB granules," *Water Research*, vol. 29, no. 11, pp. 2449–2454, 1995.

[101] F. M. Cuervo-López, F. Martinez, M. Gutiérrez-Rojas, R. A. Noyola, and J. Gómez, "Effect of nitrogen loading rate and carbon source on denitrification and sludge settleability in upflow anaerobic sludge blanket (UASB) reactors," *Water Science and Technology*, vol. 40, no. 8, pp. 123–130, 1999.

[102] D. J. Batstone and J. Keller, "Variation of bulk properties of anaerobic granules with wastewater type," *Water Research*, vol. 35, no. 7, pp. 1723–1729, 2001.

[103] F. O. Martínez, J. Lema, R. Méndez, F. Cuervo-López, and J. Gómez, "Role of exopolymeric protein on the settleability of nitrifying sludges," *Bioresource Technology*, vol. 94, no. 1, pp. 43–48, 2004.

[104] J. Wu, H.-M. Zhou, H.-Z. Li, P.-C. Zhang, and J. Jiang, "Impacts of hydrodynamic shear force on nucleation of flocculent sludge in anaerobic reactor," *Water Research*, vol. 43, no. 12, pp. 3029–3036, 2009.

[105] M. S. M. Jetten, L. V. Niftrik, M. Strous, B. Kartal, J. T. Keltjens, and H. J. M. Op Den Camp, "Biochemistry and molecular biology of anammox bacteria biochemistry and molecular biology of anammox bacteria M.S.M. Jetten et al.," *Critical Reviews in Biochemistry and Molecular Biology*, vol. 44, no. 2-3, pp. 65–84, 2009.

[106] M. G. Klotz, M. C. Schmid, M. Strous, H. J. M. Op Den Camp, M. S. M. Jetten, and A. B. Hooper, "Evolution of an octahaem cytochrome c protein family that is key to aerobic and anaerobic ammonia oxidation by bacteria," *Environmental Microbiology*, vol. 10, no. 11, pp. 3150–3163, 2008.

[107] M. C. Schmid, A. B. Hooper, M. G. Klotz et al., "Environmental detection of octahaem cytochrome c hydroxylamine/hydrazine oxidoreductase genes of aerobic and anaerobic ammonium-oxidizing bacteria," *Environmental Microbiology*, vol. 10, no. 11, pp. 3140–3149, 2008.

[108] T. T. Chen, P. Zheng, and L. D. Shen, "Growth and metabolism characteristics of anaerobic ammonium-oxidizing bacteria aggregates," *Applied Microbiology and Biotechnology*, vol. 97, no. 12, pp. 5575–5583, 2013.

[109] J. D. Bryers and F. Drummond, "Local macromolecule diffusion coefficients in structurally non-uniform bacterial biofilms using fluorescence recovery after photobleaching (FRAP)," *Biotechnology and Bioengineering*, vol. 60, no. 4, pp. 462–473, 1998.

[110] D. de Beer, P. Stoodley, and Z. Lewandowski, "Measurement of local diffusion coefficients in biofilms by microinjection and confocal microscopy," *Biotechnology and Bioengineering*, vol. 53, no. 2, pp. 151–158, 1997.

[111] L. W. Hulshoff Pol, W. J. de Zeeuw, C. T. M. Velzeboer, and G. Lettinga, "Granulation in UASB-reactors," *Water Science and Technology*, vol. 15, no. 8-9, pp. 291–304, 1983.

[112] L. Tijhuis, B. Hijman, M. C. M. van Loosdrecht, and J. J. Heijnen, "Influence of detachment, substrate loading and reactor scale on the formation of biofilms in airlift reactors," *Applied Microbiology and Biotechnology*, vol. 45, no. 1-2, pp. 7–17, 1996.

[113] J. Chen, Q. Ji, P. Zheng, T. Chen, C. Wang, and Q. Mahmood, "Floatation and control of granular sludge in a high-rate anammox reactor," *Water Research*, vol. 44, no. 11, pp. 3321–3328, 2010.

[114] A. Dapena-Mora, J. L. Campos, A. Mosquera-Corral, M. S. M. Jetten, and R. Méndez, "Stability of the ANAMMOX process in a gas-lift reactor and a SBR," *Journal of Biotechnology*, vol. 110, no. 2, pp. 159–170, 2004.

[115] A. Dapena-Mora, B. Arrojo, J. L. Campos, A. Mosquera-Corral, and R. Méndez, "Improvement of the settling properties of Anammox sludge in an SBR," *Journal of Chemical Technology and Biotechnology*, vol. 79, no. 12, pp. 1417–1420, 2004.

[116] Y. Ma, D. Hira, Z. Li, C. Chen, and K. Furukawa, "Nitrogen removal performance of a hybrid anammox reactor," *Bioresource Technology*, vol. 102, no. 12, pp. 6650–6656, 2011.

[117] P. An, X. Xu, F. Yang, L. Liu, and S. Liu, "A pilot-scale study on nitrogen removal from dry-spun acrylic fiber wastewater using anammox process," *Chemical Engineering Journal*, vol. 222, pp. 32–40, 2013.

[118] D. D. Ebbing and S. D. Gammon, *General Chemistry*, Houghton Mifflin, Boston, MA, USA, 9th edition, 2007.

[119] C. Tang, P. Zheng, J. Chen, X. Chen, S. Zhou, and G. Ding, "Start-up and process control of a pilot-scale Anammox bioreactor at ambient temperature," *Chinese Journal of Biotechnology*, vol. 25, no. 3, pp. 406–412, 2009.

[120] S.-Q. Ni, S. Sung, Q.-Y. Yue, and B.-Y. Gao, "Substrate removal evaluation of granular anammox process in a pilot-scale upflow anaerobic sludge blanket reactor," *Ecological Engineering*, vol. 38, no. 1, pp. 30–36, 2012.

[121] W. Driessen and G. Reitsma, "One-Step ANAMMOX Process-Water Projects Online," UK Water Project, 2011.